University of Massachusetts Amherst
ScholarWorks@UMass Amherst

Doctoral Dissertations 1896 - February 2014

1-1-2001

The influence of inter-domain interactions on the physical properties of polyurethanes.

Xiaodong Wu
University of Massachusetts Amherst

Follow this and additional works at: https://scholarworks.umass.edu/dissertations_1

Recommended Citation
Wu, Xiaodong, "The influence of inter-domain interactions on the physical properties of polyurethanes." (2001). *Doctoral Dissertations 1896 - February 2014*. 1017.
https://doi.org/10.7275/yt91-fd13 https://scholarworks.umass.edu/dissertations_1/1017

This Open Access Dissertation is brought to you for free and open access by ScholarWorks@UMass Amherst. It has been accepted for inclusion in Doctoral Dissertations 1896 - February 2014 by an authorized administrator of ScholarWorks@UMass Amherst. For more information, please contact scholarworks@library.umass.edu.

UMASS/AMHERST
312066 0275 8535 5

THE INFLUENCE OF INTER-DOMAIN INTERACTIONS ON THE PHYSICAL PROPERTIES OF POLYURETHANES

A Dissertation Presented

by

XIAODONG WU

Submitted to the Graduate School of the
University of Massachusetts Amherst in partially fulfillment
of the requirements for the degree of

DOCTOR OF PHILOSOPHY

September 2001

Polymer Science and Engineering

© Copyright by Xiaodong Wu 2001
All Rights Reserved

THE INFLUENCE OF INTER-DOMAIN INTERACTIONS ON THE PHYSICAL PROPERTIES OF POLYURETHANES

A Dissertation Presented

by

XIAODONG WU

Approved as to style and content by:

Shaw Ling Hsu, Chair

Richard J. Farris, Member

Thomas J. McCarthy, Member

Howard D. Stidham, Member

Thomas J. McCarthy, Department Head
Polymer Science and Engineering

To my parents.

ACKNOWLEDGMENTS

I would first like to acknowledge my advisor, Professor Hsu, for his guidance through my graduate education. I am grateful for the opportunity to work on several interesting projects and interact with both the scientific and industrial communities by his generous funding of trips to various meetings and workshops. I also thank him for always reminding me the big picture of my research and helping me focus on the scientific issues of each project.

I also wish to express my appreciation to Professor Thomas McCarthy, Professor Richard Farris and Professor Howard Stidham for serving on my committee. Their helpful comments and instructions gave me a lot of input in this dissertation work. Besides, I enjoyed the short courses on spectroscopy offered by Professor Stidham since I was the only student in the class.

I would like to extend my gratitude to the staff of PSE department. Without them, I can't imagine what my graudate life could be at UMass. First I thank Eileen Besse for her meticulous work and humor, John Domian for his timeless help on the machine shop work, Andre Mel'cuk for his assistance on my computer questions, and Sophie Hsu for her kind help on group matters.

There are several people at DOW Chemical to whom I owe much. I would like to thank Dr. Ralph Priester Jr. for organizing numerous meetings to advance the research. Other people include Dr. Werner Lidy, Dana Gier, Dr. Michael Mazor, Dr. Chris Christenson and Dr. Jozef Bicerano for the stimulating discussions and invaluable comments on the progress of my polyurethane research.

I believe everyone will agree that your coworkers are as important as your advisor. I would like to thank Dr. Dorie Yontz for helping me when I started the project on polyurethane research. I would also like to express my appreciation to Amy Heintz,

Shuhui Kang, Daniel Duffy, Dr. Andrei Stolov, Amanda Chaparro, Michael Williams and Visiting Professor Xiaozhen Yang for their friendship and discussion inside and outside science. In addition, I am proud of being one member of the PSE family for the intensive scientific interactions throughout the department and the fun we had in the ASPIRE Program.

I would also like to acknowledge many friends outside the department for their enduring friendship, especially to Dr. Alfred Karlson, John, Terry, Dr. Jun Wang, for making my life colorful in these years.

Finally, I dedicate this dissertation to my parents for their love, sacrifice and support of my entire graduate studies in the states, especially to my father who inspired me into this fascinating field when I was a kid.

ABSTRACT

THE INFLUENCE OF INTER-DOMAIN INTERACTIONS ON

THE PHYSICAL PROPERTIES OF POLYURETHANES

SEPTEMBER 2001

XIAODONG WU, B.ENG., SHANGHAI JIAO TONG UNIVERSITY

M.S., BOWLING GREEN STATE UNIVERSITY

Ph.D., UNIVERSITY OF MASSACHUSETTS AMHERST

Directed by: Professor Shaw Ling Hsu

The phase separated structure of polyurethane foams is kinetically trapped due to the vitrification of hard segment domains, which results in an interconnecting hard domain morphology. This new morphological picture depicts the importance of the inter-connectivity provided by both the small portions of the long hard segments and the disordered regions that serve as an indirect bridge between hard domains. Deuterium substitution has been used to specify different regions of the interconnecting phase-separated structure in polyurethanes. Thin film samples were prepared isothermally using foam formulations with different water contents to obtain very different degrees of domain inter-connectivity. By analyzing the relative rate of substitution at different relative humidity and temperature of the environment, it is possible to differentiate the degree of phase-separation for various samples with different degrees of phase separation. The infrared spectroscopic features, mainly amide vibrations, of various parts of hard segments have been identified. The deuterium substitution rates measured

revealed that the size and dispersion of hard-segment domains can vary significantly as a function of reaction temperature and composition of reactants. It is also possible to differentiate the interfacial region from the phase-separated domains.

Based upon the interconnecting hard domain morphology, infrared dichroic studies further demonstrated the contribution of hard domains to reinforcement of polyurethane materials. Plastic deformation within the hard domain was observed even at small strain, giving a molecular insight to the stress-softening effect and energy hysteresis associated with polyurethanes.

The viscoelastic properties of polyurethane studied by stress relaxation experiments have again shown the importance of interconnectivity to the overall mechanical properties of this material. A correlation between the exact water placement and overall deterioration of physical properties has been established.

Lignin has been successfully incorporated as a reinforcing component to enhance polyurethanes. It was not until the dispersion state of the lignin in polyol was improved and both the processing conditions and catalyst package were optimized that the modulus and strength of the polyurethane material showed significant enhancement. It is found that lignin most likely functions as the hard segments to achieve better interconnectivity of the physical network of the hard domain morphology.

TABLE OF CONTENTS

LIST OF TABLES

LIST OF FIGURES

LIST OF SCHEMES

CHAPTER I

INTRODUCTION

1.1. Survey of Dissertation

Ever since the phase separated structure of polyurethane was proposed, [1,2] extensive researches have been carried out to understand the morphology and physical properties of polyurethanes. [3-22] The numerous reactants, the rich chemistry and various processing conditions generate a broad spectrum of applications for polyurethanes in foams, adhesives, coatings, medical devices, etc. [23]

The phase separation of the reactive processing of water-blown flexible slabstock foam system has intrigued many scientists. [19,20,24-30] The system starts as a liquid state mixture – viscous polyol, water, and liquid isocyanate and a small amount of tin and amine catalyst. In less than 5 minutes, the entire liquid system undergoes liquid-liquid phase separation, eventually intercepted by the vitrification of the hard segment domain, resulting in a solid foam.

In this thesis, polyurethane thin films and plaques were made under isothermal conditions to obtain different morphologies. The interconnecting hard domain morphology has been characterized using deuterium substitution and by the hard segment length distribution. It is found that the degree of phase separation and the interfacial region that interconnects the hard domains are crucial to the physical properties of the

material and the new morphological model by Yontz *et. al.* has been proved. Using infrared dichroism, in addition to the orientation studies for different domains, the volume change of the hard domain throughout the entire deformation process has been evaluated. The observation points to the large energy hysteresis and stress-softening effect associated with polyurethanes, even at low strains. The viscoelastic property of polyurethane has also been studied by the stress relaxation experiments to explore the water transport and plasticization mechanism. This investigation can further our understanding of the hard domain reinforcement and the importance of the interconnecting region to the overall physical properties. Based upon the new morphological picture and reinforcing mechanism we proposed, lignin as an organic filler has been successfully incorporated into the polyurethanes. Various issues to optimize the process conditions are investigated, including the improvement of the dispersion state of lignin into the polyol, and proper catalyst package for generating better phase separated morphology and interconnectivity of the hard domain. It was found that both the modulus and strength increased after lignin was properly incorporated into the polyurethanes.

This thesis is divided into seven chapters. Chapter 1 introduces the origin of the phase separation of polyurethane materials, the kinetically trapped phase separated morphology and the basic polyurethane chemistry, followed by the research objectives. Chapter 2 describes the detailed experimental procedures and processing conditions in making the polyurethane thin films and plaques. The detailed characterization techniques are also included. In Chapter 3, the deuterium substitution method has been presented to investigate the interconnecting hard domain morphology. Based upon our understanding of the new morphological model, the deformation behaviors of polyurethanes have been examined in Chapter 4 using infrared dichroism, which provides the molecular insight

into the hard domain reinforcement. The viscoelastic property of polyurethane materials under humid environment is of technological importance and it is the subject of Chapter 5. By combining the results given in the above three chapters, interconnecting hard domain morphology was shown to be important for the enhancement of the properties of polyurethane. In Chapter 6, lignin has been demonstrated as a reinforcing component to strengthen polyurethane, which has potential application in foams and adhesives. The miscibility of lignin with polyol, the optimized processing conditions, and the resulting morphology and properties are discussed. The catalytic chemistry is emphasized. Finally, a research summary and future work are addressed in Chapter 7.

1.2. Interconnecting Hard Domain Morphology of Polyurethanes

1.2.1. Phase separation

Many block copolymers, including segmented polyurethanes, are known to possess a phase separated morphological structure comprising thermodynamically incompatible hard and soft segment domains. [1,5,6,13,14,31-33] The degree of phase separation is related to an interaction parameter χ, originally introduced by Flory and Huggins for polymer solutions. [34] The thermodynamic is fundamental and the driving force to the overall phase separation. It is dictated by the equation

Equation 1.1 $$\Delta G_m = \Delta H_m - T\Delta S_m > 0$$

where ΔG_m is the free energy of mixing. For microphase separation, the following equation will also be satisfied:

Equation 1.2. $$\left(\frac{\partial^2 \Delta G_m}{\partial \phi^2}\right)_{T,P} < 0$$

where ϕ is the volume fraction of one component. [35]

Despite the tremendous investment in both theoretical and experimental studies, [8,10,16,18-20,25,33,36-39] it has been virtually impossible to relate the fundamentals of chemical reaction to the phase separation behavior in polyurethanes and their mechanical properties. For virtually more than thirty years, polyurethane phase separation is generally believed to be due to chemical immiscibility between hard and soft segments and specific interactions between hard segments. [40] In addition, the excluded volume of the rigid segments is a crucial factor in the determination of the phase separation structure. [13,14] Even polyurethanes that do not hydrogen bond still phase separate. [41-43] In most cases, the hard domain formation is not complete due to the rising viscosity of the reacting system and the distribution of the hard segment lengths. There is a certain amount of dispersed hard segments dissolved in the soft matrix. The phase mixing may also involve a small amount of soft segments dissolved in the hard domain, which increases the hard domain volume fraction. [32]

The final morphology is critically controlled by the kinetic process and temperature profile. The complexity of the polyurethane structure is strongly influenced by both reactant composition and processing conditions. During the polymerization process, the rising temperature profile can change the reaction kinetics dramatically.

[24,29] The chemical crosslinking and phase separation are competing processes, which will determine the degree of phase mixing against the phase separation in the final morphology of the system. [44] If a kinetically trapped phase separated morphology exists, ordered and disordered hard domains and dispersed hard segments must coexist. In addition, the presence of an interfacial region is also a possibility. [45,46] However, these two aspects of the structure have never been characterized fully.

A number of techniques have been used to characterize polyurethane structures. These include scattering, [6,17,47] spectroscopy, [3,40,48-52] EXAFS, [53] thermal methods, [45,54] NMR, [43,55] and mechanical testing. [5,56] Deuterium substitution adds to the structural information available, particularly regarding the dispersed phase and interfacial regions, two structural aspects not well covered by the techniques listed above.

In-situ studies of structure development during the reactive processing of model flexible polyurethane foam systems using FTIR spectroscopy and synchrotron SAXS has been carried out by Ryan's group. [18-20] The polymerization began with a homogeneous liquid mixture, and then went through a microphase separation transition, where the phase separation followed a spinodal decomposition mechanism. [57,58] At later stage, the expanding foam raised in the modulus resulted from microphase separation being intercepted and arrested by vitrification of the hard segments. [19] The important conclusion from this study is that the vitrification of the hard segments freezes in the morphology at the Berghmans point [27] and results in the interconnecting physical network of the hard segment domain morphology. [18-20] The interconnecting hard domain morphology can most likely account for the physical network formed by the hard domain, which has been shown to enhance the physical properties of polyurethane

materials. [5,59-61] Based upon the percolation theory, above 16% volume fraction of the hard domain can form interlocking morphology. [62] The volume fraction of these systems is well above this value and it is possible that interconnecting hard domain morphology exists in these structures. The interconnecting phenomenon has already been known in other fields, such as rodlike liquid crystalline materials. [63] It tends to form a physical network by aggregation of the rigid segments as shown in Figure 1.1.

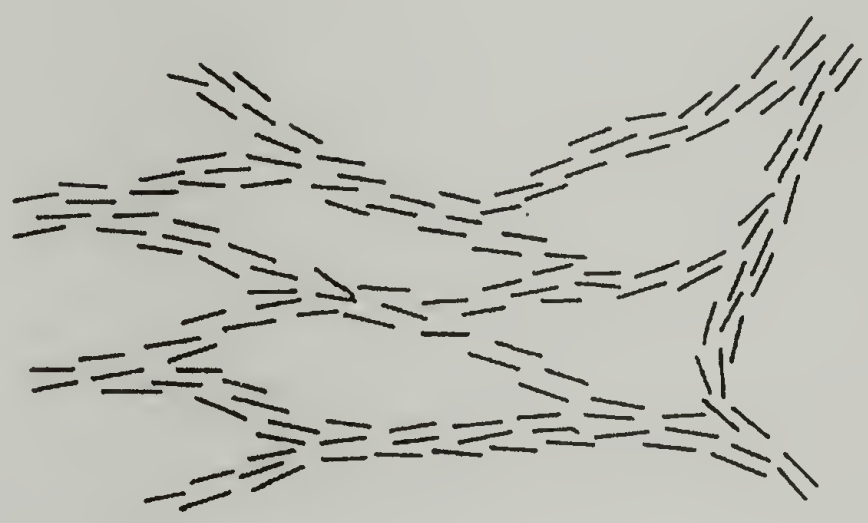

Figure 1.1. Model for networks formed by aggregation of rigid rodlike polymers [63]

Even though several experimental studies have shown that the interconnecting morphology has higher mechanical properties, quantitative modeling of its reinforcing mechanism is still a challenge. It has been suggested that traditional filler models are not sufficient to describe the modulus and strength. [64-72] A quantitative description of the interconnecting hard domain morphology and its deformation behavior is needed for further understanding.

The interconnectivity has been classified under three possible types as shown in Figure 1.2: (i) Molecular. The connecting elements are individual, soft chains with junctions being the dispersed glassy concentrated phase. (ii) Continuous phase connectivity. This provides through the continuity of the glassy phase itself in the otherwise expanded system. (iii) Adhesive phase connectivity. Here again the glassy phase provides the connectivity but through adhesive contact of glassy particles forming ramifying aggregates, called paste consistency. [27]

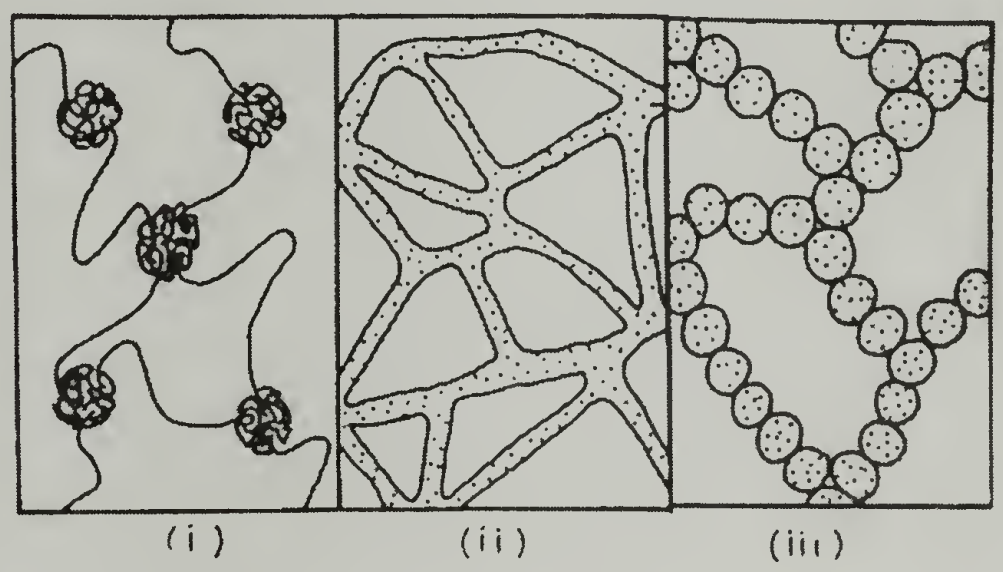

Figure 1.2. A schematic illustration of the three classes of gel: (i) molecularly connected, (ii) phase connected (continuous), (iii) phase connected (adhesive) [27]

Yontz conducted research on the morphology of model polyurethane systems. [44,64] Based upon AFM and TEM results, the observed morphology for samples made at 50 °C has not only the highly organized hard domain, but also the interconnecting rigid material between domains. In contrast, the samples made at 150 °C point to a phase mixed morphology with some loosely aggregated hard segments. It was concluded that the crosslinking rate was faster than phase separation at 150 °C, the gelling reaction increases the viscosity of the reacting system and restricted the mobility of the hard

segments, resulting in a phase mixed morphology. [44,64] Yontz also examined the hard segment length distribution for various polyurethane systems using MALDI-TOF. Hard

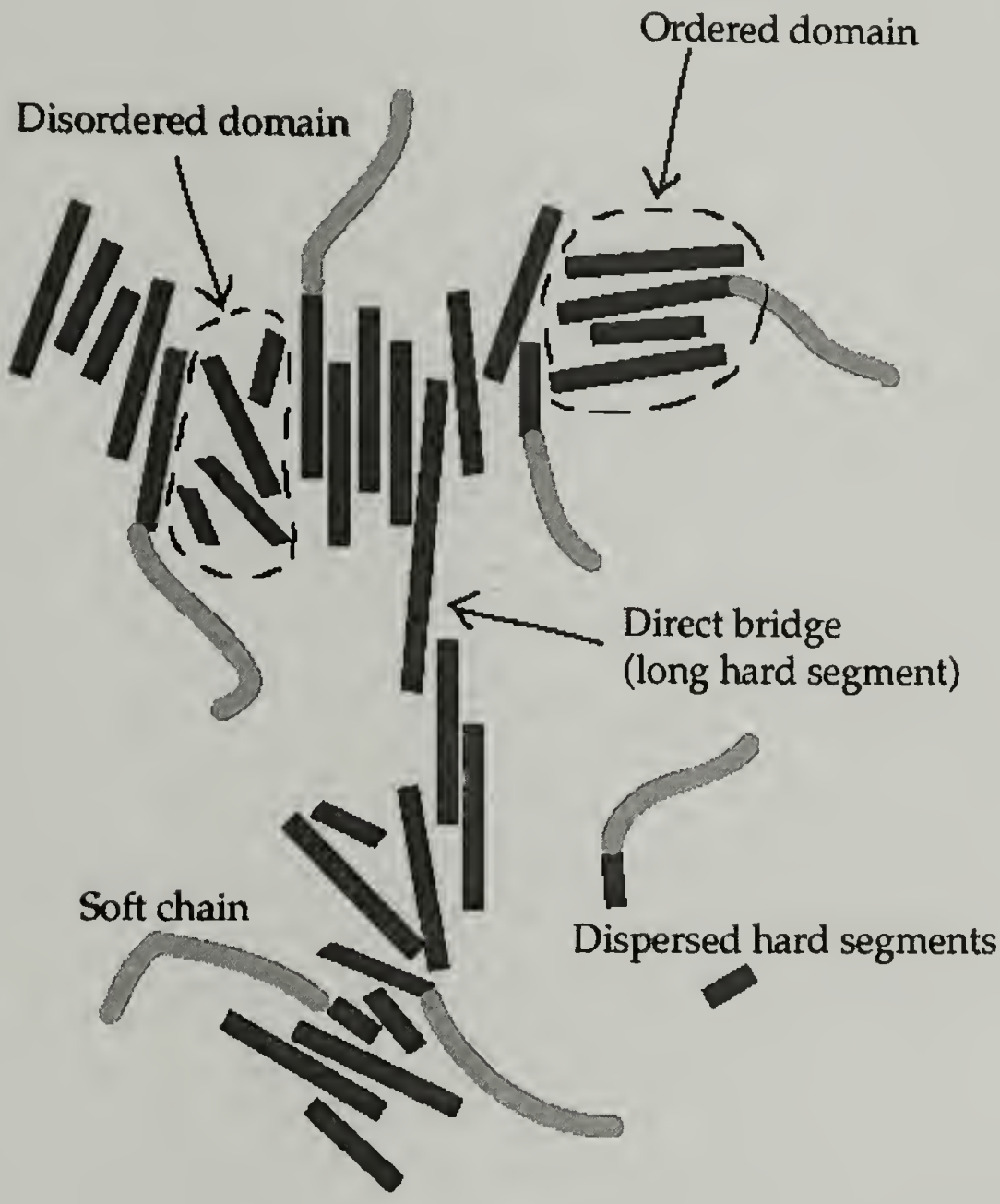

Figure 1.3. Interconnecting hard domain morphology

segment length is a one of the parameters in determining equilibrium degree of phase separation and phase separation kinetics. [9,10,13] The result of the long hard segments in

the phase separated morphology led to the idea of their function as the direct interconnecting bridge between domains. [73]

The performance of polyurethanes is severely degraded in humid environment. [74-76] Since foam materials have a large surface area, the understanding of the change in morphology and property of polyurethanes upon moisture absorption is technologically important. Several mechanisms have been proposed based upon earlier studies, correlating the effect of moisture sorption to the lowering of mechanical properties. Gibson suggested that absorption of moisture disrupts the original bonds. [77] It was proposed that the mechano-sorptive behavior due to moisture allows an increase in molecular mobility. [78] A widely accepted concept which suggested that the humid aged compression set (HASET) is due to water penetrating hard domains and interfering with hydrogen bonding. [79] This has served as the basis for the several subsequent studies. [80-82] However, the interpretation lacks exact information of where water goes in certain sites of the hard domain structures. Later a combined effect of rubber elasticity of the covalent network and a plasticization effect of temperature and humidity was proposed. [74-76] In this dissertation, D_2O vapor sorption is shown to be unique in studying the water plasticization mechanism. The high sensitivity and characteristic bands for certain groups in infrared spectroscopy can specify where absorbed D_2O are located, and allows understanding diffusion behavior within the accessible regions and interactions with these regions.

1.2.2. Polyurethane Chemistry

The basic ingredients of a polyurethane material are diisocyanate, a chain extender and the hydroxyl or amino-ended polyol or polyester chains. The complete description of the polyurethane foam components is listed in Appendix A. Diisocyanates can be either aromatic or aliphatic. Aromatic compounds are more reactive. The typical aromatic diisocyanates include 4,4'-methylenebis(phenyl isocyanate) (MDI) and toluene diisocyanate (TDI). The chain extenders often are short chain alcohols or amines. Reaction between diisocyanate and a hydroxyl group forms the urethane group, while reaction between diisocyanate and an amine group forms the urea group. The reaction schemes are summarized in Figures 1.4 and 1.5. Water is also an important chain extender, especially in making flexible slabstock foams. [83]

Figure 1.4. Urethane formation reaction

Figure 1.5. Urea formation reaction

Water reacts with isocyanate group to form carbamate group. After decomposing into carbon dioxide (blowing) and amine as illustrated in the Figure 1.6, the resulting amine reacts with another isocyanate group to form the urea linkage.

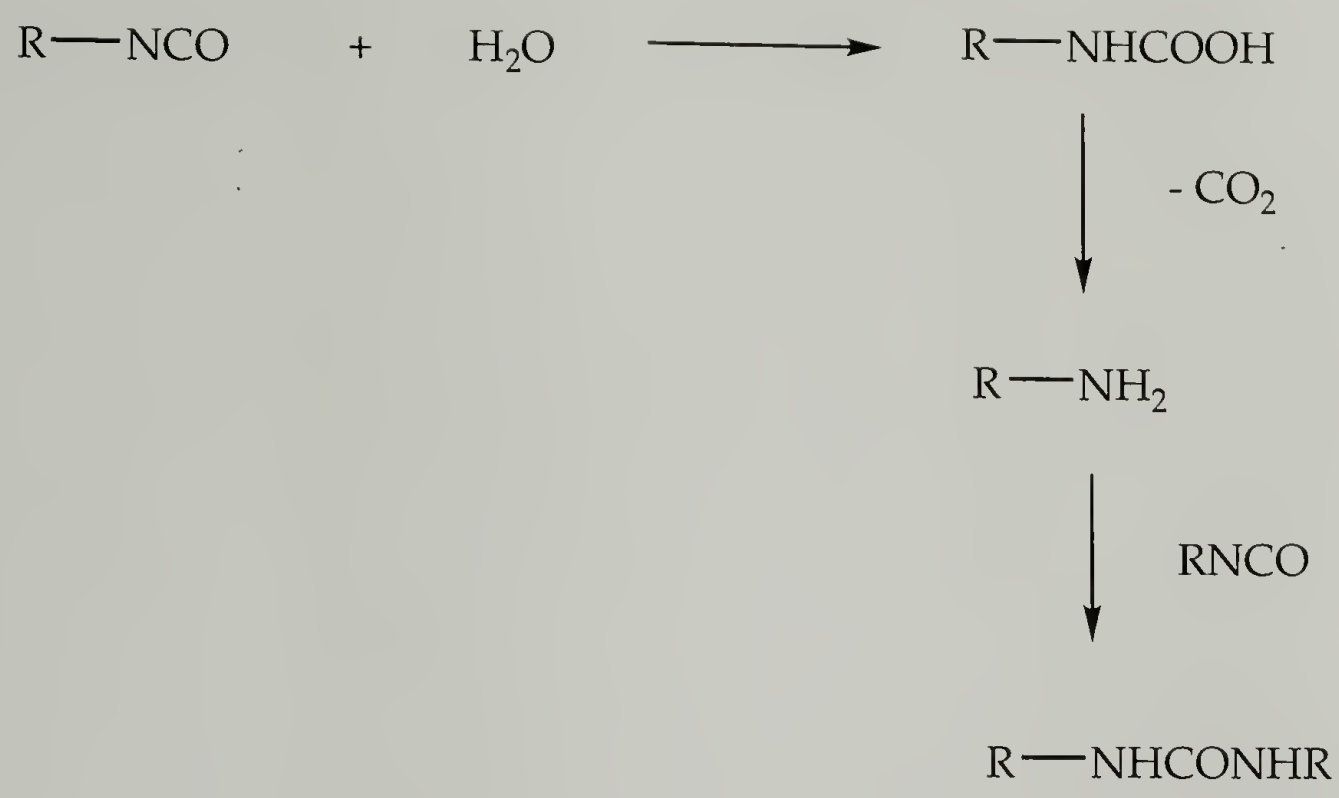

Figure 1.6. Water blow reaction to generate urea hard segment

Usually urea groups form the oligmers at certain chain length, as indicated by the degree of polymerization *m* in Figure 1.7. These hard segments will aggregate to form the hard domain during microphase separation. The urethane linkage at each end connects the soft polyether chains to the hard segment and the resulting structure of polyurethanes can be expressed as following:

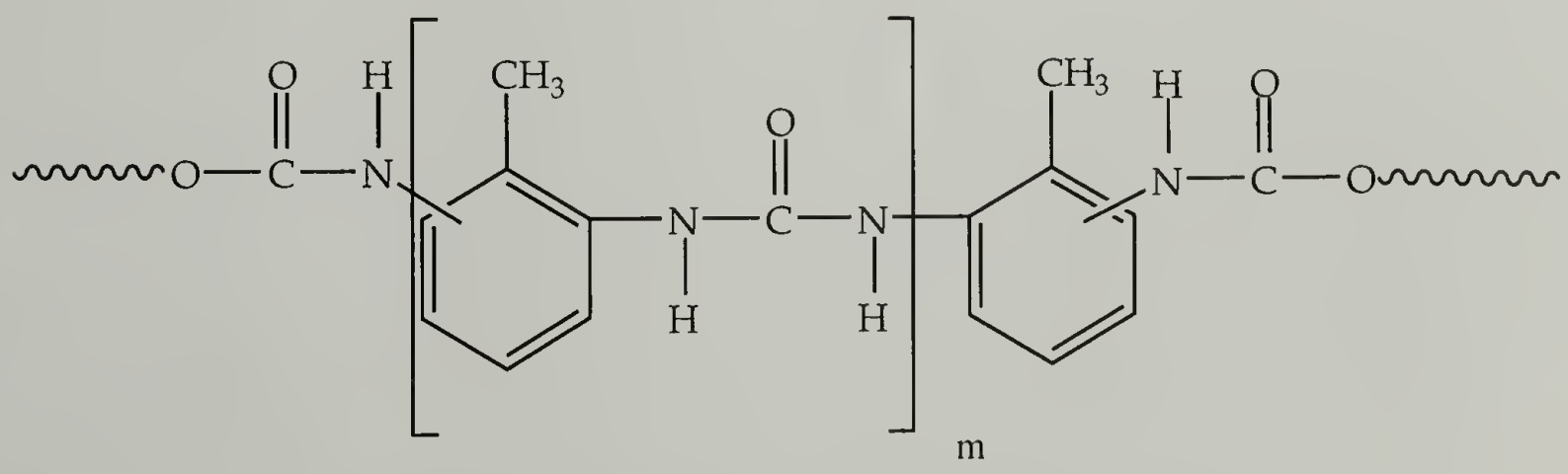

Figure 1.7. Chemical structure of polyurethane urea

Another important aspect of polyurethane chemistry is the side reactions, which include trimerization and additional reactions of the isocyanate with the urea and urethane groups to form biuret and allophanate, respectively. [84,85] These side reactions as shown in Figures 1.8-1.10 will cause chain branching and crosslinking. [86-90] Based upon the MALDI-TOF analysis, there is also a very small percentage (2~4%) of cyclic structures in the final morphology. [73]

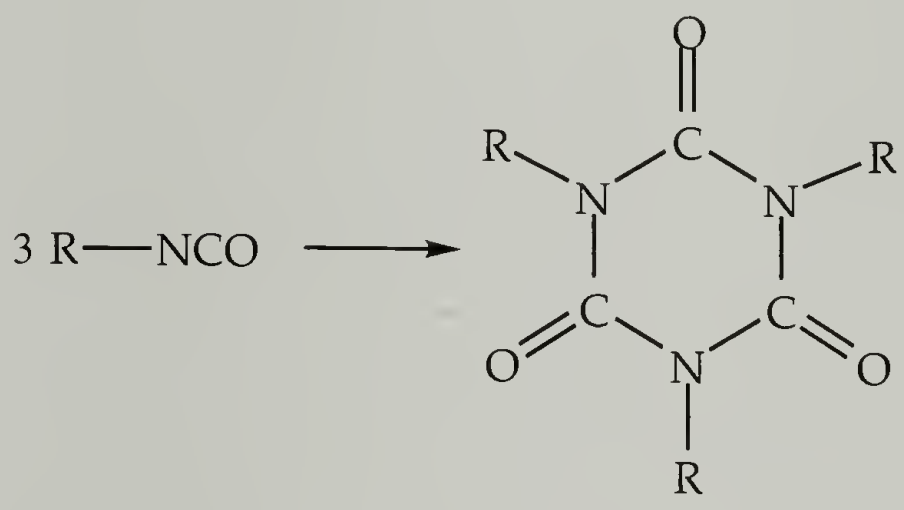

Figure 1.8. Trimerization reaction of isocyanate

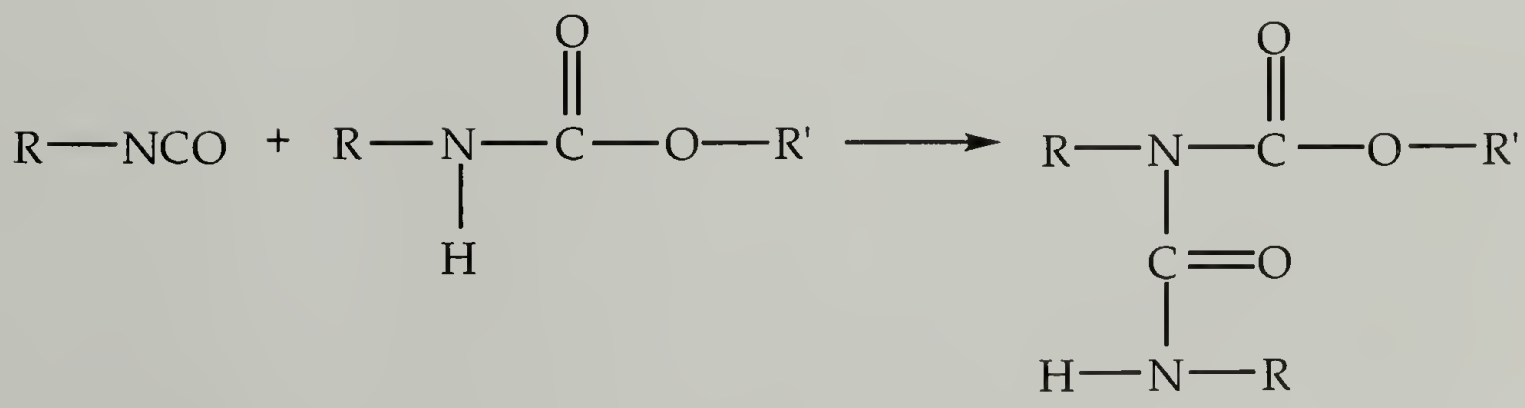

Figure 1.9. Allophanate formation reaction

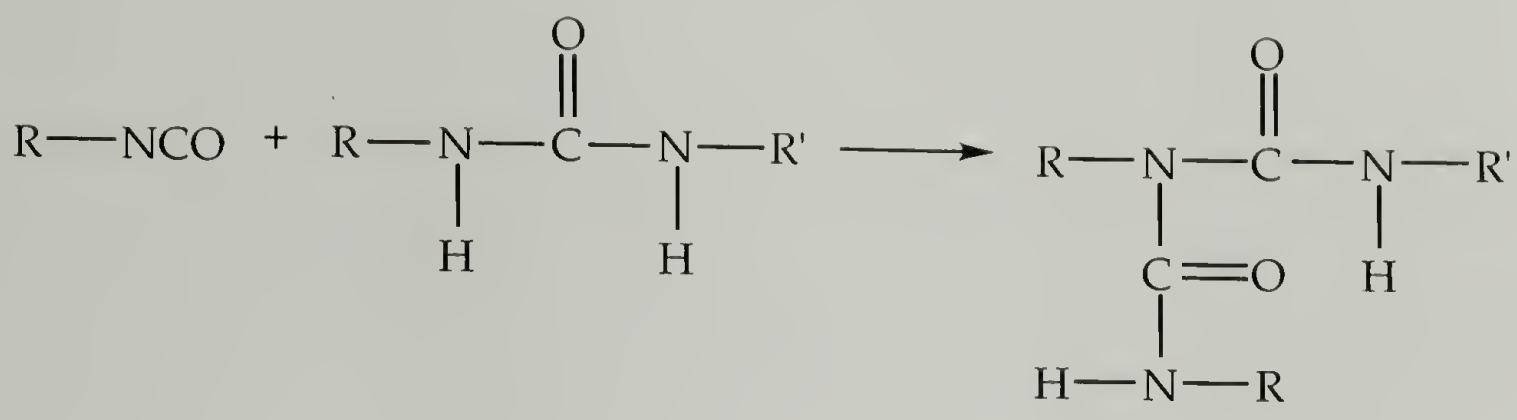

Figure 1.10. Biuret formation reaction

1.3. Research Objectives

The deuterium substitution method will be used to study quantitatively on the dispersion state of hard domain morphology and specify the surface, the interfacial and the bulk hard domain. This method has been proven to be useful in exploring the conformational change of lysozyme in D_2O solution by studying the kinetics of hydrogen-deuterium exchange. [91] The structural features of keratin and other model proteins have also been characterized using this technique. [92,93] Based upon the different diffusion rates in different regions of the hard domain, the extent of adsorption of deuterated water at the surface and the disordered region of the hard domains in polyurethanes can be monitored by infrared spectroscopy. Therefore a quantitative description of the relative fraction of surface, disordered and bulk ordered regions of the hard domains can be realized. The schematic plot is demonstrated in Figure 1.11.

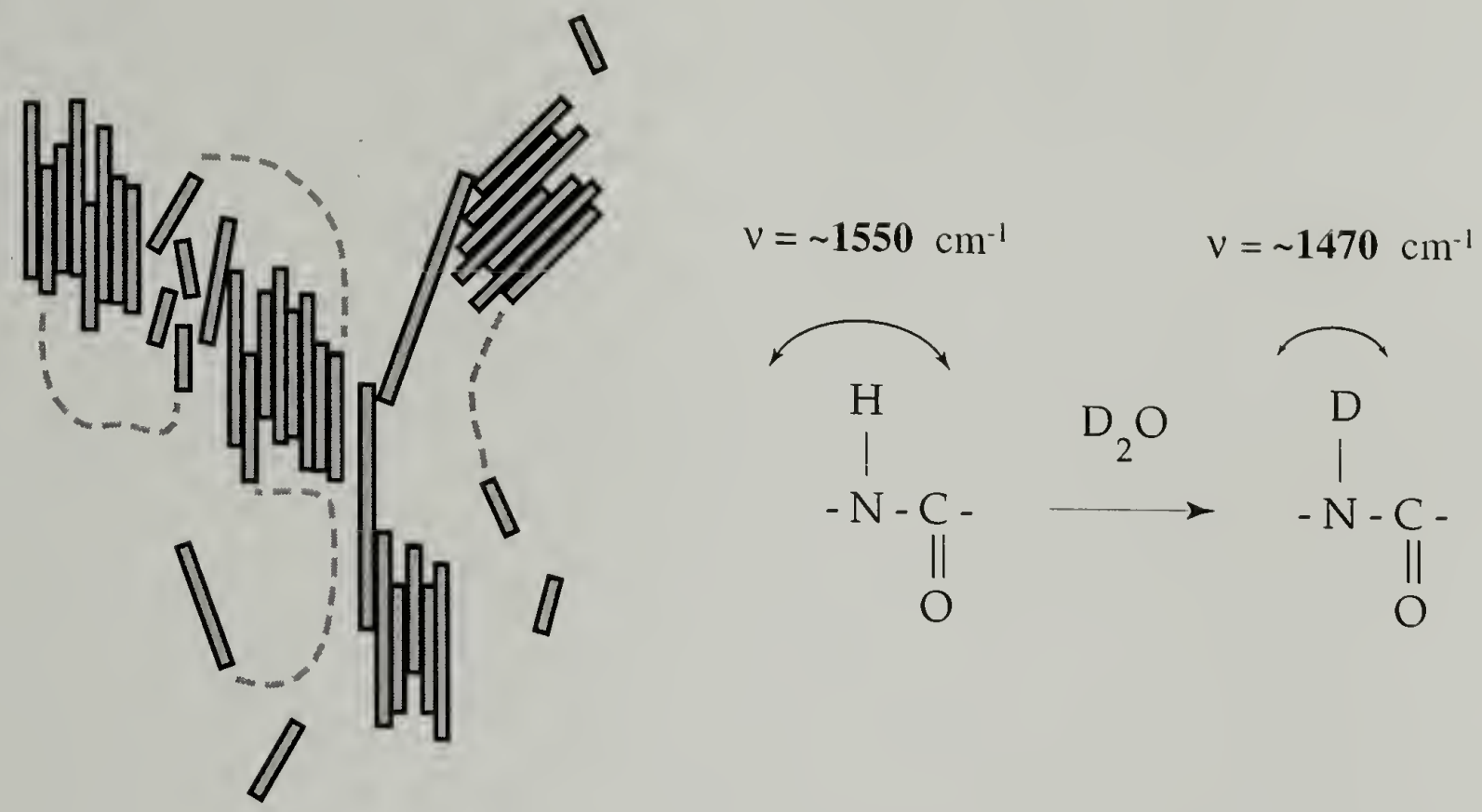

Figure 1.11. Deuterium Substitution – D_2O diffuses into a thin film sample to probe the dispersion state of hard domain within the soft matrix

The interfacial region connects the hard domains or lies between a hard domain and adjacent soft matrix, plays a role in enhancing the mechanical properties of the material. This can be investigated by infrared dichroism. To understand the deformation behavior of polyurethanes better, the response of the Amide II band to uniaxial stretching will be observed using infrared dichroic measurement. Based upon the knowledge obtained from deuterium substitution experiments on these samples, the two major components within the amide II region will be intensively studied and associated with ordered urea hard domain and urethane groups at the boundary between the domains with some dispersed hard segments. This observation allows study of the deformation behavior based upon morphological features in a quantitative way using the amide II

band. It also provides experimental evidence for theoretical modeling work to understand the true reinforcement and mechanical properties of the materials.

The viscoelastic properties of polyurethane samples in humid environments can be studied using stress relaxation and *in situ* monitoring the accessibility of moisture. Combined with deuterium substitution, the D_2O sorption experiment demonstrates a direct evidence of large distortion of hard domain under plasticization since D_2O functions as a marker indicating where water reaches in the specific region of the hard domain. The swelling stress relaxation experiment also provides a unique way to study the transport properties of moisture in thin film samples.

Incorporating lignin as an organic filler to enhance the mechanical properties not only provides an effective way to utilize this biomass to solve environmental problems, but also gives potential to reduce the isocyanate consumption in polyurethane productions. Lignin can be used to enhance the interconnecting hard domain morphology and thus to strengthen the physical properties of polyurethanes. To succeed in making the lignin polyblend materials, the miscibility and the dispersion state of lignin in polyol before polymerization will be studied. The catalytic package in the processing conditions will also be examined and improved to control the final morphology and physical properties of polyurethanes. The reinforcing mechanism of this composite material will also be explored.

1.4. References

1) Cooper, S. L.; Tobolsky, A. V. *J. Appl. Polym. Sci.* **1966**, *10*, 1837-1844.

2) Bonart, R.; Morbitzer, L.; Hentze, G. *J. Macromol. Sci.-Phys.* **1969**, *B3*, 337-356.

3) Ishihara, H.; Kimura, I.; Saito, S.; Ono, H. *J. Macromol. Sci. Phys.* **1974**, *B10*, 591-618.

4) Schneider, N. S.; Paik Sung, C. S.; Matton, R. W.; Illinger, J. L. *Macromolecules* **1975**, *8*, 62-67.

5) Paik Sung, C. S.; Smith, T. W.; Sung, N. H. *Macromolecules* **1980**, *13*, 117-121.

6) Koberstein, J. T.; Stein, R. S. *J. Polym. Sci., Part B: Polym. Phys.* **1983**, *21*, 2181-2200.

7) Koberstein, J. T.; Russell, T. P. *Macromolecules* **1986**, *19*, 714-720.

8) Armistead, J. P.; Wilkes, G. L. *J. Appl. Polym. Sci.* **1988**, *35*, 601-629.

9) Lee, H. S.; Wang, Y. K.; Hsu, S. L. *Macromolecules* **1987**, *20*, 2089.

10) Lee, H. S.; Wang, Y. K.; MacKnight, W. J.; Hsu, S. L. *Macromolecules* **1988**, *21*, 270-273.

11) Meuse, C. W.; Yang, X.; Yang, D.; Hsu, S. L. *Macromolecules* **1992**, *25*, 925-932.

12) Meuse, C. W.; Tao, H.-J.; Hsu, S. L.; MacKnight, W. J. *Polym. Prepr. (Am. Chem. Soc., Div. Polym. Chem.)* **1993**, *34*, 266-267.

13) Tao, H.-J.; Meuse, C. W.; Yang, X.; MacKnight, W. J.; Hsu, S. L. *Macromolecules* **1994**, *27*, 7146-7151.

14) Tao, H.-J.; Fan, C. F.; MacKnight, W. J.; Hsu, S. L. *Macromolecules* **1994**, *27*, 1720-1728.

15) Tao, H. J.; MacKnight, W. J.; Gagnon, K. D.; Lenz, R. W.; Hsu, S. L. *Macromolecules* **1995**, *28*, 2016-2022.

16) Lee, H. S.; Hsu, S. L. *Macromolecules* **1989**, *22*, 1100-1105.

17) Creswick, M. W.; Lee, K. D.; Turner, R. B.; Huber, L. M. *J. Elast. Plast.* **1989**, *21*, 179-96.

18) Elwell, M. J.; Mortimer, S.; Ryan, A. J. *Macromolecules* **1994**, *27*, 5428-5439.

19) Elwell, M. J.; Ryan, A. J.; Grunbauer, H. J. M.; Van Lieshout, H. C. *Polymer* **1996**, *37*, 1353-1361.

20) Elwell, M. J.; Ryan, A. J.; Grunbauer, H. J. M.; Van Lieshout, H. C. *Macromolecules* **1996**, *29*, 2960-2968.

21) Neff, R.; Macosko, C. W. *A Model for Modulus Development in Flexible Polyurethane Foam*: Chicago, IL, **1995**, pp 344-352.

22) Neff, R.; Adedeji, A.; Macosko, C. W.; Ryan, A. J. *J. Polym. Sci., Part B: Polym. Phys.* **1998**, *36*, 573-581.

23) Oertel, G. *Polyurethane Handbook*; Hanser/Gardner Publications, Inc.: Cincinnati, **1993**.

24) Priester, R. D.; McClusky, J. V.; O'Neill, R. E.; Harthcock, M. A.; Davis, B. L. *33rd Annual Polyurethane Technical/Marketing Conference* **1990**, *September 30-October 3*, 527-538.

25) Artavia, L. D.; Macosko, C. W. *J. Cell. Plast.* **1990**, *26*, 490-511.

26) Artavia, L. D.; Macosko, C. W.; Priester, R. D., Jr.; Shrock, A. K.; Turner, R. B. *An Integrated View of Reactive Urethane Foaming*: Nice, France, **1991**, pp 509-517.

27) Callister, S.; Keller, A.; Hikmet, R. M. *Makromol. Chem. Macromol. Symp.* **1990**, *39*, 19-54.

28) Grunbauer, H. J. M.; Folmer, J. C. W. *J. Appl. Polym. Sci.* **1994**, *54*, 935-949.

29) Van Gheluwe, P.; Leroux, J. *J. Appl. Polym. Sci.* **1983**, *28*, 2053-2067.

30) Mertes, J.; Stutz, H.; Schrepp, W.; Kreyenschmidt, M. *J. Cell. Plast.* **1998**, *34*, 526-543.

31) Seymour, R. W.; Allegrezza, A. E.; Cooper, S. L. *Macromolecules* **1973**, *6*, 896-902.

32) Yang, C. Z.; Li, C.; Cooper, S. L. *J. Polym. Sci., Polym. Phys. Ed.* **1991**, *29*, 75-86.

33) Turner, R. B.; Wilkes, G. L. *Structure vs. Properties of Flexible Urethane Foams Used in the Home Furnishing Industry (Polymer-Morphology)*; Technomic Publishing Co., Inc.: Aachen, Federal Republic of Germany, **1987**, pp 935-939.

34) Flory, P. J. *Principles of Polymer Chemistry*; Cornell University Press: Ithaca, NY, **1953**.

35) Ryan, A. J.; Stanford, J. L.; Still, R. H. *Polym. Comm.* **1988**, *29*, 196-198.

36) McClusky, J. V.; O'Neill, R. E.; Priester, R. D. J.; Ramsey, W. A. *J. Cell. Plast.* **1992**, *30*, 224-241.

37) McClusky, J. V.; Priester, R. D., Jr.; O'Neill, R. E.; Willkomm, W. R.; Heaney, M. D.; Capel, M. A. *J. Cell. Plast.* **1994**, *30*, 338-360.

38) Rossmy, G. R.; Kollmeier, H. J.; Lidy, W.; Schator, H.; Wiemann, M. *J. Cell. Plast.* **1977**, *13*, 26-35.

39) Wilkinson, A. N.; Naylor, S.; Elwell, M. J.; Draper, P.; Komanschek, B. U.; Stanford, J. L.; Ryan, A. J. *Polym. Commun.* **1996**, *37*, 2021-2024.

40) Wang, C. B.; Cooper, S. L. *Macromolecules* **1983**, *16*, 775-786.

41) Culbertson, B. M. *Multiphase Macromolecular Systems*; Plenum Publishing Corporation: New York, **1989**.

42) Harrell, L. L., Jr. *Macromolecules* **1969**, *2*, 607-612.

43) Kornfield, J. A.; Spiess, H. W.; Nefzger, H.; Eisenbach, C. D. *Macromolecules* **1991**, *24*, 4787-4795.

44) Yontz, D. J.; Hsu, S. L.; Lidy, W. A.; Gier, D. R.; Mazor, M. H. *J. Polym. Sci., Polym. Phys.* **1998**, *36*, 3065-3077.

45) Petrovic, Z. S.; Javni, I. *Journal of Polymer Science: Part B: Polymer Physics* **1989**, *27*, 545-560.

46) Yang, C. Z.; Hwang, K. K. S.; Cooper, S. L. *Makromol. Chem.* **1983**, *184*, 651-668.

47) Li, Y.; Ren, Z.; Zhao, M.; Yang, H.; Chu, B. *Macromolecules* **1993**, *26*, 612-622.

48) Siesler, H. W. *Polymer Bulletin* **1983**, *9*, 382-389.

49) West, J. C.; Cooper, S. L. *J. Polym. Sci., Polym. Symp.* **1977**, *60*, 127-150.

50) Hocker, J. *J. Appl. Polym. Sci.* **1980**, *25*, 2879-2889.

51) Coleman, M. M.; Lee, K. H.; Skrovanek, D. J.; Painter, P. C. *Macromolecules* **1986**, *19*, 2149-2157.

52) Brunette, C. M.; Hsu, S. L.; MacKnight, W. J. *Macromolecules* **1982**, *15*, 71-77.

53) Grady, B. P.; O' Connell, E. M.; Yang, C. Z.; Cooper, S. L. *J. Polym. Sci., Part B: Polym. Phys.* **1994**, *32*, 2357-2366.

54) Koberstein, J.; Gancarz, I. *Journal of Polymer Scienc: Part B: Polymer Physics* **1986**, *24*, 2487-2498.

55) Clayden, N. J. N., C.; and Eeckhaut, G. *Macromolecules* **1998**, *31*, 7820-7828.

56) Gorce, J.-N.; Hellgeth, J. W.; Ward, T. C. *Polym. Eng. Sci.* **1993**, *33*, 1170-1176.

57) Strobl, G. *The Physics of Polymers*; 2nd ed.; Springer-Verlag: Berlin, **1997**.

58) Reich, S. *Dynamics of Late Stage Phase Separation in Polymer Blends*; Rabin, Y. and Bruinsma, R., Ed.; Plenum Press: New York, **1994**, pp 73-98.

59) Seymour, R. W.; Cooper, S. L. *J. Polym. Sci., Polym. Symp.* **1974**, *46*, 69-81.

60) Miller, J. A.; Lin, S. B.; Hwang, K. K. S.; Wu, K. S.; Gibson, P. E.; Cooper, S. L. *Macromolecules* **1985**, *18*, 32-44.

61) Martin, D. J.; Meijs, G. F.; Gunatillake, P. A.; Yozghatlian, S. P.; Renwick, G. M. *J. Appl. Polym. Sci.* **1999**, *71*, 937-952.

62) Levon, K.; Margolina, A.; Patashinsky, A. Z. *Macromolecules* **1993**, *26*, 4061-4063.

63) Uematsu, I.; Uematsu, Y. *Polypeptide Liquid Crystals*; Gordon, M., Ed.; Springer-Verlag: Berlin, **1984**.

64) Yontz, D. J. *An Analysis of Molecular Parameters Governing Phase Seperation in a Reacting Polyurethane System*; University of Massachusetts: Amherst, MA, **1999**, pp 329.

65) Bicerano, J.; Brewbaker, J. L. *J. Chem. Soc. Faraday Trans.* **1995**, *91*, 2507-2513.

66) Pukanszky, B. *Makromol. Chem. Macromol. Symp.* **1993**, *70/71*, 213-223.

67) Halpin, J. C. *Revised Primer on Composite Materials: Analysis*; Technomic Publishing Co., Inc.: Lancaster, **1984**.

68) Laws, N.; McLaughlin, R. *J. Mech. Phys. Solids* **1979**, *47*, 1-13.

69) Brodnyan, J. G. *Trans. Soc. Rheol.* **1959**, *3*, 61-68.

70) Mooney, M. *J. Colloid Sci.* **1951**, *6*, 162-170.

71) Guth, E. *J. Appl. Phys.* **1945**, *16*, 20-25.

72) Smallwood, H. M. *J. Appl. Phys.* **1944**, *15*, 758-766.

73) Yontz, D. J.; Hsu, S. L. *Macromolecules* **2000**, *33*, 8415 - 8420.

74) Moreland, J. C.; Wilkes, G. L. *Journal of Applied Polymer Science* **1991**, *43*, 801-815.

75) Dounis, D. V.; Wilkes, G. L.; Turner, R. B. *Polym. Prepr. (Am. Chem. Soc., Div. Polym. Chem.)* **1994**, *35*, 781-82.

76) Broos, R.; Herrington, R. M.; Casati, F. M. *Journal of Cellular Plastics* **2000**, *36*, 207-245.

77) Gibson, L. J.; Ashby, M. F. *Proc. Roy. Soc. Lond. A* **1982**, *382*, 43-59.

78) Van der Put, T. A. C. M. *Wood Fiber Sci.* **1989**, *21*, 219.

79) Herrington, R. M.; Klarfeld, D. L. *Humid Aged Compression Set Phenomena in All Water Blown HR Molded Foams*; Technomic Publishing Co., Inc.: Lancaster, PA., **1983**, pp 177-182.

80) Moreland, J. C.; Wilkes, G. L.; Turner, R. B. *Viscoelastic Behavior of Flexible Slabstock Polyurethane Foams as a Function of Temperature and Relative Humidity*: Nice, France, **1991**, pp 500-508.

81) Dounis, D. V.; Moreland, J. C.; Wilkes, G. L.; Dillard, D. A.; Turner, R. B. *J. Appl. Polym. Sci.* **1993**, *50*, 293-301.

82) Dounis, D. V.; Wilkes, G. L. *Polymer* **1997**, *38*, 2819-2828.

83) Herrington, R.; Hock, K. *Flexible Polyurethane Foams*; 2 ed.; The Dow Chemical Company: Midland, **1997**.

84) Balon, W. J. *Trifunction Isocyanate Trimers*; E.I. duPont de Nemours and Company: USA, **1957**.

85) Korzyuk, E. L.; Zharkov, V. V.; Emelin, E. A. *J. Appl. Chem. USSR* **1981**, *54*, 1320-1324.

86) Spirkova, M.; Kubin, M.; Dusek, K. *J. Macromol. Sci.-Chem.* **1987**, *A24*, 1151-1166.

87) Sandridge, R. L.; Morecroft, A. S.; Hardy, E. E.; Saunders, J. H. *J. Chem. Eng. Data* **1960**, *5*, 495-498.

88) Merten, R.; Lauerer, D.; Dahm, M. *J. Cell. Plast.* **1968**, *4*, 262-275.

89) Kurzer, F. *Chem. Rev.* **1956**, *56*, 95-197.

90) Kricheldorf, H. R.; Meier-Haack, J. *Makromol. Chem.* **1992**, *193*, 2631-2645.

91) Tsuboi, M.; Nakanishi, M. *Adv. Biophys.* **1979**, *12*, 101-130.

92) Bendit, E. G. *Biopolymers* **1966**, *4*, 539-559.

93) Chen, C. C.; Krejchi, M. T.; Tirrell, D. A.; Hsu, S. L. *Macromolecules* **1995**, *28*, 1464-1469.

CHAPTER II

EXPERIMENTAL PROCEDURES AND CHARACTERIZATION TECHNIQUES

2.1. Experimental Procedures

2.1.1. Materials

The polyurethane system is used to make flexible slabstock foams. Tolylene diisocyanate (TDI) was used as received from Aldrich (80% 2,4-TDI, 20% 2,6-TDI) and the chemical structures are illustrated in Figure 2.1. The position of isocyanate groups actually determines the reactivity as indicated in the scheme. The difference in reactivity is critical in the final morphology of the product. [1]

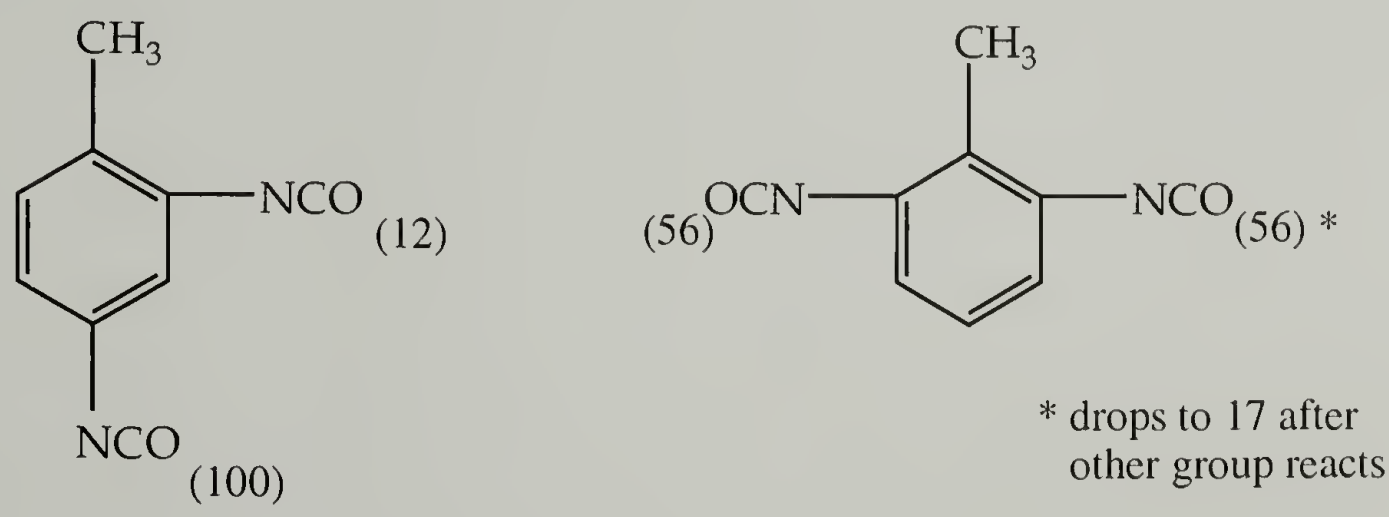

Figure 2.1. Diisocyanate TDI structures

The polyol used in the formulation was Voranol 3137 from DOW Chemical. The structure is shown in Figure 2.2. It is a copolymer with propylene oxide and about 13%wt ethylene oxide randomly incorporated into the backbone. The average molecular weight is 3000 g/mol, and the average functionality is 2.79. The chemical composition of the polyol has been studied using MALDI-TOF. [2] It is noted that the composition of ethylene oxide and propylene oxide can determine the solubility and dispersion state of water before the polymerization takes place. [2]

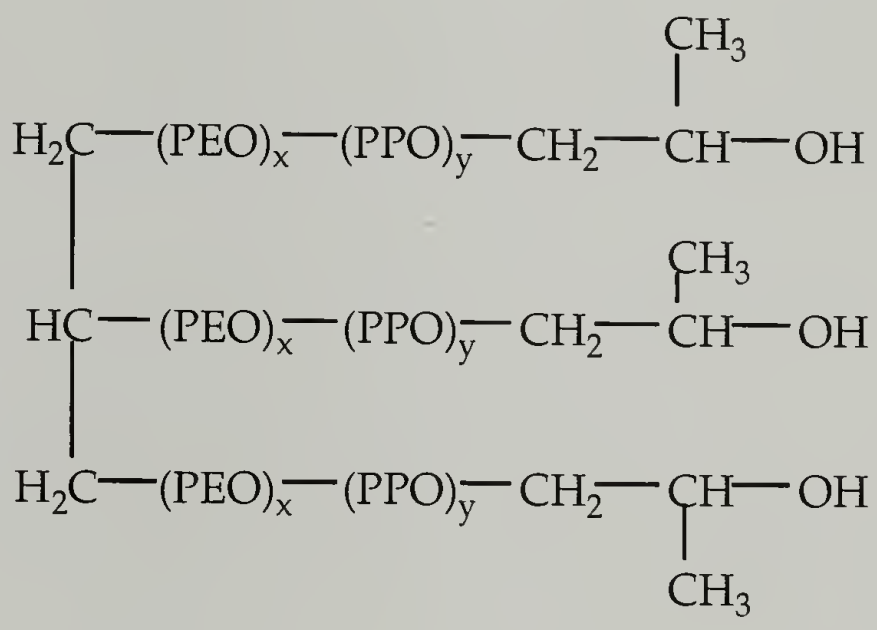

Figure 2.2. Chemical structure of Voranol® 3137

Water plays a role as a chain extender in the formulation to generate urea hard segments. Urea has two active hydrogens that can form stronger hydrogen bonding than urethane groups. [3-7] Deionized water was used as received from EM Science.

Catalysis plays a vital role in the preparation of urethane and urethane-urea polymers, because it not only affects the rates of the chemical reactions responsible for

chain propagation, extension, crosslinking and side reactions, but also affects the ultimate properties of the resulting polymers. [8-17] The catalytic mechanisms are illustrated in Appendix B. Tin and amine catalysts were used as received from Air Products. The DABCO T-9 catalyst is stannous octoate as indicated in Figure 2.3 and is basically a gelling catalyst that catalyzes the reaction between isocyanate and hydroxyl groups.

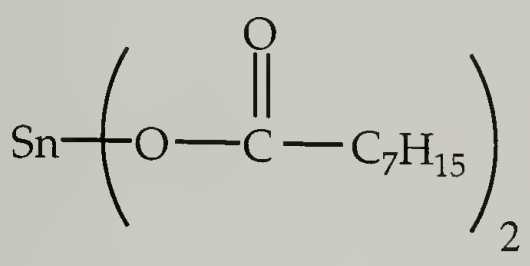

Figure 2.3. Chemical structure of DABCO® T-9 tin catalyst

The DABCO 33-LV, as shown in Figure 2.4, is the amine catalyst, a slight blowing catalyst. [18] It is a solution of diazobicyclo[2,2,2] octane, 1,4-(33%) in dipropylene glycol. It catalyzes the gelling reaction between TDI and polyol.

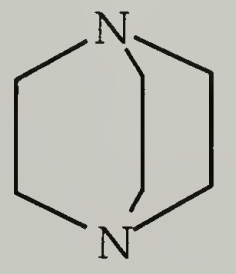

Figure 2.4. Chemical structure of DABCO® 33-LV amine catalyst

Another amine catalyst, DABCO BL-11, as shown in Figure 2.5, is a blowing catalyst. It accelerates the isocyanate-water reaction more intensely than the isocyanate-

polyol reaction due to stronger hydrogen bonding interaction with water. It is composed of 70% bis(dimethylaminoethyl) ether in a solution of dipropylene glycol. It can also be available under the name of Niax A-1 by Osi Specialties-Witco.

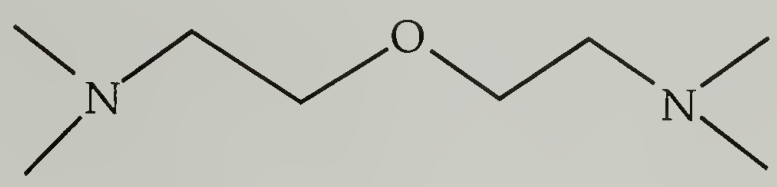

Figure 2.5. DABCO® BL-11 amine catalyst

2.1.2. Lignin

Lignin exists in wood as a random, three-dimensional network polymer comprised of phenylpropane units linked together in different ways. [19] The constitutional structural units of lignin are shown in Figure 2.6. The molecular weight is estimated around 5000 g/mol. [20]

The most significant and urgent problem is the profitable utilization of the vast quantities of lignin available as waste products or byproducts of the forest-using industries and the pulp and paper industry. [21] Lignin as a biomass has been found useful in engineering polymeric materials. [21-24] It not only solves the environment problems, but also provides an alternative to petroleum-based constituents and confers biodegradability on finished products. [25-27]

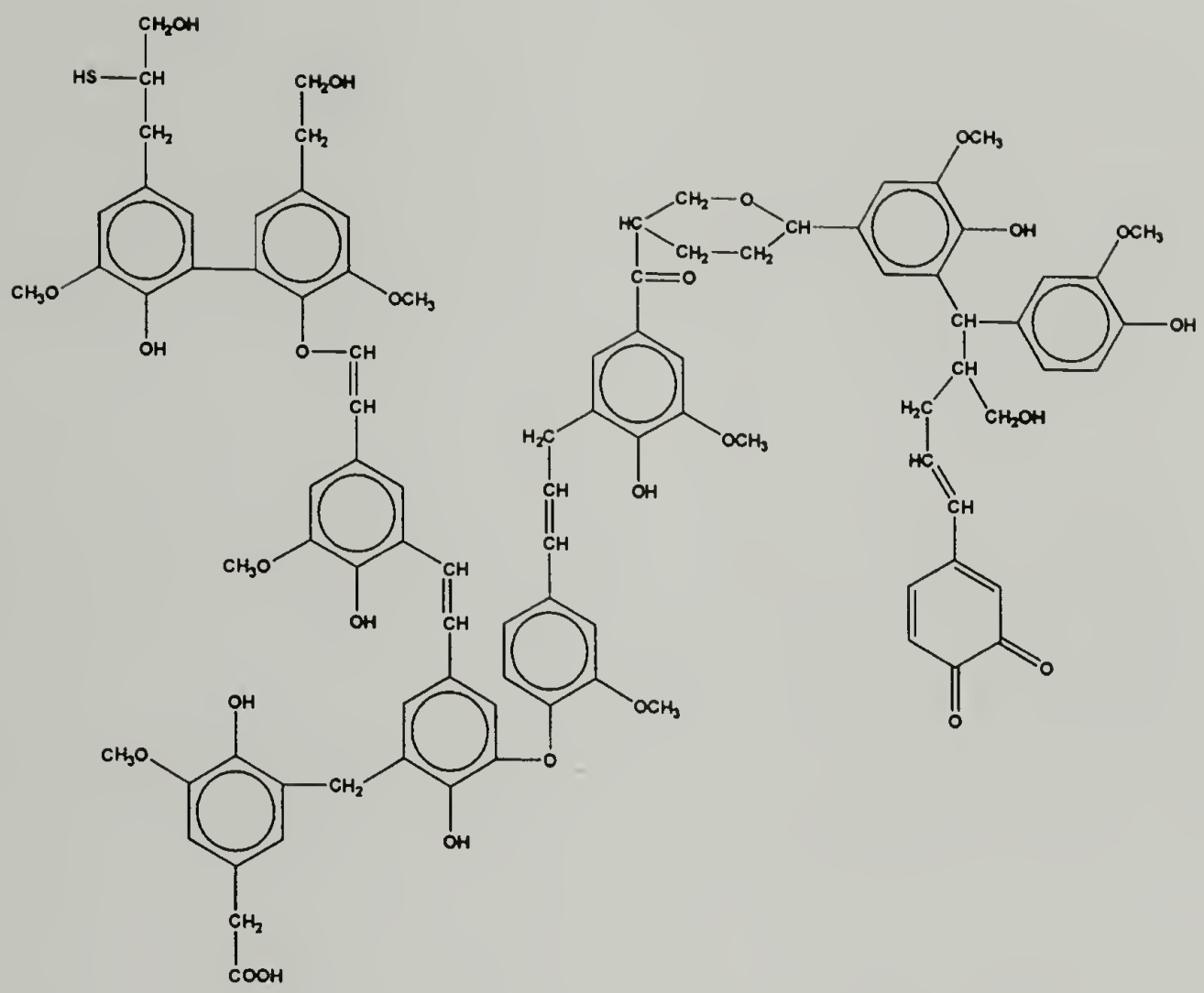

Figure 2.6. Structural units for kraft lignin

2.1.3. Processing Conditions

2.1.3.1. Plaque Preparation

Plaque samples were prepared in a steel mold provided by the DOW Chemical Company. The mold was coated with a fluorocarbon release agent (Fluoroglide ®) and preheated to a designated temperature in a press with electrically heated platens before

polymerization. To make plaques, polyol was mixed with an appropriate amount of Dabco T-9 catalyst; water and TDI were weighed into separate syringes. Catalysts and water were weighed to within 0.002 g of the formulation weight, and polyol and TDI were weighed to within 0.02 g. Amine catalysts were weighed and mixed into the polyol/T-9 mixture into a plastic beaker before polymerization. Water was then added and stirred until the solution was clear. TDI was added and mixed for 15 seconds when the foaming started. Then the mixture was poured into the preheated mold within 20-25 seconds of TDI addition. The mold was closed at 40-45 seconds and 15,000 lbs force was applied after 3 1/2 minutes. Sample was left at the mold temperature for one hour before cooling began by running water through the press plates. Plaques produced in this manner were around 1 mm thick and exhibited very few macroscopic defects such as bubbles or cracks. The reason to make plaque samples is tend to directly study the morphology and properties of the polyurethane materials without the complexity from the cellular structure of the foams.

A U-T naming system is used throughout the thesis to identify the plaques and films. The number U refers to the urea content and lists the theoretical number of ureas per chain, either four or six. Based upon the formulation, the weight fraction of urea hard segment for 4- and 6-samples are 28% and 35%, respectively. The calculation of the formulation is illustrated in previous work. [28] It is reported that the density of the hard domain phase is 1.251 g/cc. [29] From the Material Safety Data Sheet provided by the polyol supplier, the density of the soft segment is 1.019 g/cc. [28] The volume fraction of the hard segment is calculated to be 0.24 and 0.30 for the 4- and 6-series samples, respectively. The second number T refers to the isothermal reaction temperature in degrees Celsius. Therefore 4-80 refers to a sample with four ureas per chain that was synthesized at 80 °C.

2.3.1.2. Thin Film Prepraration

The thin films were prepared isothermally at three temperatures of 50, 70 and 80 °C using the composition previously described in earlier work. [30] Similarly, polyol was mixed well with T-9 organotin catalyst and Dabco 33-LV and Dabco BL-11 amine catalysts. Deionized water as chain extender was added to the mixture and stirred until the solution became clear. TDI was poured into the mixture while stirring, the timer was started, and stirring continued. At 25 seconds, the foamed liquid was poured onto a preheated polished stainless steel plate covered with FEP (fluorinated ethylene propylene) film. After a certain period of waiting time, the top plate covered with FEP film was added. This assembly was then placed in a press equipped with steel platens heated at that temperature. Force was rapidly applied to around 16,000 lbs. and polymer was cured in the press at constant temperature for one hour. After curing, a film was produced with a thickness of below 20 μm.

2.2. Characterization Techniques

2.2.1. Fourier Transformed Infrared Spectroscopy (FTIR)

Most of the infrared spectra were obtained using a Bruker IFS 113v vacuum spectrometer. The spectra were averaged from 128 co-added scans at a resolution of 4 cm^{-1}. Low temperature measurements were conducted using a cold finger apparatus of

load design and construction. The thin film sample was clamped on the cold finger. The sample chamber was evacuated and liquid nitrogen was poured in the Dewar to cool the system. The spectra will be demonstrated in Chapter 3.

A traditional technique for solid sample measurement is the mineral oil (Nujol) mull method. A small amount of solid sample is mulled in a mortar with a small amount of Nujol to yield a paste, which is then pressed between salt windows. [31] The best mulls display interference fringes when viewed between salts in visible light.

2.2.2. Attenuated Total Reflectance (ATR)

For the thick plaques and foam samples, transmission infrared is impossible. Attenuated total reflectance (ATR) spectra were obtained with a Perkin Elmer Spectrum 2000 Fourier Transformed Infrared Spectrometer. The spectra were averaged from 64 co-added scans at a resolution of 0.5 cm^{-1}. A 10 X 5 X 1 mm single-pass parallelepiped KRS-5 crystal (n=2.4) was used.

One example of applications of ATR is as follows: the foam samples provided by the DOW Chemical Company as specified in Table 2.1 were studied by ATR to obtain evidence characterizing the phase separated morphology of this series of samples. The spectra are shown in Figures 2.7(a)-(b).

Table 2.1. A Series of Foam Samples from DOW Chemical Company

Reference	224-30-2	224-37-1	224-37-2	224-37-3	224-37-4	224-37-5	224-37-6	224-37-7
Voranol 3040	100	100	100	100	100	100	100	100
T-80	56.5	52.1	45	47.4	49.8	54.5	52.1	52.1
Isocyanate Index	120	110	95	100	105	115	110	110
water	4	4	4	4	4	4	4	4
Dabco 33LV	0.12	0.12	0.12	0.12	0.12	0.12	0.12	0.12
Niax A-1	0.04	0.04	0.04	0.04	0.04	0.04	0.04	0.04
Tegostab BF 2370	0.8	0.8	0.8	0.8	0.8	0.8	0.8	0.8
T-9	0.13	0.18	0.25	0.22	0.20	0.16	0.18	0.18

Samples 224-37-6 and 224-37-7 had a small amount of crystallizable polyester polyol. Conclusions can be drawn from the spectra as follows:

1) 224-30-02 sample had the poorest degree of phase separation, as shown by the augmented intensity of free N-H stretching and amide I and II bands, relative to the other samples.

2) 224-37-1 had very similar morphology to 224-37-7, except the latter had a little weaker hydrogen bonding intensity.

3) 224-37-5 had the second poorest degree of phase separation based upon the amide I region; while 224-37-2 and 224-37-3 had the highest degree of phase separation.

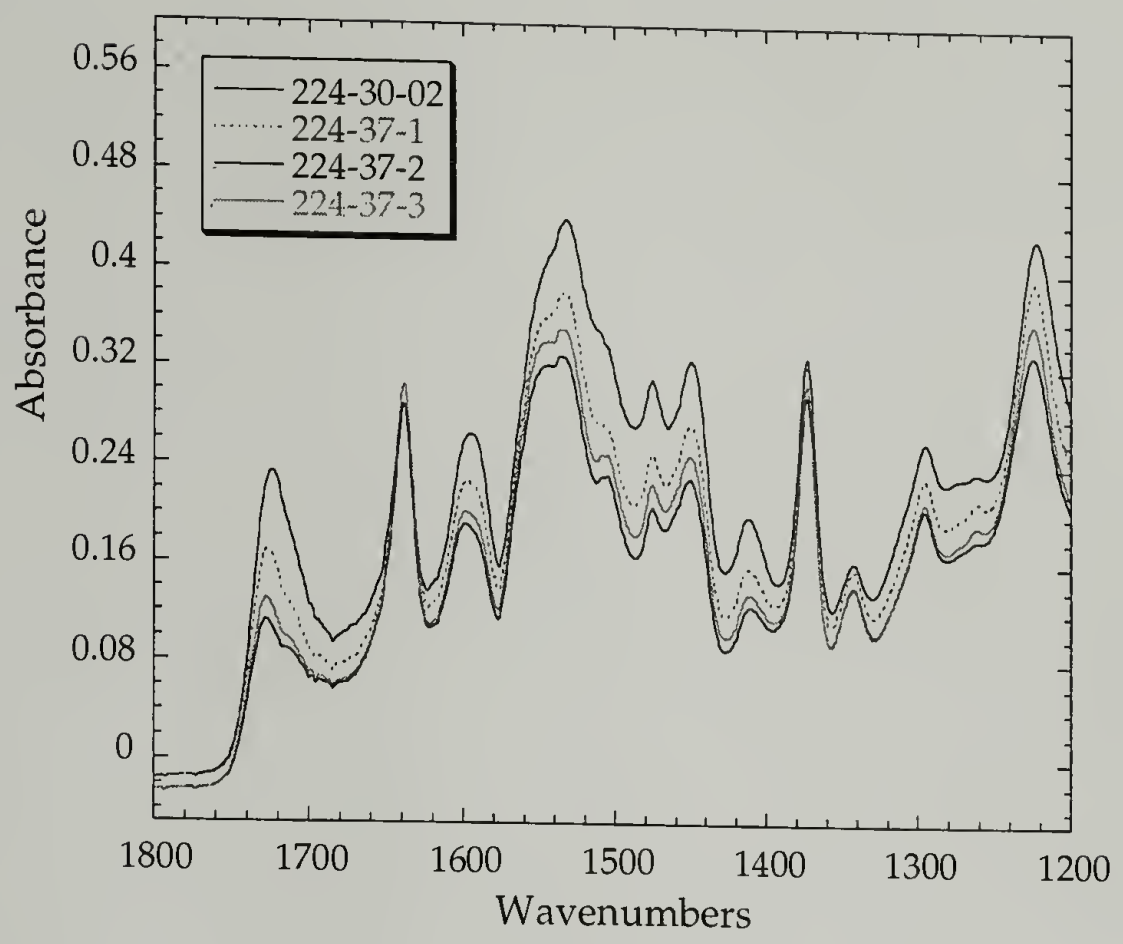

(A)

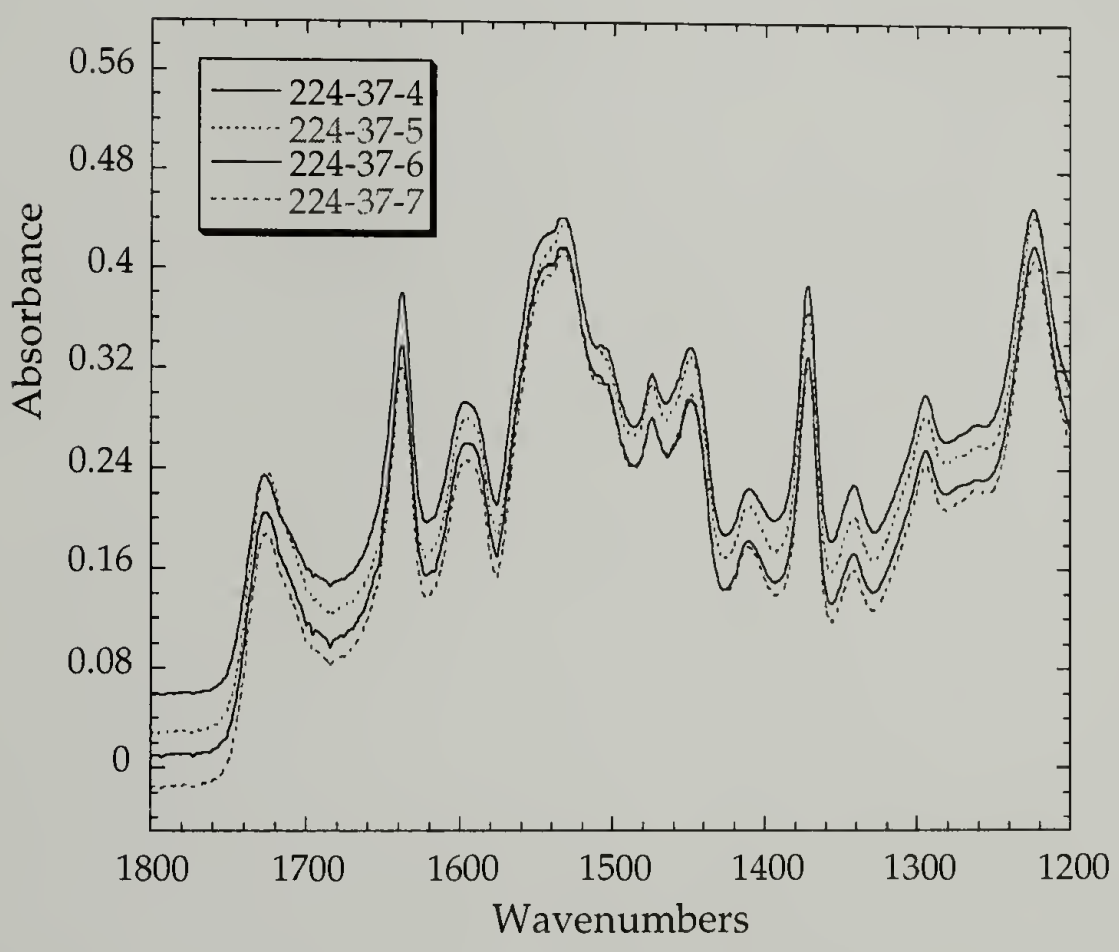

(B)

Figure 2.7. ATR-FTIR spectra of foam samples

4) The order of the degree of phase separation should be

Poorest 30-02 < 37-5 < 37-1, 37-6, 37-7 < 37-4 < 37-1, 37-2 Best

5) All these foam samples showed evidence of residual unreacted isocyanate.

It is interesting to note that the degree of phase separation in these foams was directly related to the isocyanate index in the formulation. Therefore using ATR-FTIR is a powerful and convenient tool to characterize phase separation in foam and plaque samples.

2.2.3. Infrared Dichroic Measurement

The infrared dichroic measurement was made on the Bruker IFS-113v FTIR spectrometer equipped with a liquid nitrogen cooled mercury-cadimium-telluride (MCT) detector. The principles of this method will be covered in Chapter 4. Thin film samples were stretched with a hand uniaxial stretcher at 10% strain intervals. The whole deformation process could be followed by this means. The polarized infrared source is obtained by using a polarizer from Graseby Specac of CPS Products Div. The parallel and perpendicular spectra were collected 5 ~ 10 minutes after the sample was stretched. It is assumed that after such a period of time the stress relaxation of the sample was close to the steady state. The changes in the sample thickness during elongation were normalized against the structural absorbance in the C-H stretching region for the soft matrix.

2.2.4. Deuterium Substitution

For D_2O vapor sorption studies, a special cell with CaF_2 windows was built to fit in the spectrometer for *in situ* infrared measurements. The relative humidity of D_2O inside the cell was controlled by a saturated sodium chloride solution. A constant flow of dried nitrogen gas bubbled through two serially connected bubble tubes filled with sodium chloride saturated D_2O solution before transferring into the cell to deliver D_2O onto the thin film. A heating apparatus built inside the cell was used for deuterium substitution studies at elevated temperatures.

2.2.5. Stress Relaxation

The viscoelastic properties of phase separated polyurethane can be studied using stress relaxation. A stress relaxation apparatus was designed and built. This apparatus was made to fit in the spectrometer for *in situ* infrared measurement. The initial strain is set for the sample before stretching. A small motor is used to stretch the sample at constant strain rate to reach initial strain at 20%. The stress relaxation results were recorded in the computer.

The swelling stress experiment is conducted as follows: A dry sample was stretched at certain strain in the stress relaxation apparatus. During the dry stage of stress relaxation, a dry air purge is used to dry the surface of the sample and prevent moisture uptake. After the film reaches an apparent equilibrium stress for 5 hours, the water vapor carried by the same air source is introduced into the chamber. The stress was found to decay and the transient stress data were recorded in the computer using a data acqusition

software from LabView. The desorption experiment was conducted by purging the "wet" sample using the dry air immediately following moisture plasticization.

The swelling stress experiment was combined with deuterium substitution studies, allowing *in-situ* water plasticization studies to be conducted. Using D_2O for plasticization provides direct evidence of large distortions of hard domains under plasticization. D_2O as a marker indicates where water reaches in the specific regions of the hard domain.

2.2.6. Others

Mechanical properties were tested on an Instron 4468 Univeral Testing System. Tensile bars were cut with a die of ASTM D-1708-84 for microtensile test specimen. The strain rate was 1.0 mm/min. The stress-strain behavior for plaque samples were obtained as shown in Figures 2.8-2.9.

The modulus results listed in Table 2.2 represent the initial tangent modulus. Samples made at lower temperature and larger volume fraction of hard domain have much higher strengths. Rubbers and elastomers are normally found in the 2-3 MPa range at 100% elongation. [32,33]

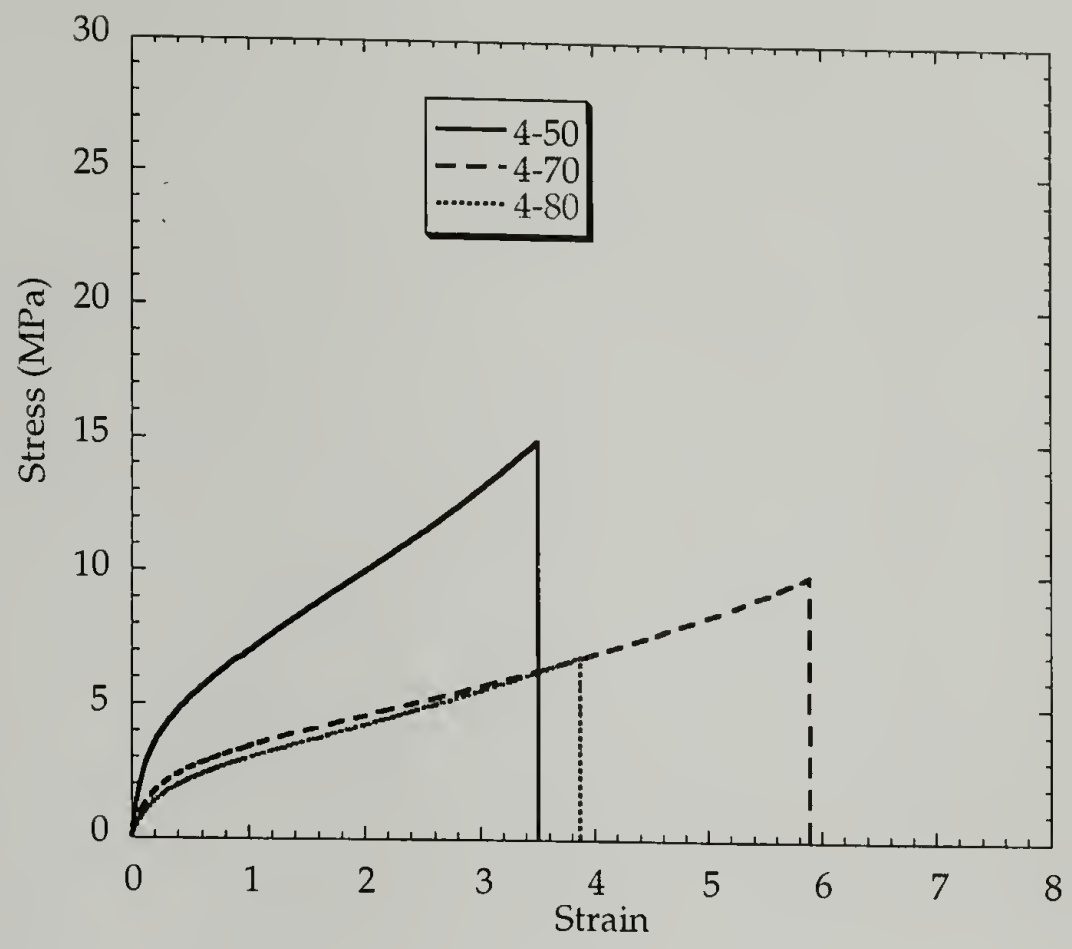

Figure 2.8. Mechanical properties of 4-urea series samples

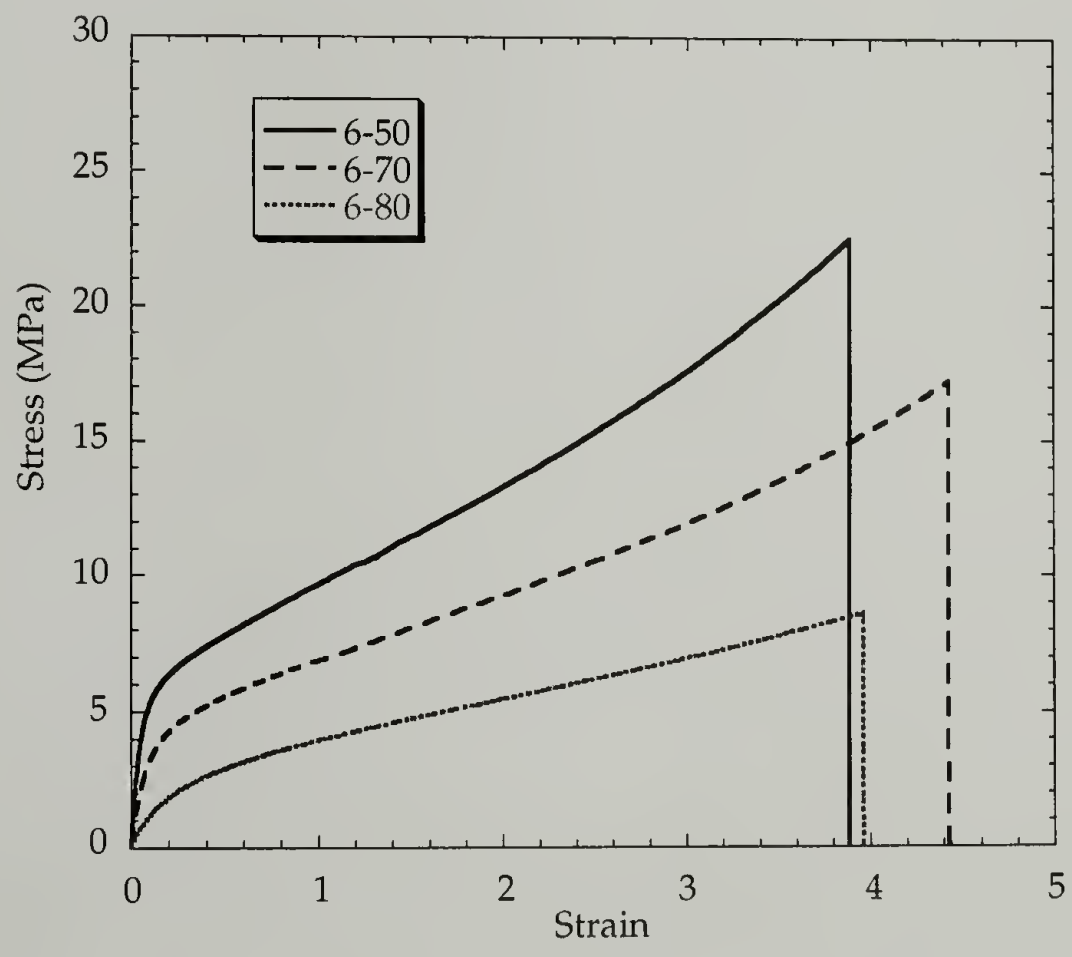

Figure 2.9. Mechanical properties of 6-urea series samples

Table 2.2. Mechanical Properties of Polyurethane Plaques Made at Different Temperatures

	Modulus (MPa)	Tensile Strength at 100% Strain (MPa)	Elongation (%)
4-50	38	7.1	351
6-50	100	9.8	338
4-70	14	3.3	588
6-70	51	6.8	453
4-80	11	3.0	463
6-80	17	4.5	267

Other characterization techniques include optical microscopy, thermal analysis techniques (DSC and TGA), SEM, SAXS, and rheometric measurements. Optical microscopy was performed in reflection mode using an Olympus BX60 microscope. The glass transition temperature was measured with a Perkin Elmer DSC 7 Differential Scanning Calorimeter. The TGA analysis was conducted with a TGA 2050 Thermogravimetric Analyzer from TA Instruments, Inc. The viscosity measurement was performed on the Advanced Rheometric Expansion System (ARES) from Rheometric Scientific, Inc. Small angle X-ray scattering (SAXS) of the polyurethane samples has also been attempted for the study of phase separation. It was, however, found that for slabstock foam sample, there was no periodicity peak in the scattering profile, which indicated a broad distribution of domain structures in the phase separated morphology and poor correlation between domains.

2.3. References

1) Herrington, R.; Hock, K. *Flexible Polyurethane Foams*; 2 ed.; The Dow Chemical Company: Midland, **1997**.

2) Suen, W.; Percy, J.; Hsu, S. L. *In Preparation* **2000**.

3) Garrett, J. T.; Runt, J.; Lin, J. S. *Macromolecules* **2000**, *33*, 6353-6359.

4) Coleman, M. M.; Sobkowiak, M.; Pehlert, G. J.; Painter, P. C.; Iqbal, T. *Macromol. Chem. Phys.* **1997**, *198*, 117-136.

5) McClusky, J. V.; Priester, R. D., Jr.; O'Neill, R. E.; Willkomm, W. R.; Heaney, M. D.; Capel, M. A. *J. Cell. Plast.* **1994**, *30*, 338-360.

6) Bailey, F. E. J.; Critchfield, F. E. *J. Cell. Plast.* **1981**, *17*, 333-339.

7) Neff, R.; Macosko, C. W. *A Model for Modulus Development in Flexible Polyurethane Foam*: Chicago, IL, **1995**, pp 344-352.

8) Hostettler, F.; Cox, E. F. *Ind. Eng. Chem.* **1960**, *52*, 609-610.

9) Wong, S.-W.; Frisch, K. C. *J. Polym. Sci. Part A: Polym. Chem. Ed.* **1986**, *24*, 2867-2875.

10) Malwitz, N.; Wong, S. W.; Frisch, K. C.; Manis, P. A. *J. Cell. Plast.* **1987**, *23*, 461-502.

11) Listemann, M. L.; Savoca, A. C.; Wressell, A. L. *J. Cell. Plast.* **1992**, *28*, 360-398.

12) Sojecki, R.; Trzcinski, S. *Eur. Polym. J.* **1998**, *34*, 1793-1799.

13) Sojecki, R. *Acta Polym.* **1992**, *43*, 96-98.

14) Sojecki, R. *Acta Polym.* **1991**, *42*, 411-414.

15) Sojecki, R. *Acta Polym.* **1991**, *41*, 518-520.

16) Sojecki, R. *Acta Polym.* **1989**, *40*, 487-492.

17) Sojecki, R. *Eur. Polym. J.* **1994**, *30*, 725-729.

18) Farkas, A.; Flynn, K. G. *J. Am. Chem. Soc.* **1960**, *82*, 642-645.

19) Goring, D. A. I. *Lignin: Properties and Materials*; Glasser, W. G. and Sarkanen, S., Ed.; American Chemical Society: Toronto, Ontario, Canada, **1988**; Vol. 397, pp 1-10.

20) Robinson, P., Personal Communication.

21) Wang, J.; St. John Manley, R.; Feldman, D. *Prog. Polym. Sci.* **1992**, *17*, 611-646.

22) Stephanou, A.; Pizzi, A. *Holzforschung* **1993**, *47*, 439-445.

23) Chen, R.; Wu, Q. *J. Appl. Polym. Sci.* **1994**, *52*, 437-443.

24) Rosch, J.; Mulhaupt, R. *Polym. Bull.* **1994**, *32*, 361-365.

25) Wilkinson, S. L. *C & EN News* **2001**, *79*, 61-62.

26) Hatakeyama, H.; Hirose, S.; Hatakeyama, T. *J. Macro. Sci.-Pure Appl. Chem.* **1995**, *A32*, 743-750.

27) Yoshida, H.; Morck, R.; Kringstad, K. P.; Hatakeyama, H. *J. Appl. Polym. Sci.* **1987**, *34*, 1187-1198.

28) Yontz, D. J. *An Analysis of Molecular Parameters Governing Phase Seperation in a Reacting Polyurethane System*; University of Massachusetts: Amherst, MA, **1999**, pp 329.

29) Creswick, M. W.; Lee, K. D.; Turner, R. B.; Huber, L. M. *J. Elast. Plast.* **1989**, *21*, 179-96.

30) Wu, X.; Hsu, S. L. *PMSE Preprints* **2000**, *82*, 369.

31) Colthup, N. B.; Daly, L. H.; Wiberly, S. E. *Introduction to Infrared and Raman Spectroscopy*; 3rd ed.; Academic Press, Inc.: Boston, **1990**.

32) Mullins, L.; Tobin, N. R. *Journal of Applied Polymer Science* **1965**, *9*, 2993-3009.

33) Medalia, A. I. *Rubber Chemistry and Technology* **1973**, *46*, 877-896.

CHAPTER III

MORPHOLOGICAL CHARACTERIZATION OF THE INTERCONNECTING PHASE SEPARATED POLYURETHANE

3.1. Chapter Review

In Chapter 3, the interconnecting hard domain morphology is studied using deuterium substitution. The motivation of this investigation is to obtain a more accurate morphological picture that can help understand the physical properties of polyurethanes and design the morphology for better properties. In Section 3.1, several studies are described that validate deuterium substitution, including model compounds, foam kinetics, and low temperature measurement, to understand the morphological features of the hard domain structure, and the specific band assignments for the Amide I and II regions. The deuterium substitution studies on different morphological samples are covered in Section 3.2. The bulk of the hard domain, the disordered hard domain, and the surface of the hard domain have been quantitatively characterized. Based upon the percolation theory, above 16% volume fraction of the hard domain can form interlocking morphology. [1] The volume fraction of our system is well above this value and thus it is reasonable to have interconnecting hard domain morphology. The disordered hard domain plays an important role as interfacial region to interconnect the bulk hard domains or between hard domain and soft matrix. This supports the interconnecting morphological view in which the domains are bridged through either the disordered hard domain or directly by long hard segment bridges. The soft segments constrained in these disordered hard domains increases the effective volume fraction of the hard domain, and

this leads to an increase in the modulus of the material. The decrease in the modulus for the samples made at higher temperatures is attributed to an increase in the degree of phase mixing morphology and an attendant decrease of the size of the interconnecting region for the higher temperature samples. The above conclusion will be evaluated through the analysis of the data obtained from three different morphologies generated at different reaction temperatures.

3.2. Band Assignments and Deuteration Studies

3.2.1. Different temperature samples

The spectra of three thin films made isothermally at 50, 70 and 80 °C are shown in Figures 3.1(a)-(b). The spectra were normalized to the intensity of the most intense band in the C-H stretching region between 3010 and 2700 cm^{-1}. From previous studies, the samples reacted at lower temperature exhibit larger ordered domains and more complete phase separation. [2,3] Qualitatively, the degree of phase separation was less for the samples made at higher temperatures. The sample made at 50 °C had the best phase separated morphology, as indicated by the sharp amide I band of bidentated urea at 1640 cm^{-1} as shown in Figure 3.2. [4-10] The lower intensity of 1640 cm^{-1} and higher intensity at around 1670 cm^{-1} suggested the higher degree of phase mixing for the high temperature

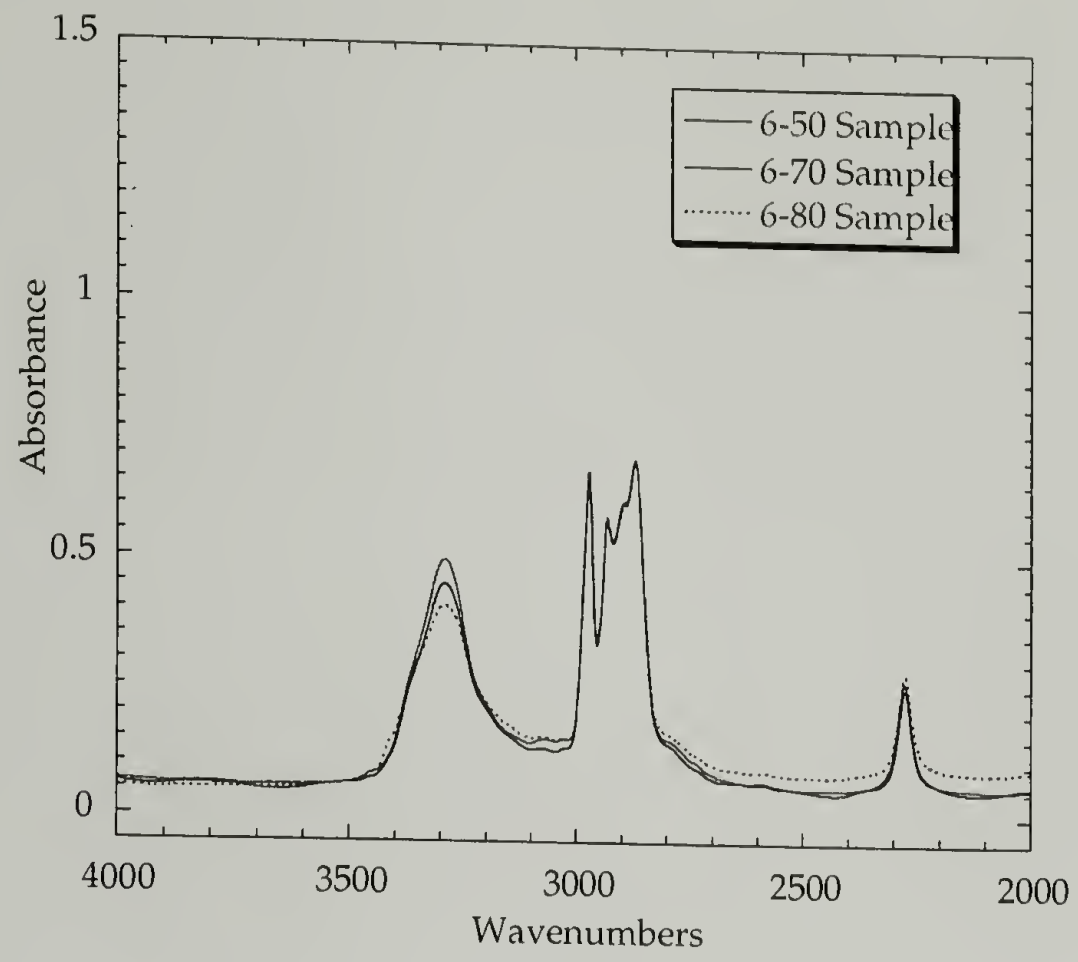

(A)

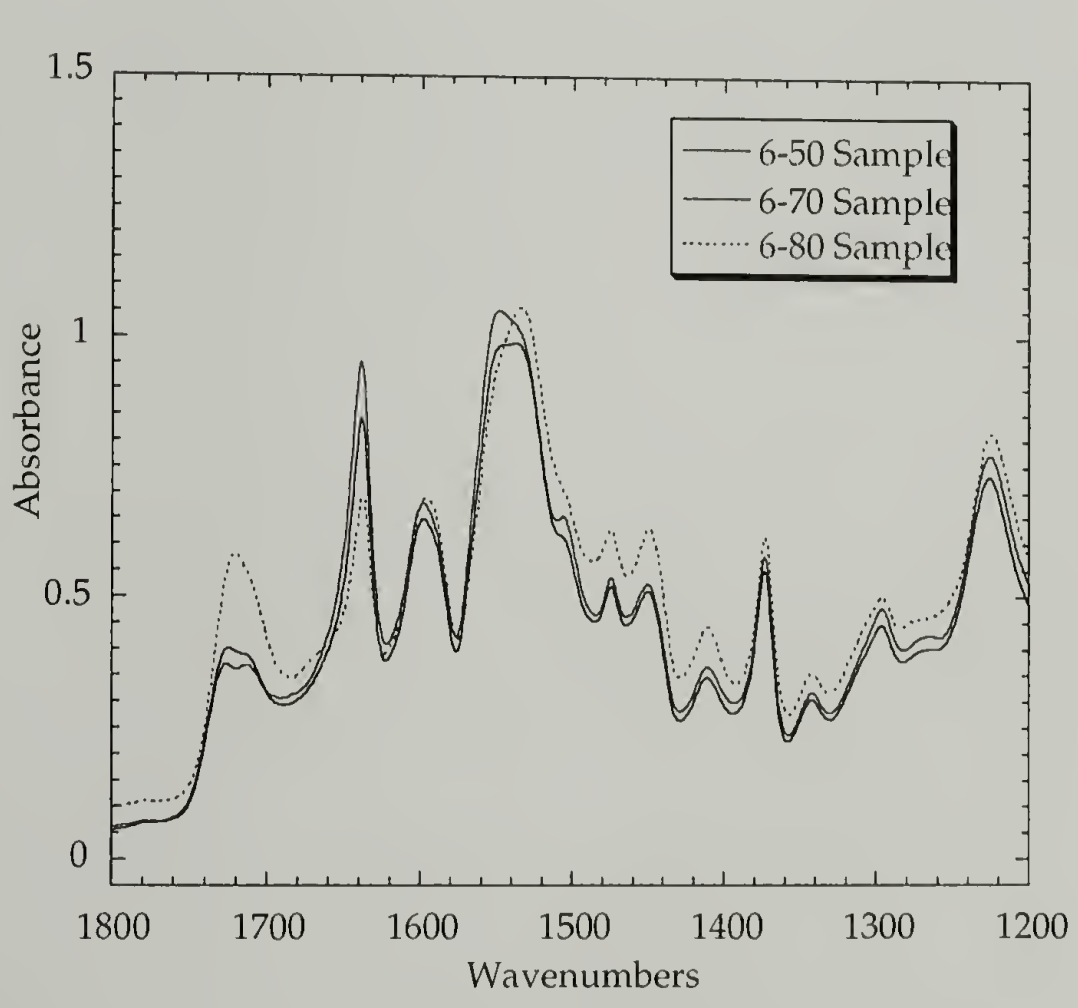

(B)

Figure 3.1. FTIR spectra of polyurethane 6-urea samples

temperature sample. The intensity of the N-H stretching band was extremely sensitive to the strength of hydrogen bonds formed. [11-14] In the N-H stretching region, a sample prepared at 80 °C showed the least integrated intensity, indicating the poorest hydrogen bonding in the sample and highest degree of phase mixing of the three. In addition, there

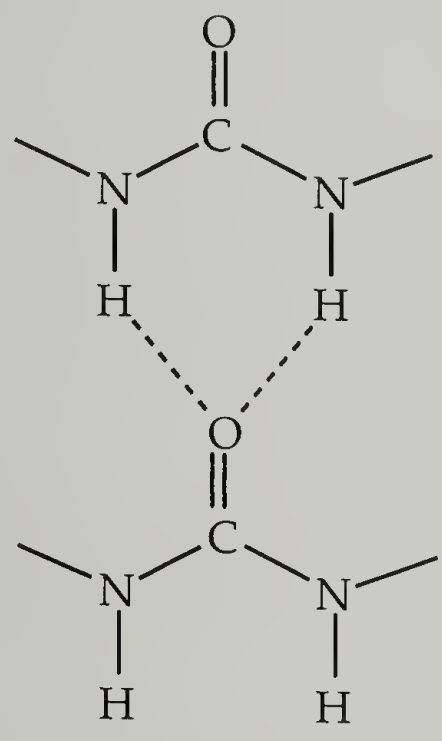

Figure 3.2. Chemical structure of bidentate urea

was a small shoulder at 3410 cm^{-1} for the 80 °C sample which is associated with the N-H stretching in the absence of hydrogen bonding. In the urethane amide I region between 1730 and 1710 cm^{-1}, two distinct bands can be observed for the non-hydrogen bonded and hydrogen bonded urethane carbonyl stretching bands in the 50 °C sample. In the spectrum of the sample made at 80 °C, there was one broad band at 1720 cm^{-1}. This showed a trend of higher degree of phase mixing for the samples prepared at higher temperatures. The spectroscopic differences were characterisitc of the different sample morphology as expected. [2,3]

3.2.2. Band assignments of Amide vibration regions

There have been many infrared studies of various polyurethane materials. [4,15-24] In order to validate the use of deuterium substitution, the model compound 1,3-diphenyl urea before and after substitution was studied as shown in Figures 3.3(a)-(b). It is interesting to note that for crystalline 1,3-diphenyl urea soaked in D_2O, deuterium substitution hardly took place. After the crystal was dissolved in dried acetone, deuterium substitution was fast upon exposure to D_2O. The N-H stretching, amide I, phenyl ring, amide II and amide III regions were all sensitive to deuteration. The N-H stretching band decreased and the water band from the substitution product increased, while the N-D stretching band appeared in the 2400-2500 cm^{-1} region. Amide I band shifted from 1648 cm^{-1} to 1634 cm^{-1}. The decrease of ring vibration at 1600 cm^{-1} suggested that it was not a pure ring vibration mode and it contained a contribution of N-H bending component. [25] But the direct quantitative indication was from the Amide II, as suggested by several authors. [26-29] The N-D in plane bending vibration appeared at 1467 cm^{-1}.

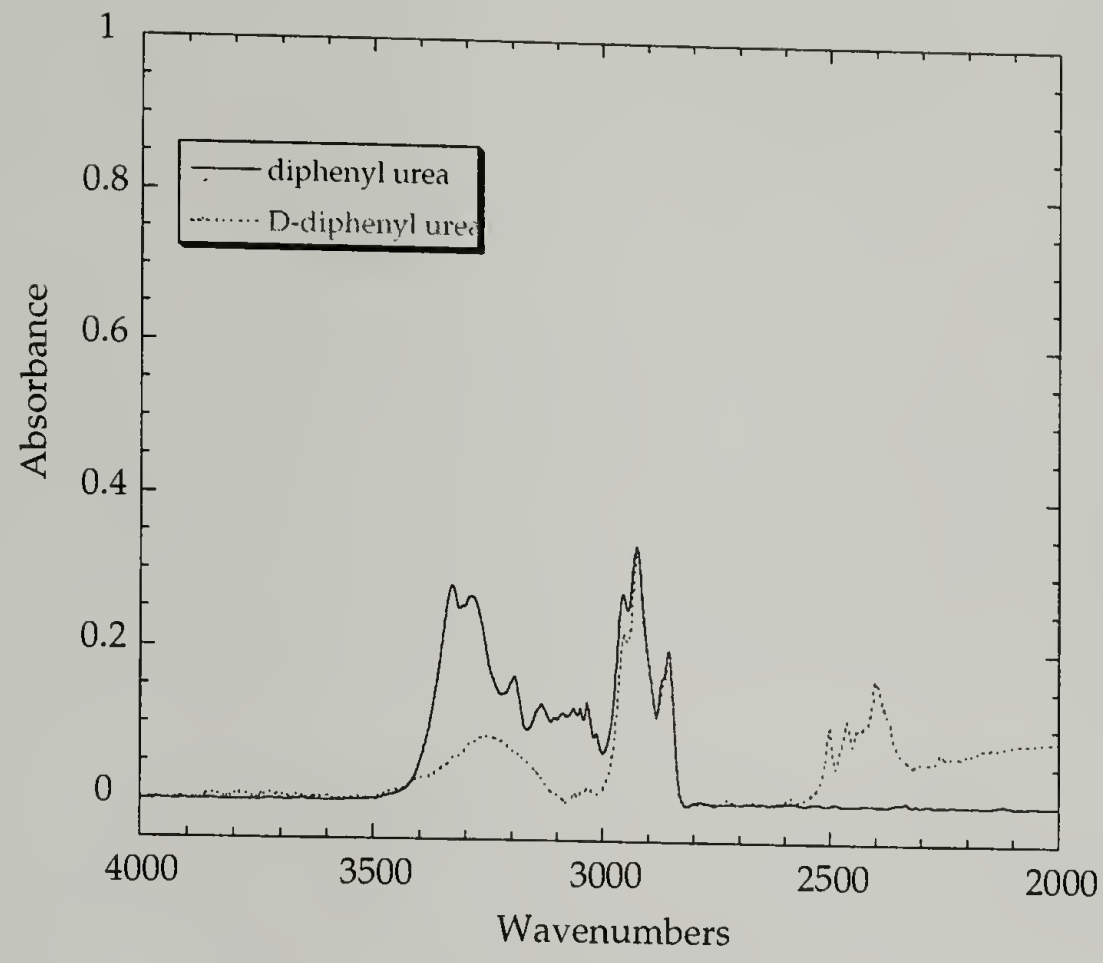

(A)

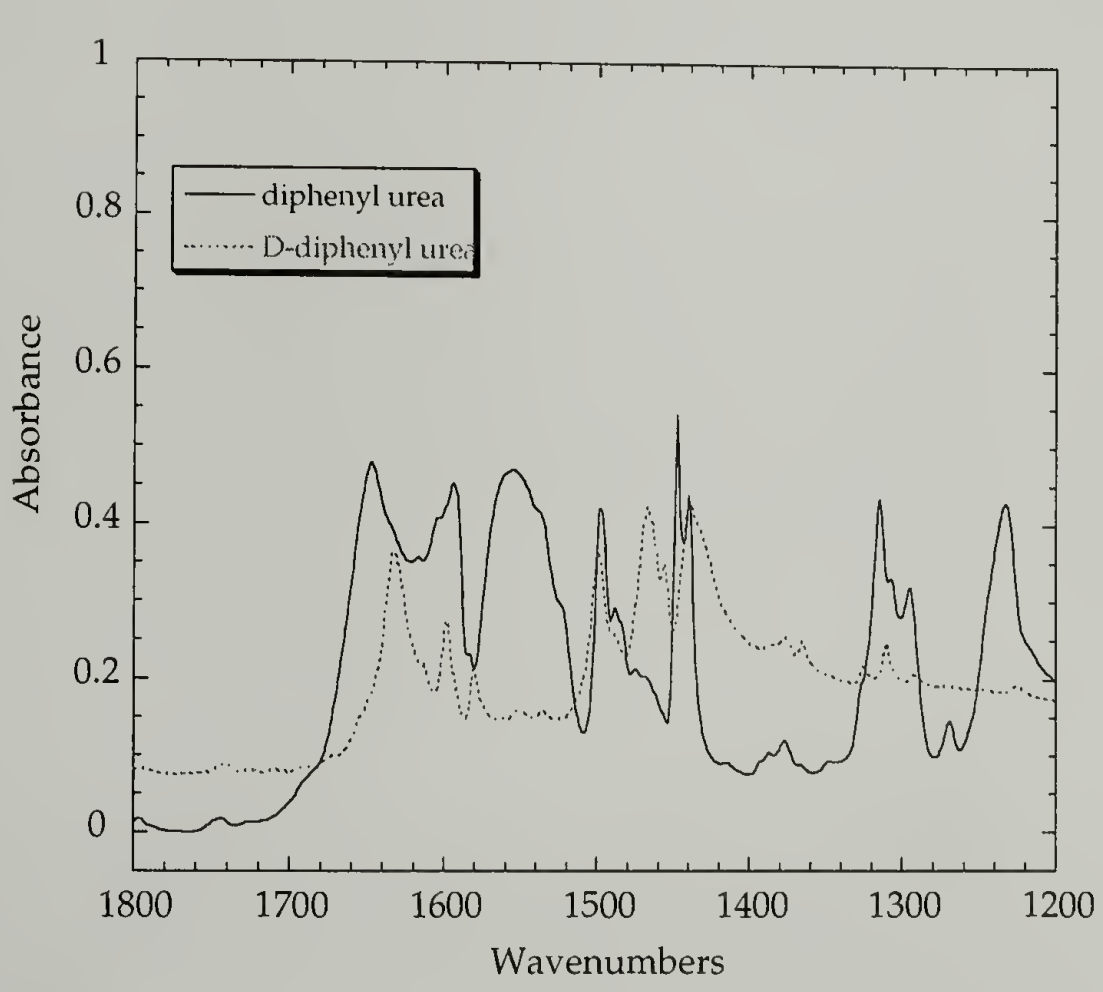

(B)

Figure 3.3(b). FTIR spectra of model compound 1,3-diphenyl urea

In order to study the morphological development and help the band assignments using infrared spectroscopy, the foam kinetics at room temperature was simulated using H_2O and D_2O as the chain extender in the foam formulation. Right after the mixing of all the components, infrared spectra of the foaming mixture were collected. The spectra of samples using H_2O as the chain extender are shown in Figures 3.4(a)-(b). It was found that as the polymerization proceeded, the O-H stretching band intensity of hydroxyl groups from water and polyol decreased and at the same time the N-H stretching band increased indicating urea and urethane formation. The band at 2275 cm^{-1} is characteristic of the isocyanate group. The decrease of intensity suggests the reaction kinetics. After 60 minutes almost all the isocyanates were consumed.

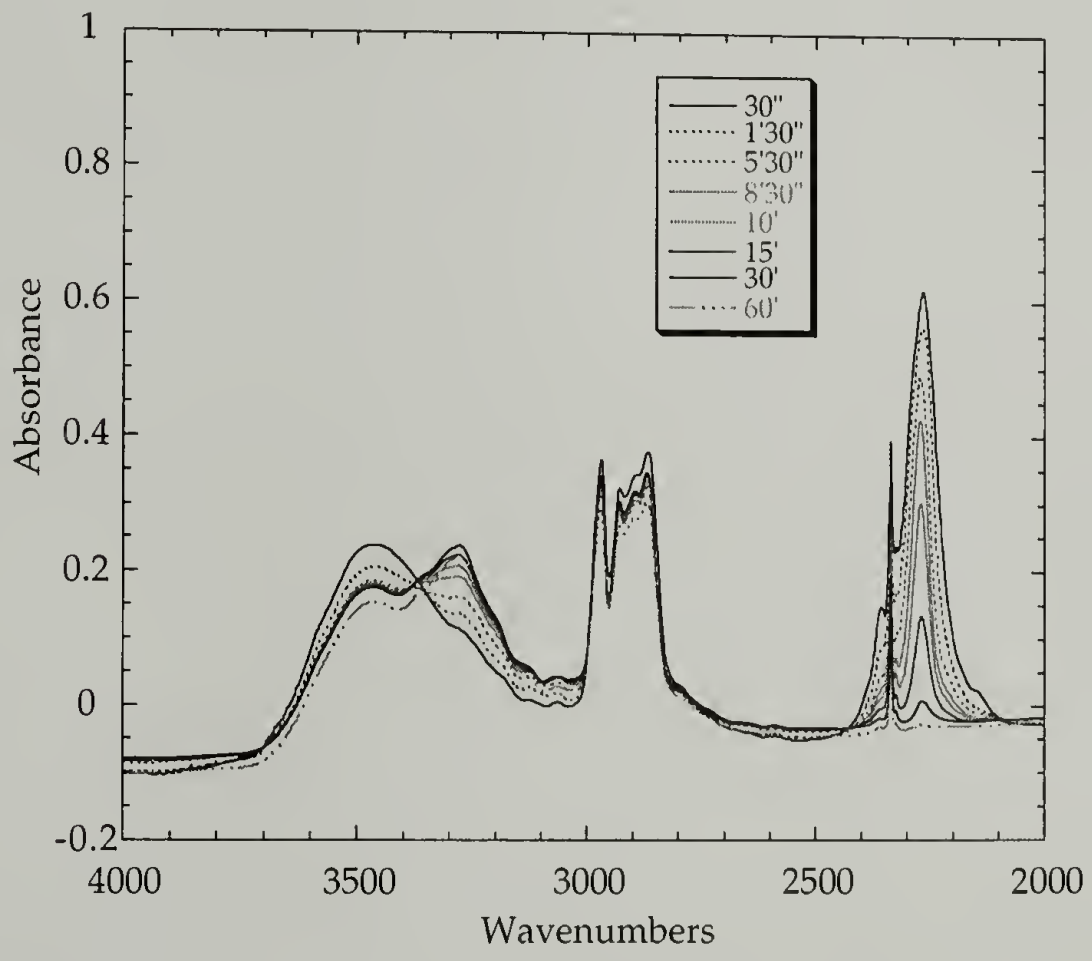

(A)

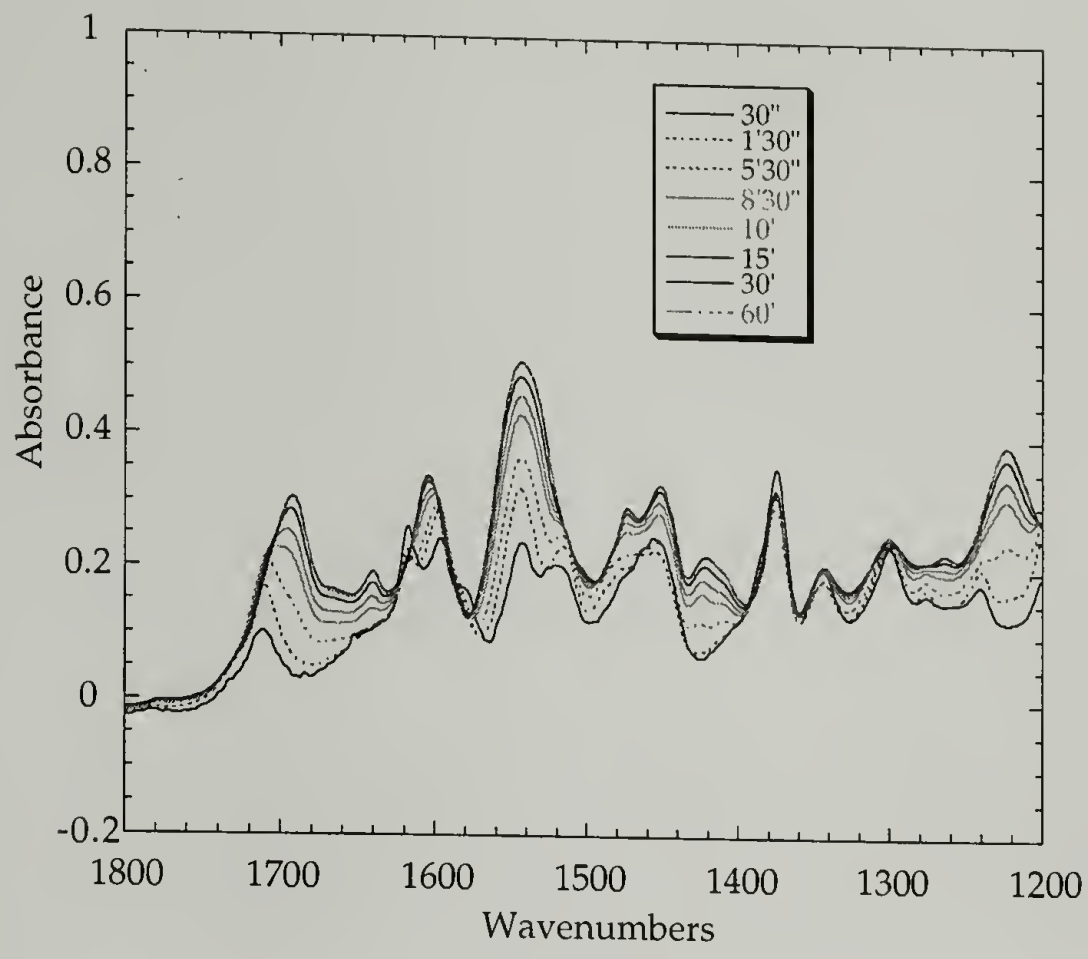

(B)

Figure 3.4. FTIR spectra monitoring the foam kinetics (H_2O as chain extender)

Initially the amide I band of the urethane group appeared at 1710 cm^{-1}, soon after the band moved to lower frequency, suggesting that hydrogen bonding interaction with urea and polyol took place. After 15 minutes the 1640 cm^{-1} band appeared indicating that urea groups started to aggregate and phase separate. It was also found that the band characteristic of phenyl ring of 2,4-TDI including 1617 and 1580 cm^{-1} decreased as reaction proceeded, and simultaneously a new broader band between 1570 and 1500 cm^{-1} was developing along with the urea and urethane groups formed by consumption of isocyanate.

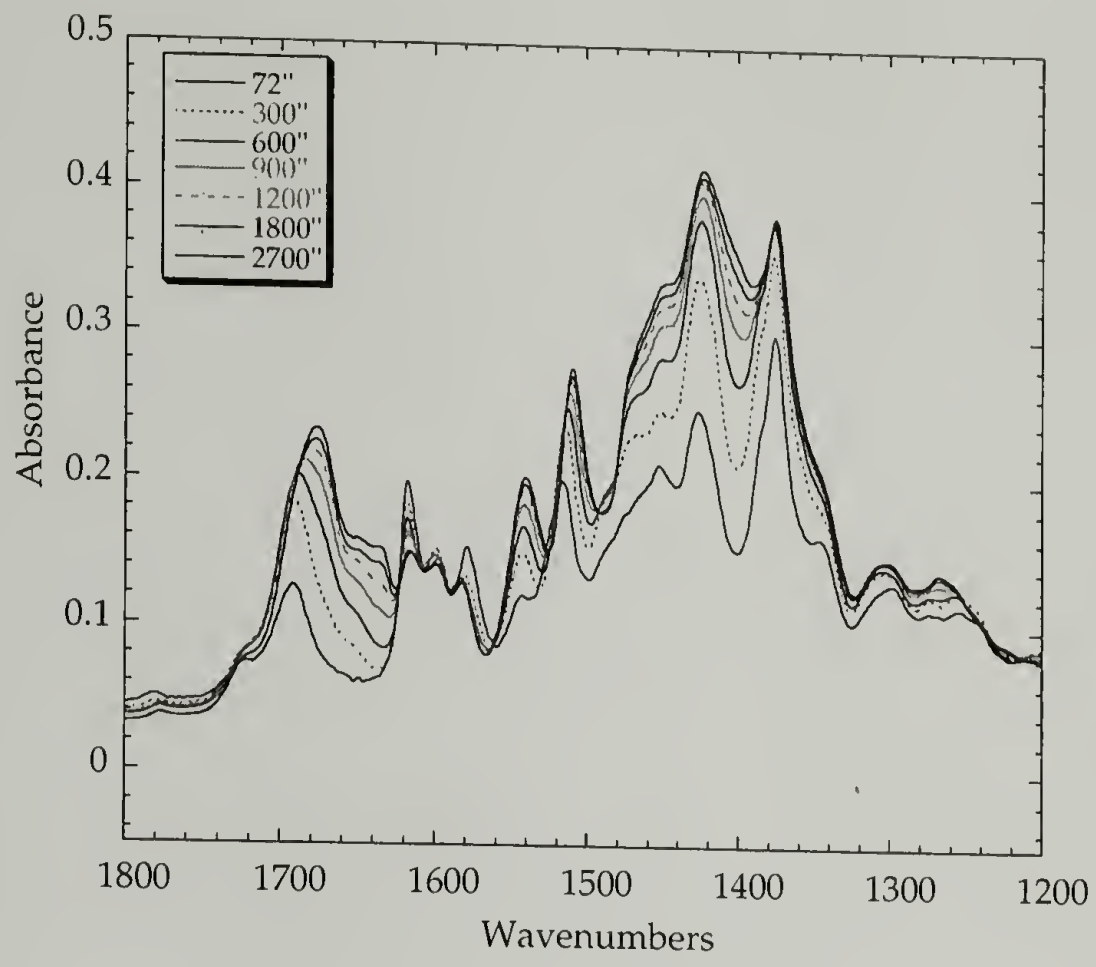

Figure 3.5. FTIR spectra monitoring the foam kinetics (D_2O as chain extender)

D_2O was then used as the chain extender as shown in Figure 3.5. The Amide I band for D-urethane group began at 1723 cm^{-1}, and the free D-urea group started at 1692 cm^{-1}. Later after about 15 minutes, a new band started to appear at 1635 cm^{-1}, indicating the D-urea groups started to aggregate and phase separate. The ring vibration showed little change compared with the H-counterpart, and only the characteristic bands of 2,4-TDI decreased.

To further study the amide II region, low temperature measurements were made. Because of different hydrogen bonds formed, some Amide vibrations associated with urethane and urea units were broad and often overlap making definitive observations difficult. [30] By lowering the temperature of the sample, it was possible to increase the

specificity since bands were sharper and easier to differentiate. The spectra obtained at room temperature and low temperature are compared in Figures 3.6(a)-(b). A higher intensity is generally expected at low temperature as shown in C-H stretching region, which was attributed to the stronger interaction of the polymer chains under volume contraction and slower motion at lower temperature. The bands that can be affected by hydrogen bonding would not only have a higher intensity, but also a shift to lower frequency at low temperature. [14] The N-H stretching region moved towards the lower frequency with higher intensity. The same as in all the amide I region where the carbonyl stretching bands shifted towards lower frequency. The amide II region made a higher frequency shift and behaved the same way as hydrogen bonding strength increased

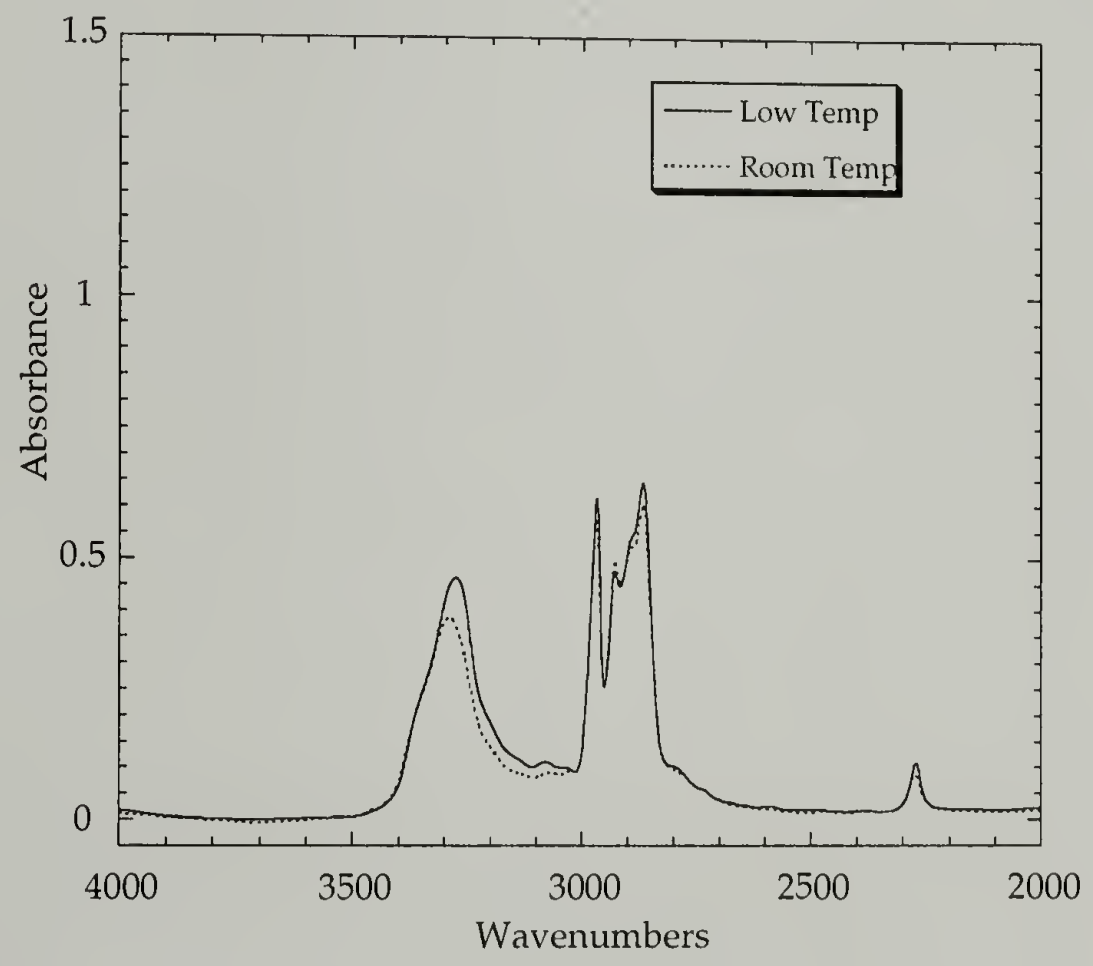

(A)

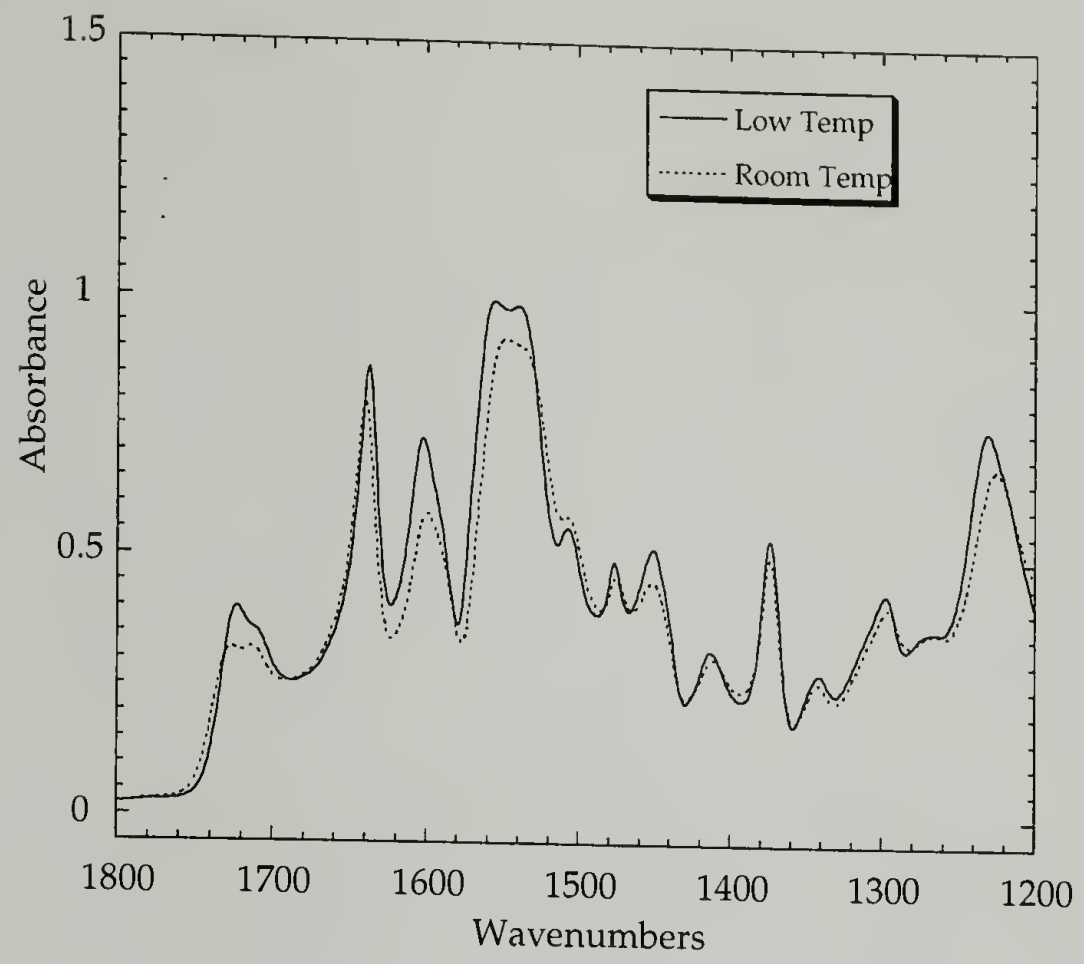

(B)

Figure 3.6. FTIR spectra of cryo-measurement of polyurethane 6-50 sample

at lower temperature. [31] The amide III band at around 1220 cm^{-1} showed a shift to higher frequency. The amide II region showed two distinct peaks at lower temperature. This led to the idea that the hard domain and the urethane groups at the boundary between domains respond differently at lower temperature. The hard domain, which is already in its glassy state at room temperature, would be affected less than would the urethane groups where the Tg is below room temperature. There was only 1 cm^{-1} shift with respect to the bulk ordered hard domain, while 3 cm^{-1} shift occurred for the surface and interfacial region of the hard domain. Lastly, the band at 1508 cm^{-1} showed intensity increase without frequency shift strongly suggesting that this band was associated with the phenyl ring of TDI.

The band assignments for the Amide I region of the polyurethane urea system are summarized in Table 3.1. In the Amide I region (1640-1730 cm^{-1}), there was no shift for the bidentated urea carbonyl stretching 1640 cm^{-1} band upon deuterium substitution,

Table 3.1. Band Assignment of Infrared Carbonyl Stretching (Amide I)

Urethane and urea (cm^{-1})		Deuterated urethane and urea (cm^{-1})	
"Free" urethane	1727	"Free" D-urethane	1723
Loosely associated urethane	1712	Hydrogen bonded D-urethane	~1694
Hydrogen bonded urethane	1700		
"Free" urea	1712	Soluble D-urea	1694
Loosely associated urea	1710, 1670, 1650		
Hydrogen bonded urea, bidendate	1640	Associated D-urea	1635

which indicated that the ordered urea hard domain is inaccessible to D_2O. The "free" urethane carbonyl at 1727 cm^{-1} shifted to 1723 cm^{-1}. Another emerging peak at 1694 cm^{-1} may be attributed to the deuterium substitution response of broad components of disordered urethane and urea groups, including the apparent 1713 cm^{-1} carbonyl peak of the hydrogen bonded urethane group and "free" urea groups. These results were consistent with results reported for similar systems. [4,19,24,32-34]

In the 1600 cm^{-1} region, which is also sensitive to deuterium substitution, [15,16] there were multiple components. The most characteristic band was the C-C stretching band from the phenyl ring. [35] In addition, the N-H bending mode coupled with the ring stretching mode appears in this region. [36] Based upon the foam simulation experiments, there was a clear difference in this region using H_2O and D_2O. Therefore it is consistent with the experimental results that the intensity of the band decreases upon deuterium substitution. However, clear band assignments remain to be made. [37-39]

Coleman, *et al.* [30] reported that the overall character of the amide II band for urethane group is similar to that of the N-H stretching vibration in that there are no obvious separate contributions from ordered and disordered hydrogen bonded domains. Based upon low temperature measurement, deuterium substitution, and infrared dichroism, which will be presented in Chapter 4, a band at 1554 cm^{-1} was assigned to urea groups in the hard domain regions. The hydrogen bonded and " free" urethane groups and the dispersed urea groups depending on the degree of phase mixing are assigned to a broad band at about 1530 cm^{-1}.

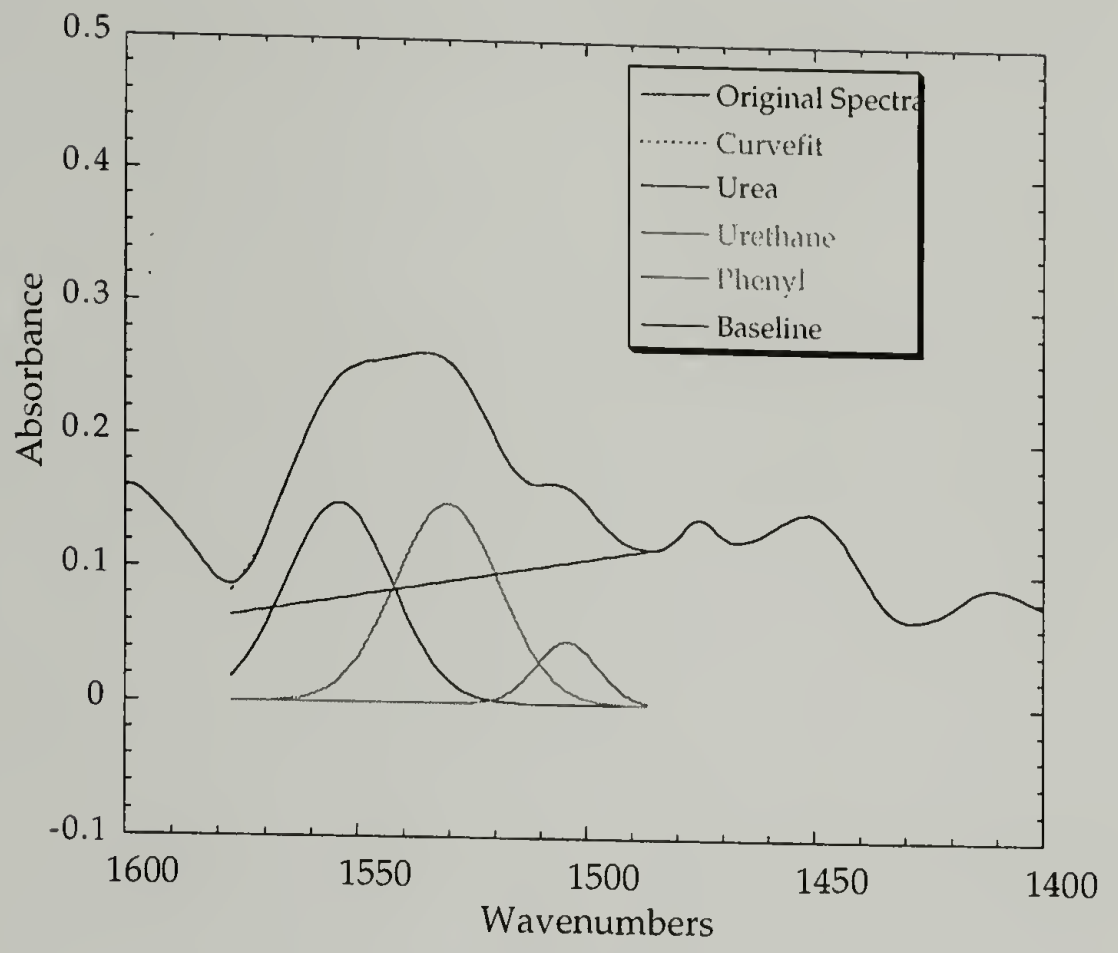

(A) Initial stage

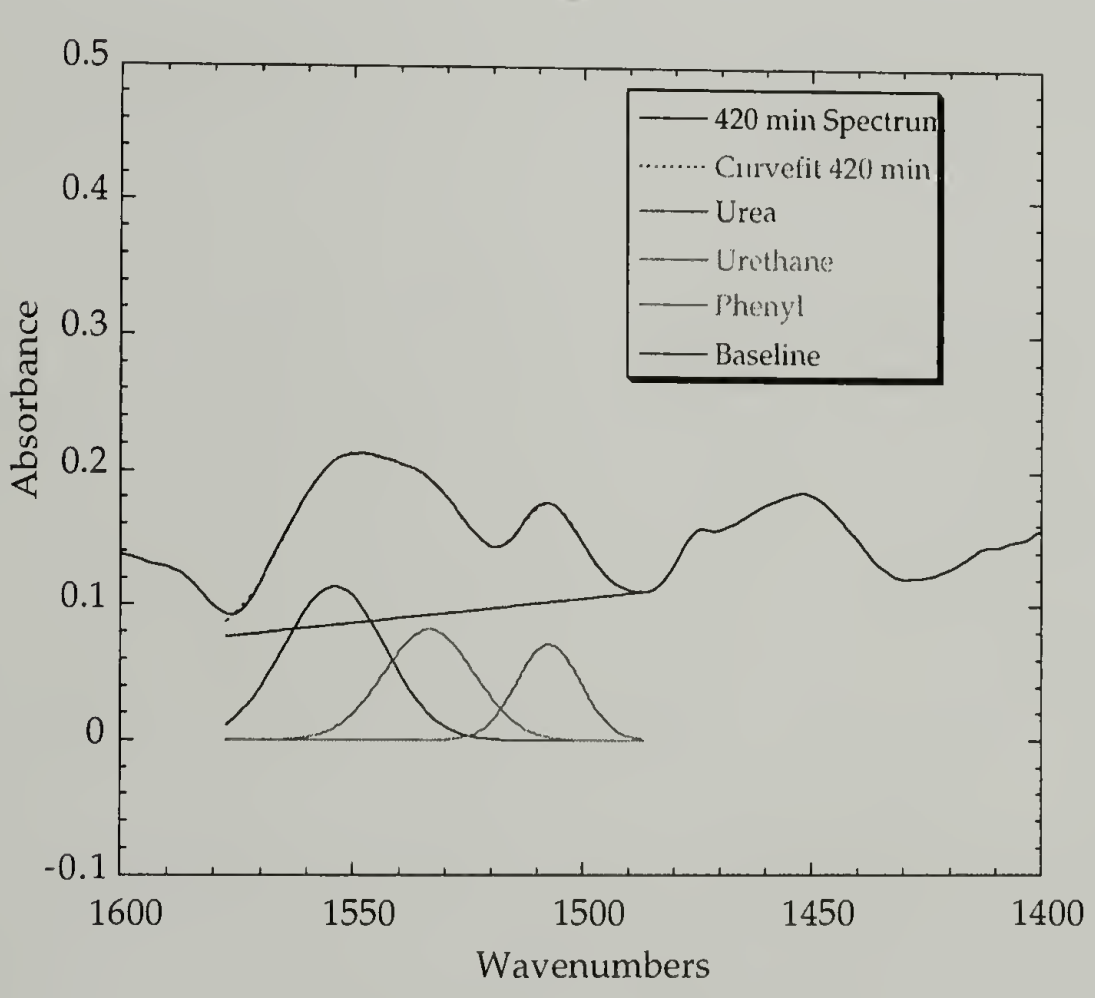

(B) Final Stage

Figure 3.7. Gaussian curve fit for the Amide II region of the 4-50 sample

The fit of the amide II region is demonstrated in Figures 3.7(a)-(b). The fitting region of amide II region between 1577 and 1486 cm^{-1} yield three Gaussian bands representing urea, urethane, and phenyl ring skeletal absorption. The inaccessible urea N-H in-plane bending obtained at a late stage of deuterium substitution indicates the peak position of the hard segment domain is actually at 1554 cm^{-1}. The band at a lower frequency of around 1530 cm^{-1} is mainly associated with the urethane groups at the domain boundary. The 1508 cm^{-1} band is associated with phenyl ring skeletal absorption. [35]

3.3. Deuterium Substitution Studies

Deuterium substitution allowed monitoring the intensities of the spectroscopic features containing contributions of N-H stretching and bending. These features would reduce in intensity and be replaced by new features because of the N-H to N-D substitution. The method is capable only of measuring the hard segments. Based upon the relative accessibility of various urea and urethane groups to D_2O, the concentration of hard segment rich domains, their surfaces, and the relative fraction of dispersed hard segments in the soft segment matrix can be estimated. The urea groups dissolved in the soft matrix are most easily accessed by D_2O. The next most easily accessible region is associated with the urea groups on the surface of the hard domain. It is difficult to differentiate between the dispersed urea groups and those on the hard domain surface. It is easy to imagine, however, that the urea groups most difficult to reach are the ones inside the hard domain. The disordered hard domain or interconnecting region can be accessed at elevated temperature. Unlike urea groups, most urethane groups are located at the surface of the hard domains and the interfacial region, and its deuterium

substitution behavior can therefore be expected to be similar to that of the urea groups on the surface or the interfacial regions.

Several infrared active features can be used to characterize the degree of phase separation and the order within phase separated domains. The Amide vibrations, particularly the Amide II and N-H stretching vibrations are especially useful. Amide II is important because it contains a significant fraction of N-H in-plane-bending contribution. 14

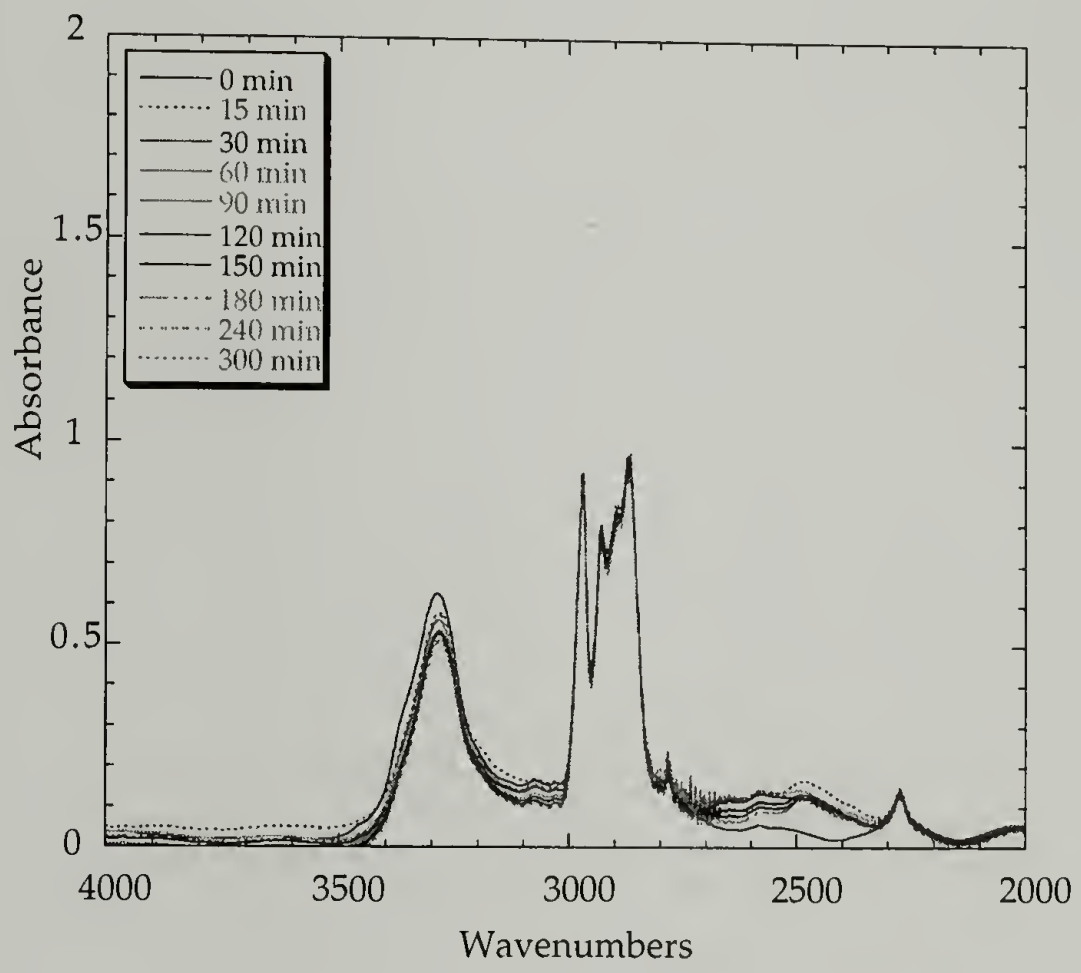

(A)

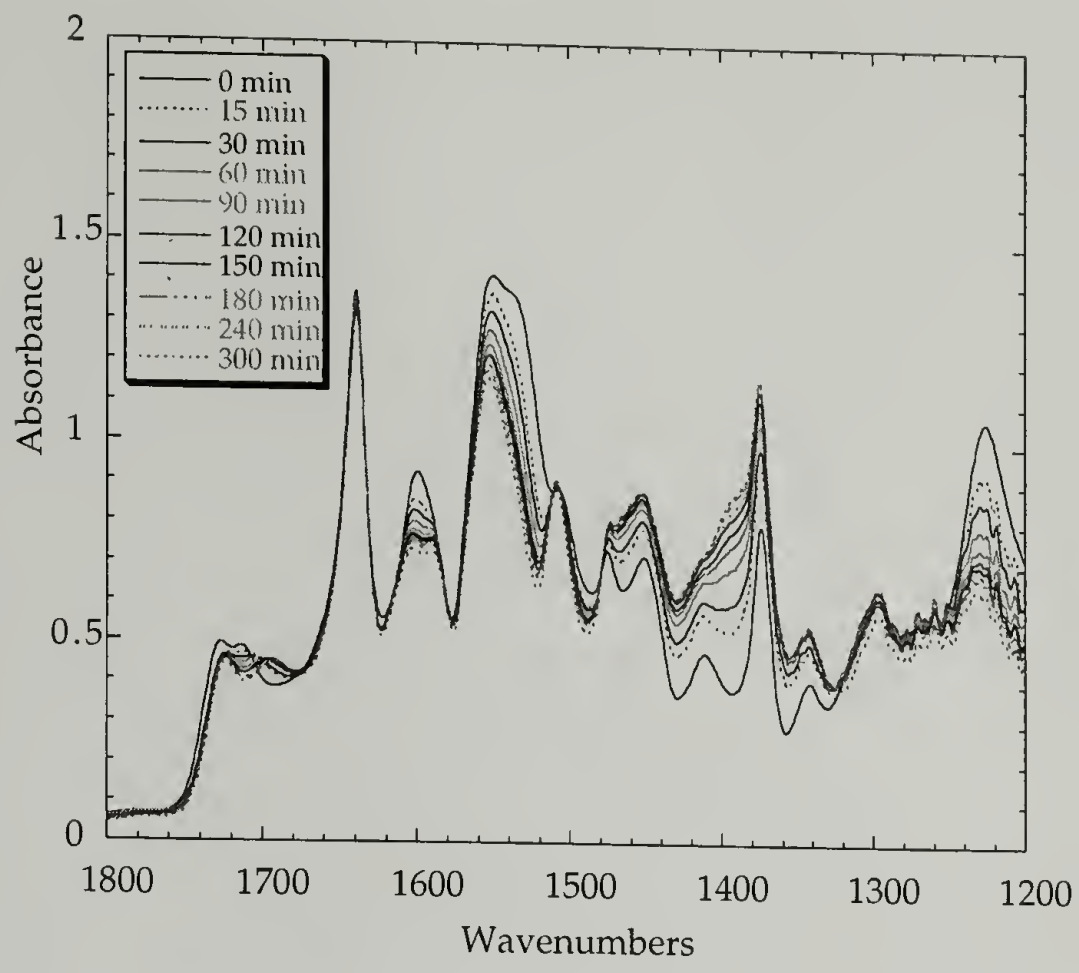

(B)

Figure 3.8. Vapor deuterium substitution of 6-50 sample at room temperature under 75% R. H.

When D_2O was introduced, the changes in the infrared spectrum for the various samples could be quite dramatic as shown in Figures 3.8(a)-(b). Urethane and urea amide I band showed the change as the simulated spectra predicted. The intensities of the Amide II and N-H stretching bands decreased as the deuterium substitution proceeded. The lower component Amide II band at around 1530 cm^{-1} was reduced substantially in intensity. A broad band increase between 1475 and 1320 cm^{-1} was observed. Although the Amide II containing N-D should be shifted to around 1470 cm^{-1}, unfortunately it overlaps the broad absorption of the O-H deformation bands of H_2O or HOD, the exchange reaction products in the thin film. It should also be noted that the intensity of the N-H stretching region decreased with a corresponding increase in the N-D stretching at around 2400-2500 cm^{-1} region. The N-H stretching region was not ideal for

quantitative analysis because the absorption coefficient of this band increases with the increasing hydrogen bonding strength. [11] This region will be discussed in the next section to help understand the hydrogen bonding strength difference in different regions of the hard domain.

The intensity change of two bands in the Amide II region demonstrates the exchange accessibility of the phase separated morphology. The percentage of the inaccessible region can be calculated using Equation 3.1 by the ratio of intensity at the experimental time to the intensity in the initial state as plotted in Figure 3.9.

Equation 3.1. $$\text{Inaccessible urea group} = \frac{\text{Urea intensity at time t}}{\text{Urea intensity at t} = 0} \times 100$$

During the first 60 minutes in Figure 3.9, the intensity of both urea and urethane decreased quickly. The peak intensity of both groups reached a plateau after 240 minutes, indicating that the portion of the hard domain and the urethane groups remained relatively inaccessible to D_2O. For the 6-50 urea sample, the inaccessible region of urea groups was 78%. This demonstrated a large amount of urea groups hidden in the hard domains and the sample maintained a well phase separated morphology.

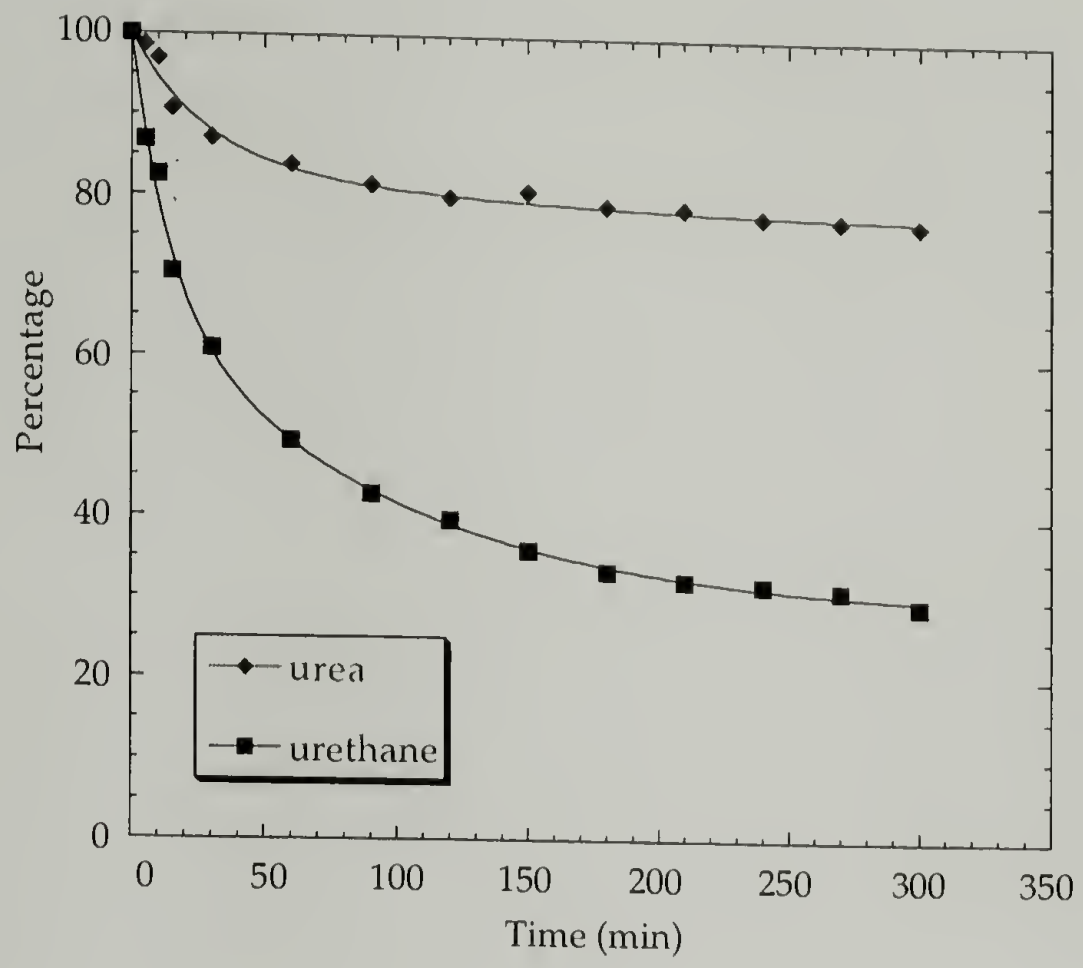

Figure 3.9. Percentage of Inaccessible region of 6-50 sample at room temperature

About 30% of urethane groups were inaccessible at room temperature. The hard segment length distribution was characterized in two samples after hydrolysis and MALDI-TOF analysis. [40] It was revealed that the hard segment length distribution was similar except for the extremely long segments containing eight urea units or more. [40] From the data obtained, it was obvious that hard segments were not all in ordered hard segment rich domains. But the fact that even urethane units could be inaccessible is consistent with the hypothesis that connectivity may exist shielding some of the urethane units. The morphology of this region may be sufficiently ordered to prevent easy D_2O penetration. We changed the D_2O vapor concentration by adjusting the relative humidity in the exchange cell. It was found that the equilibrium state was reached at a different time, but the inaccessible regions for both urea and urethane groups exhibited the same

amount of inaccessible region. These interconnecting regions may be designated as bridges across the hard segment domains.

Table 3.2. Morphological features of urea groups at different regions of the hard domain of polyurethanes made at 50 °C

	Surface	Interfacial/ Interconnecting	Bulk
4-50	28%	20%	52%
6-50	22%	24%	54%

It is found that in the Table 3.2 of deuterium substitution results for the 50 °C samples, the inaccessible region of urea groups was 72% for 4-50 sample. If we assume the shape of the hard domain is similar in 4-50 and 6-50 samples, the domain size R can be roughly compared using the equation $R = V/S$, where V and S are the volume fraction and surface area of the hard domain, respectively. The result was surprisingly high and the hard domain size of 6-50 sample is 59% higher than that of 4-50 sample. This is consistent with the morphological studies previously reported. [2,3] The difference calculated reflects the fact that the volume fraction of the hard domain dominates the difference in morphology.

In order to explore the relatively inaccessible regions further, the deuterium substitution temperature was raised. The same D_2O adsorption experiment was conducted at 45 °C. The temperature was kept below the curing temperature to prevent the sample morphology being perturbed. In this case, the change in the infrared band features was almost the same as that for room temperature, but the exchange reaction proceeded much faster and reached equilibrium earlier as illustrated in Figure 3.10. It is also important to note that at 45°C, the disappearance of the lower component of the Amide II band indicated the surface and interconnecting/interfacial regions have been accessed, and most of the urethane groups or dispersed hard segments have been reached.

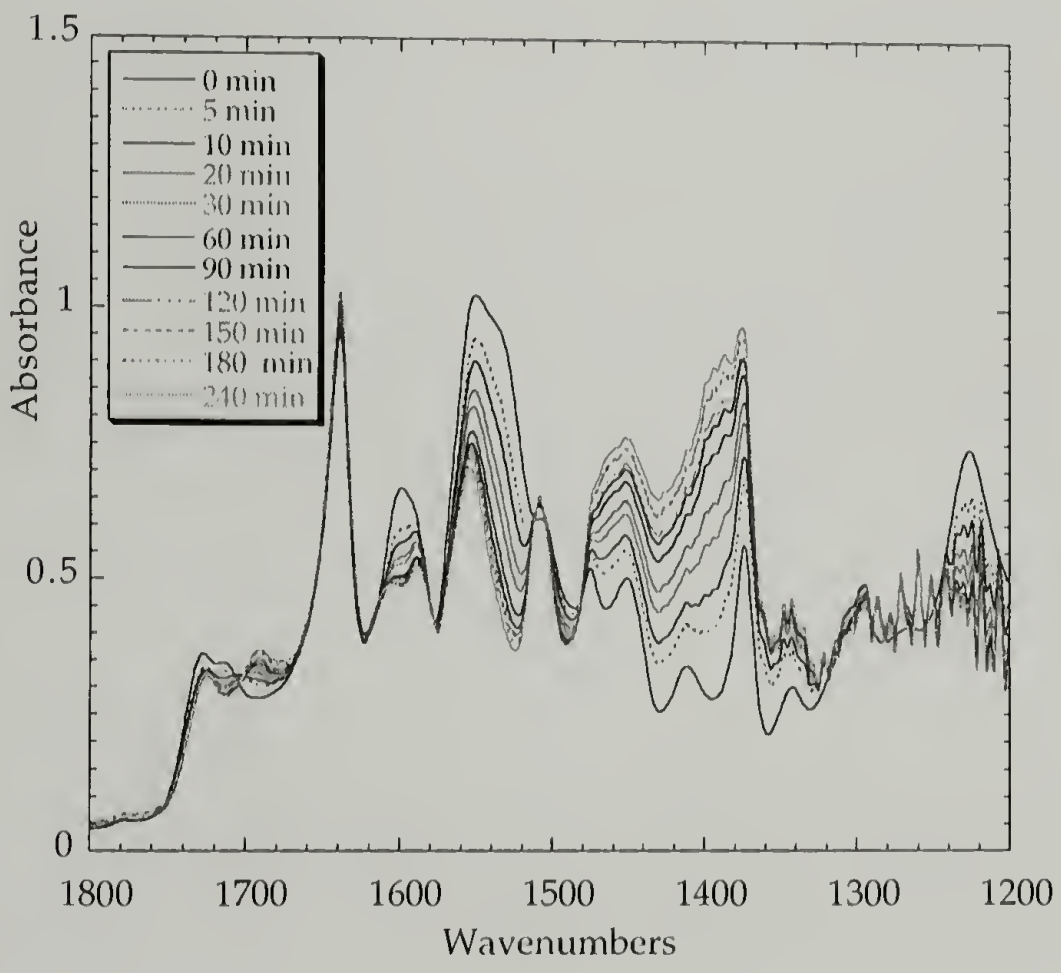

Figure 3.10. Vapor D_2O substitution of 6-50 sample at 45 °C under 75% R. H.

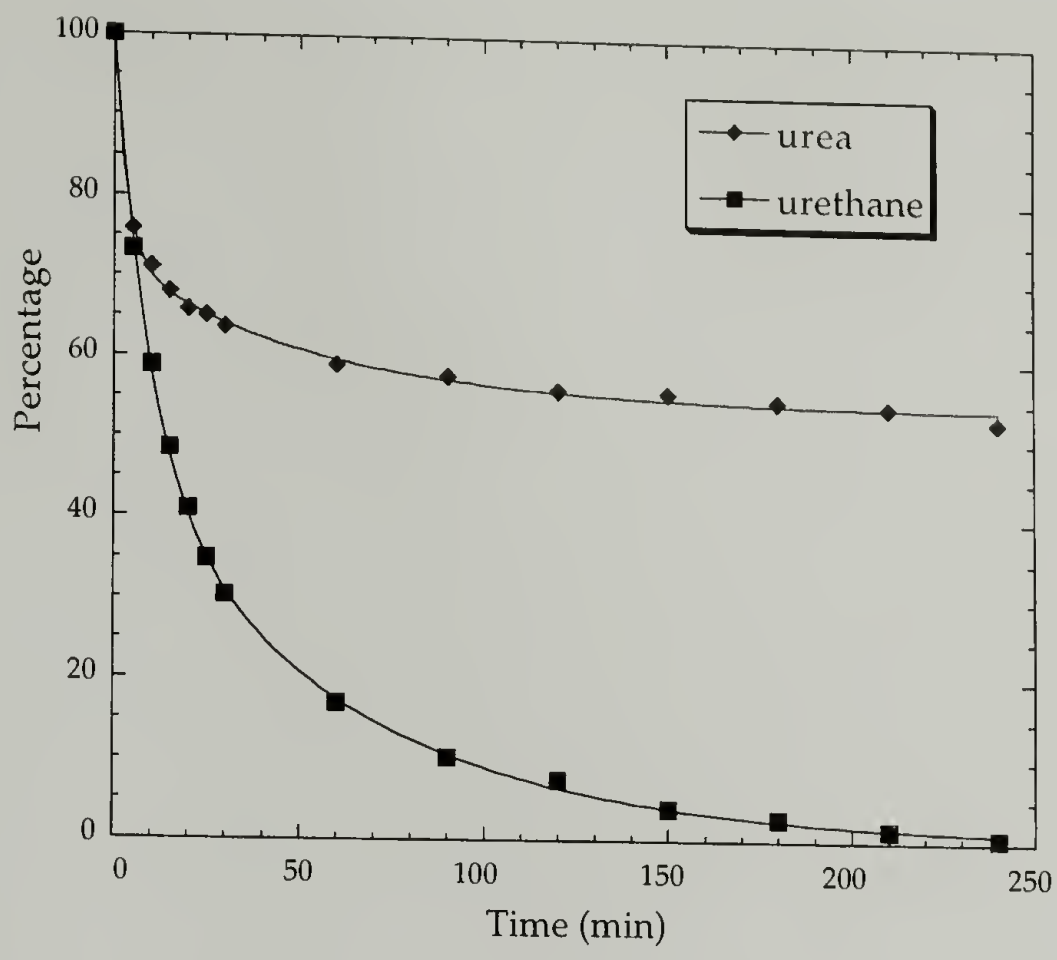

Figure 3.11. Percentage of inaccessible region of 6-50 sample at 45 °C under 75% R. H.

From Figure 3.11, the intensity of urea groups that remain at the higher component of the Amide II region represented the inner portion of ordered hard domain. This time the inaccessible region for the urea groups was 54%. The difference in the accessible part of urea groups at these two different temperatures is indicative of the difference in dispersion, or the difference in the interfacial regions. It is found that 20% of the urea groups formed the interfacial region for the 4-50 sample, and 24% of the urea groups for 6-50 sample.

At the other extreme, deuterium substitution results for the 4-80 sample were entirely different. At room temperature, the urethane groups were all accessible to D_2O as indicated in Figures 3.12-3.13. Furthermore, more than half of the urea groups existed at the surface of the hard domain. Due to the lower volume fraction of the hard domain

and the increase in the degree of phase mixing, the morphology resulted in more isolated hard domains. Only a small amount of urea groups (5%) existed in the disordered hard domains. These were likely to be isolated units rather than to function as interconnecting bridges.

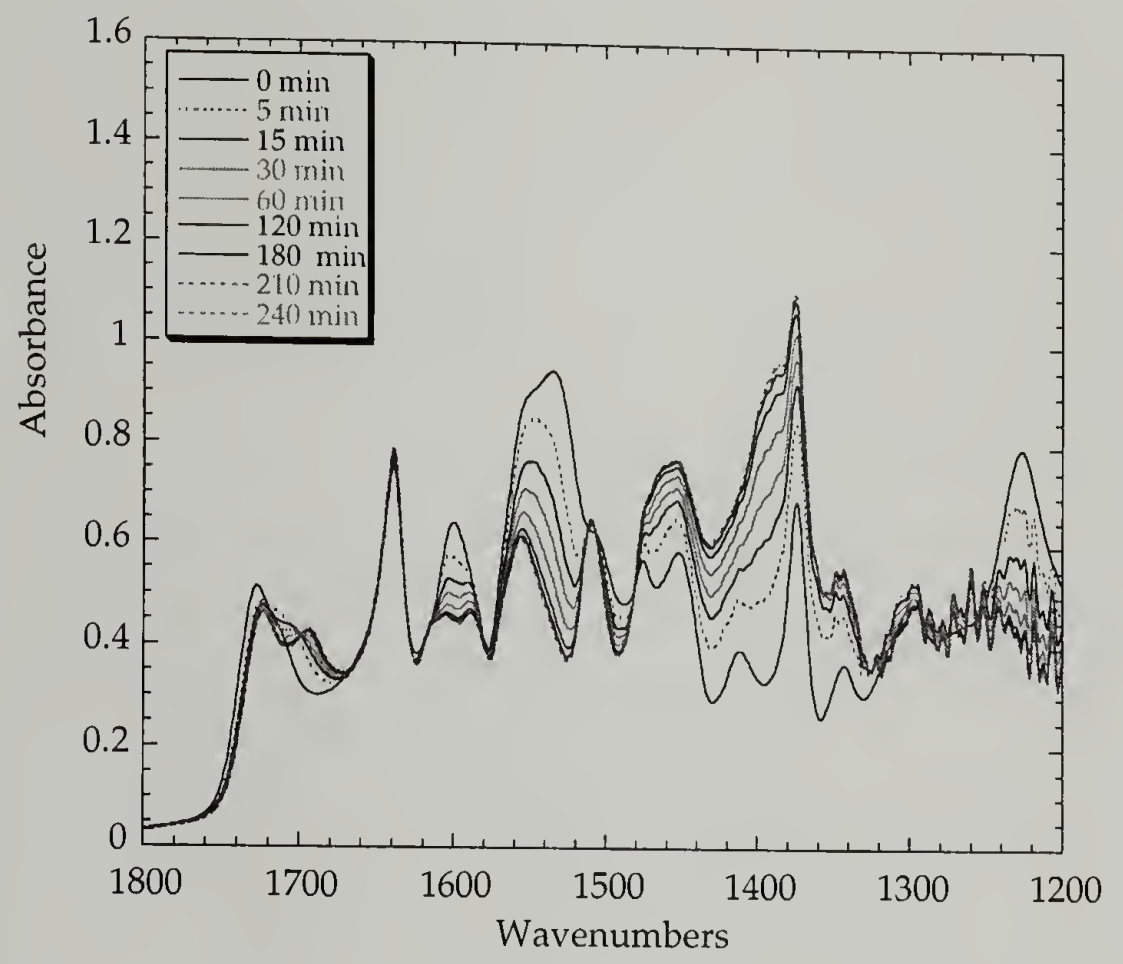

Figure 3.12. Vapor D_2O substitution of 4-80 at room temperature under 75% R.H.

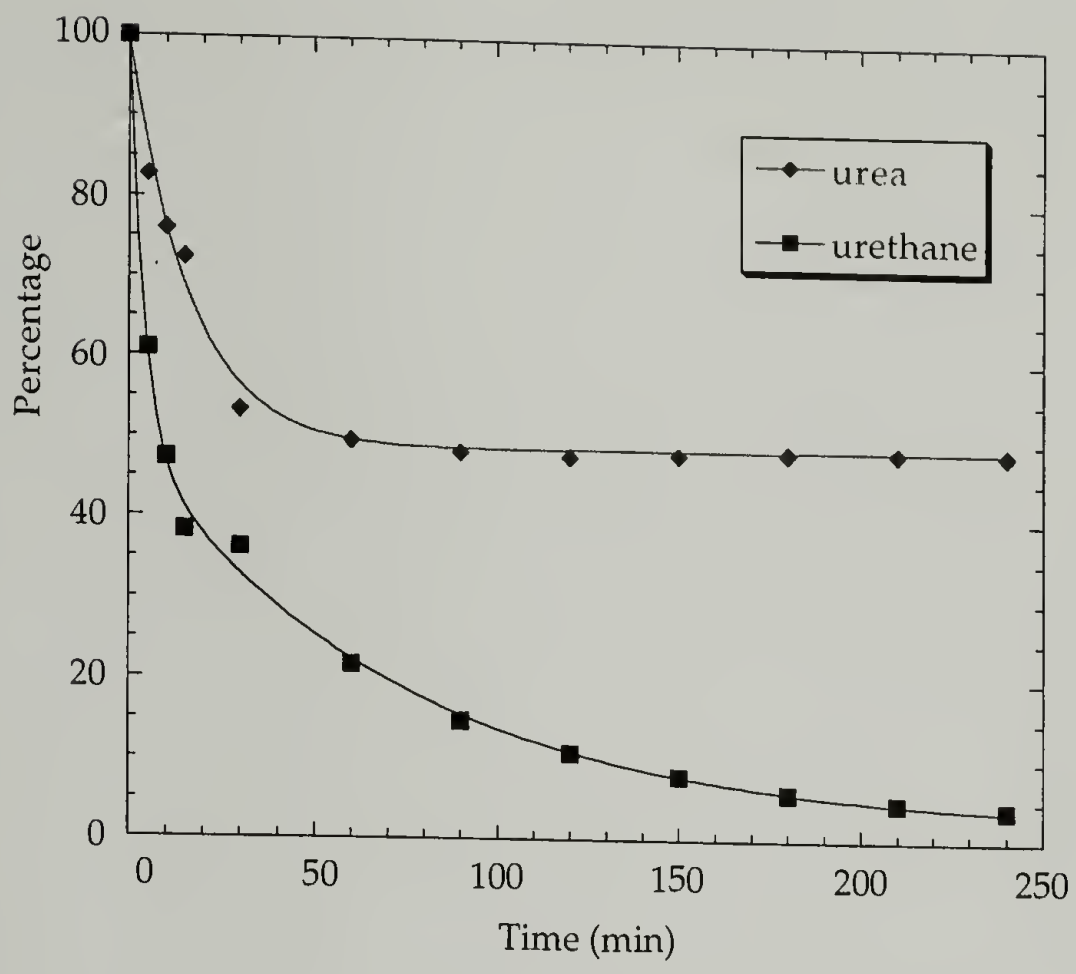

Figure 3.13. Percentage inaccessible region of 4-80 at room temperature under 75% R.H.

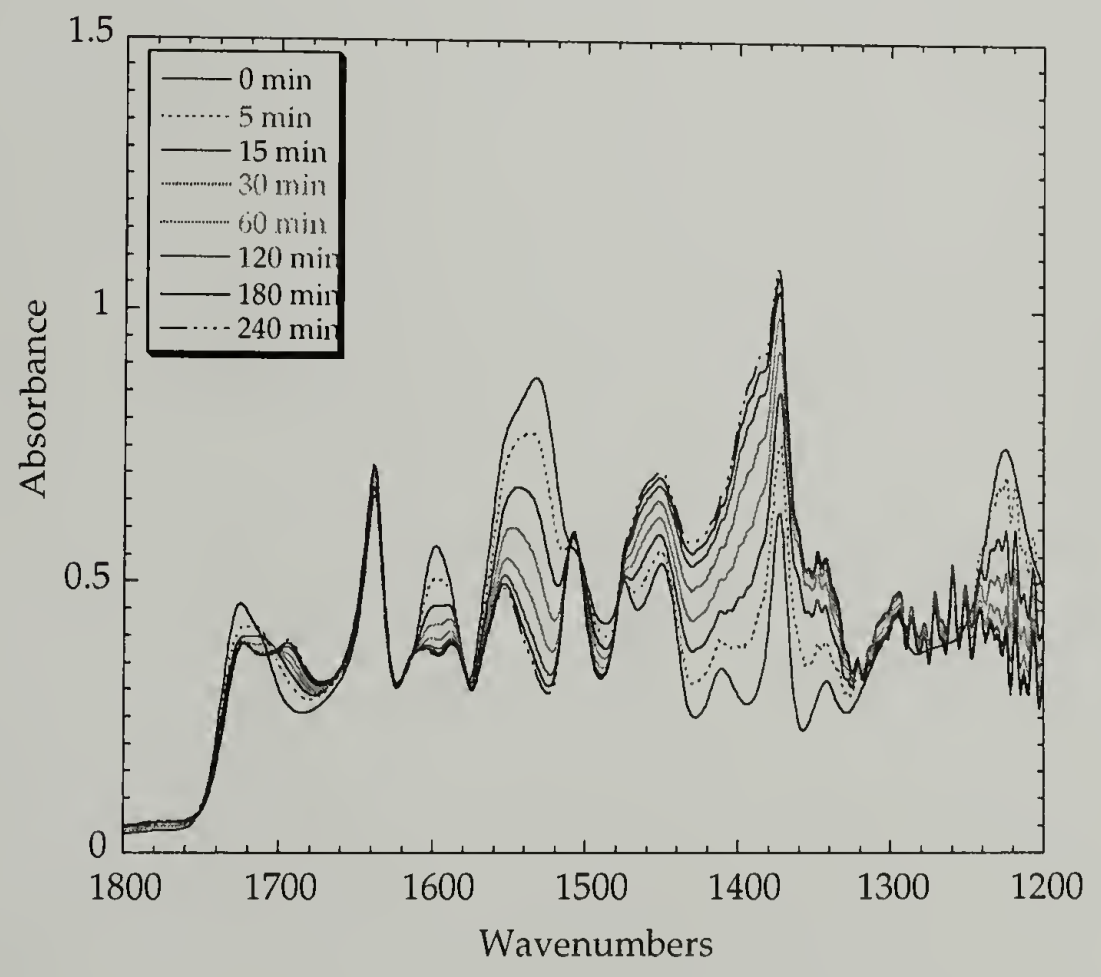

Figure 3.14. Vapor D_2O substitution of 4-80 at 45 °C under 75% R.H.

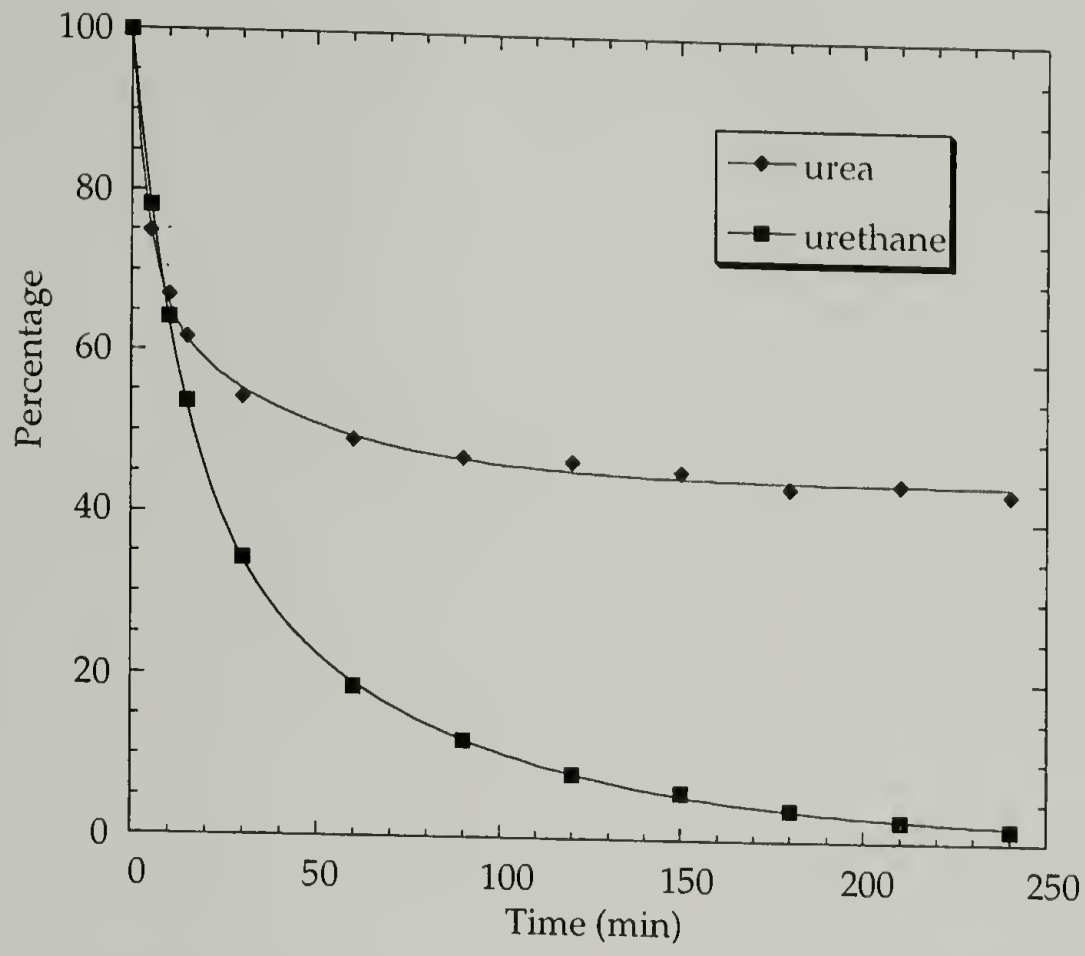

Figure 3.15. Percentage inaccessible region of 4-80 at 45 °C under 75% R.H.

As shown in Table 3.3, there was a substantial increase in the accessible region at room temperature for 80 °C samples. The accessible surface region was 51% of the urea groups for 4-80 sample and 43% of the urea groups for 6-80 sample. The results suggested increased phase mixing with larger surface area due to the smaller size of the hard domains in the higher temperature morphology. To look into the interfacial region, the sorption experiment at 45 °C (Figures 3.14-3.15) indicated that 44% of the urea groups formed the bulk of the hard domain for 4-80 sample and 47% of the urea groups for 6-80 sample. In conclusion, only 5% of the urea groups formed interfacial region for 4-80 sample and 10% for 6-80 sample. Rather than the increase in the interfacial region for the higher temperature sample, less interfacial region and more isolated hard domain existed in the morphology.

Table 3.3. Morphological features of urea groups at different regions of the hard domain of polyurethanes made at 80 °C

	Surface	Interfacial/ Interconnecting	Bulk
4-80	51%	5%	44%
6-80	43%	10%	47%

The interfacial region is important in enhancing the modulus and toughness of the material as described in the introduction. [41-44] It has been reported that under loading the stress transfer from the soft matrix onto the interconnecting interfacial region causes plastic deformation in this region before passing onto the bulk of the hard domain. [41] Deformation behavior in the interfacial region is critical for the performance of polyurethanes.

For samples reacted at 70 °C as shown in Table 3.4, it is clear that the degree of phase mixing is in between the samples prepared at 50 and 80 °C. From deuterium substitution, this difference is illustrated by the observation that 26 % of the hard domain forms the surface region in the 6-70 sample. The bulk of the hard domain has 53 % of the urea groups and the rest 21 % form the interfacial region.

Figure 3.16. Morphological pictures of 4-80 sample

Table 3.4. Morphological features of urea groups at different regions of the hard domain of polyurethanes made at 70 °C

	Surface	Interfacial/ Interconnecting	Bulk
4-70	48%	8%	44%
6-70	26%	21%	53%

If we plot the various regions of the hard domain morphology at different temperatures in Figures 3.17-3.18, it is found that the bulk hard domain doesn't change much for these samples, but there is a large change in the surface area and interfacial region of the hard domain morphology. The decrease in the modulus of higher temperature samples is due to the increase of phase mixing and decrease in the interfacial region of the hard domain morphology.

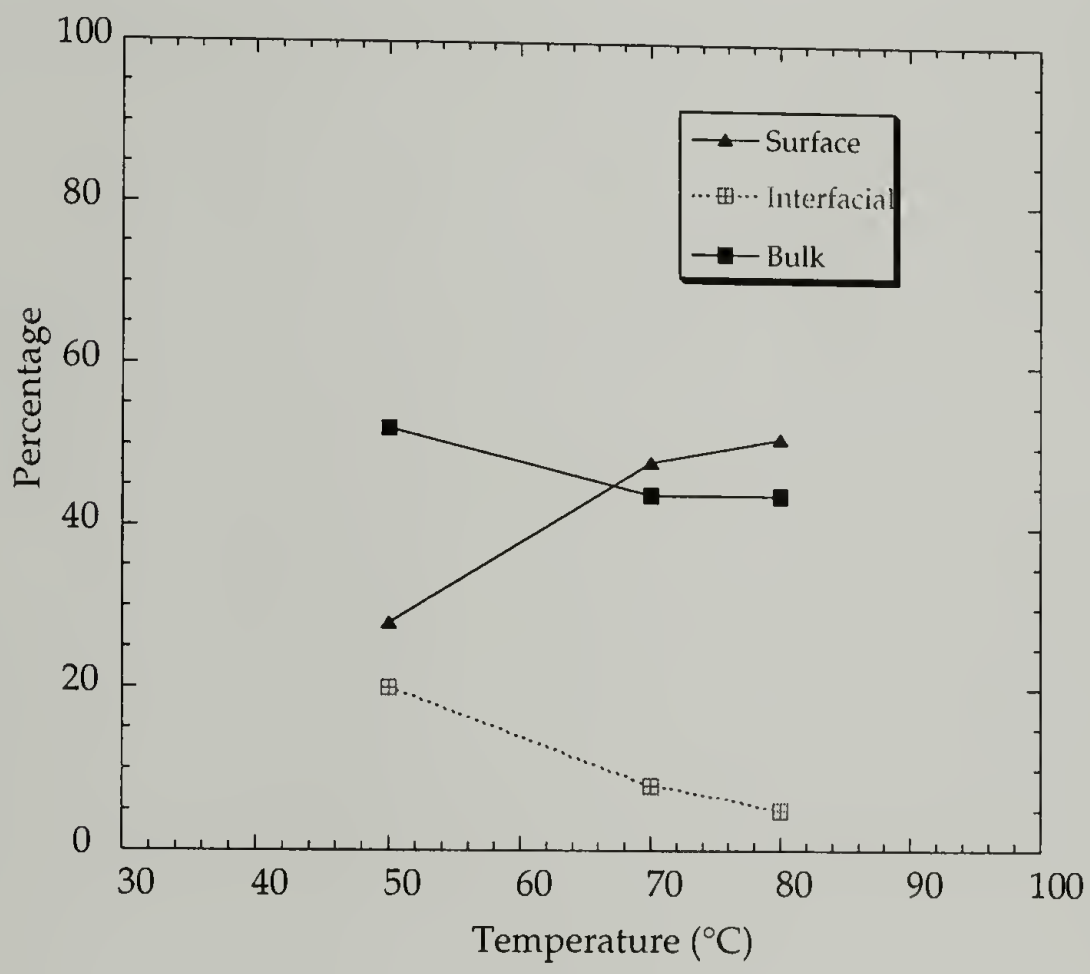

Figure 3.17. Temperature effect on the hard domain morphology of 4-urea samples

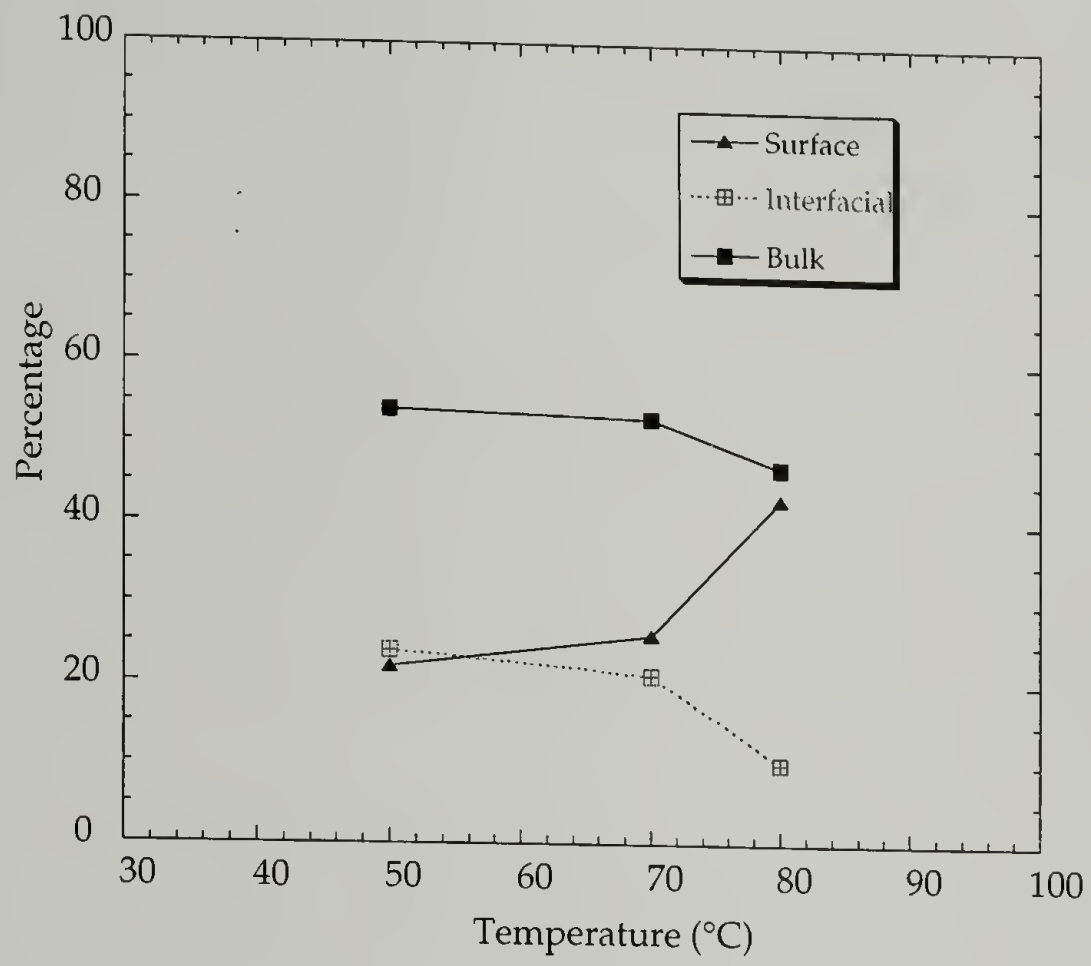

Figure 3.18. Temperature effect on the hard domain morphology of 6-urea samples

3.4. Hydrogen bonding strength difference in different regions of hard domain

Another advantage of deuterium substitution is that it allows an estimate of the hydrogen bonding strength of different regions of the hard domain. The urea groups

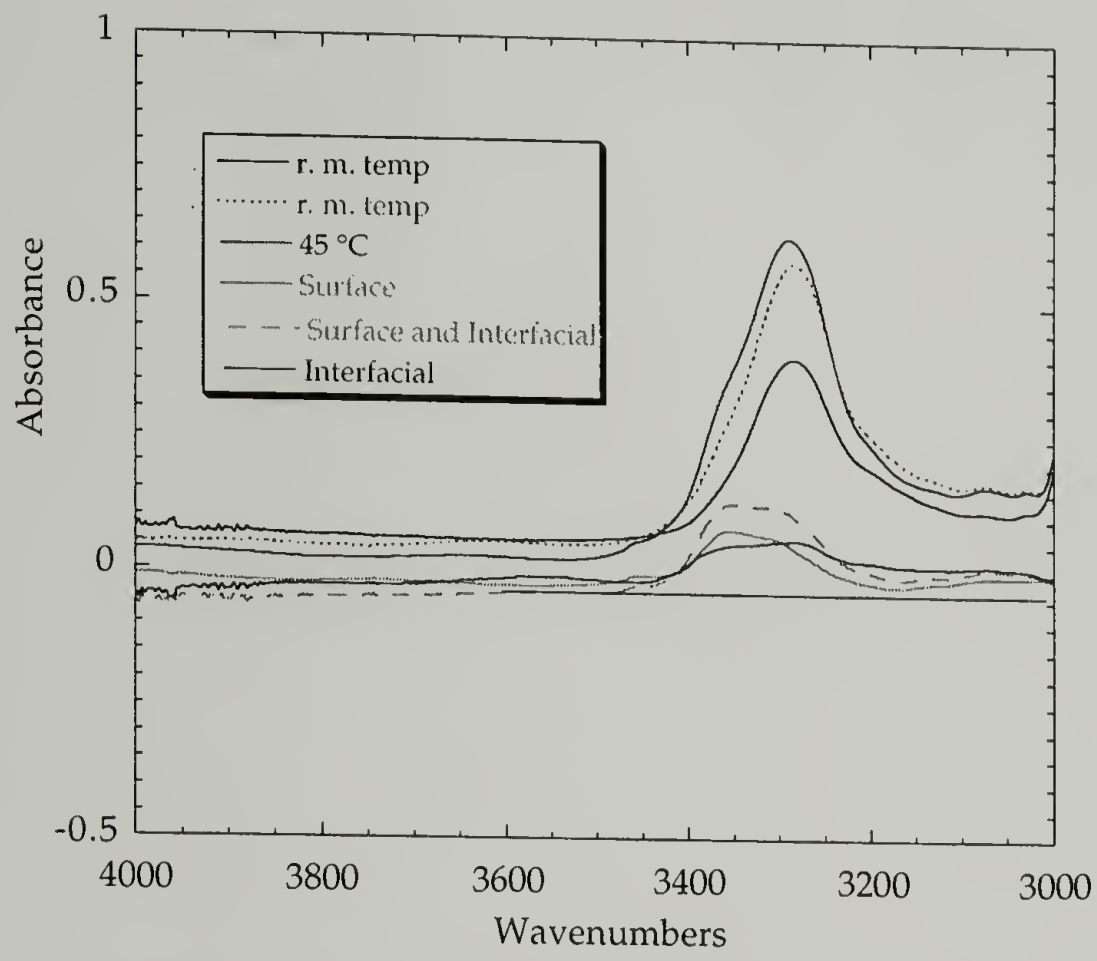

Figure 3.19. Hydrogen bonding strength difference in different regions of the hard domain morphology

at the surface have been deuterium substituted at room temperature, and the N-H stretching region of the difference spectrum of the original and deuterium substituted spectra at room temperature indicates the hydrogen bonding strength of the surface region. Neglecting the error introduced from the O-H stretching, the N-H stretching region of the difference spectrum between original and deuterated sample at 45 °C indicates the hydrogen bonding strength at surface and interfacial regions. Next, hydrogen bonding strength at both surface and interfacial regions can be differentiated by comparing the two different spectra. The difference spectra are shown in Figure 3.19. Note that the N-H stretching band for the interfacial region shifts to lower wavenumbers, indicating stronger hydrogen bonding in the interfacial region. The comparable intensity

Table 3.5. N-H stretching peak positions (cm^{-1}) for different regions of the hard domain

Samples	Bulk of hard domain	Surface	Interfacial
4-50	3287	3326	3304
6-50	3289	3325	3300
4-80	3287	3324	3301
6-80	3290	3328	3298

of the two bands demonstrates the similar amount of these two regions, which supports similar results from the amide II regions. Also for samples made at 80 °C, the decreasing intensity of N-H stretching for the interfacial region suggests a loss in the interfacial region in higher temperature samples and with a corresponding increase in phase mixing. In Table 3.5, the weight center of band position for each specific region of the hard domain is shown. The bulk hard domain has a band center at an average of 3288 cm^{-1}, the surface at 3326 cm^{-1}, and the interfacial region at 3301 cm^{-1}. The results provide further evidence that hydrogen bonding is not the major factor for phase separation. [45]

3.5. Conclusions

The deuterium substitution method has been used to study the dispersion state of the interconnecting hard domain morphology quantitatively. The surface, the disordered hard domain and the bulk hard domain have been specified for samples made at different temperatures. Based upon the new morphological picture, in addition to the direct

bridges from the longer hard segments, the disordered hard domains can interconnect the hard domains or connect between hard domain and soft matrix. The interconnecting regions of the hard domain decrease as the reaction temperature increases. The larger surface area for the higher temperature samples is consistent with the previous studies that showed that as temperature increases, the degree of phase mixing increases.

The difference in the morphological features of different temperature samples is attributed to the physical properties of the final materials. It is suggested that the degree of phase separation and the interconnecting region of the hard domain in the phase separated morphology are determining factors for the mechanical properties of polyurethanes. The reinforcing mechanism will be further discussed in Chapters 4 and 5.

3.6. References

1) Levon, K.; Margolina, A.; Patashinsky, A. Z. *Macromolecules* **1993**, *26*, 4061-4063.

2) Yontz, D. J.; Hsu, S. L.; Lidy, W. A.; Gier, D. R.; Mazor, M. H. *J. Polym. Sci., Polym. Phys.* **1998**, *36*, 3065-3077.

3) Yontz, D. J. *An Analysis of Molecular Parameters Governing Phase Seperation in a Reacting Polyurethane System*; University of Massachusetts: Amherst, MA, **1999**, pp 329.

4) Priester, R. D.; McClusky, J. V.; O'Neill, R. E.; Harthcock, M. A.; Davis, B. L. *33rd Annual Polyurethane Technical/Marketing Conference* **1990**, *September 30-October 3*, 527-538.

5) Born, L.; Hespe, H. *Colloid Polym. Sci.* **1985**, *263*, 335-341.

6) Bailey, F. E. J.; Critchfield, F. E. *J. Cell. Plast.* **1981**, *17*, 333-339.

7) McClusky, J. V.; Priester, R. D., Jr.; O'Neill, R. E.; Willkomm, W. R.; Heaney, M. D.; Capel, M. A. *J. Cell. Plast.* **1994**, *30*, 338-360.

8) Neff, R.; Macosko, C. W. *A Model for Modulus Development in Flexible Polyurethane Foam*: Chicago, IL, **1995**, pp 344-352.

9) Thomas, O.; Priester, R. D., Jr.; Hinze, K. J.; Latham, D., D. *Journal of Polymer Science: Part B: Polymer Physics* **1994**, *32*, 2155-2169.

10) Turner, R. B.; Wilkes, G. L. *Structure vs. Properties of Flexible Urethane Foams Used in the Home Furnishing Industry (Polymer-Morphology)*; Technomic Publishing Co., Inc.: Aachen, Federal Republic of Germany, **1987**, pp 935-939.

11) Tsubomura, H. *J. Chem. Phys.* **1956**, *24*, 927-931.

12) Pimentel, G. C.; Sederholm, C. H. *The Journal of Chemical Physics* **1956**, *24*, 639-641.

13) Pimentel, G. C.; L., M. A. *The Hydrogen Bond*; W. H. Freeman and Company: San Francisco, **1960**.

14) Bellamy, L. J. *The Infrared Spectra of Complex Molecules*; Chapman and Hall Ltd.: London, **1975**.

15) Nakayama, K.; Ino, T.; Matsubara, I. *J. Macromol. Sci.-Phys.* **1969**, *A3*, 1005.

16) Ishihara, H.; Kimura, I.; Saito, S.; Ono, H. *J. Macromol. Sci. Phys.* **1974**, *B10*, 591-618.

17) Paik Sung, C. S.; Schneider, N. S. *Macromolecules* **1975**, *8*, 68-73.

18) West, J. C.; Cooper, S. L. *J. Polym. Sci., Polym. Symp.* **1977**, *60*, 127-150.

19) Hummel, D. O.; Ellinghorst, G.; Khatchatryan, A.; Stenzenberger, H. D. *Die Ange. Makrom. Chem.* **1979**, *82*, 129-148.

20) Brunette, C. M.; Hsu, S. L.; MacKnight, W. J. *Macromolecules* **1982**, *15*, 71-77.

21) Coleman, M. M.; Skrovanek, D. J.; Hu, J.; Painter, P. C. *Macromolecules* **1988**, *21*, 59-65.

22) Coleman, M. M.; Graf, J. F.; Painter, P. C. *Specific Interactions and the Miscibility of Polymer Blends*; Technomic Publishing Co.: Lancaster, **1991**.

23) Artavia, L. D.; Macosko, C. W. *J. Cell. Plast.* **1990**, *26*, 490-511.

24) Elwell, M. J.; Ryan, A. J.; Grunbauer, H. J. M.; Van Lieshout, H. C. *Polymer* **1996**, *37*, 1353-1361.

25) Varsanyi, G. *Vibrational Spectra of Benzene Derivatives*; New York: Academic Press, **1969**.

26) Bendit, E. G. *Biopolymers* **1966**, *4*, 539-559.

27) Tsuboi, M.; Nakanishi, M. *Adv. Biophys.* **1979**, *12*, 101-130.

28) Siesler, H. W. *Polymer Bulletin* **1983**, *9*, 557-562.

29) Chen, C. C.; Krejchi, M. T.; Tirrell, D. A.; Hsu, S. L. *Macromolecules* **1995**, *28*, 1464-1469.

30) Coleman, M. M.; Lee, K. H.; Skrovanek, D. J.; Painter, P. C. *Macromolecules* **1986**, *19*, 2149-2157.

31) Miyazawa, T.; Blout, E. R. *J. Am. Chem. Soc.* **1961**, *83*, 712-719.

32) Hocker, J. *J. Appl. Polym. Sci.* **1980**, *25*, 2879-2889.

33) Creswick, M. W.; Lee, K. D.; Turner, R. B.; Huber, L. M. *J. Elast. Plast.* **1989**, *21*, 179-96.

34) Elwell, M. J.; Ryan, A. J.; Grunbauer, H. J. M.; Van Lieshout, H. C. *Macromolecules* **1996**, *29*, 2960-2968.

35) Colthup, N. B.; Daly, L. H.; Wiberly, S. E. *Introduction to Infrared and Raman Spectroscopy*; 3rd ed.; Academic Press, Inc.: Boston, **1990**.

36) Wang, F. C.; Feve, M.; Lam, T. M.; Pascault, J. *J. Polym. Sci., Part B: Polym. Phys.* **1994**, *32*, 1315-1320.

37) Yang, X.; Hsu, S. L. *Macromolecules* **1993**, *26*, 1465.

38) Kim, P. K.; Chang, C.; Hsu, S. L. *Polymer* **1986**, *27*, 34-46.

39) Fukushima, K.; Zwolinski, J. B. *J. Chem. Phys.* **1969**, *50*, 737-749.

40) Yontz, D. J.; Hsu, S. L. *Macromolecules* **2000**, *33*, 8415 - 8420.

41) Smith, T. L. *Polymer Engineering and Science* **1977**, *17*, 129-143.

42) Paik Sung, C. S.; Smith, T. W.; Sung, N. H. *Macromolecules* **1980**, *13*, 117-121.

43) Pukanszky, B. *Makromol. Chem. Macromol. Symp.* **1993**, *70/71*, 213-223.

44) Martin, D. J.; Meijs, G. F.; Gunatillake, P. A.; Yozghatlian, S. P.; Renwick, G. M. *J. Appl. Polym. Sci.* **1999**, *71*, 937-952.

45) Eisenbach, C. D.; Stadler, E. *Macromol. Chem. Phys.* **1995**, *196*, 1981-1997.

CHAPTER IV

DICHROIC STUDIES OF INTERCONNECTING MORPHOLOGY OF POLYURETHANES

4.1. Chapter Review

In this chapter, the deformation behavior of polyurethane is discussed based upon the interconnecting hard domain morphology proposed in Chapter 3. Infrared dichroism was used to give insight into hard domain reinforcement. The principles of the infrared dichroic method are outlined in Section 4.2. The dichroic results are given in Section 4.3. The Amide II band provides quantitative information of hard domain volume change throughout the deformation. The role of bulk hard domain, interfacial region and dispersed hard segment chains in contributing to the overall mechanical properties of polyurethanes is discussed. These observations not only point to the large hysteresis and stress softening phenomena associated with the polyurethane materials, even at small strains, but also shed light on interconnecting hard domain reinforcement.

The understanding of mechanical properties of polyurethane is often limited by the poor understanding of its phase separated morphology. In the previous chapter, the interconnecting hard domain morphology is quantitatively characterized using deuterium substitution and the interconnecting region of the hard domain is specified. It is noted that the interconnecting interfacial region and the degree of phase separation are the determining factors for the enhancement of both the modulus and strength of the material and thus the whole deformation process. [1-3] This chapter will suggest the contribution of

the interfacial region to the mechanical properties of polyurethanes. The observation of orientation and plastic deformation of the hard domain during the stretching process gives a complete molecular interpretation of energy dissipation and hard domain reorganization, which helps explain the large hysteresis and stress softening effect; characteristic phenomena associated with polyurethanes. [4-6]

4.2. Principles of Infrared Dichroism

The studies on the molecular orientation and its specification in some quantitative form are essential to a full understanding of a variety of properties such as mechanical and dielectric, etc. Among the common techniques such as birefringence, X-ray scattering, NMR spectroscopy, polarized fluorescence, Raman depolarization and sonic techniques, infrared dichroism has been widely used to study the orientation of polymers. [7]

When an oriented polymer is investigated with linearly polarized radiation, the absorbance A of a single group in the polymer chain is proportional to the square of the scalar product of its transition moment vector $\bar{M}$ and the electric vector $\bar{E}$ of the incident polarized radiation:

Equation 4.1. $$a \propto \left(\bar{M} \cdot \bar{E}\right)^2 = (ME)^2 \cos^2 \gamma$$

where $\left|\bar{M}\right| = M, \left|\bar{E}\right| = E$ and γ is the angle between the transition moment and the electric vector. Thus the maximum absorption takes place when the electric vector is parallel to

the transition moment of the vibrating groups, but no light will be absorbed when its electric vector is perpendicular to the transition moment. The actually observed absorbance A is equal to the sum of absorbance contributions of all structural units:

Equation 4.2. $$A \propto \int_{n} \left(\bar{M} \cdot \bar{E}\right)^2 dn$$

where the integral refers to the summation over all molecules. When these atomic groups and their associated transition moments are randomly oriented within the polymer, the measured absorbance is independent of the polarization direction of the incoming light. For anisotropic distribution of the transition moments, the observed net absorbance varies with the direction of the electric vector $\bar{E}$ of the polarized radiation. [8] The effect of anisotropy on a particular absorption band in the IR spectrum of a polymer is characterized by the dichroic ratio R in Equation 2.1:

Equation 4.3. $$R = \frac{A_{//}}{A_{\perp}}$$

where $A_{//}$ and $A_{\perp}$ are the absorbances measured with radiation polarized of parallel and perpendicular to the draw direction, respectively. If R is larger than 1.0, the band is called a parallel band; if R is smaller than 1.0, it is called a perpendicular band. This nomenclature refers not only to the stretching direction but also to the chain axis that is preferentially oriented in the stretching direction.

In order to represent the orientation, it is supposed that all the molecular chains are displaced by the same angle θ from parallelism with the draw direction as shown in Figure 4.1.

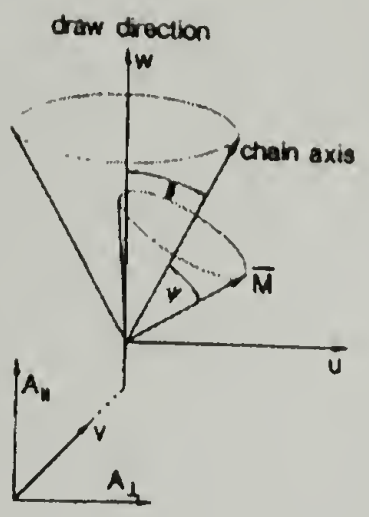

Figure 4.1. Distribution of transition moments of a particular vibration in a uniaxially oriented polymer with respect to the draw direction[8]

The second order orientation function can then be expressed as follows:

Equation 4.4. $$\langle P_2(\cos\theta)\rangle = \frac{1}{2}\left(3\langle\cos^2\theta\rangle - 1\right)$$

It is obvious that for perfect parallel alignment, i.e. $\theta = 0°$, the orientation function f is equal to 1. If all the chains perfectly align perpendicularly to the draw direction, i.e. $\theta =$ 90 °, the orientation function f is equal to -0.5.

The orientation function f can be related to the dichroic ratio by using the following equation:

Equation 4.5. $$\langle P_2(\cos\theta)\rangle = \frac{(R-1)(R_0+2)}{(R+2)(R_0-1)} = f$$

where R_0 is the dichroic ratio for perfect alignment and is equal to $2\cot^2\psi$, where ψ is the angle between the transition moment vector for the vibration and the local chain axis. As ψ varies from 0 to $\pi/2$, R_0 varies from ∞ to 0, and no dichroism (R_0 =1) will be observed when $\psi = 54°44'$.

The primary advantage of this deduction is that the orientation functions determined by independent methods (e.g. X-ray diffraction, birefringence, NMR) may be coupled with the results derived from IR dichroic measurements of absorption bands which are representative of the appropriate phase.

The infrared dichroic method can be used to study the orientation not only of the ordered structure, but also the disordered structure, since the molecules vibrate locally in different phases and yield different infrared characteristic bands. The orientation function f of an absorption band having its transition moment perpendicular to the chain axis ($\psi = 90°$) can be calculated using equation 4.6. The carbonyl stretching (Amide I) and symmetric C-H stretching vibrations of samples 4-50 through 6-80 are assumed to be perpendicular to the polymer chain axis. The amide I was also reported to be 78 ° with the chain axis. [3,9]

Equation 4.6. $$f = (-2)\frac{(R-1)}{(R+2)}$$

The N-H in-plane bending (Amide II) transition moment is assumed to be parallel to the polymer chain axis ($\psi = 0°$) and the orientation function f is calculated as

Equation 4.7. $$f = \frac{(R-1)}{(R+2)}$$

The structural absorbance has been chosen as intensity for quantitative analysis because it eliminates the influence of changing orientation on the actual intensity of an absorption band. [10-12] The structural absorbance A_0 is calculated as

Equation 4.8. $$A_0 = \frac{A_{//} + 2A_{\perp}}{3}$$

For example, during elongation of a semi-crystalline polymer several different process, such as elastic deformation of the original spherulitic superstructure, transformation of a spherulitic into a fibrillar sturcture, plastic deformation of microfibrils by slippage processes and elongation of molecular chains in the amorphous regions may occur simultaneously, successively, or partly superimposed. [13-15] One of the advantages of IR spectroscopy is that under certain conditions these complex processes may be resolved into the individual components. Thus, the crystalline and amorphous phase of a semi-crystalline polymer can be characterized separately by evaluating the dichroic effects of absorption bands that are peculiar to these regions. [13-15]

Finally, it is worth mentioning a few of the sources of errors in dichroic measurements. The determination of dichroic ratio encounters the same difficulties as ordinary intensity measurements as soon as various absorption bands overlap where it becomes uncertain how to measure the background intensity for an individual band. Other effects include the polarizer efficiency, insufficient resolution of the spectrometer, false radiation due to spectral dilution and scattered light, and beam convergence. [9]

4.3. Results and Discussion

The orientation of the hard domain in various polyurethane systems has been extensively studied using infrared dichroic measurements. [3,11,16-22] All authors agree that Amide I bands are used for qualitative characterization and it is shown that in most of the systems the hard domain tends to have negative orientation when the sample starts to deform. [3,11,17,23] This unique feature in the deformation of polyurethane occurs because the bulk hard segment domain tends to rotate transverse to the stretching direction. This is interpreted as bulk lamellar-like hard domain with the long-axis direction perpendicular to the polymer chain axis. [17] The idea came from the studies of spherulitic deformation of polyethylene. [24] On the other hand, the soft chains and the hard segment chains that disperse in the soft matrix tend to align with the stretch direction. The orientation of the urethane groups at the boundary between domains is affected by the soft chains and thus they are stretched parallel to the stretch direction. The hard domain undergoes disruption when the sample is stretched at above 100% strain [17,23] where the orientation of the hard domain begins to increase from the negative minimum as shown in Scheme 4.1. [23] Despite these findings, it is still not sufficient to understand the actual hard domain reinforcement throughout the deformation process since only orientation is

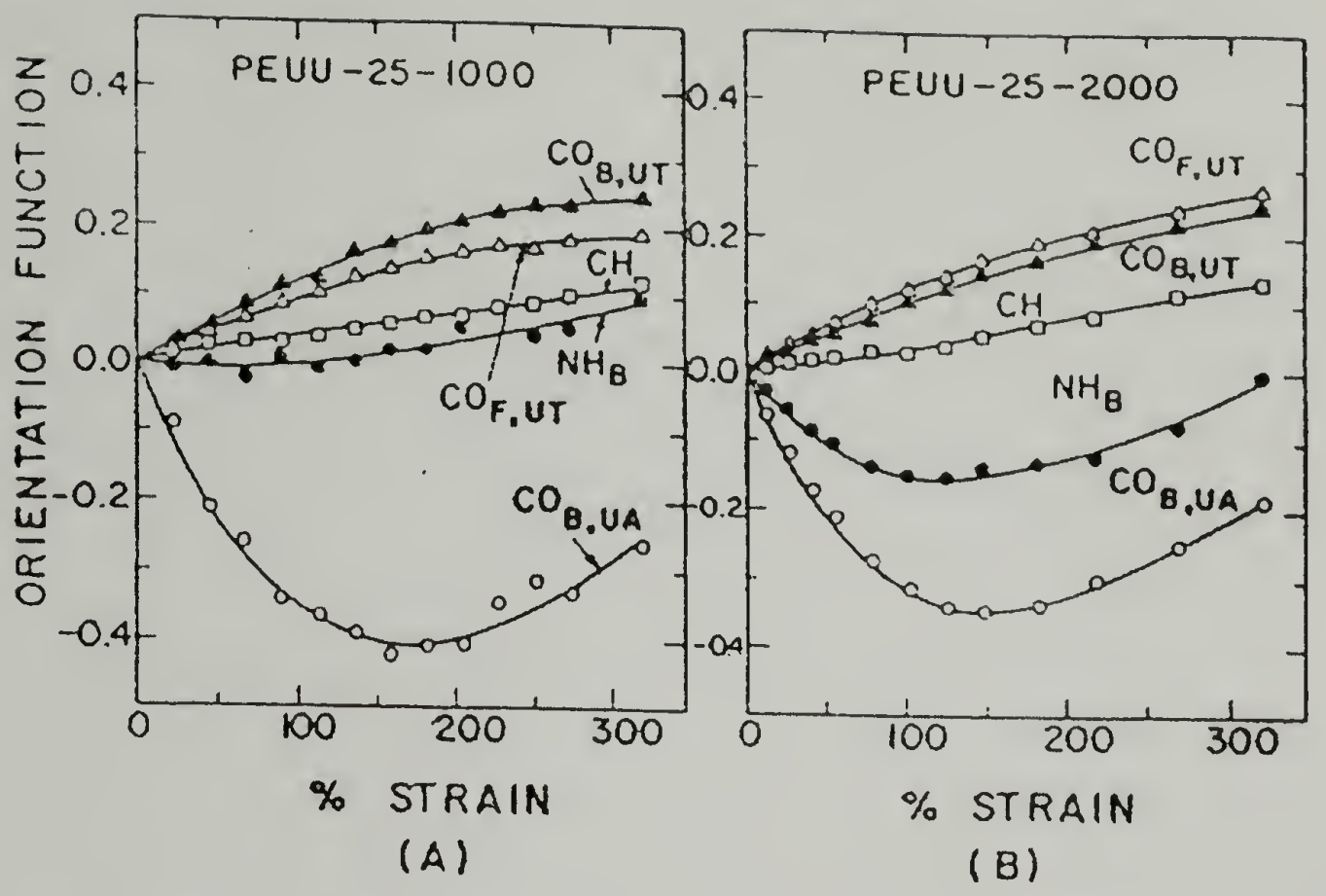

Scheme 4.1. Orientation function vs. elongation curves of (A) PEUU-25-1000 and (B) PEUU-25-2000 [23]

followed for both domains. Another reason is that there is no direct link between specific hard domain region and the corresponding infrared band in previous studies. With the help of deuterium substitution, the problem can be resolved using the amide II band. An evaluation of the plastic deformation of hard domain based upon interconnecting morphology becomes possible.

Figures 4.2 - 4.4 show a series of dichroic spectra of 6-50 thin film sample collected before, in the middle and at the end of the deformation process. In the spectra, the parallel spectrum is shown as solid line indicated as par; the perpendicular spectrum is shown as dotted line indicated by per. Since the difference spectra $A_{sub} = A_{//} - A_{\perp}$ is

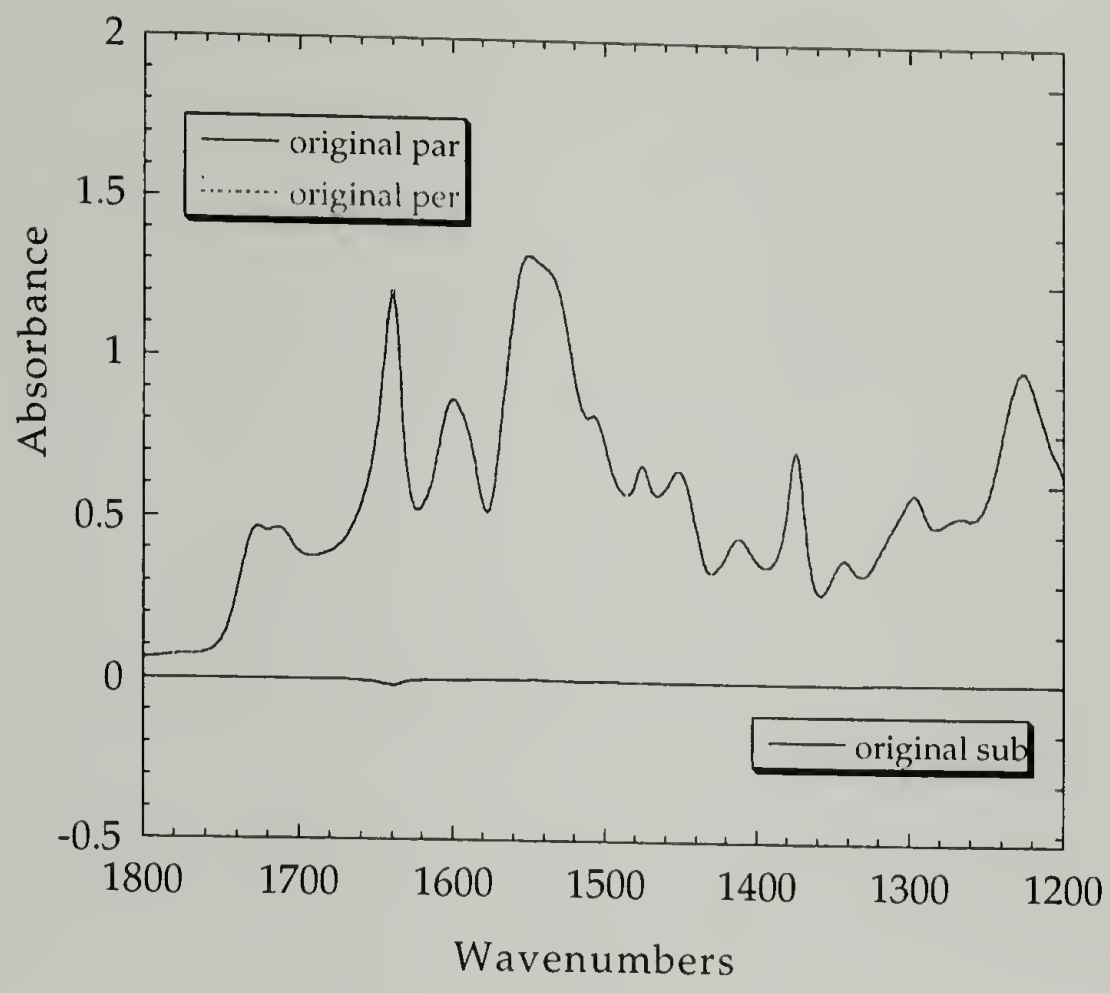

Figure 4.2. Infrared dichroic spectra of 6-50 sample before stretching

found easy to visualize the change of each band and thus the orientation of the specific group, a difference spectrum is included under each pair of spectra at a certain draw ratio. Before stretching the sample as shown in Figure 4.2, there was no orientation since the parallel and perpendicular spectra were almost identical, which indicated that the hard domain was randomly distributed throughout the material. After the sample was stretched at a certain strain at 60%, the dichroic spectra are shown in Figure 4.3. It can be seen from the difference spectrum, suggesting the orientation of different regions of the morphology. First, it is found that both the Amide I and the Amide II bands can be correlated. The urethane amide I band and lower component of Amide II which

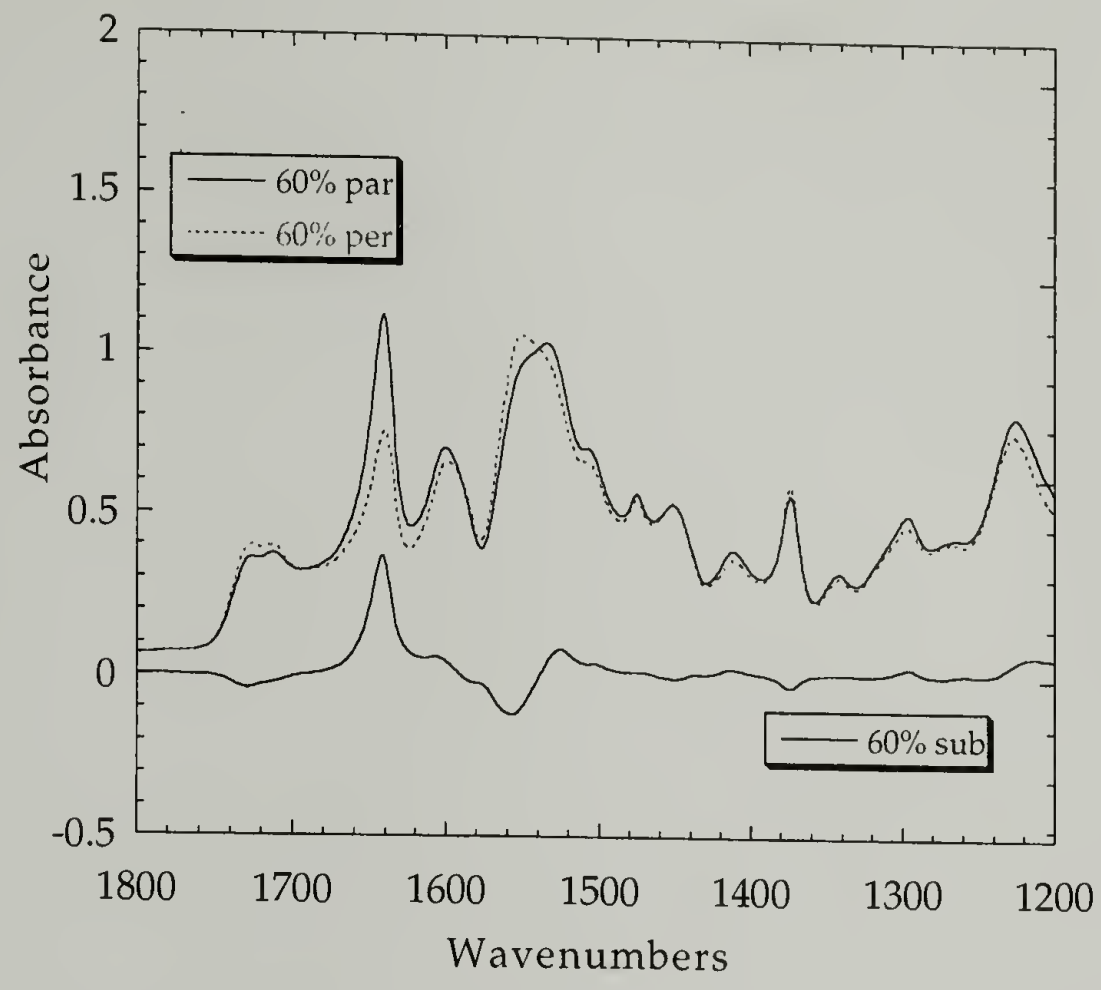

Figure 4.3. Infrared Dichroic Spectra of 6-50 sample stretched at 60% Strain

both represents the dispersed hard segment chains and urethane groups at the boundary between domains will orient towards the stretching direction, as positive orientation reflected on the difference spectra. While for ordered urea groups which form the hard domain with its characteristic amide I band at 1640 cm^{-1}, pairing with the higher component of the amide II region behaves similarly transverse the uniaxial stretch as negative orientation. At the strain up to 160%, the increase in orientation for the hard domain would not be due to the change in the hard segment chain conformation (either urethane or urea). Therefore the peak position for the hard domain is maintained the same throughout the deformation process. In conclusion, this observation further verifies the band assignments made on deuterium substitution that was described in Chapter 3.

The peak position of the higher component at 1554 cm^{-1} of the amide II region would be a strong indication of the bulk of the hard domain, the lower component at around 1530 cm^{-1} represents the dispersed hard segment chains and urethane groups at the boundary between domains. These two bands behave exactly in an opposite way. The ordered hard domain showed negative orientation while the urethane groups and dispersed hard segments tended to align with the soft chains along the stretching direction.

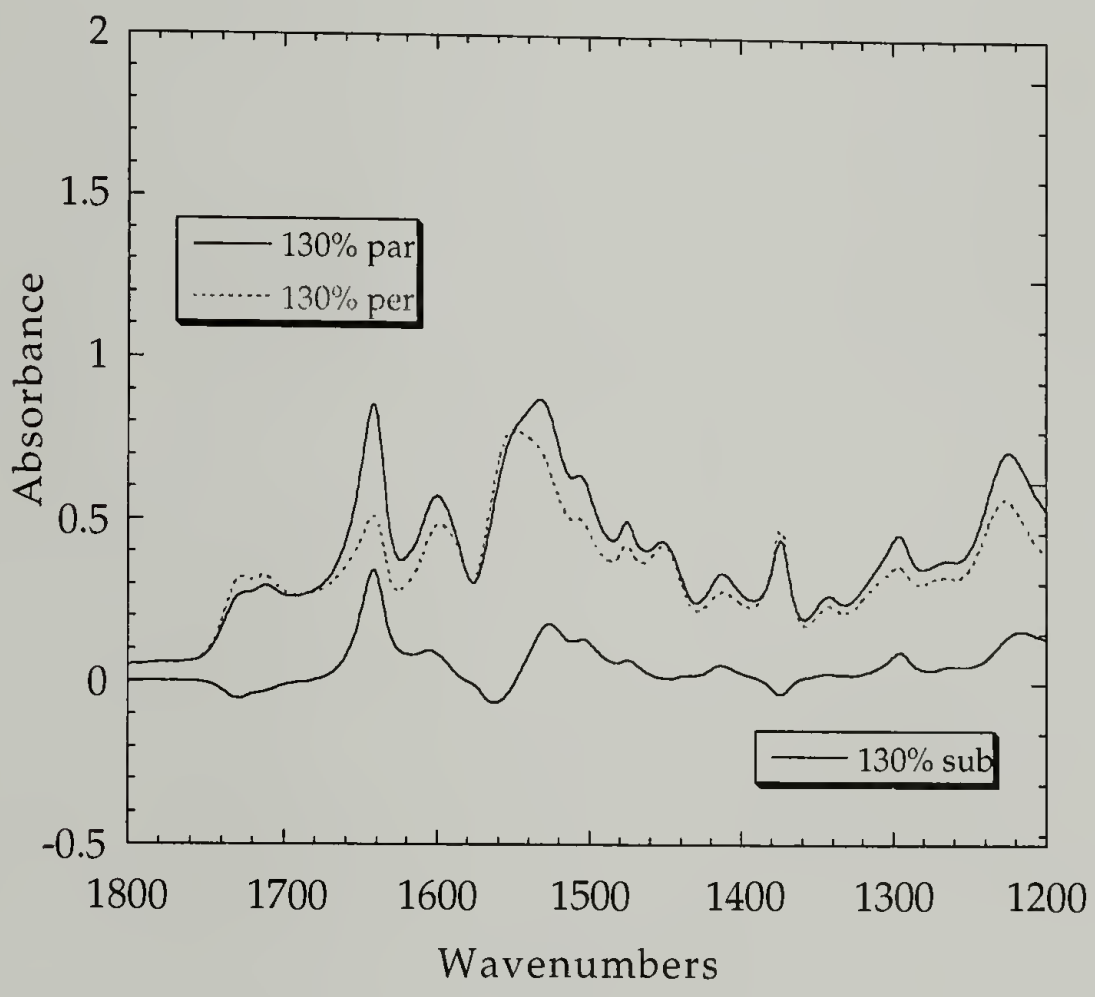

Figure 4.4. Infrared Dichroic Spectra of 6-50 Sample Before Break at 130% Strain

In Figure 4.5, the orientation of hard domain became more negative, even though the individual parallel and perpendicular band intensities decreased as thickness decreases. It was important to notice that there was an increase in intensity in the difference spectra for the lower component of the Amide II band and a decrease in the

higher component of the Amide II band. This suggested that the volume fraction of the hard domain was changing during the deformation process.

Second, it is clear in Figure 4.5 that the hard domain, as represented by 1640 cm^{-1} band, showed increasing negative orientation up to –0.4, close to –0.5 with increasing the draw ratio before the sample broke while soft chains showed only slight increase in the

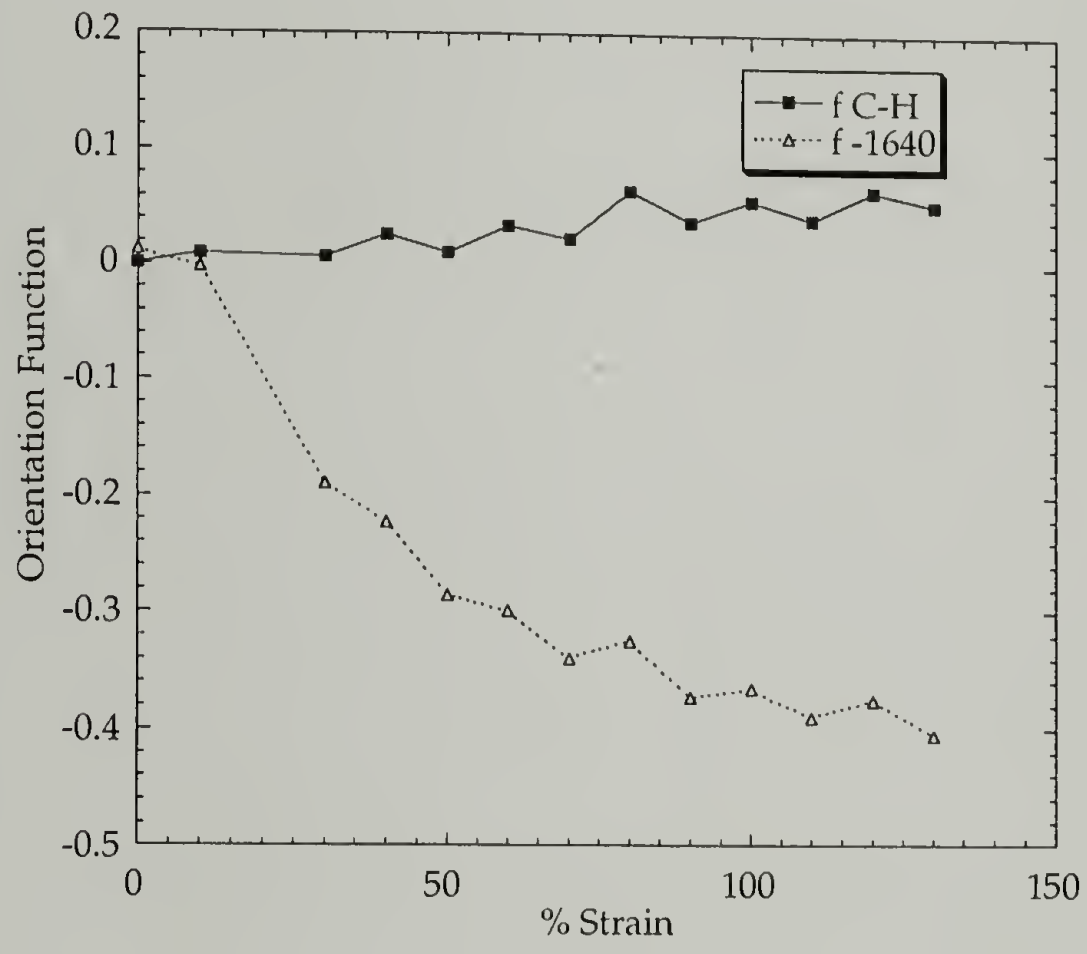

Figure 4.5. The Orientation Function of Soft and Hard Domain for polyurethane 6-50 samples

positive orientation. It is reasonable to think that during stress relaxation after 5 minutes of stretching, the soft chains tended to relax back to the original state indicating the stress had been transferred onto the hard domain through the weaker interfacial

regions. This could cause plastic deformation of the interfacial region, because in the less well packed interfacial region, the stress on soft chains sufficed to break the hydrogen bonding and other interactions between hard segments. This results in the hard segment chains either sliding away from the original position or being pulled out from the interfacial region into the soft matrix. During stress relaxation, hard domain reorganization occurred.

With the help of deuterium substitution, the two components of the Amide II region were studied quantitatively. These two components from parallel and perpendicular spectra were used to calculate the structural absorbance. The integrated intensity of C-H stretching representing the soft matrix was used for calibration of the

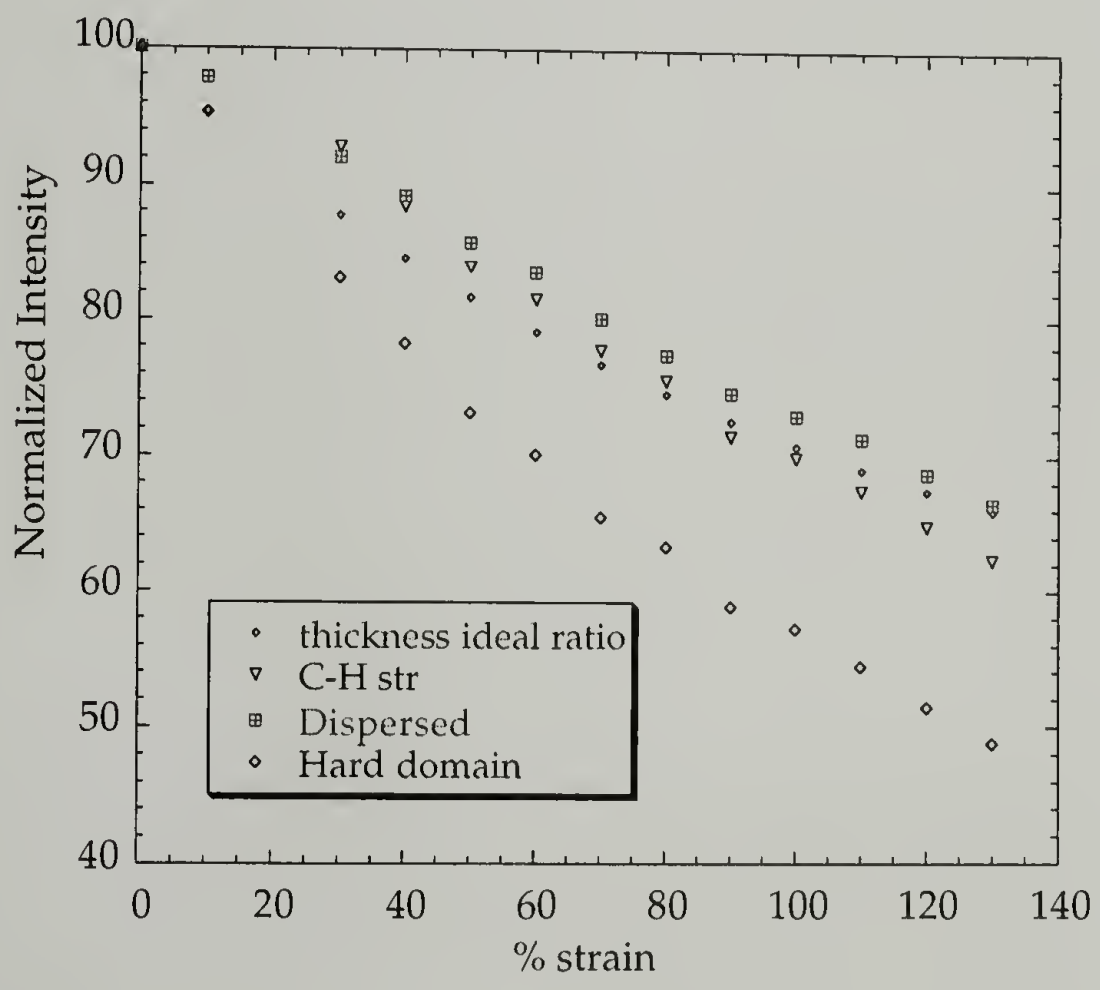

Figure 4.6. Intensity Change within the Hard Domain vs. Dispersed Hard Segments of 6-50 sample under Deformation

thickness decrease upon stretching. The structural absorbance of the sample at each draw ratio was calculated as indicated in Figure 4.6. It is found that the hard domain decreases faster than the thickness decreases, while the dispersed hard segment seemed to decrease more slowly. The normalization was then performed against the C-H stretching region to account for the thickness decrease. In this way, information can be obtained on both hard domain change and dispersed hard segment and urethane group intensity change. Figure 4.7 shows that the volume of hard domain was decreasing throughout the entire

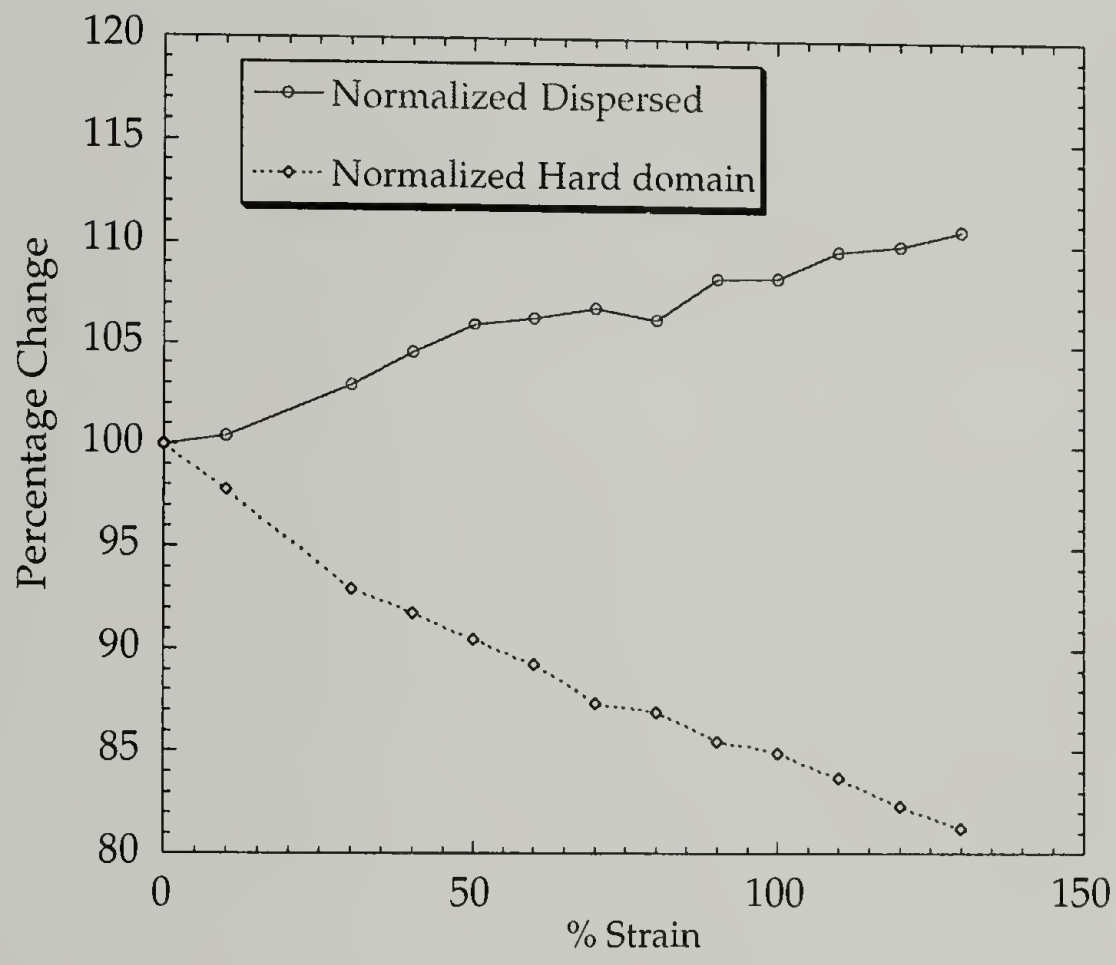

Figure 4.7. Normalized Percentage Change within Hard Domain vs. Dispersed Hard Segments for 6-50 Sample

deformation process. Before the sample broke, there was about 19%wt of the hard domain were pulled into the soft matrix and of course the dispersed portion of the urea and urethane groups increased.

These experimental results showed the hard domain undergoes plastic deformation, even at small strain, suggesting that energy hysteresis and stress-softening exist at low strain or stress levels. [25] The crystallization of soft matrix is not applicable to this system due to the majority of propylene oxide units (87 wt%) along the soft chains. Since the hard segment chains were pulled out into the soft matrix, the reinforcing quality of hard segments was lost and the modulus dropped. After removing the stress, the elastic properties of the chemically crosslinked soft matrix allowed the hard domain to reorganize into a new state.

Another sample, the 4-80 thin film, which has a more phase mixed morphology, is also presented here as shown in Figures 4.8-4.10. The dichroic results follow a similar trend. The sample began with homogeneous material and different domains responsing to the stretching differently. The hard domain tended to align perpendicular to the stretching direction, while the soft matrix showed little positive orientation as shown in Figure 4.11. The hard domain of 4-80 sample is smaller, weaker, and more isolated than the 4-50 sample. Plastic deformation is more easily induced in small weaker domains. Due to the higher degree of phase mixing, more hard domain is involved in the reorganization. About 22% of the hard segment domain was pulled out into the soft matrix as shown in Figure 4.13.

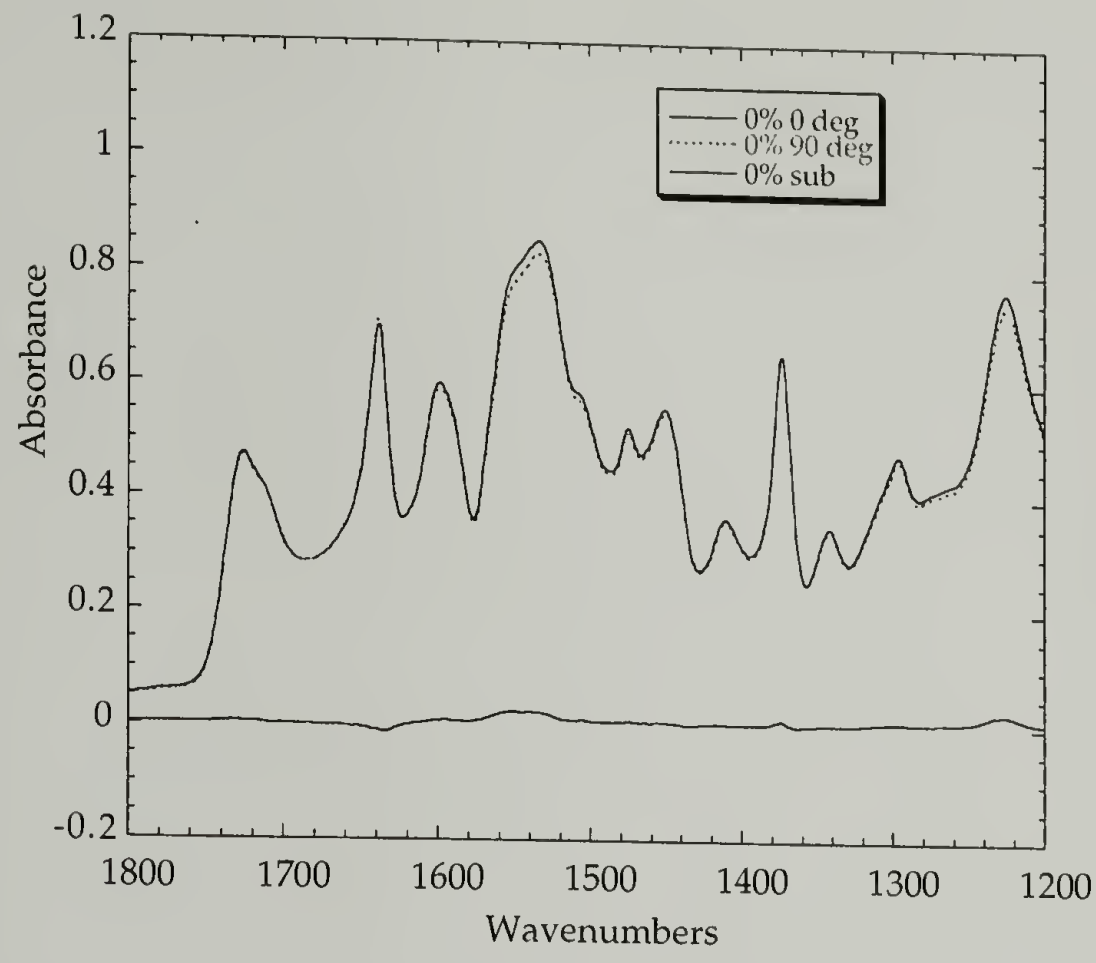

Figure 4.8. Infrared Dichroic Spectra of 4-80 sample before stretching

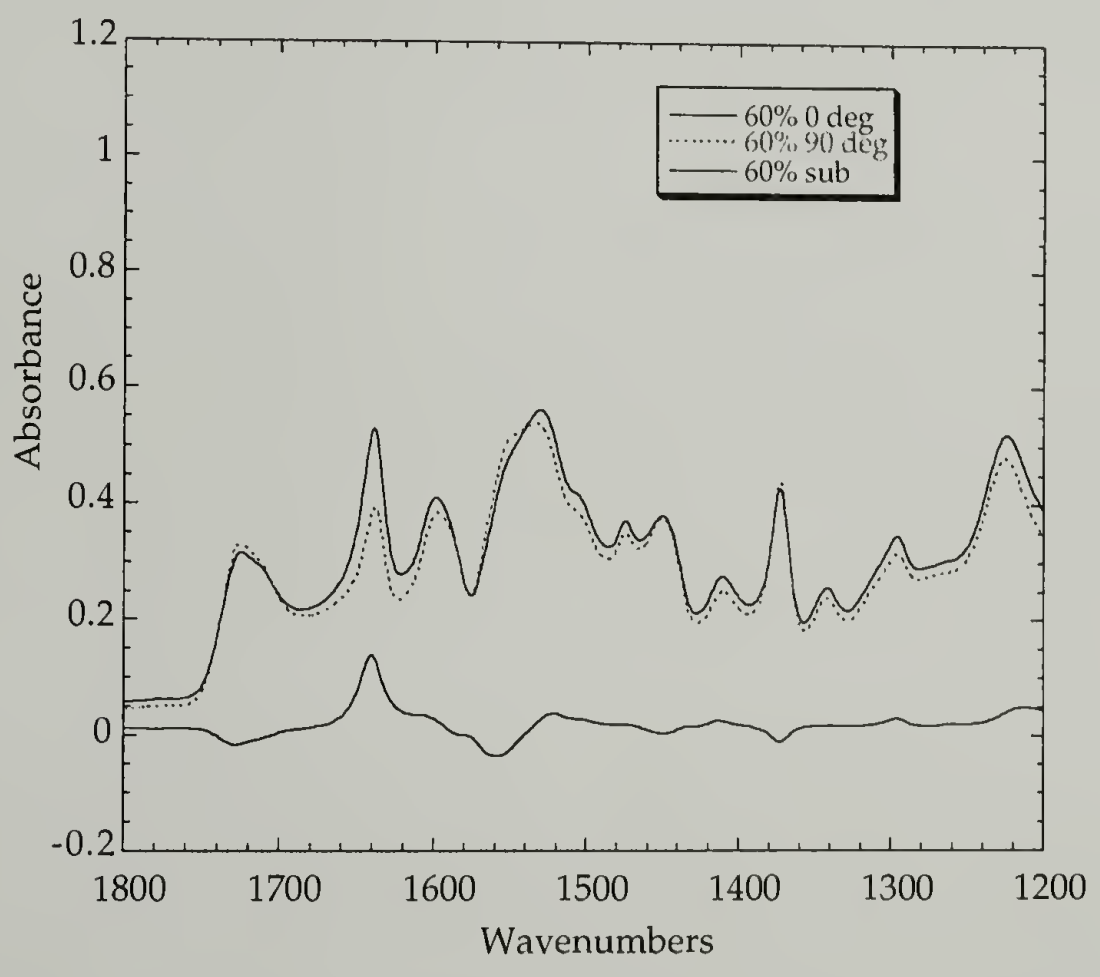

Figure 4.9. Infrared Dichroic Spectra of 4-80 sample stretched at 60% Strain

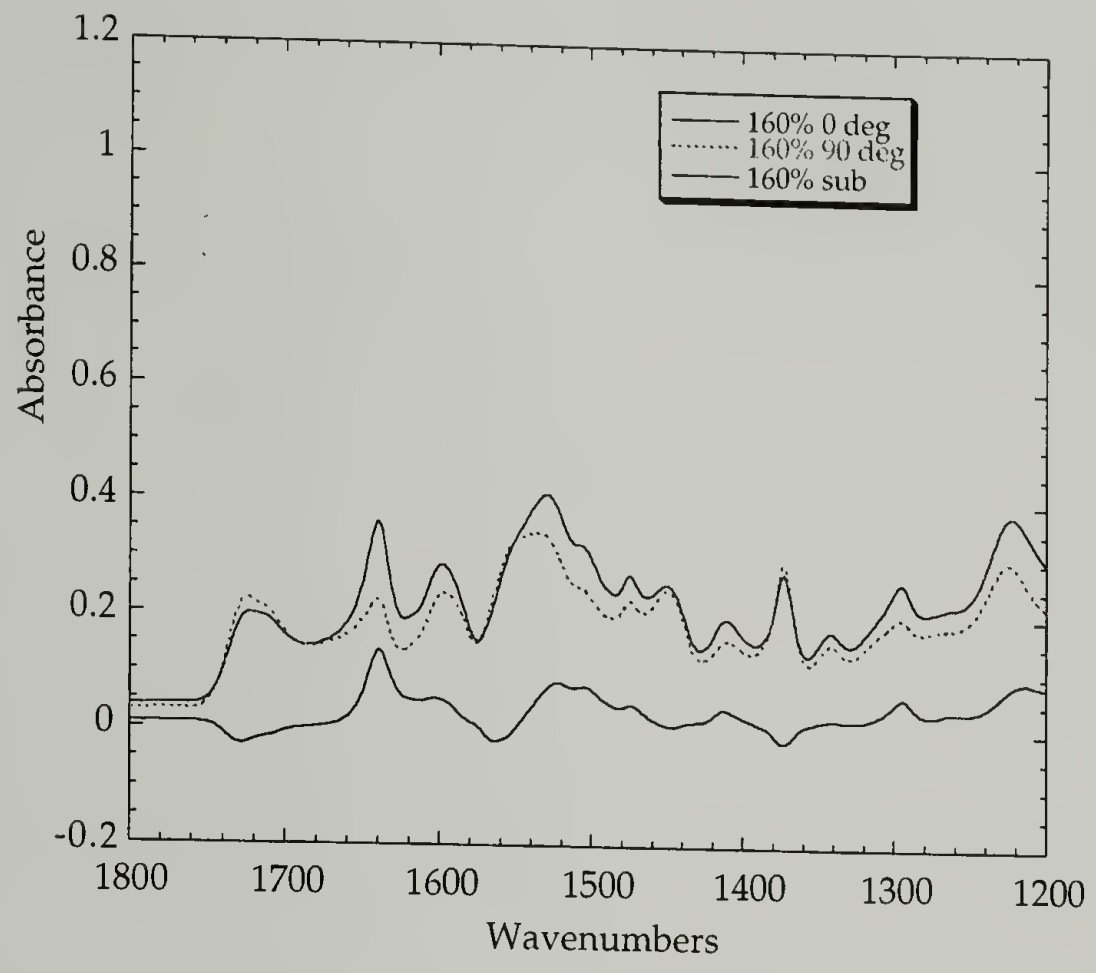

Figure 4.10. Infrared Dichroic Spectra of 4-80 sample stretched at 160% Strain

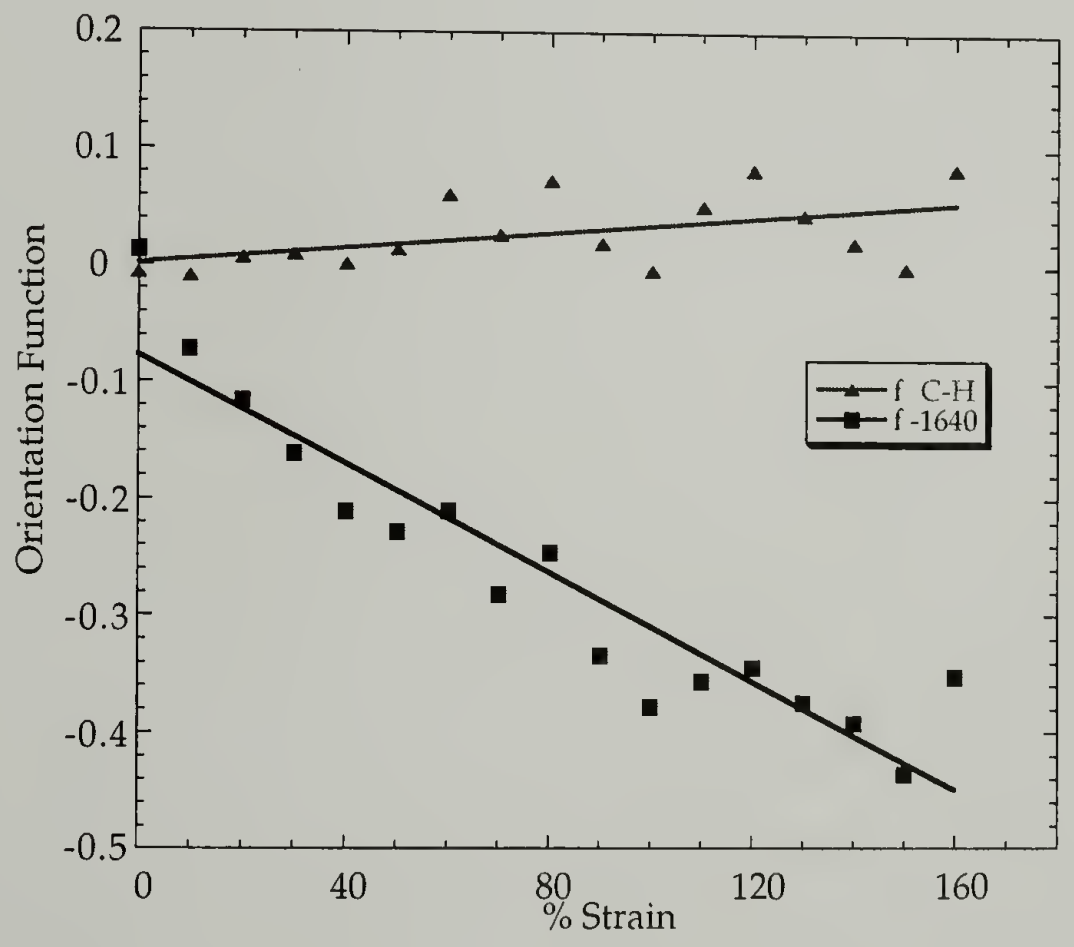

Figure 4.11. The Orientation Function of Soft and Hard Domain for the Polyurethane 4-80 sample

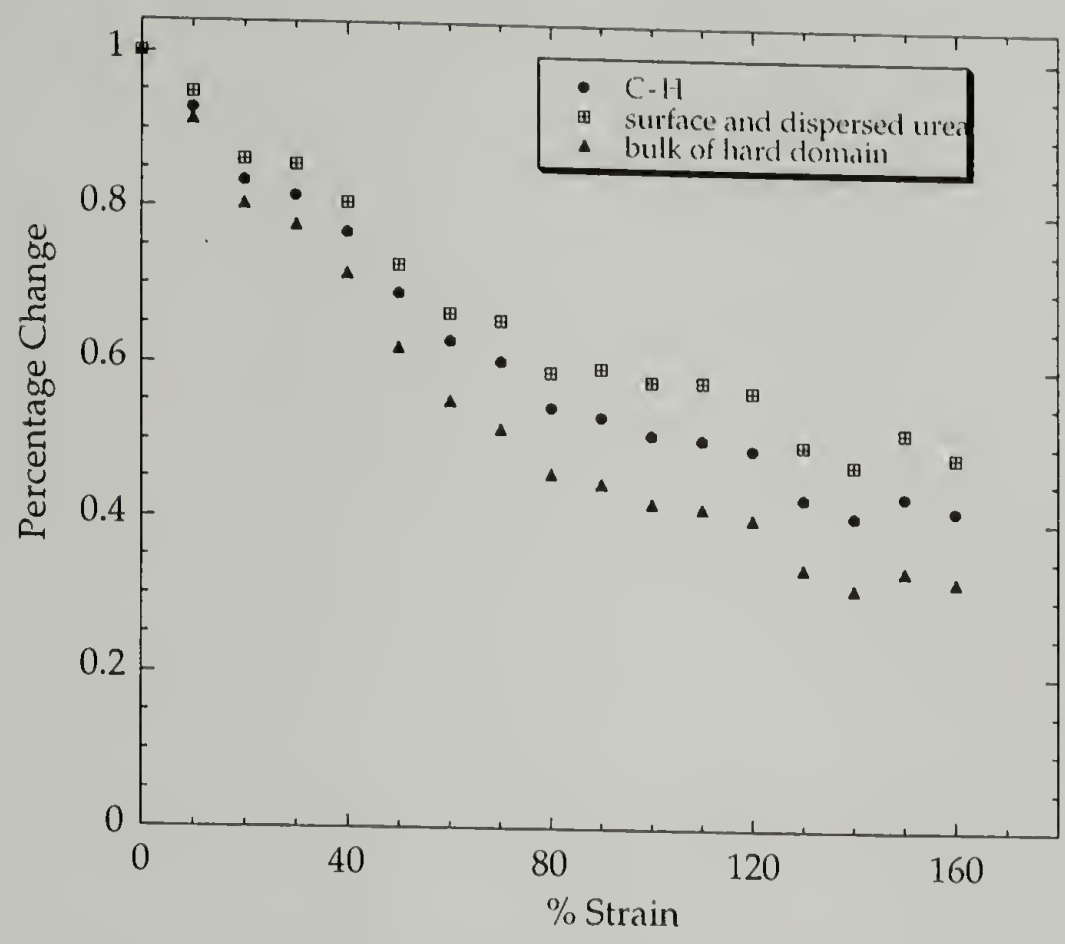

Figure 4.12. Intensity Change within the Hard Domain vs. Dispersed Hard Segments of 4-80 sample under Deformation

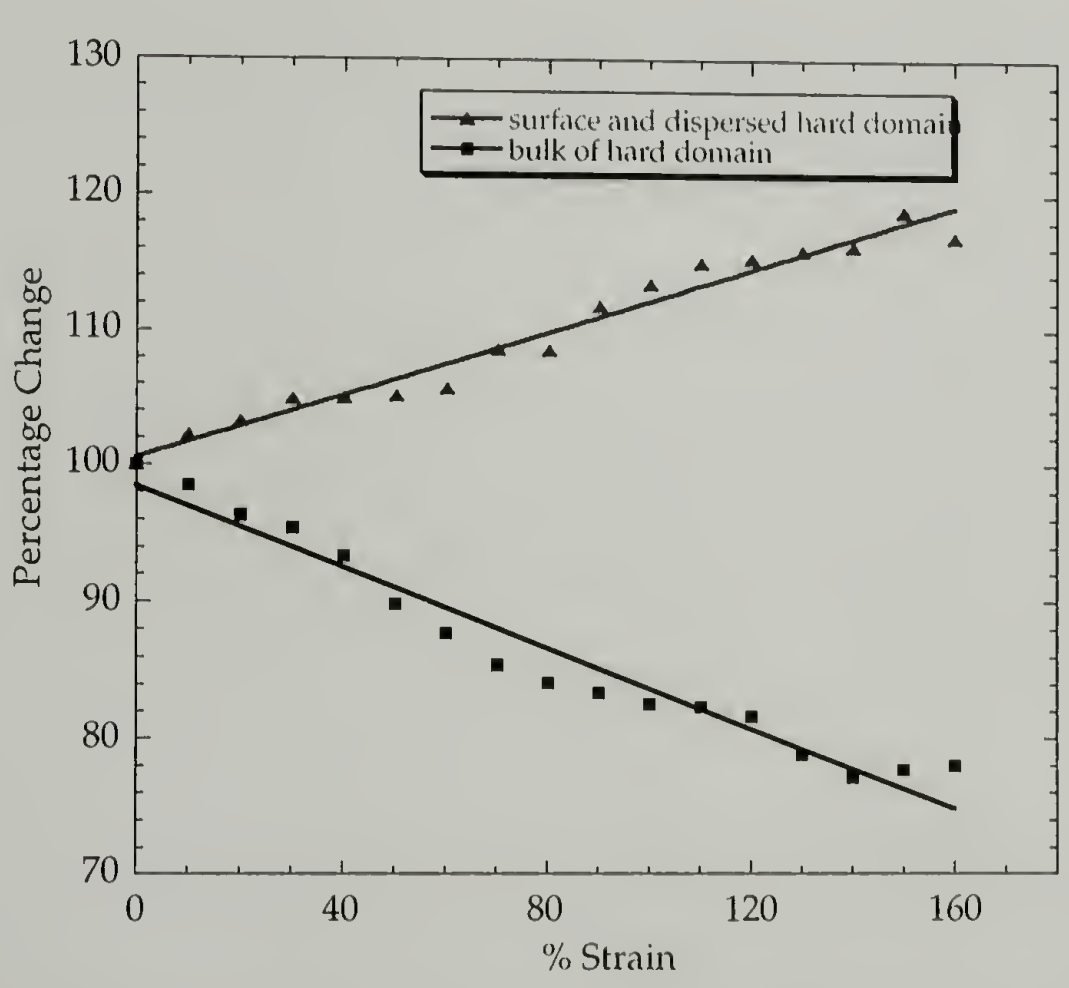

Figure 4.13. Normalized Percentage Change within Hard Domain vs. Dispersed Hard Segments for 4-80 Sample

Two other samples, including 4-50 and 6-80, were studied using infrared dichroism. The results are summarized in Table 4.1. At 100% strain, the percentage change of the hard domain increases for higher volume fraction 6-series samples. Also samples made at higher temperature showed larger change due to higher degree of phase mixing.

Table 4.1. The Percentage Change in the Weight Fraction of Hard Domain upon Stretching

	at 100% Strain	at break
4-50	6%	14%
6-50	15%	19%
4-80	18%	22%
6-80	20%	20%

4.4. Conclusions

The deformation behavior of a polyether urethane urea system has been studied using infrared dichroic measurement. In addition to the amide I region, the amide II region was shown to be important for quantification of the deformation process on a molecular level. The hard domain is not "undeformable" but it rather participates in stretching throughout the deformation process, even at small strains. The interconnecting hard domain region takes the load and distributes the stress evenly to eliminate stress concentration. It is believed that the interfacial region and the degree of phase separation

are crucial for the final mechanical properties of the material. Within the interfacial region, the soft chains are constrained by hard segments. The effective hard domain volume fraction increases and interconnectivity between hard domains contributes to the higher modulus of the material. Upon deformation, the polyether soft chains transfer the stress through the interconnecting interfacial region onto the bulk of the hard domain during stress relaxation. The bulk of the hard domain tends to rotate transverse to the stretching direction. The lower modulus of the interconnecting regions will experience plastic deformation. This allows chains in these regions to slide away from the original position or to pull out into the soft matrix and become dispersed hard segments. The observation using infrared dichroism demonstrated large plastic deformation in the hard domain. This explains the large hysteresis and stress softening effect for polyurethanes, even at small strains. For design of high performance polyurethane materials, the interconnecting morphology and the compromise between bulk hard domain and interconnecting interfacial regions determines the final performance of the material. Controlling the right morphology is important for obtaining high modulus and more durable polyurethane materials.

4.5. References

1) Smith, T. L. *Polymer Engineering and Science* **1977**, *17*, 129-143.

2) Paik Sung, C. S.; Smith, T. W.; Sung, N. H. *Macromolecules* **1980**, *13*, 117-121.

3) Lin, S. B.; Hwang, K. S.; Tsay, S. Y.; Cooper, S. L. *Colloid Polym. Sci.* **1985**, *263*, 128-140.

4) Gorce, J.-N.; Hellgeth, J. W.; Ward, T. C. *Polym. Eng. Sci.* **1993**, *33*, 1170-1176.

5) Godovsky, Y., K.; Bessonov, N. P.; Mironova, N. N. *Colloid & Polymer Science* **1989**, *267*, 414-420.

6) Paik Sung, C. S.; Smith, T. W.; Hu, C. B.; Sung, N.-H. *Macromolecules* **1979**, *12*, 538-540.

7) Siesler, H. W. *Rheo-Optical Fourier-Transform Infrared Spectroscopy: Vibrational Spectra and Mechanical Properties of Polymers*; Springer-Verlag: Berlin, **1984**; Vol. 65.

8) Siesler, H. W.; Holland-Moritz, K. *Infrared and Raman Spectroscopy of Polymers*; Marcel Dekker, Inc.: New York, **1980**.

9) Zbinden, R. *Infrared Spectroscopy of High Polymers*; Academic Press, Inc.: New York, **1964**.

10) Fraser, R. D. B. *J. Chem. Phys.* **1953**, *21*, 1511.

11) Siesler, H. W. *Berichte Der Bunsen-Gesellschaft-Physical Chemistry Chemical Physics* **1988**, *92*, 641-645.

12) Siesler, H. W. *Polymer Bulletin* **1983**, *9*, 382-389.

13) Samuels, R. J. *J. Macromol. Sci. - Phys.* **1970**, *B4*, 701-759.

14) Samuels, R. J. *J. Polym. Sci., A* **1965**, *3*, 1741-1763.

15) Peterlin, A. *Plastic Deformation of Polymers*; Marcel Dekker, Inc.: New York, **1971**.

16) Estes, G. M.; Seymour, R. W.; Cooper, S. L. *Macromolecules* **1971**, *4*, 452-457.

17) Ishihara, H.; Kimura, I.; Saito, S.; Ono, H. *J. Macromol. Sci. Phys.* **1974**, *B10*, 591-618.

18) Seymour, R. W.; Allegrezza, A. E.; Cooper, S. L. *Macromolecules* **1973**, *6*, 896-902.

19) Petrovic, Z. S.; Ferguson, J. *Prog. Polym. Sci.* **1991**, *16*, 695.

20) Yamamoto, T.; Shibayama, M.; Nomura, S. *Polymer Journal* **1991**, *23*, 311-320.

21) Lee, H. S.; Hsu, S. L. *Journal of Polymer Science: Part B: Polymer Physics* **1994**, *32*, 2085-2098.

22) Moreland, J. C.; Wilkes, G. L. *Journal of Applied Polymer Science* **1991**, *43*, 801-815.

23) Wang, C. B.; Cooper, S. L. *Macromolecules* **1983**, *16*, 775-786.

24) Read, B. E.; Stein, R. S. *Macromolecules* **1968**, *1*, 116.

25) Yontz, D. J. *An Analysis of Molecular Parameters Governing Phase Seperation in a Reacting Polyurethane System*; University of Massachusetts: Amherst, MA, **1999**, pp 329.

CHAPTER V

WATER TRANSPORT AND PLASTICIZATION MECHANISM IN POLYURETHANES

5.1. Chapter Review

This chapter will cover the viscoelastic properties of polyurethane under humid environment. It is important to understand how moisture causes the structural and morphological change and thus affects the performance and mechanical properties of polyurethanes. The study aims to explore the water plasticization mechanism and also demonstrate again the importance of the interconnecting hard domain region to the overall properties of polyurethanes. The preliminary stress relaxation data are presented in Section 5.2 to understand the dry and "wet" samples. The swelling stress method presented in Section 5.3 studies the moisture transport properties in polyurethane thin films. The diffusion coefficient of water obtained using this method has been related to the phase separated morphology. In Section 5.4, the swelling stress method is combined with deuterium substitution, and the water plasticization mechanism is further investigated. The increased accessible region of the hard domain and low recovery of stress from the desorption process indicate the hard domain undergoes irreversible plastic deformation at surface and interfacial regions in the stretched state, in addition to the large softening effect in the soft matrix.

5.2. Stress Relaxation Experiments

In a preliminary stress relaxation study shown in Figure 5.1, thin films of a 6-50 sample before and after water plasticization were stretched at 10% initial strain. The strain rate was kept high and constant. The initial stress measured for the dry sample was 7.1 MPa. After water plasticized for 270 minutes, the initial stress was 5.9 MPa. The results were normalized using the initial stress value and plotted on a log-log diagram shown in Figure 5.2. The stress decay for the dry sample obeys a power law as shown in Equation 5.1.

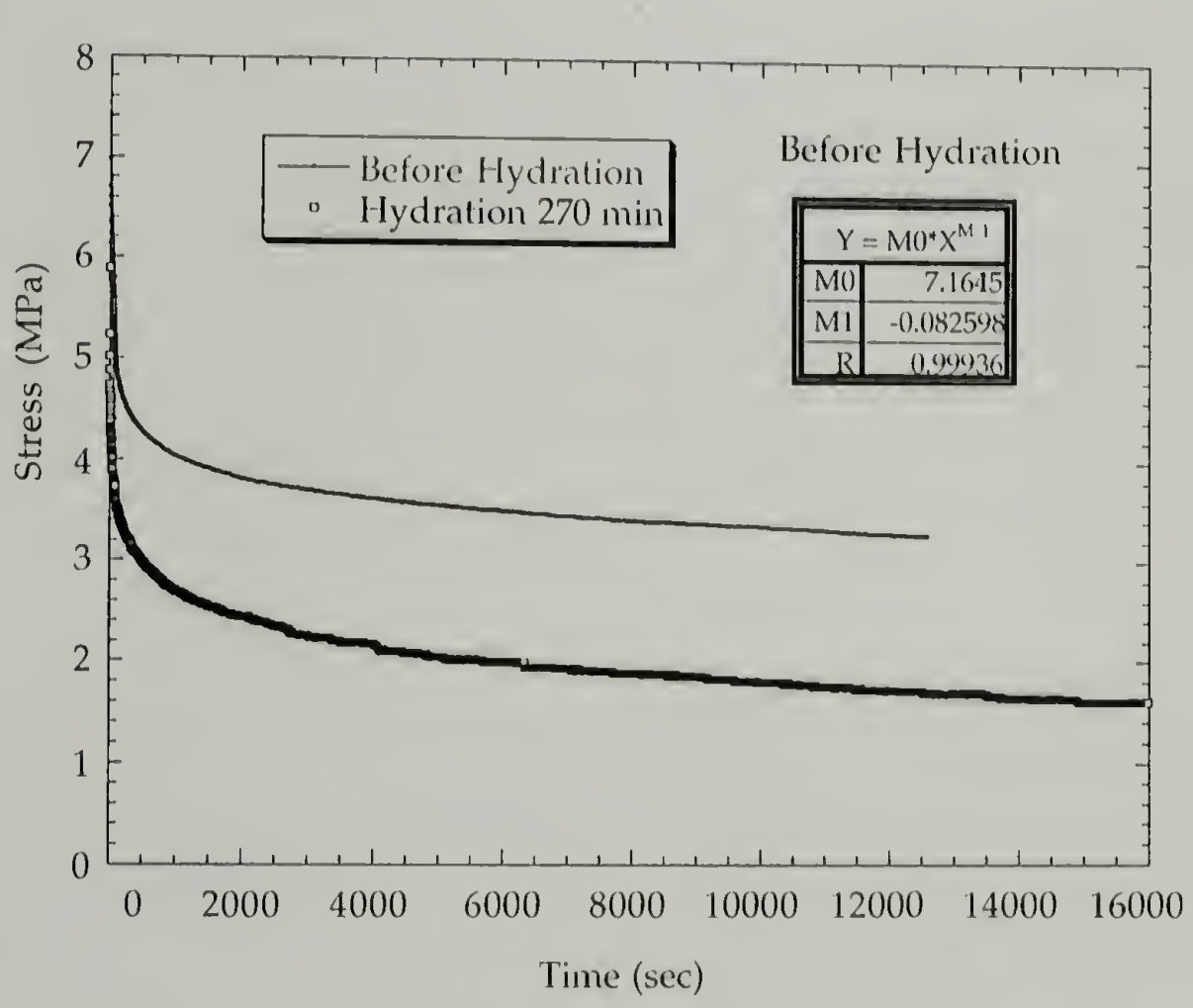

Figure 5.1. Stress relaxation of 6-50 samples before and after hydration

Even though a power-law relationship applies to a variety of systems, including foams, the exact mechanism is still unknown. [1-3]

Equation 5.1. $$\sigma(t) = 7.16t^{-0.083}$$

The time of half decay of the initial stress for the dry and "wet" samples

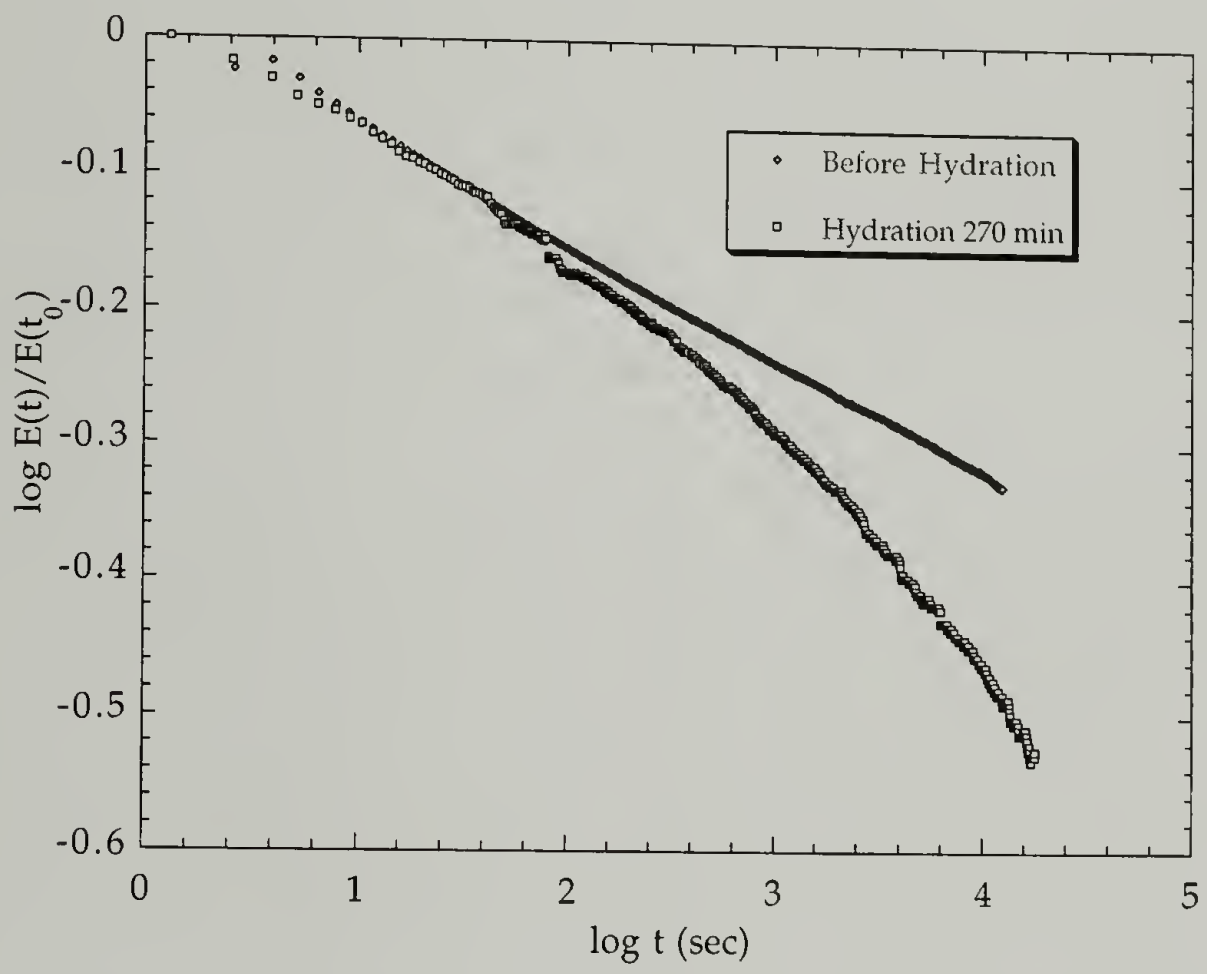

Figure 5.2. Log-log plot of stress relaxation of 6-50 sample before and after hydration

was 6310 and 1230 seconds, respectively. The stress of the "wet" sample decayed five times faster than that of the dry sample. Furthermore, at longer times the decrease of the stress of the "wet" sample accelerates, which indicates plastic flow of the material after

being plasticized. The viscoelastic response of the block copolymers is a direct consequence of a plastic deformation of the hard phase. The soft matrix can be considered to respond essentially in an elastic manner. [4-7] This phenomenon can be attributed to water softening effects on the hard domain since the plastic deformation of the hard domain contributes to the relaxation at longer times. The plasticization mechanism will be discussed in more detail in the following sections.

5.3. Water Transport Properties

The swelling stress method has been shown to be an effective way to study the transport properties of moisture in thin film samples. [8-10] For constant strain, the sample is initially stretched to a certain strain. After stress relaxation to the steady state, water vapor is introduced into the chamber, and the changes in stress monitored *in situ*. This change in the stress is called swelling stress, which is associated with moisture diffusion. It has been shown that the swelling stress is proportional to the mass uptake, and the mass diffusivity can be retrieved from the data. [9]

In Figure 5.3, a typical swelling stress experiment has been conducted on a polyurethane thin film. A dry 4-50 sample was initially stretched at 20% strain and the stress relaxed for about 10 hours. Moisture at 75% relative humidity was introduced into the testing chamber. The sample showed a further decrease in stress soon after moisture absorption. The second stage of the stress relaxation can be used to measure moisture transport properties in polyurethane thin film.

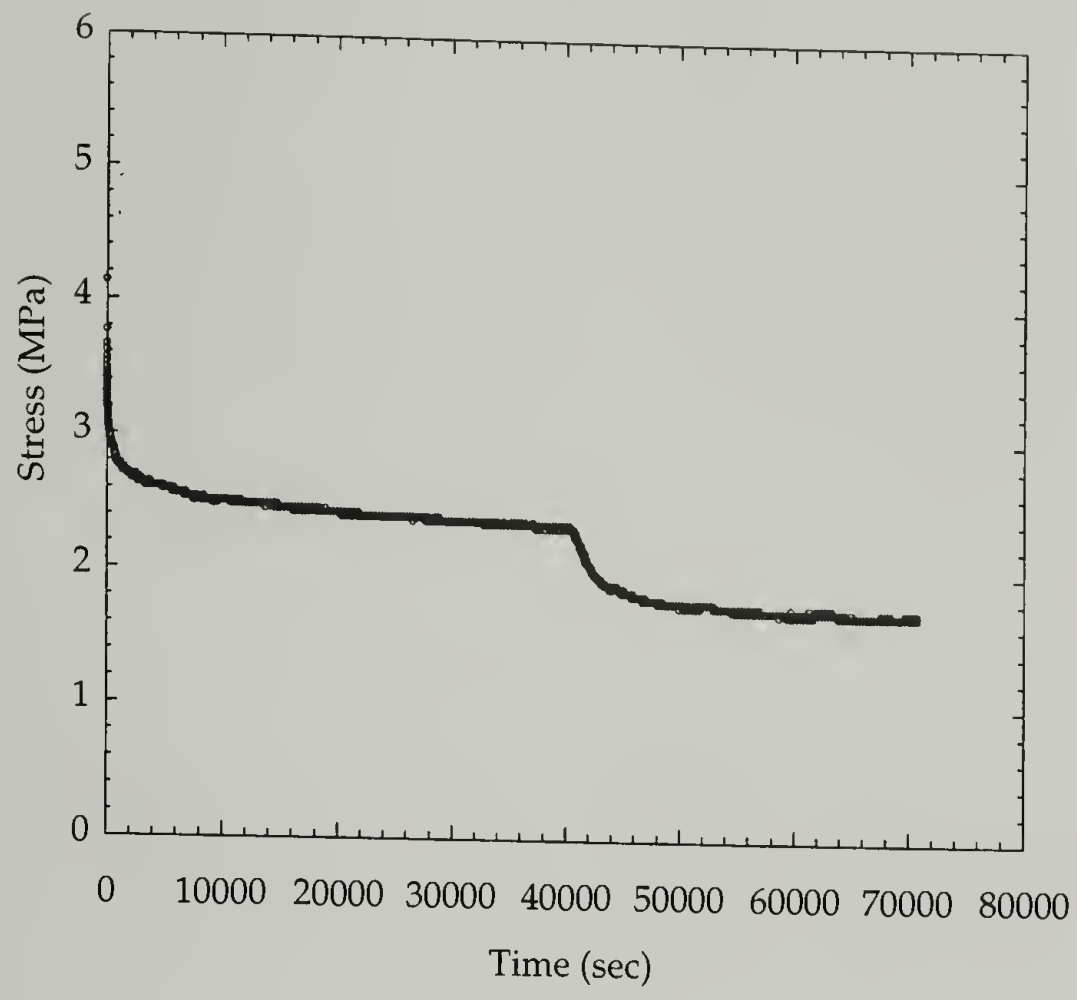

Figure 5.3. Swelling stress experiment on 4-50 sample

Based upon diffusion of small molecules in polymers studied at constant temperature and vapor pressure, [11-14] the increase in weight of a sheet of thin film of thickness l and hence the rate of the mass uptake of water vapor. The solution of the diffusion equation is written as:

Equation 5.2. $$\frac{M_t}{M_\infty} = 1 - \frac{8}{\pi^2}\sum_{m=0}^{\infty}\frac{1}{(2m+1)^2}\exp\left\{-D(2m+1)^2\pi^2 t/l^2\right\}$$

The application of this equation is based on the assumption that immediately the thin film is placed in the vapor the concentration at each surface attains a value

corresponding to the equilibrium uptake for the vapor pressure, and remains constant afterwards. The value of the half time for which $M_t/M_\infty = 0.5$, is given by

Equation 5.3. $$\left(\frac{t}{l^2}\right)_{1/2} = -\frac{1}{\pi^2 D}\ln\left\{\frac{\pi^2}{16} - \frac{1}{9}\left(\frac{\pi^2}{16}\right)^9\right\}$$

Thus the diffusion coefficient D can be obtained as:

Equation 5.4. $$D = \frac{0.049}{\left(\frac{t}{l^2}\right)_{1/2}}$$

Or using the initial slope, the diffusion coefficient can be calculated as:

Equation 5.5. $$D_{eff} = 3.14\left[\frac{(slope)(l)}{4}\right]^2$$

In this way, the kinetics of stress decrease during moisture adsorption may be followed and the transport properties of moisture in the polyurethane thin films can be studied by initial slope and half-time methods. If the diffusion is Fickian, the diffusion coefficient obtained by these two methods should be identical, but different for non-Fickian diffusion.

As shown in Figure 5.4, the half time method was applied to obtain the diffusion coefficient of water. The half time $t_{1/2}$ was 1778 seconds and the film thickness was 21 μm. Using Equation 5.4, the diffusion coefficient was calculated as $1.22*10^{-10}$ cm^2/sec.

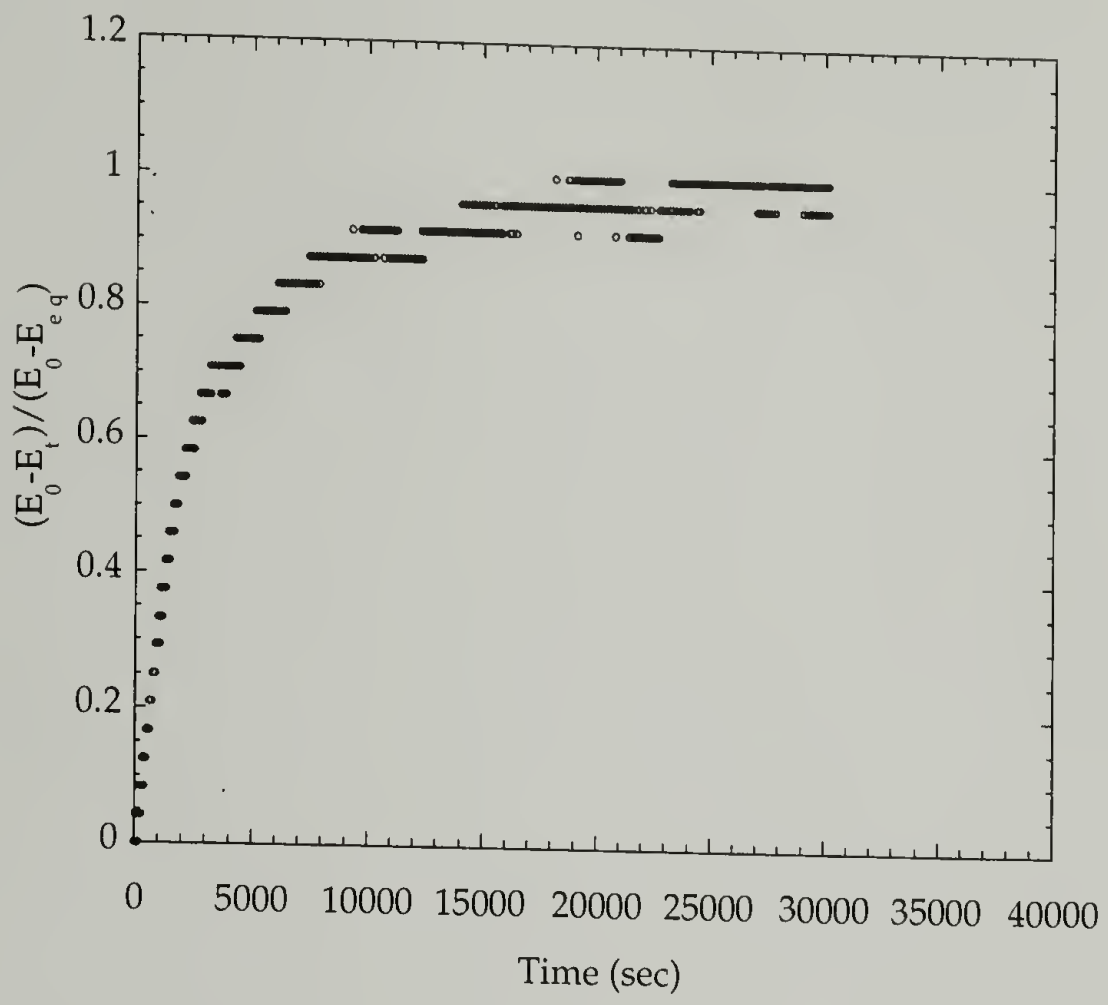

Figure 5.4. Normalized plot to calculate mass diffusivity in half-time method

For short times, the plot depicted in the Figure 5.5 of M_t/M_∞ vs. $t^{1/2}$ was linear up to $M_t/M_\infty = 0.6$. The initial slope was 0.018 $s^{-1/2}$, and using the initial slope method of Equation 5.5, another diffusion coefficient value was obtained as $2.65*10^{-10}$ cm^2/sec. The results are listed in Table 5.1.

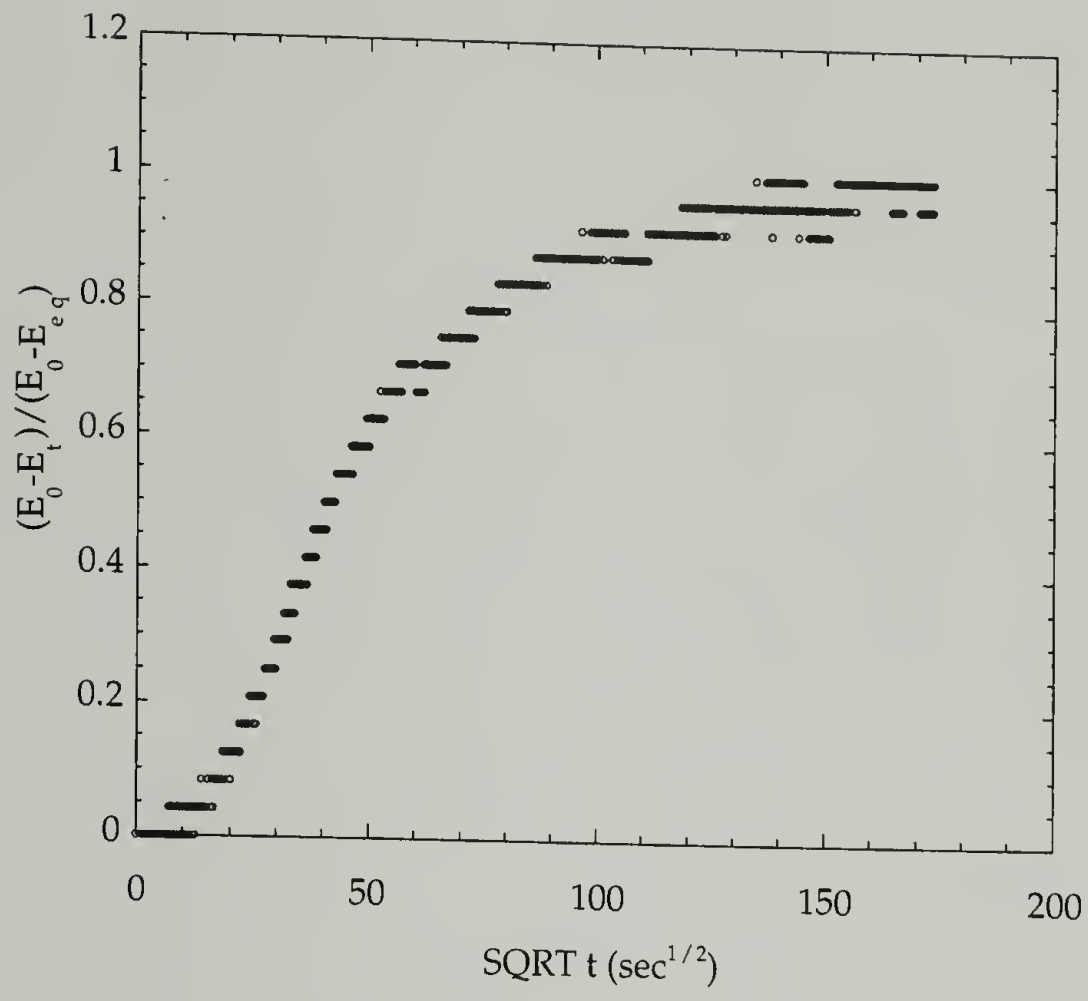

Figure 5.5. Normalized plot to calculate mass diffusivity in initial slope method

From Table 5.1, the higher temperature sample apparently has a higher diffusion coefficient, which suggests that the rate of water penetration is greater. Furthermore, the results by two methods for the 50 °C sample are more consistent, indicating a Fickian diffusion for the low temperature sample, while for the 80 °C sample, a large difference in the diffusion coefficient results suggests a non-Fickian characteristic.

The diffusion behavior of moisture in polyurethane can be related to the phase separated morphology. Water accessible regions for phase separated polyurethane thin film at room temperature is largely in the soft matrix but partially also in the surface of the hard domain and the boundary between hard and soft domains. [15] Water diffusion

follows Fick's law in these regions. This is found to be true for the samples made at 50 °C. The larger discrepancy in the diffusion coefficients for 80 °C samples by these two methods suggests that moisture competes with hydrogen bonding in the soft matrix as more hard segments are dispersed in the soft matrix due to an increase in the degree of phase mixing. Thus, the diffusion behavior becomes non-Fickian.

Table 5.1. Diffusion coefficient obtained from swelling stress method

Diffusion Coefficient (cm^2/sec)	Initial slope	Half time
4-50	$2.65*10^{-10}$	$1.22*10^{-10}$
6-50	$2.38*10^{-10}$	$9.18*10^{-11}$
4-80	$1.30*10^{-8}$	$2.31*10^{-10}$
6-80	$6.24*10^{-8}$	$8.69*10^{-10}$

5.4. Water Plasticization Mechanism

Combined with deuterium substitution, D_2O accessibility can serve as a probe to indicate where water goes in the specific regions of the phase separated morphology of polyurethanes. The real time infrared spectra are shown in Figure 5.6. The inaccessible

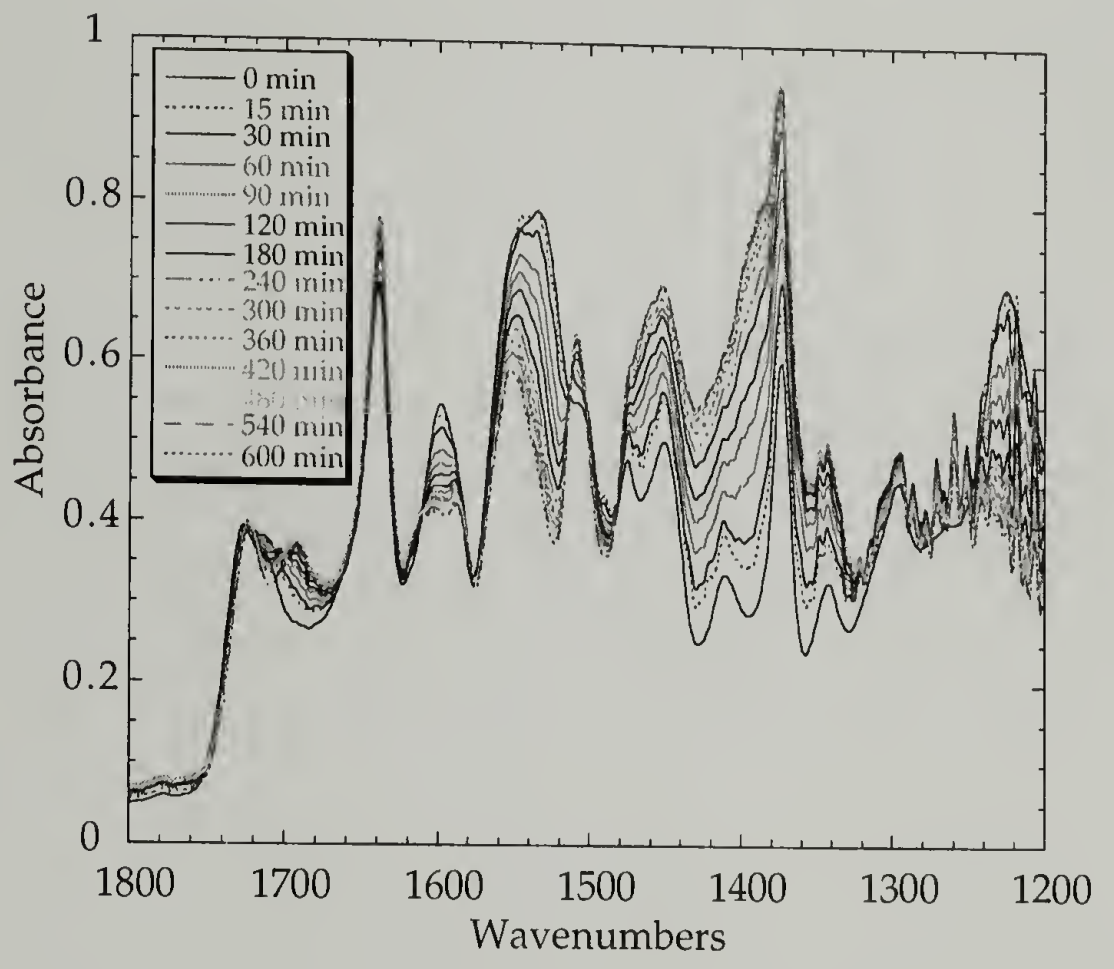

Figure 5.6. Infrared spectra of deuterium substitution on stretched 4-50 sample

region of the urea hard domain was 62% for a stretched 4-50 sample as shown in Figure 5.7. The accessible region was increased by around 10% compared to unstretched samples. The same happened for 6-50 sample, in which the inaccessible region of urea groups was 69%, an increase of 9% above the unstretched state. The increased

accessibility suggests that the accessible hard domain regions underwent plastic deformation. Some hard segment chains were pulled away from the hard domain through surface and interfacial regions. Thus more hard domain could be accessed.

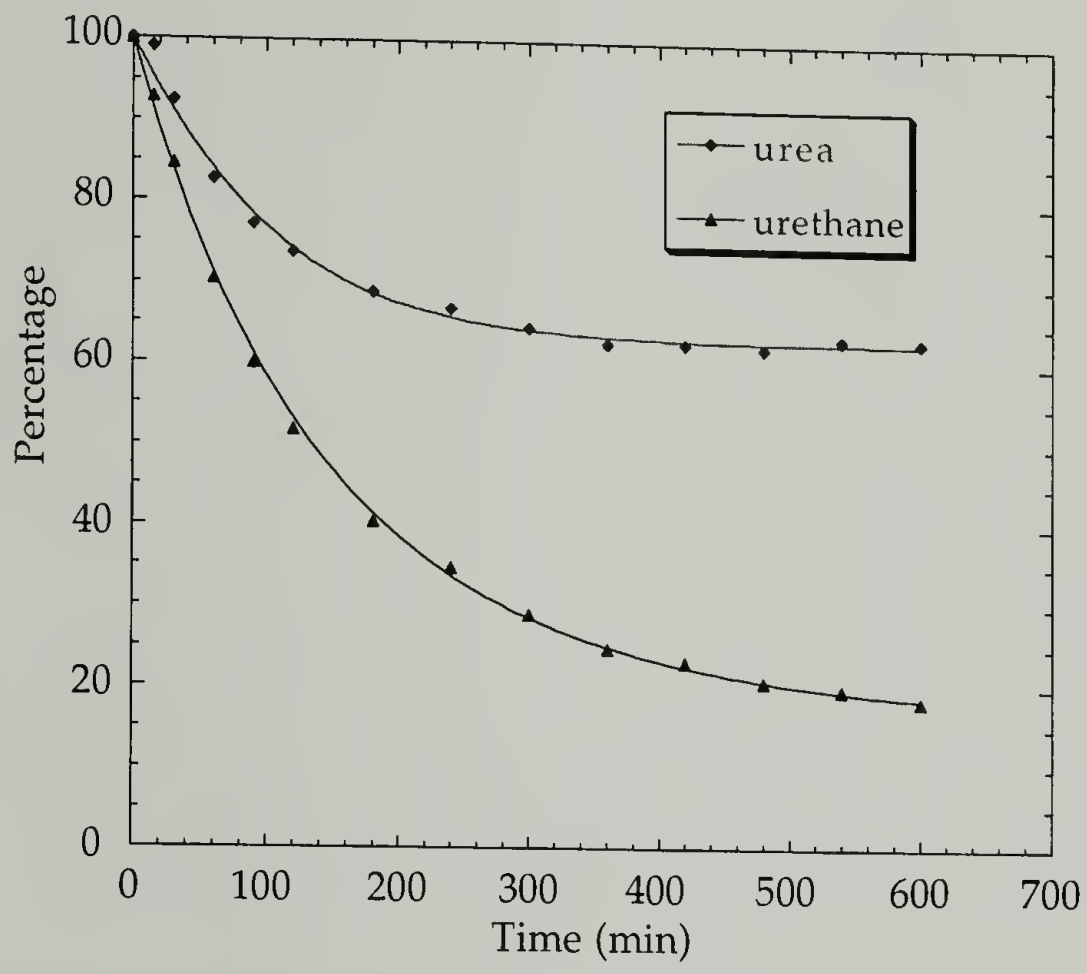

Figure 5.7. Percentage of inaccessible region of 4-50 sample under stretched state

Based upon the deuterium substitution results obtained in the previous chapter, the surface and interconnecting regions of the hard domain are accessible at room temperature, and the surface region will be weakened. Infrared dichroism showed that the hard domain tends to rotate transversely to the stretch direction under deformation. [16-18] The difficulty of rotational motion of the hard domains is related to the overall modulus measured. [19] It is expected that the hard domain can rotate more easily after plasticization at the surface region. This could be one of the reasons for lower modulus in water plasticized sample.

Another interesting observation can be obtained by investigating the kinetics of the extent of substitution reactions of both urea and urethane groups. Deuterium substitution is a diffusion controlled chemisorption process. The kinetics of the extent of substitution can be followed if we plot $\frac{(Q_0 - Q_t)}{(Q_0 - Q_{eq})}$ vs. t, as show in Figure 5.8, where Q_0

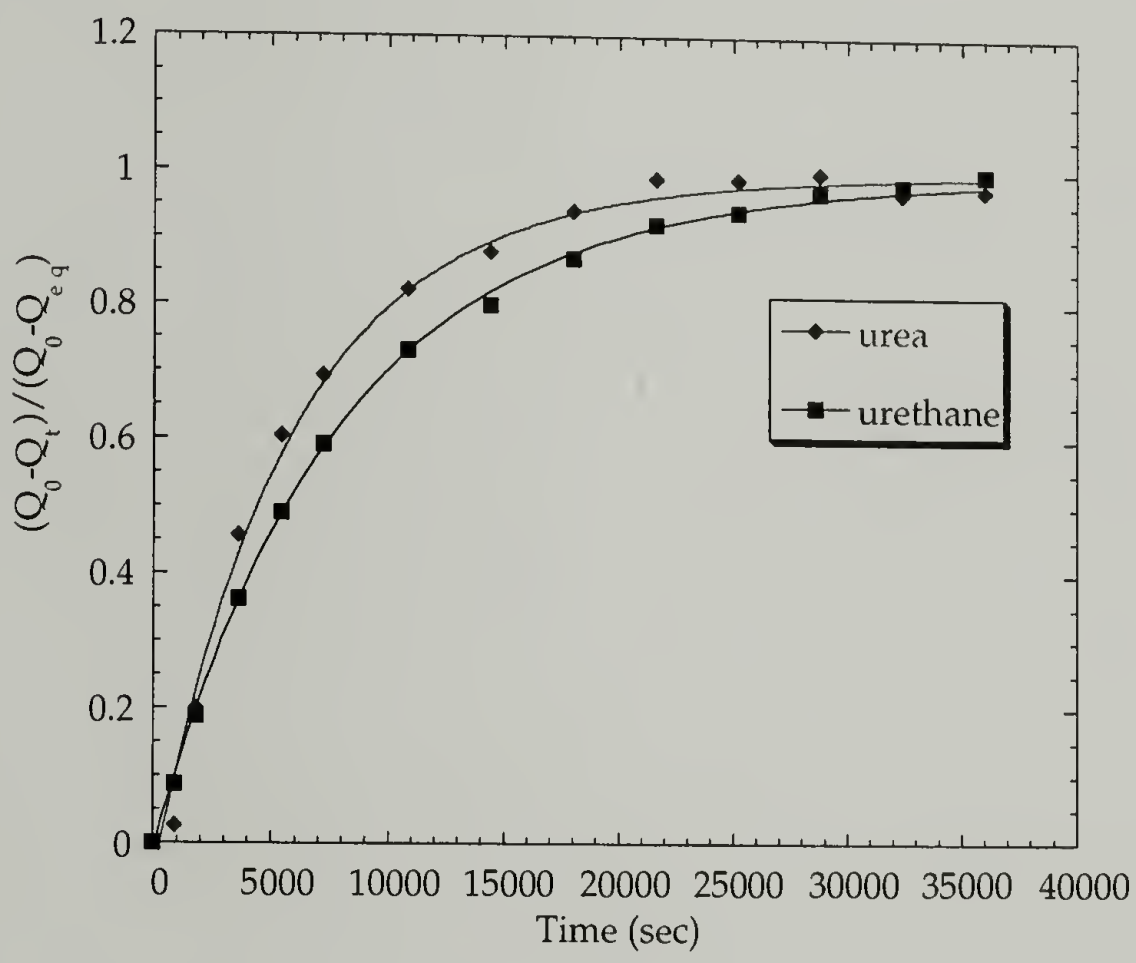

Figure 5.8. Kinetics of the extent of substitution

is the initial intensity of a group and is treated as 100 after normalization; Q_t and Q_{eq} are the normalized intensity of the inaccessible regions at time t and in the equilibrium state. Furthermore, the interaction of moisture with different regions of the separated

morphology can be studied in a unique way as shown in Figure 5.9. The initial linear slope for urethane groups suggested that the moisture interaction of urethane groups or dispersed hard segments obeyed was Fickian, while that of urea groups, which is a glassy state forming the hard domain, deviated and followed non-Fickian behavior.

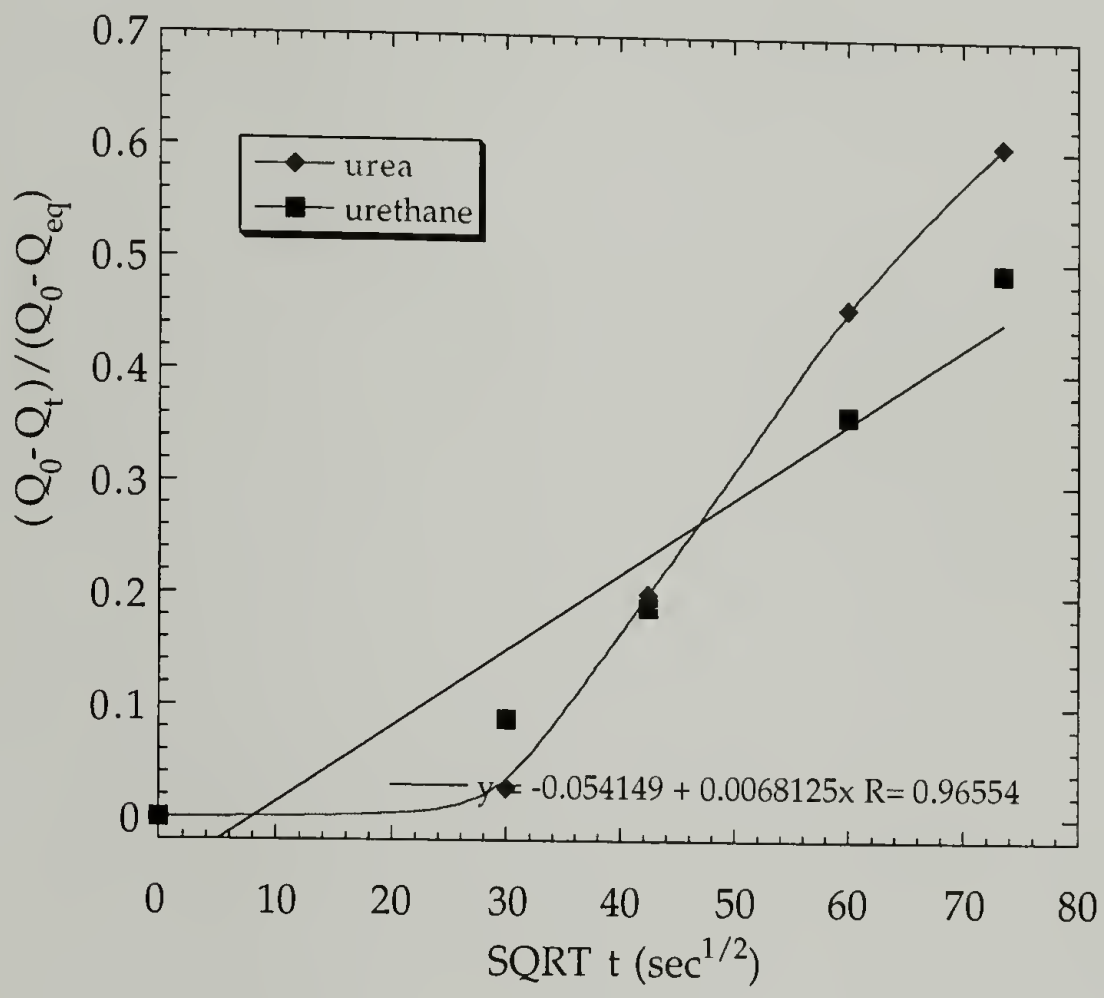

Figure 5.9. Kinetics of the extent of substitution

The interconnecting regions, either the small portion of the direct bridge from the long segments or the disordered hard domain, are also vulnerable to moisture attack, which could result in a decrease of interconnectivity. It can be concluded that both weakening phenomena participated in stress depression and modulus decrease of the plasticized samples. The weaker hydrogen bonds at the surface of the hard domain and the interconnecting region can cause hard segment chains to slide away from the original

position and pull out into the soft matrix. This could further induce plasticization in these regions and progressive substitution can account for an increase in the accessibility of the hard domain. Stress relaxation combined with deuterium substitution can reveal the reinforcement of the physical network of the interconnecting hard domain morphology.

It is expected that plastic deformation of the hard domain and decrease in the interconnectivity within the plasticized sample could account for irreversible stress recovery as shown in Figure 5.10. The initial stress was 5.8 MPa. After the first dry

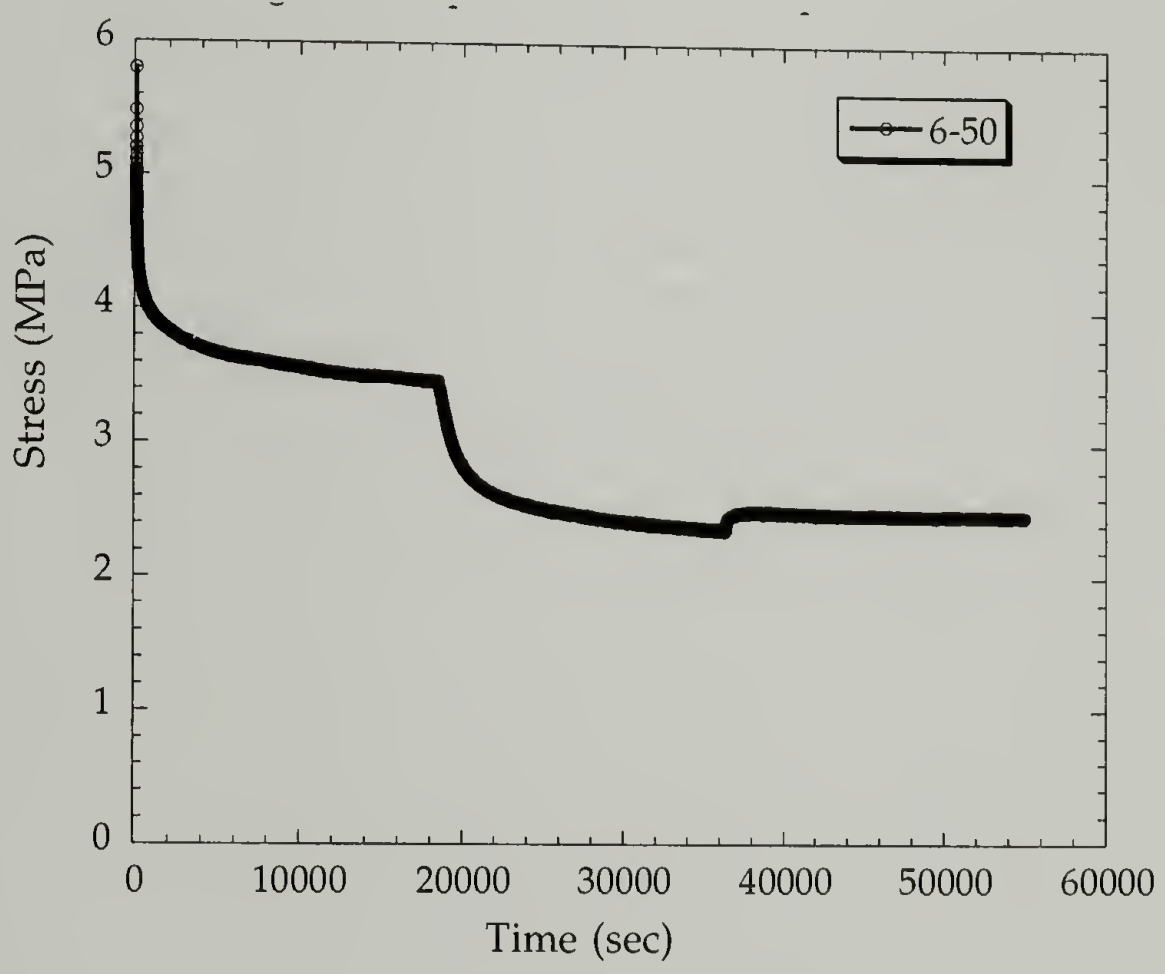

Figure 5.10. Swelling stress experiment of 6-50 sample including desorption

stage of stress relaxation for about 5 hours, the stress reduced to 3.5 MPa, a 40% decrease from the initial value. Upon moisture plasticization at the second stage of about 5 hours, a 32% stress depression from the equilibrium stress was observed. Finally only 3% of the

stress recovered during the desorption procedure. We seek the contribution of the interconnecting elements to both elastic and viscoelastic responses of polyurethanes. The decrease in interconnectivity as a result of moisture weakening were largely attributed to small recovery in the desorption period. Presumably the moisture could desorb from the sample through the soft matrix. This phenomenon was also observed in the dynamic creep experiment under cyclic moisture condition for automotive seating foam samples. [2,15,20-22]

It should be noted that deuterium substitution does not indicate any contribution from the soft matrix even though moisture diffuses through it. Since the amount of moisture sorbed is proportional to the weight fraction of the soft matrix, indicating that water is absorbed in this phase predominantly, the role of the soft matrix is substantial. [15]. Our work emphasizes the role of the surface and the interconnecting regions of the hard domain in the overall stress relaxation process under humid condition.

5.5. Conclusions

The swelling stress experiment has been conducted to understand the transport properties of moisture in the polyurethane thin film samples. Using D_2O as a probe allows simultaneous study of where the absorbed water is and the extent of interaction with specific regions of the hard domain. It is known that the surface and interfacial regions of the interconnecting hard domain morphology are accessible. The excess accessibility of the hard domain morphology of a thin film sample upon stretching compared with that of the undeformed sample suggests that the hard domain undergoes large plastic deformation in these regions where under stress. The small irreversible

stress recovery at desorption period indicates a large decrease in the interconnectivity of the hard domain morphology. The diffusion coefficient of moisture in the polyurethane thin films can be determined by swelling stress measurements. The emphasis on the hard domain contribution to lower mechanical properties under water plasticization has been presented.

5.6. References

1) Paik Sung, C. S.; Smith, T. W.; Sung, N. H. *Macromolecules* **1980**, *13*, 117-121.

2) Moreland, J. C.; Wilkes, G. L.; Turner, R. B. *Viscoelastic Behavior of Flexible Slabstock Polyurethane Foams as a Function of Temperature and Relative Humidity*: Nice, France, **1991**, pp 500-508.

3) Rubinstein, M.; Obukhov, S. P. *Macromolecules* **1993**, *26*, 1740-1750.

4) Smith, T. L.; Dickie, R. A. *J. Polymer Sci. Part C* **1969**, *26*, 163-187.

5) Arnold, K. R.; Meier, D. J. *J. Appl. Polym. Sci.* **1970**, *14*, 427-440.

6) Kamykowski, G. W.; Ferry, J. D.; Fetters, L. J. *J. Polym. Sci: Polym. Phys. Ed.* **1982**, *20*, 2125-2134.

7) Bard, J. K.; Chung, C. I. *Modeling the Elastic Behavior of Poly(Styrene-b-Butadiene-b-Styrene) Block Copolymers*; Legge, N. R., Holden, G. and Schroeder, H. E., Ed.; Hanser: Munich, **1987**.

8) Jou, C.; Sackinger, S. T.; Farris, R. J. *J. Coatings Technol.* **1995**, *67*, 71-77.

9) Sackinger, S. T. *The Determination of Swelling Stresses in Polyimide Film*; University of Massachusetts: Amherst, **1990**.

10) Vrtis, J. K. *Stress and Mass Transport in Polymer Coating and Films*; University of Massachusetts: Amherst, **1995**.

11) Crank, J. *The Mathematics of Diffusion*; Oxford University Press: Oxford, **1956**.

12) Yamamura, H.; Kuramoto, N. *J. Appl. Polym. Sci.* **1959**, *2*, 71-80.

13) Schneider, N. S.; Dusablon, L. V.; Snell, E. W.; Prosser, R. A. *J. Macromol. Sci.-Phys.* **1969**, *B3*, 623-644.

14) Yang, D. K.; Koros, W. J.; Hopfenberg, H. B.; Stannett, V. T. *J. Appl. Polym. Sci.* **1985**, *30*, 1035-1047.

15) Broos, R.; Herrington, R. M.; Casati, F. M. *Journal of Cellular Plastics* **2000**, *36*, 207-245.

16) Ishihara, H.; Kimura, I.; Saito, S.; Ono, H. *J. Macromol. Sci. Phys.* **1974**, *B10*, 591-618.

17) Seymour, R. W.; Allegrezza, A. E.; Cooper, S. L. *Macromolecules* **1973**, *6*, 896-902.

18) Siesler, H. W. *Polymer Bulletin* **1983**, *9*, 382-389.

19) Petrovic, Z. S.; Ferguson, J. *Prog. Polym. Sci.* **1991**, *16*, 695.

20) Huang, J. S.; Gibson, L. J. *J. Mater. Sci* **1991**, *26*, 637-646.

21) Dounis, J.; Moreland, J. C.; Wilkes, G. L.; Turner, R. B. *Polym. Prepr. (Am. Chem. Soc., Div. Polym. Chem.)* **1992**, *33*, 284-85.

22) Dounis, D. V.; Moreland, J. C.; Wilkes, G. L.; Dillard, D. A.; Turner, R. B. *J. Appl. Polym. Sci.* **1993**, *50*, 293-301.

CHAPTER VI

HIGH PERFORMANCE POLYURETHANES INCORPORATING LIGNIN

6.1. Chapter Review

Based upon our understanding of the interconnecting hard domain morphology in the previous chapters, lignin can function as a reinforcing component that effectively enhances the polyurethane materials. This chapter will describe how lignin incorporates into polyurethanes.

Lignin is a polymer consisting of both aromatic and aliphatic portions. It exists in wood as a random three-dimensional network of phenylpropane units linked together in different ways. Lignin is a high-impact strength, thermally resistant thermoset polymer with elastic modulus estimated as 6.6 GPa and a glass transition temperature ranging from 127-193°C. [1,2] It is the skeletal substance of plants and the second most abundant biopolymer after cellulose in nature. Lignin imparts a number of desirable qualities to wood, such as strength. [3] A structural analysis of lignin is carried out in Section 6.2. In Section 6.3, the miscibility and dispersion of lignin in polyol is found to be crucial for effective incorporation of lignin to enhance the properties of polyurethanes. Several studies that include DSC, FTIR, optical microscopy, and viscosity will be presented in the section. Finding the optimized processing condition to make lignin incorporated polyurethane plaques is discussed in Section 6.4. The catalyst package is the important issue to be solved because the diversity of functionality of lignin affects the catalytic ability for urethane chemistry. A better plaque sample can be made once the above two

issues have been addressed and the morphology and mechanical properties of the polyurethane with lignin incorporated are evaluated in the same section. The reinforcing mechanism after incorporating lignin is explored in Section 6.5. The thermal performance of the plaque samples is also investigated.

6.2. Structural Analysis of Lignin

The major structural units for the hardwood and softwood lignins were studied by NMR and infrared spectroscopy. The results are shown in Figures 6.2 - 6.4. The hydroxyl groups can be best characterized using infrared spectroscopy as identified with a broad O-H stretching region at 3600-3100 cm^{-1}. The absorption band in the region 1700-1720 cm^{-1} suggests that there is some contribution from non-conjugated keto groups in the β-position of the phenylpropane side chain. [4] The abundance of

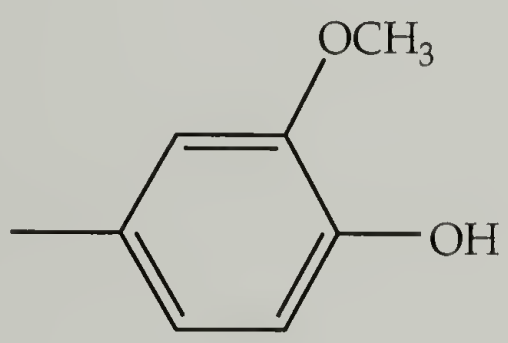

Figure 6.1. Chemical structure of guaiacyl group

guaiacyl groups in softwood lignin is indicated by its characteristic band at 1275 cm^{-1}. The chemical structure of guaiacyl group is shown in Figure 6.1. [5] The aromatic methoxy groups in hardwood lignin are suggested by an infrared band at 1190 cm^{-1}.

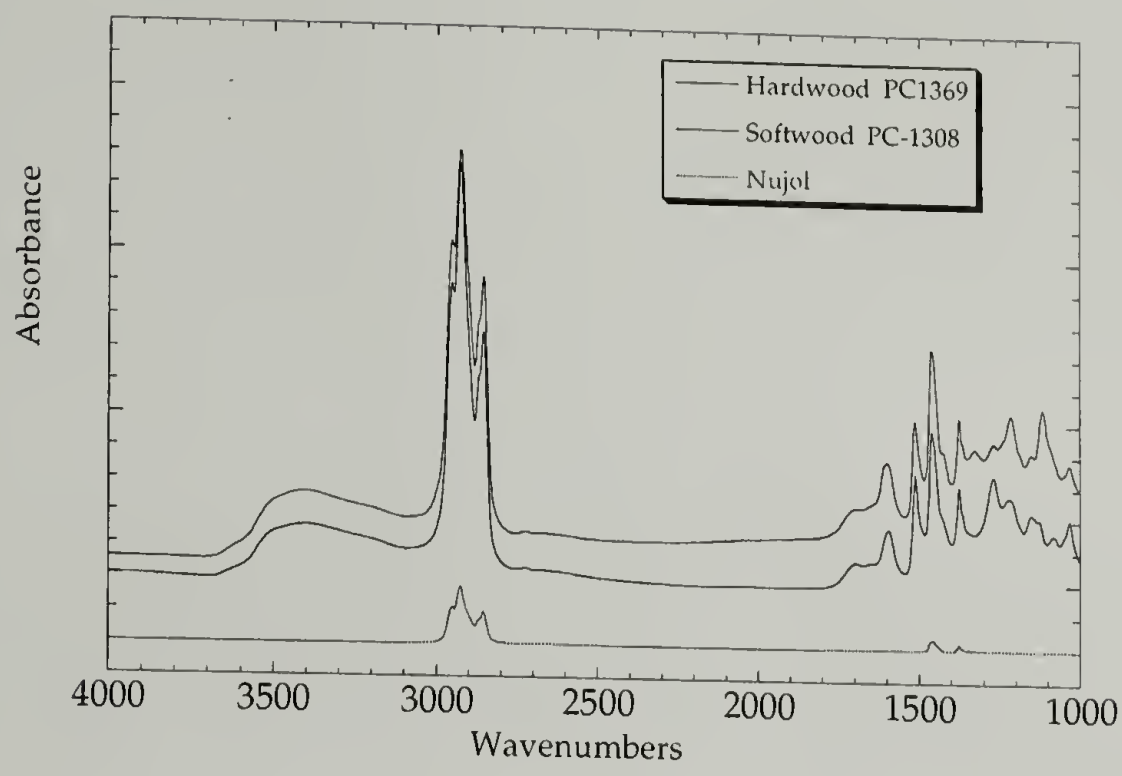

Figure 6.2. FTIR spectrum of lignin samples (Nujol)

The NMR results further verified the existence of certain structural features, such as CH_3CO-, -OCH_3, -OCH_2-, in the hardwood and softwood lignin. Based upon the difference in the chemical shift, the ratio of aromatic (between 6 and 8 ppm) to aliphatic (between 0 and 2.5 ppm) could be estimated from integration results. It was found that the ratio was 2.0 for hardwood lignin and 1.6 for softwood lignin. The ratio is believed to be an important parameter of thermostability of lignin samples. [6]

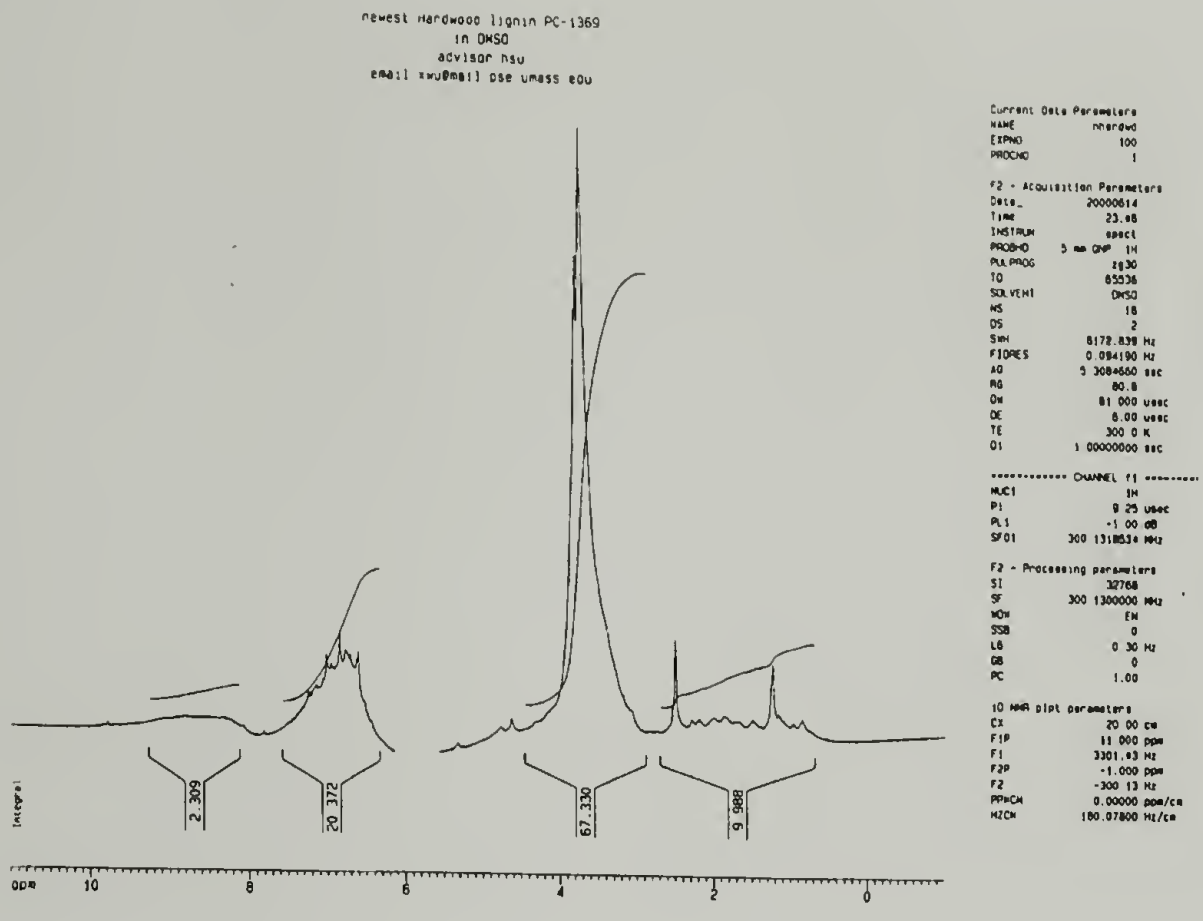

Figure 6.3. NMR spectrum of Hardwood lignin (PC 1369)

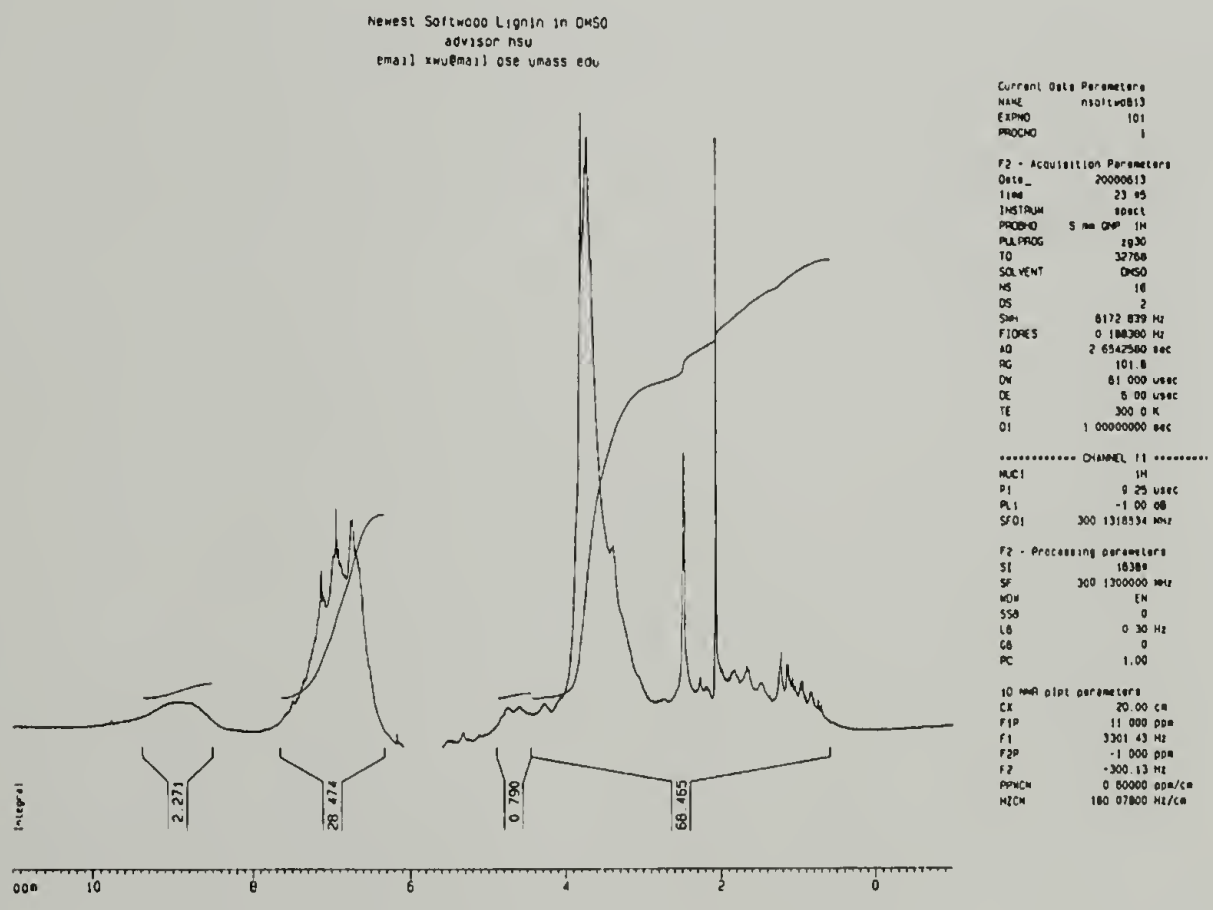

Figure 6.4. NMR spectrum of Softwood Lignin (PC-1308)

It is these structural features that impart lignin with multi-functionality for potential chemical reactions and interactions with other polymeric matrices. The excellent colloidal and rheological properties of lignin particles allow the incorporation of lignin into various polymeric matrices and may eliminate the small local defects for better reinforcement. [7] High aromatic content imparts high stiffness to the materials thus enhancing the properties and possibly thermostability and flame retardance. Lignin can often be used as an organic filler or incorporated into copolymers and polyblends. [8-10] The drawback of lignin, however, is its chemical and molecular weight inhomogeneity due to different resources and processing conditions. [7]

6.3. The Miscibility and the Dispersion State of Lignin in Polyol

Reinforcement, defined by Parkinson, will imply the incorporation into rubber of substances having small particles which give to the vulcanizate high abrasion resistance, high tear and tensile strength and some increase in stiffness. [11] The major limitations of lignin in the application to polyurethane systems are its miscibility with polyol and the change in the reaction kinetics of polyurethane chemistry. Microscopic studies of the reinforcement of elastomers by fillers involve the determination of (1) the size and shape of the filler particles, (2) their distribution or dispersion, (3) filler-polymer wetting phenomena, (4) the adhesion of a filler particle to the matrix. [12,13]

The mechanical behavior of polymer reflects both bulk and localized changes in polymer structure. While elastic modulus is an integral characteristic of a material, strength and toughness are sensitive predominantly to the presence of relatively tiny

structural defects. [14] The primary failure mode for a polymer-filler composite is usually interfacial debonding. The stress concentration at the local defects lowers the strength of the material. [15,16] Therefore the dispersion of lignin in polyol before polymerization is very important. Furthermore, the dispersion and miscibility of lignin with polymeric matrices is important in determining uniformity and structural material properties of lignin incorporated polymers. [17]

It has been reported that the chemical modification of lignin by hydroxyalkylation – forming hydroxypropyl lignin derivatives – builds toughening elements and improves the viscoelastic properties as prepolymers. [18,19] Another method described lignin dissolved in a suitable solvent, such as glycol and reacted with diisocyanate. [20] Also through chemical grafting, the preparation of renewable polymer-synthetic polymer graft copolymers of controlled structures with precise control has been developed. [21] It is found that by heating the dispersion state of lignin can be improved in certain polyol systems. Among the methods reported above, which includes chemical modification, using solvent, chemical grafting and heating, the most economical approach is obviously the heat treatment, since it eliminates the synthesis, purification and extraction steps of the others.

The dispersion state of lignin in polyol is strongly affected by the intra- and inter-molecular interactions and is studied using optical microscopy and infrared spectroscopy, In Figures 6.5-6.6, it is found that before heat treating, the direct mixing sample has lignin particles estimated at the range of 17±3 μm size dispersed in the polyol. After heating with stirring, the size of lignin was reduced to 5±1 μm and was dispersed in

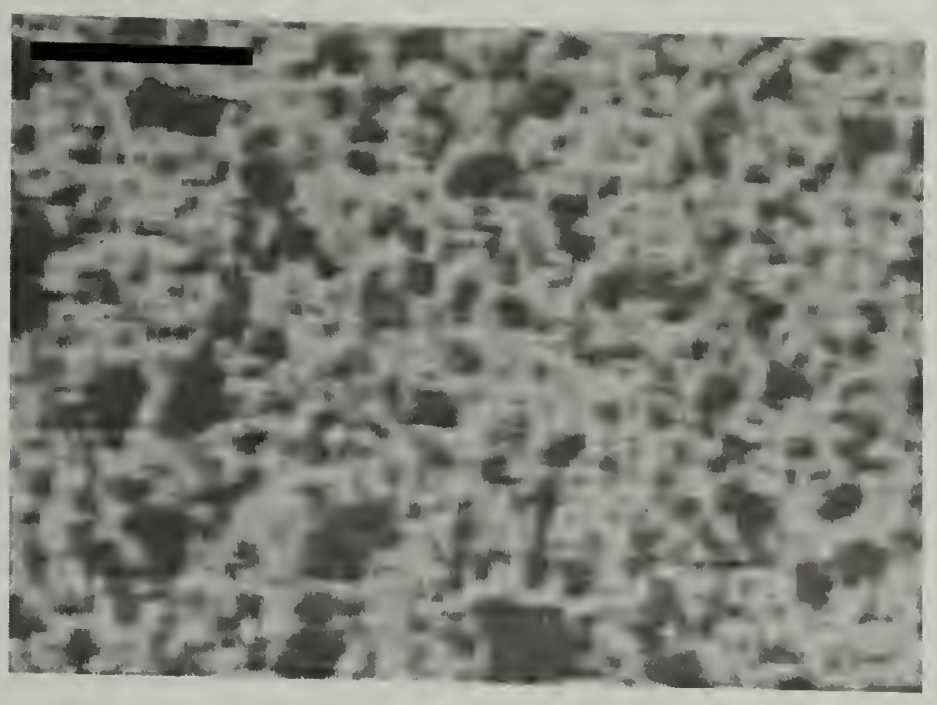

Figure 6.5. Optical microscopy image of 5% hardwood lignin direct mixed in polyol (100 μm bar)

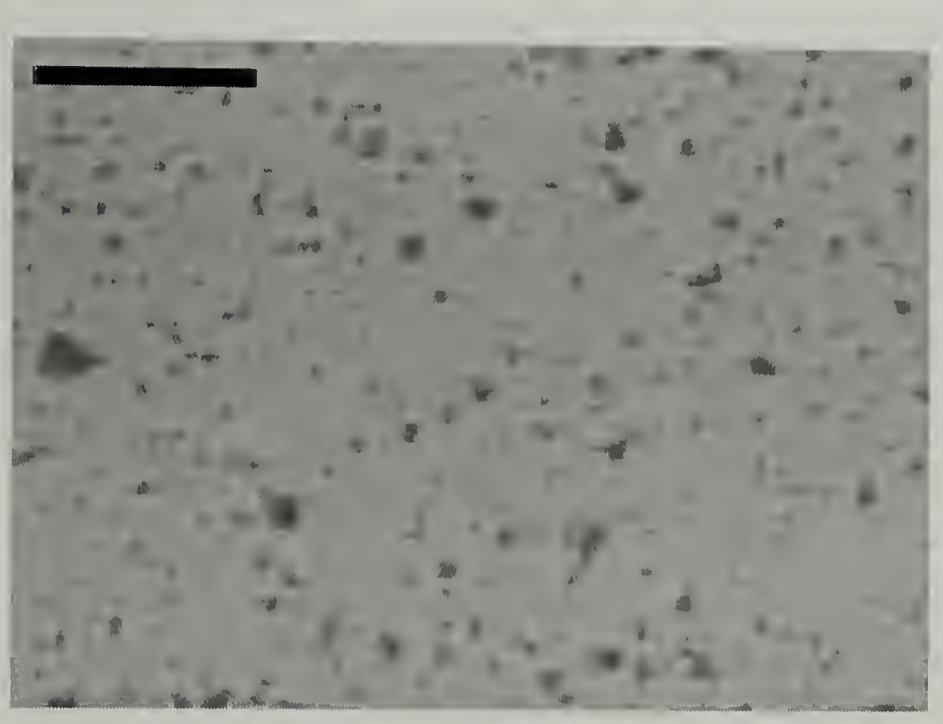

Figure 6.6. Optical microscopy image of 5% hardwood lignin in polyol after heat treatment (100 μm bar)

polyol in a more homogenous way. Before heat treatment lignin forms aggregates through intra- or inter-hydrogen bonding. These hydrogen bonds, however, can be

disrupted and reorganized upon heat treatment and the new interactions with the ether chains and the hydroxyl group of polyol improve the miscibility. This is evident by the infrared measurements of these mixtures under controlled thickness of 50 μm, as shown in Figure 6.7. Before heat treatment, the mixture of lignin and polyol simply showed addition in the free hydrogen bonding

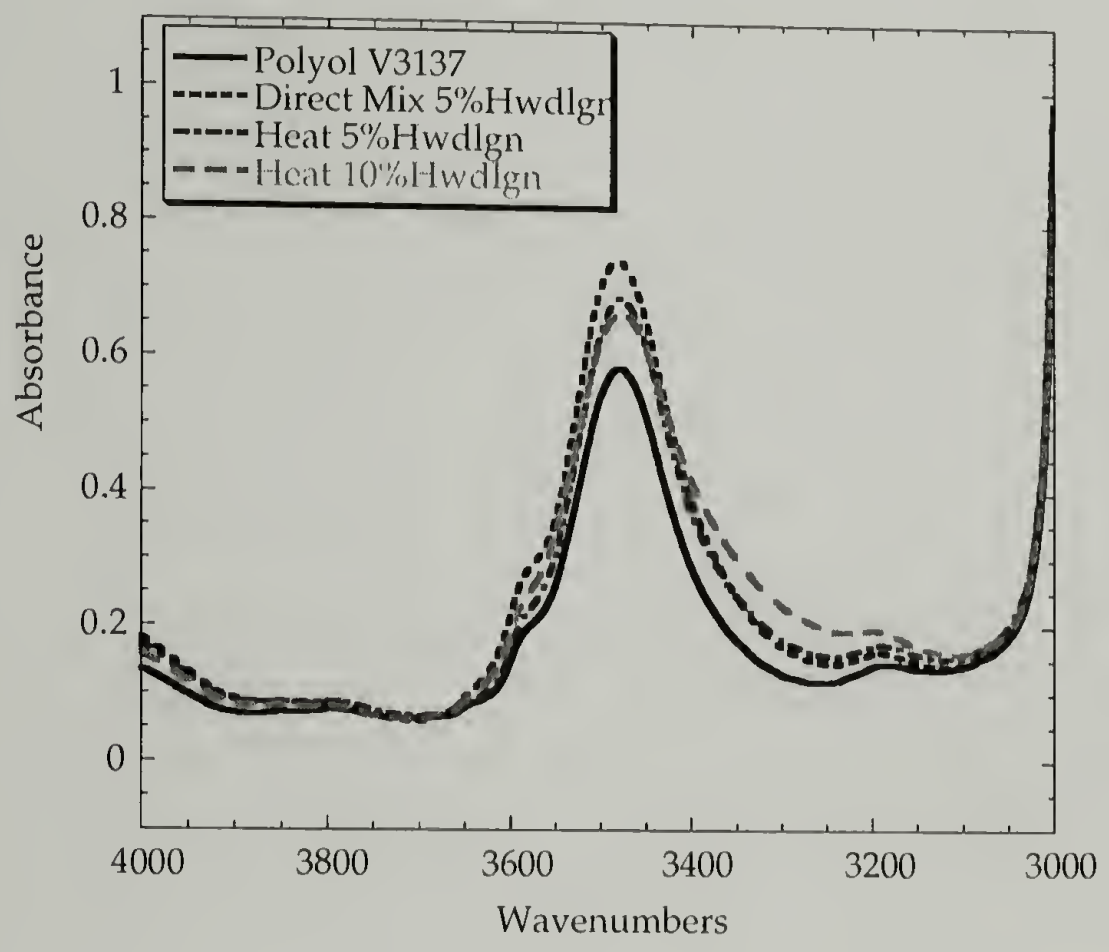

Figure 6.7. Infrared spectra of lignin incorporated polyol (O-H stretch region)

hydroxyl stretching band at 3588 cm^{-1}. After heat treatment, there was an obvious decrease in the intensity of the free hydrogen bonding band, with a corresponding increase in the hydrogen bonding component of the hydroxyl stretching at lower frequency (3400-3200 cm^{-1}), suggesting that the hydrogen bonding between lignin and polyol was promoted by heat treatment. For 10%wt lignin sample, the decreased free

hydrogen bond component and increased hydrogen bonded component showed hydrogen bonding was enhanced between lignin and polyol.

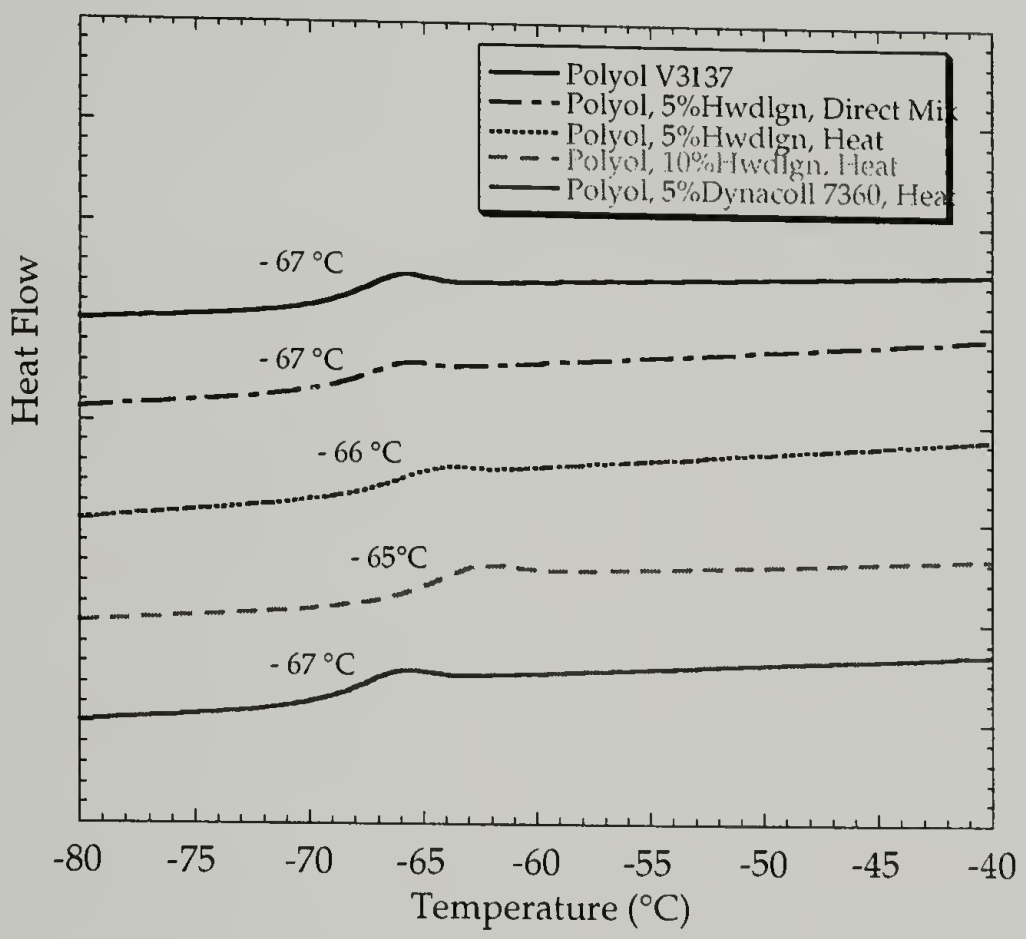

Figure 6.8. DSC curves of lignin incorporated polyol samples

Differential scanning calorimetry (DSC) is often used to study the miscibility of two different polymers. DSC results are shown in Figure 6.8. For pure polyol Voranol 3137, the Tg appeared at –67 °C. After direct mixing with 5% of hardwood lignin, the Tg showed no shift and stayed at –67 °C, indicating that the two polymers were not miscible. The Tg of a polyol sample with 5% Dynacoll 7360 showed no shift and remained at –67 °C. After lignin was mixed with polyol and the mixture heated to 80 °C for an hour, the Tg showed a small shift to –66 °C. When the lignin content was

increased to 10%, the Tg shifted to –65 °C. The errors involved in these measurements were less than 1 °C and Tg increased slightly after incorporating lignin. This suggests that the miscibility between lignin and polyol was improved.

Viscosity measurement were made to measure the viscosity change upon incorporation of lignin. The results are plotted in Figure 6.9. The polyol and the mixture of polyol and 5% lignin acted as Newtonian fluids. The viscosity of pure polyol was 0.37 Poise (Pa· S) at room temperature and decreased as temperature increased. The sample mixed with 5% Hardwood lignin after heat treatment showed the highest viscosity measured at ambient temperature. Possibly the hydrogen bonding enhances the interactions between lignin particles and polyol chains restricting mobility of polyether

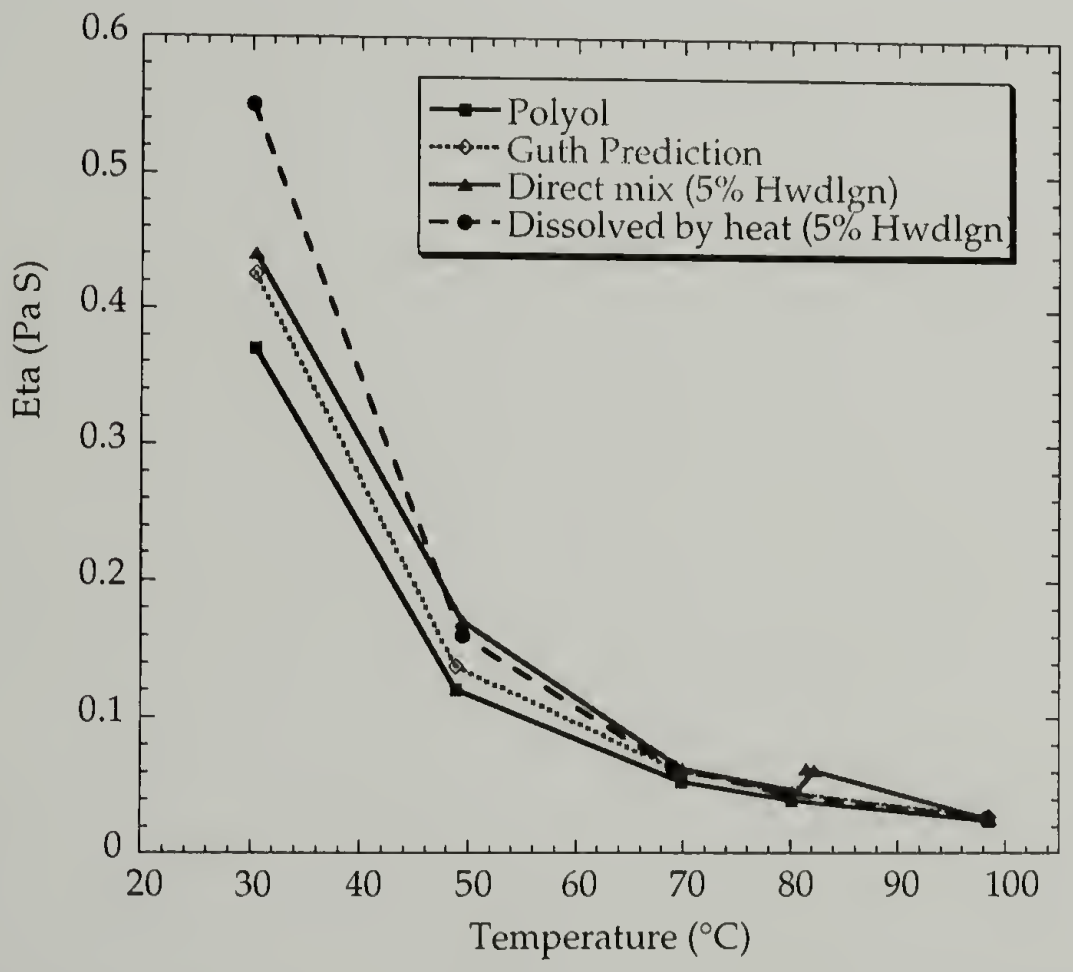

Figure 6.9. Viscosity measurements of lignin incorporated polyol samples

chains. The viscosity before heat treatment was lower due to lack of interactions shown in the infrared spectrum. It is interesting to note that for samples heated to 80 °C or above there was a small increase in the viscosity. The Guth equation 6.1 predicts the behavior of the unheated mixture very well. Upon heating, the viscosity increases at all temperatures measured, suggesting an increase in viscosity for the heated samples

Equation 6.1. $$\eta^* = \eta\left[1 + 2.5c + 14.1c^2\right]$$

where η^* and η are the viscoisty of the emulsion and solvent, and c is the volume concentration. At higher temperature above 70 °C, the hydrogen bonding weakened thus the viscosity followed the Guth prediction well.

Heat treatment of the mixture of lignin and polyol improved the dispersion of lignin into polyol. The specific interaction through hydrogen bonding improved the wetting properties of unmodified lignin into polyol and later adhesion between lignin and the polyurethane matrix in reactive processing.

6.4. The morphology and physical properties of lignin incorporated polyurethane plaques

Polyurethane plaque samples were made to study the mechanical properties of the material. Stress-strain curves were obtained for each of these samples. Before optimizing the catalyst packages, the mechanical properties from the stress strain curve are summarized in Figures 6.10-6.11 and Tables 6.1-6.2. 4-50 sample has fewer hard segments, and both the modulus and the strength decreased for those direct mixing samples. The more lignin was incorporated, the lower the strength the sample could

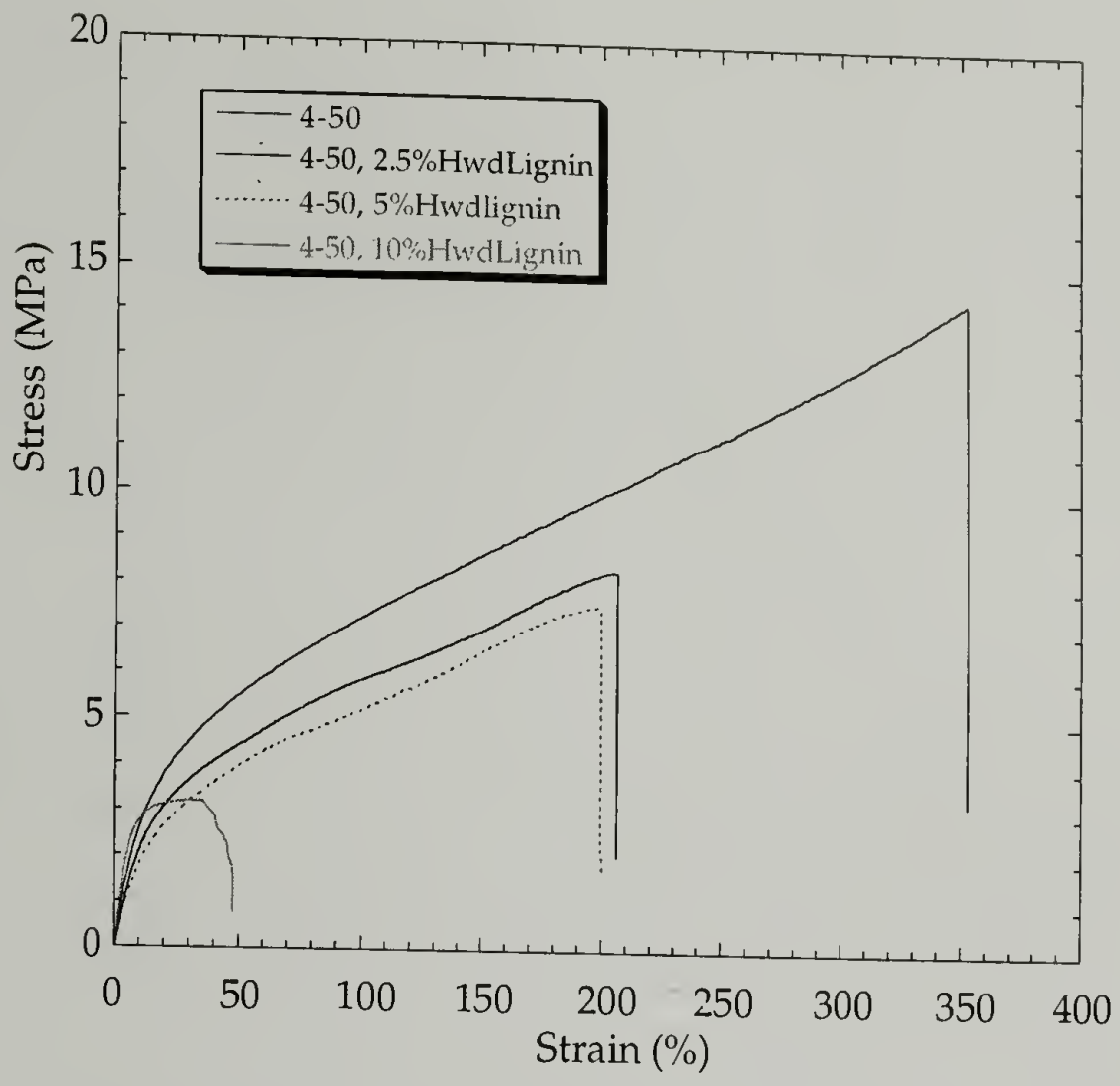

Figure 6.10. Mechanical Properties of 4-50 Plaques Incorporated with lignin

Table 6.1. Mechanical Properties of 4-50 Plaques Incorporated with lignin

	Modulus (MPa)	Tensile Strength at 100% Strain (MPa)	Elongation (%)
4-50	37	7.2	352
4-50, 2.5% Hwdlgn, (Direct Mix)	31	5.8	206
4-50, 5% Hwdlgn, (Direct Mix)	27	5.2	200
4-50, 10% Hwdlgn, (Direct Mix)	64	Failed	47
4-50, 5% Hwdlgn, (Methanol)	13	4.0	262
4-50, 10% Hwdlgn, (Methanol)	23	3.6	204

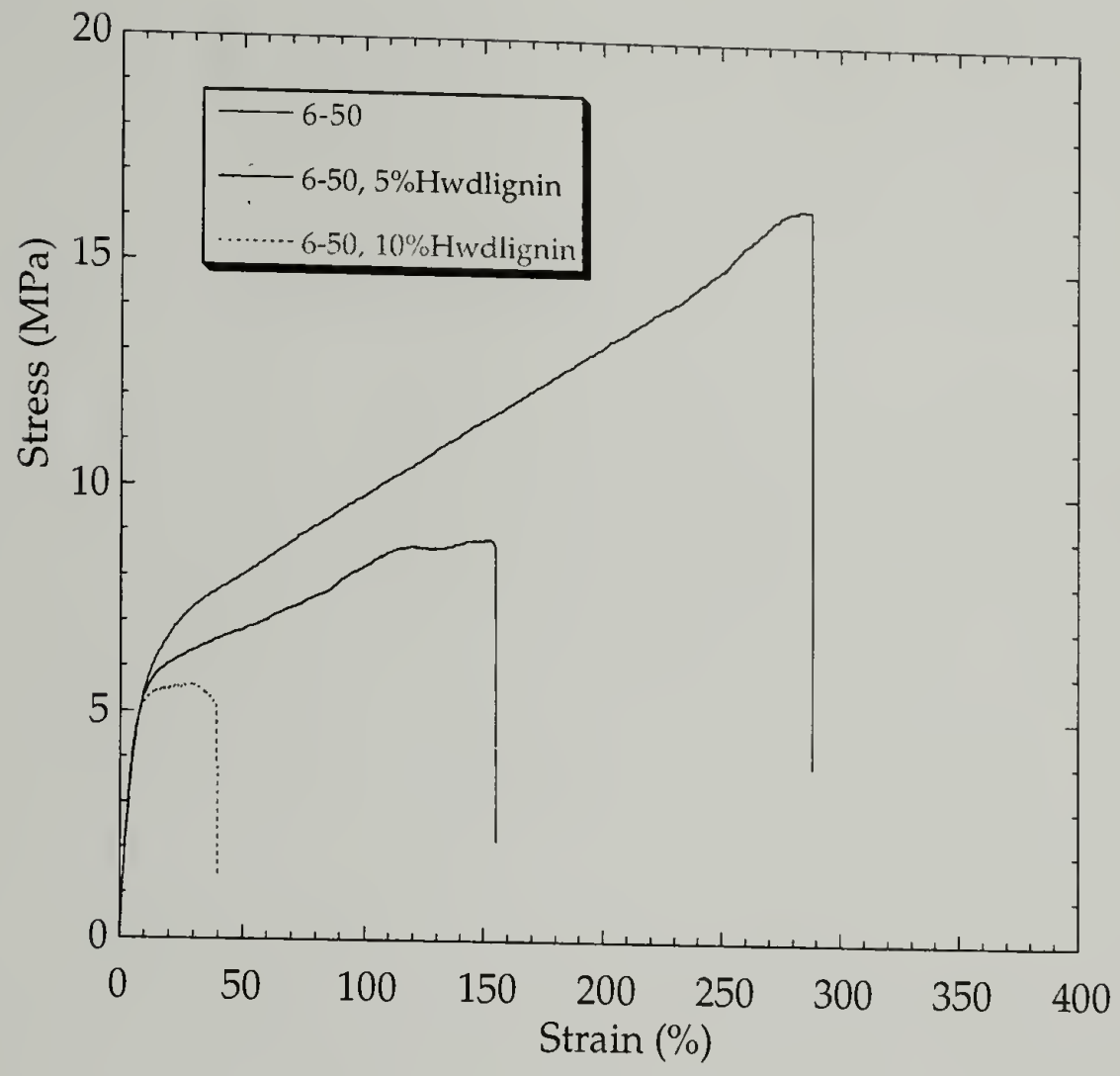

Figure 6.11. Mechanical properties of 6-50 plaques incorporated with lignin

Table 6.2. Mechanical Properties of 6-50 Plaques Incorporated with lignin

	Modulus (MPa)	Tensile Strength at 100% Strain (MPa)	Elongation (%)
6-50	94	9.8	288
6-50, 5% Hwdlgn, (Direct Mix)	109	8.2	154
6-50, 10% Hwdlgn, (Direct Mix)	138	Failed	39
6-50, 5% Hwdlgn, (Methanol)	57	6.2	452
6-50, 10% Hwdlgn, (Methanol)	104	6.6	243

achieve. When 10 wt% of lignin was incorporated, the material failed at much lower strain level. These samples lost elastomeric properties after incorporation of lignin. For 6-50 sample which contains higher volume fraction of the hard segments, the modulus showed improvement but the strength suffered a large decrease. Similarly at 10 wt% lignin incorporation, the sample broke at early strain before 50%.

Methanol (CH_3OH) was chosen to improve the mixing. The solvent was removed after mixing by vacuum distillation. However, it is suspected that residual solvent in the polyol mixtures participated in the polyurethane reactions. It was found that the modulus decreased and the strength decreased almost 50% for the final polyurethane materials.

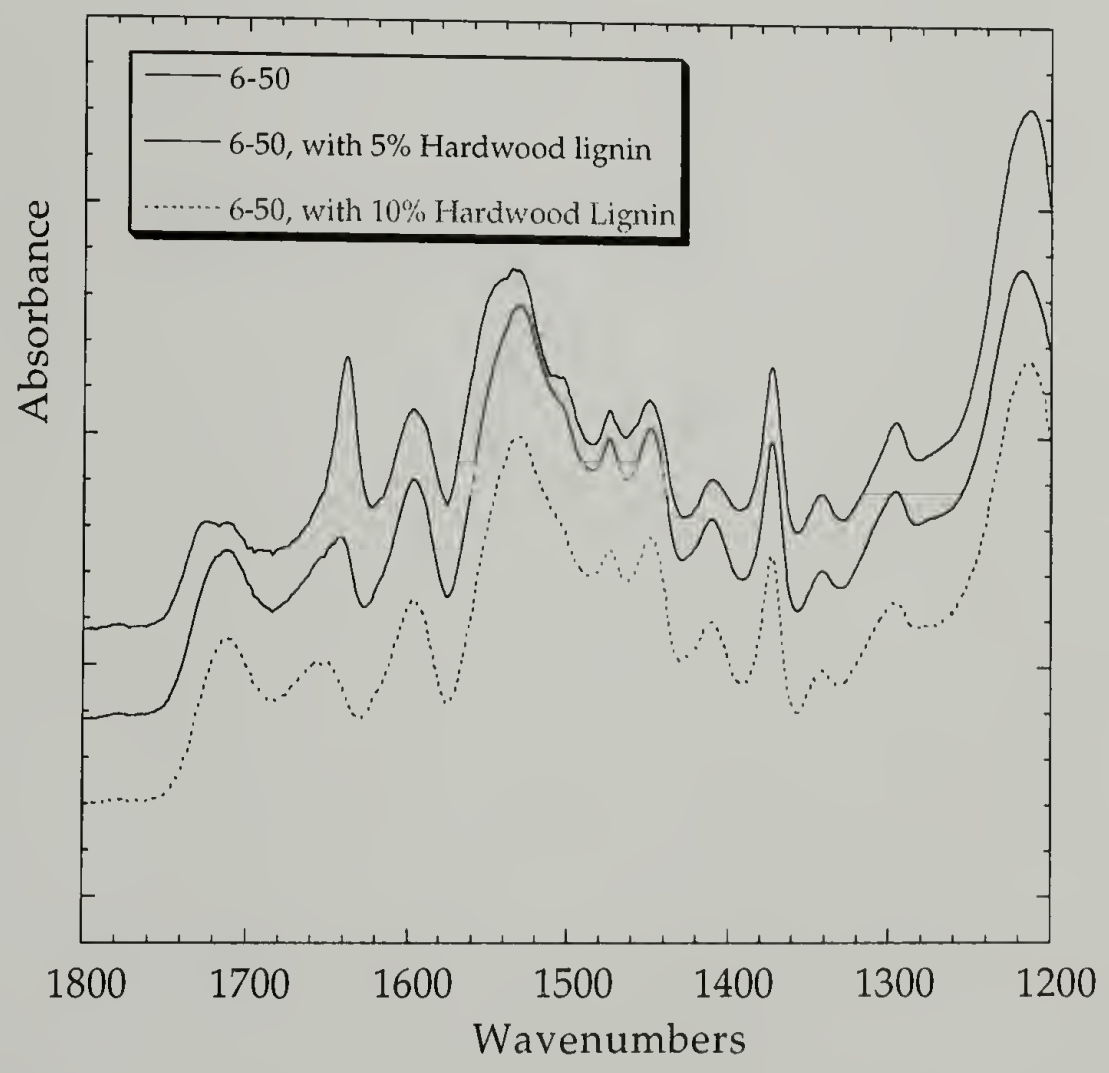

Figure 6.12. ATR-FTIR spectra of lignin incorporated polyurethane plaque samples (before raising the catalyst levels)

Therefore using solvent to improve miscibility is not a suitable approach.

In order to understand the decrease in the mechanical properties of these samples, the phase separated morphology was characterized by using ATR-FTIR as shown in Figure 6.12. It is clearly noticed that the 1640 cm^{-1} band representing the ordered hard domain was decreasing as more lignin was incorporated into the polymer matrix. Incorporating lignin destroyed the phase separated morphology of the polyurethane matrix. In addition, poor dispersion and adhesion between lignin and polyurethane matrix generated local defects and resulted in poor reinforcement. For 4-50 sample, this effect was more substantial since lower volume fraction of the hard domain existed in the material. After losing the reinforcing hard domain, the mechanical properties decreased significantly.

One possible reason for the poor final morphology is that the diversity of functionality of lignin hampers the catalytic activity of common organotin and amine catalysts. The function and mechanisms of the catalyst package are discussed in Appendix B. It is found that using the normal amount of catalysts, the reaction proceeded very slowly and was not suitable for foam applications and plaque preparation. The mechanisms are: (1) The surface active properties of lignin compete with stannous octanoate for action on the hydroxyl groups of the polyol. (2) The acidity of lignin compounds reacts with amine catalysts before the catalytic activity becomes effective. When using the normal amount of catalyst, smaller amounts of catalyst was available to water, polyol and isocyanates, the foaming process slowed and so did the curing process. This led to poor final phase separated morphology as shown in Figure 6.13, and in decreased chemical crosslinking, which resulted in the lower mechanical properties observed.

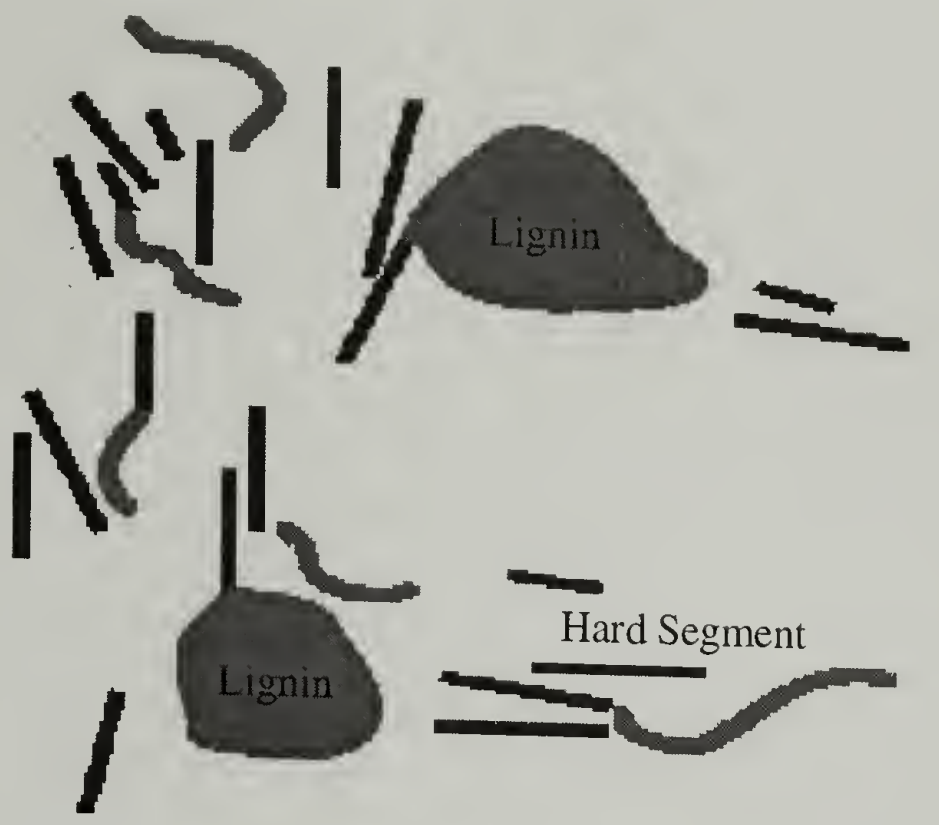

Figure 6.13. Morphological picture of lignin incorporated polyurethanes (poor mixing)

To optimize process conditions, foam rise and curing time are important issues.[22] Better phase separated morphology is required to obtain enhanced mechanical properties of polyurethanes. By raising the catalyst level, these problems could be overcome. The morphology before and after optimizing the dispersion state and process condition was studied using ATR-FTIR. The spectra are shown in Figure 6.14. By raising the catalyst level, 2X, 3X, 4X, the degree of phase separation showed significant improvement. The 1640 cm^{-1} band was sharp, indicative of a well phase separated morphology. By investigating of the ratio of 1640 cm^{-1} band and the urethane amide I band, the degree of phase separation can be roughly estimated. Double or triple amounts (2X and 3X) of the catalyst packages gave the most phase separation. At 4X, the degree of phase separation decreased to some extent, probably due to the faster exothermic reaction and higher temperature profile.

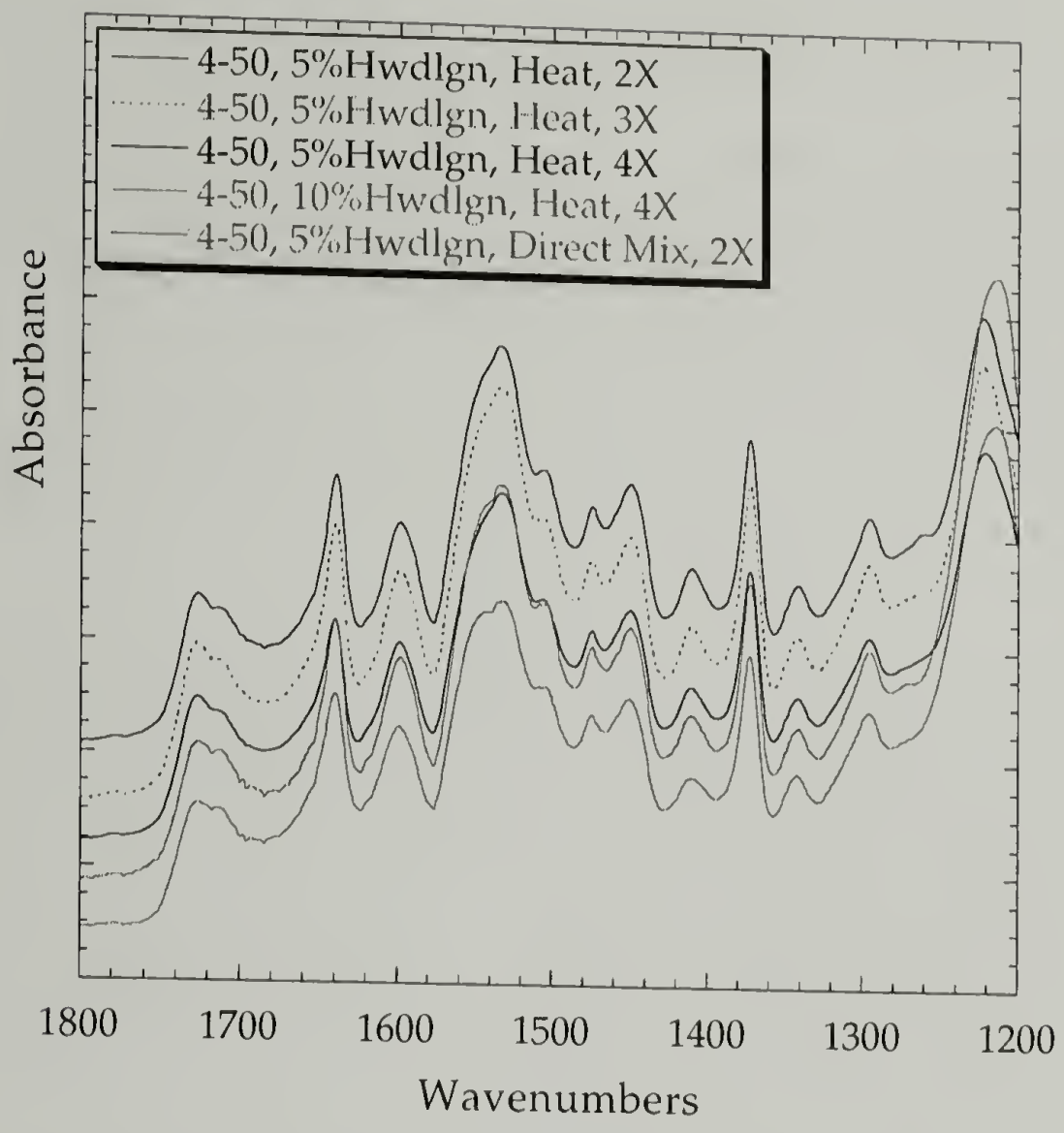

Figure 6.14. ATR-FTIR spectra of lignin incorporated polyurethane plaque samples (after raising the catalyst levels)

The mechanical properties of the plaque samples have also been evaluated using the stress-strain curve. The modulus and strength of the material is summarized in Figures 6.15-6.16 and Tables 6.3-6.4.

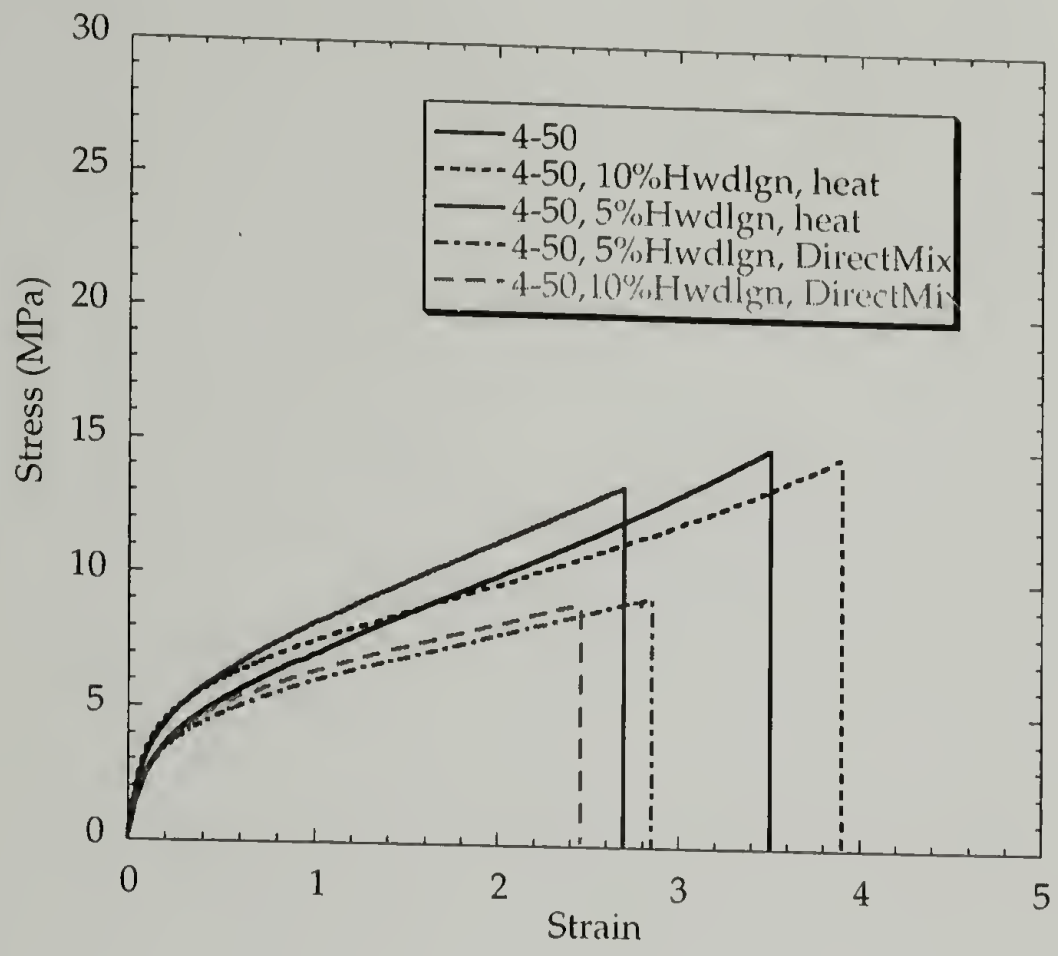

Figure 6.15. Mechanical properties of lignin incorporated 4-50 polyurethane plaque samples (after optimized processing condition)

Table 6.3. Mechanical properties of lignin incorporated 4-50 polyurethane plaque samples (after optimized processing condition)

	Modulus (MPa)	Tensile Strength at 100% Strain (MPa)	Elongation (%)
4-50	39	7.0	351
4-50, 5% Hwdlgn, Direct Mix	41	6.0	285
4-50, 5% Hwdlgn, Heating	63	8.1	270
4-50, 10% Hwdlgn, Direct Mix	37	6.3	245
4-50, 10% Hwdlgn, Heating	53	7.5	390

The lignin incorporated samples demonstrated higher modulus and strength after increasing the catalyst, compared with previous results. The elongation is generally affected by local defects in the sample. The direct mixing samples showed lower elongation. After heat treatment, defects are decreased.

It is important to note that after improving the miscibility of lignin and polyol, and optimizing the process conditions, both the modulus and strength have shown increase for 5% hardwood lignin incorporated samples, compared to the direct mixing.

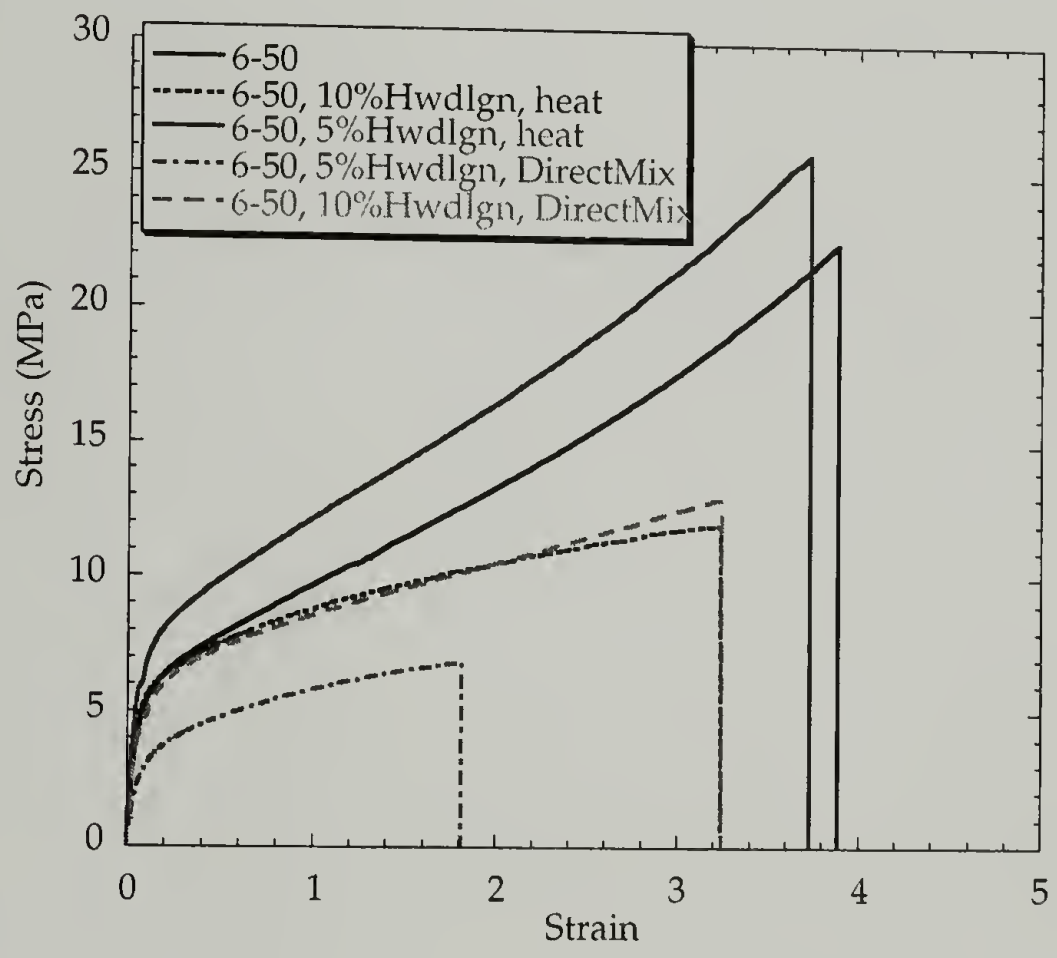

Figure 6.16. Mechanical properties of lignin incorporated 6-50 polyurethane plaque samples (after optimized processing condition)

Table 6.4. Mechanical properties of lignin incorporated 6-50 polyurethane plaque samples (after optimized processing condition)

	Modulus (MPa)	Tensile Strength at 100% Strain (MPa)	Elongation (%)
6-50	108	9.7	388
6-50, 5% Hwdlgn, Direct Mix	65	5.8	181
6-50, 5% Hwdlgn, Heating	160	12.1	373
6-50, 10% Hwdlgn, Direct Mix	95	8.5	325
6-50, 10% Hwdlgn, Heating	124	8.8	325

For 4-50 sample, 60% of the modulus increase and 15% of the strength increase at 100% strain can be found for the improved lignin mixing sample. The same for the 6-50 sample, 48% of the modulus increase and 24% of the strength increase can be found for the sample after the heat treatment.

When 10% lignin was incorporated into the polyurethane, the catalyst package seemed not to be able to overcome the perturbation of lignin particles. This resulted in slower morphology development and final cure of the samples. For 4-50 sample, higher strength at 100% strain was found but at higher elongation the strength was lower than the original sample. Overall, the 10% lignin incorporated polyurethane samples were stiffer with some sacrifice in the strength.

6.5. Reinforcing mechanism

In earlier studies, the increase in Tg of the soft matrix was attributed to vitrification of the hard domain. [23-25] For both the 4-50 and 6-50 samples, about 20 °C increase in Tg on polymerization is strong evidence of hard domain vitrification. [26-28]

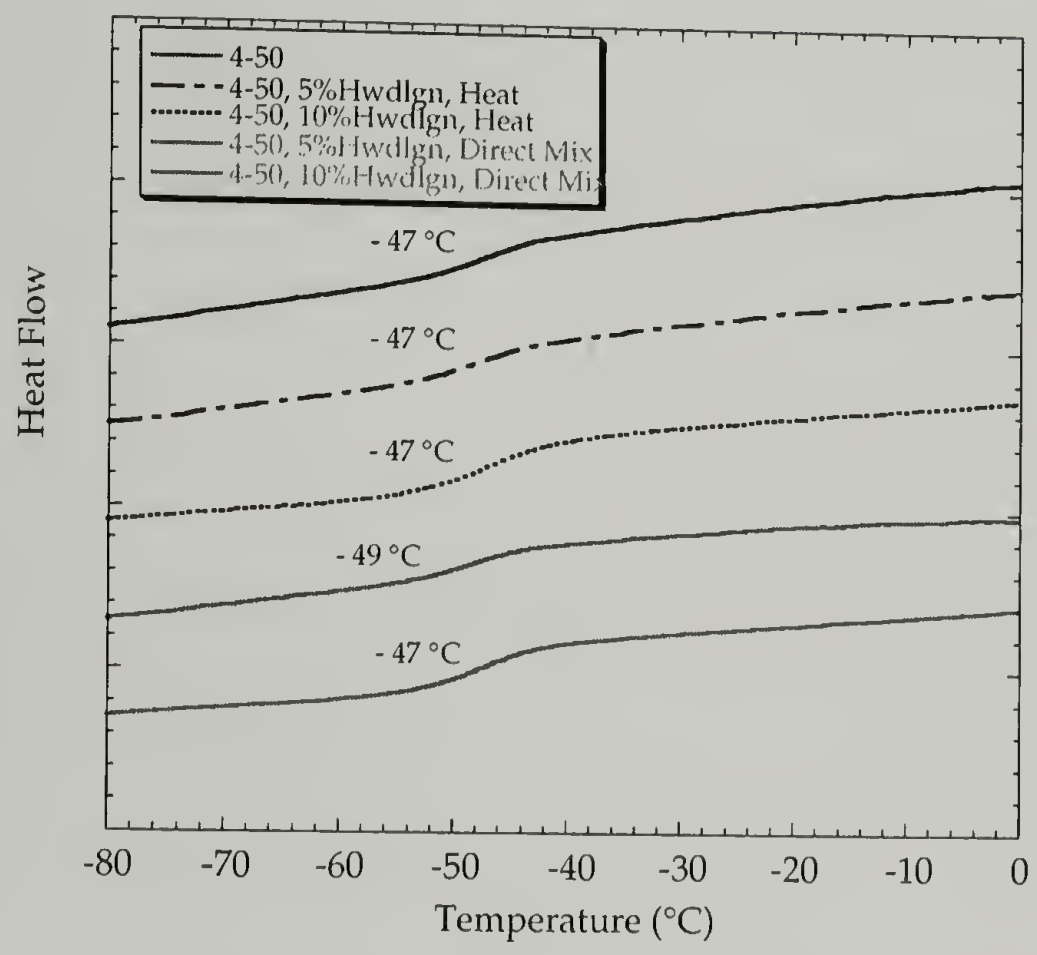

Figure 6.17. DSC curves of lignin incorporated polyol

Before incorporating lignin the glass transition temperature for the soft matrix was at –47 °C for the 4-50 sample. The DSC curve is shown in Figure 6.17. After incorporating lignin with improved dispersion, the Tg remained at –47°C. The soft matrix was not strengthened by lignin, even though the miscibility was improved through hydrogen

bonding. In fact, the active functional groups of lignin could serve as many anchor sites to react with the isocyanate groups to bridge among the hard domains, thus enhancing the interconnectivity.

The DSC results for the direct mixing samples showed a surprisingly opposite trend, and the Tg appeared at lower temperature at -49 °C. One possible reason is the lignin as a separated phase could consume isocyanate groups and showed little effect on the enhancement of soft domain. As a result, less isocyanate was available for the polyol, and the increase in Tg was diminished.

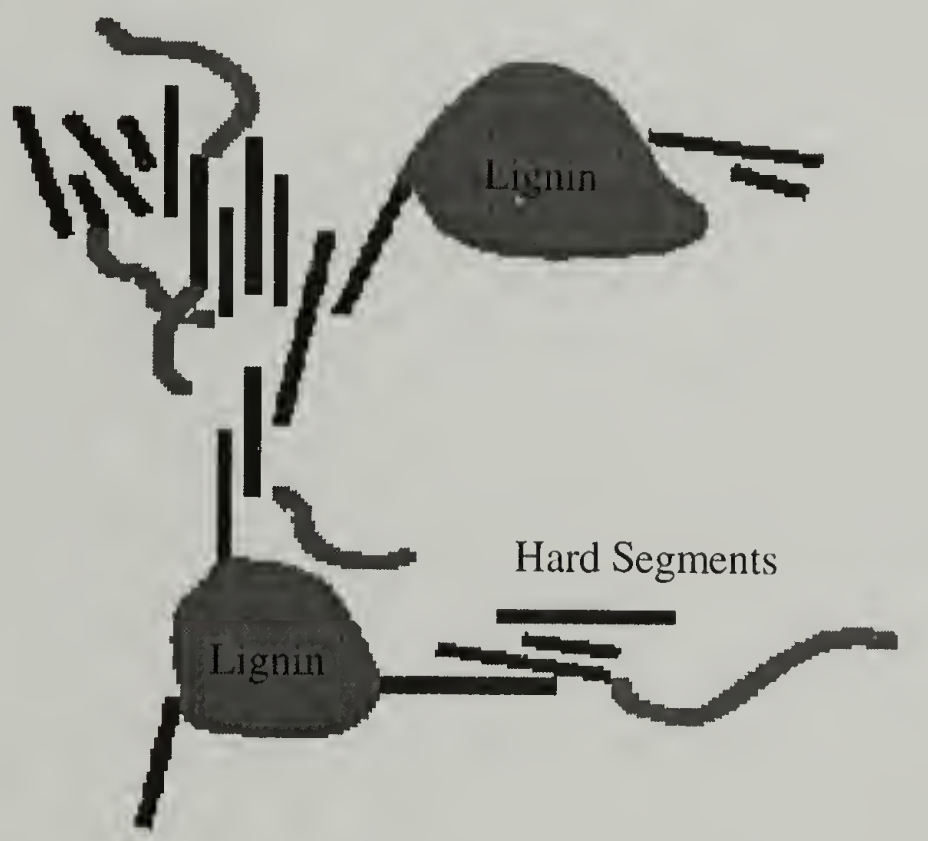

Figure 6.18. Morphological picture of lignin incorporated polyurethanes (interconnectivity enhanced)

The reinforcing mechanism in lignin incorporated polyurethanes is suggested in Figure 6.18. The lignin functions as hard segments. The multiple reaction sites in lignin provides anchors for the reactions between lignin and isocyanate that could enhance the

interconnectivity with the hard domains. Compared with the polyurethane sample without added lignin, the unchanged Tg of the soft matrix of the miscible lignin incorporated polyurethane suggested that lignin did not effectively reinforce the soft matrix but played an important role as the hard segments and enhanced the interconnectivity. The mechanical properties were thus improved.

The fractured plaque sample morphology was studied by scanning electron microscopy (SEM) on the fractured surface of the tensile bar. The results are shown in

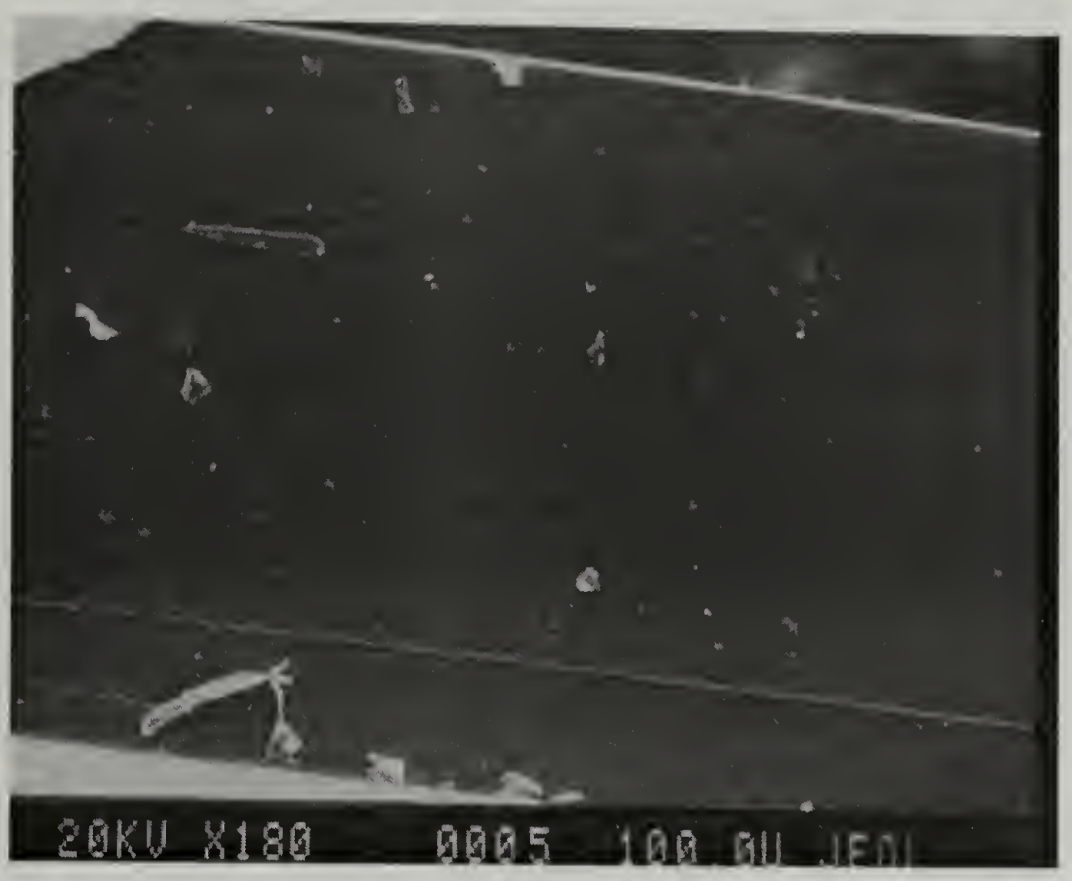

Figure 6.19. Fractured surface of tensile bar from 6-50 polyurethane sample

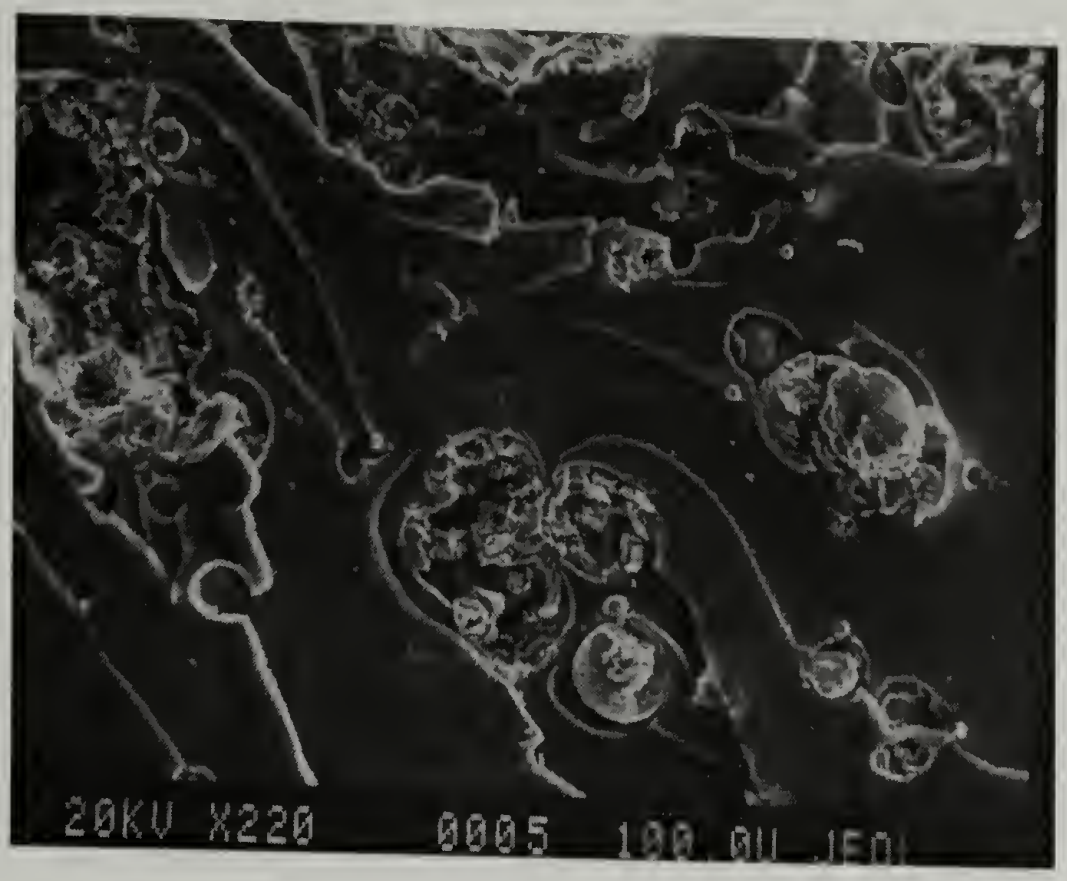

Figure 6.20. Fractured surface of tensile bar from 5% lignin incorporated 6-50 sample (direct mixing and poor catalyst package)

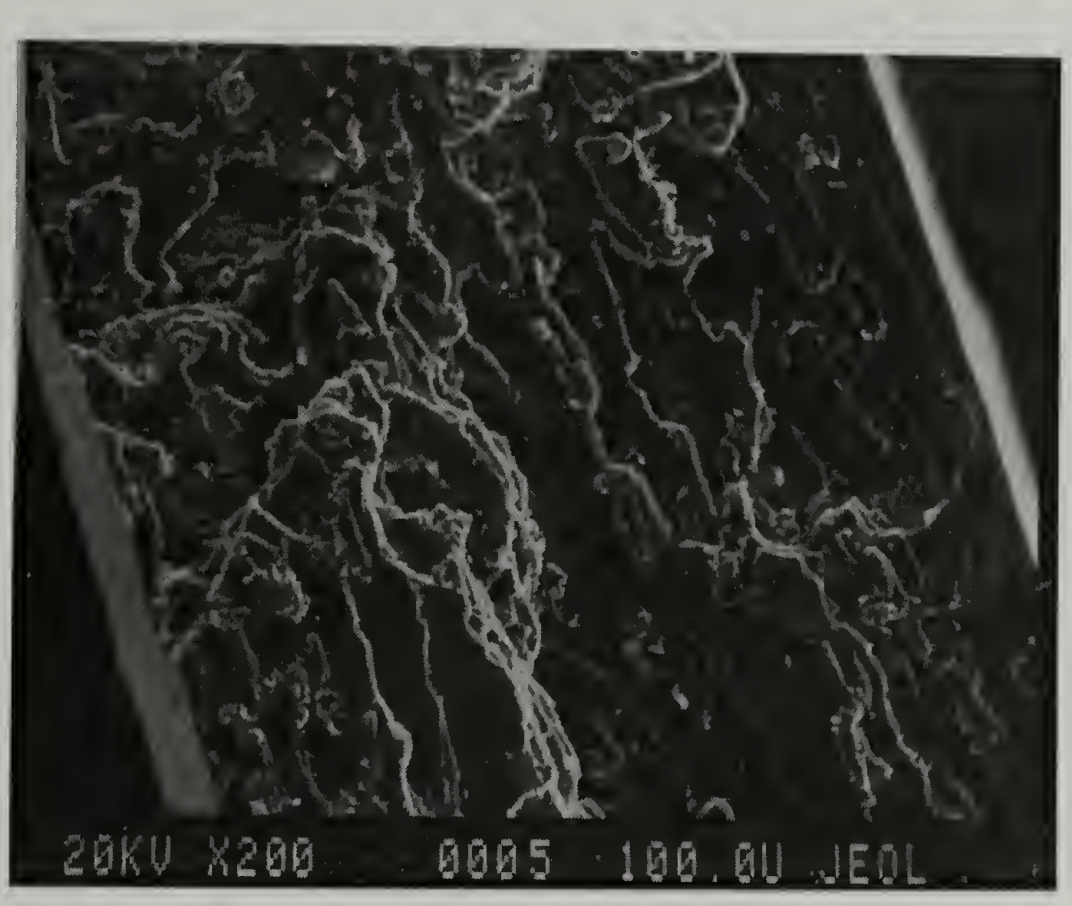

Figure 6.21. Fractured surface of tensile bar from 5% lignin incorporated 6-50 sample (direct mixing and improved catalyst package)

Figures 6.19 – 6.23. The fracture surface of the original sample is shown in Figure 6.19. The surface was smooth and no features could be found as expected at the scale the sample was amplified.

For 5% lignin direct mixing with poor phase separation polyurethane samples as shown in Figure 6.20, large lignin aggregates up to 70 μm were dispersed in the polyurethane matrix. Poor adhesion between particles and matrix appears as a clear boundary observed on the fractured surface. Therefore local defects lowered the strength of this composite material and gave the potential for early failure.

A sample of 5% lignin direct mixing with good phase separation morphology after raising the catalyst level is shown in Figure 6.21. The fact that fewer large particles could be observed at the fractured surface suggests that the higher catalyst level improved the dispersion state of lignin, which may be attributed to the higher temperature profile at higher catalyst level. Improved dispersion decreased the local defects. Thus the strength of the material was enhanced.

For 5% lignin mixed sample after heat treatment and optimized processing condition, a significant change in the SEM image can be noted in Figure 6.22. First the lignin particles were more homogeneously distributed throughout the polyurethane matrix after the heat treatment. The lignin particle size decreased tremendously. At higher magnification as shown in Figure 6.23, no clear boundary could be observed between lignin and matrix on the fracture surface, indicating good adhesion.

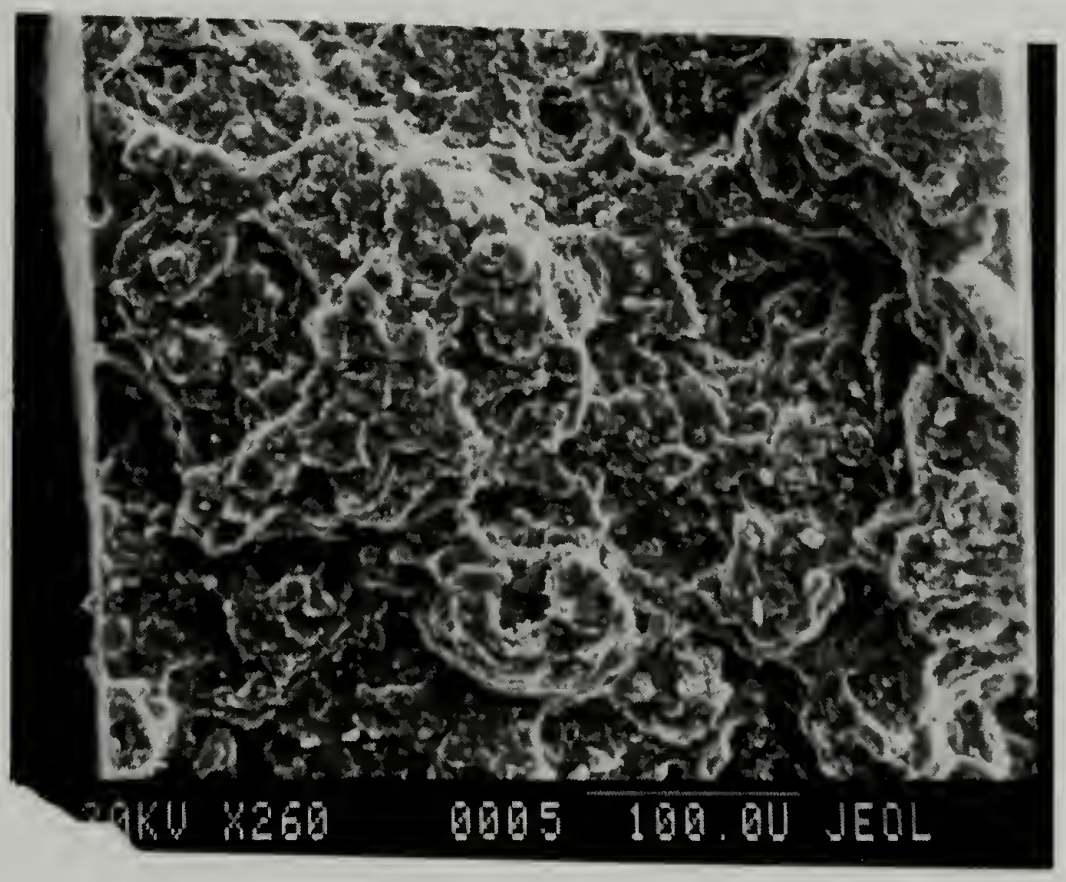

Figure 6.22. Fractured surface of tensile bar from 5% lignin incorporated 6-50 sample (heat treatment and improved catalyst package)

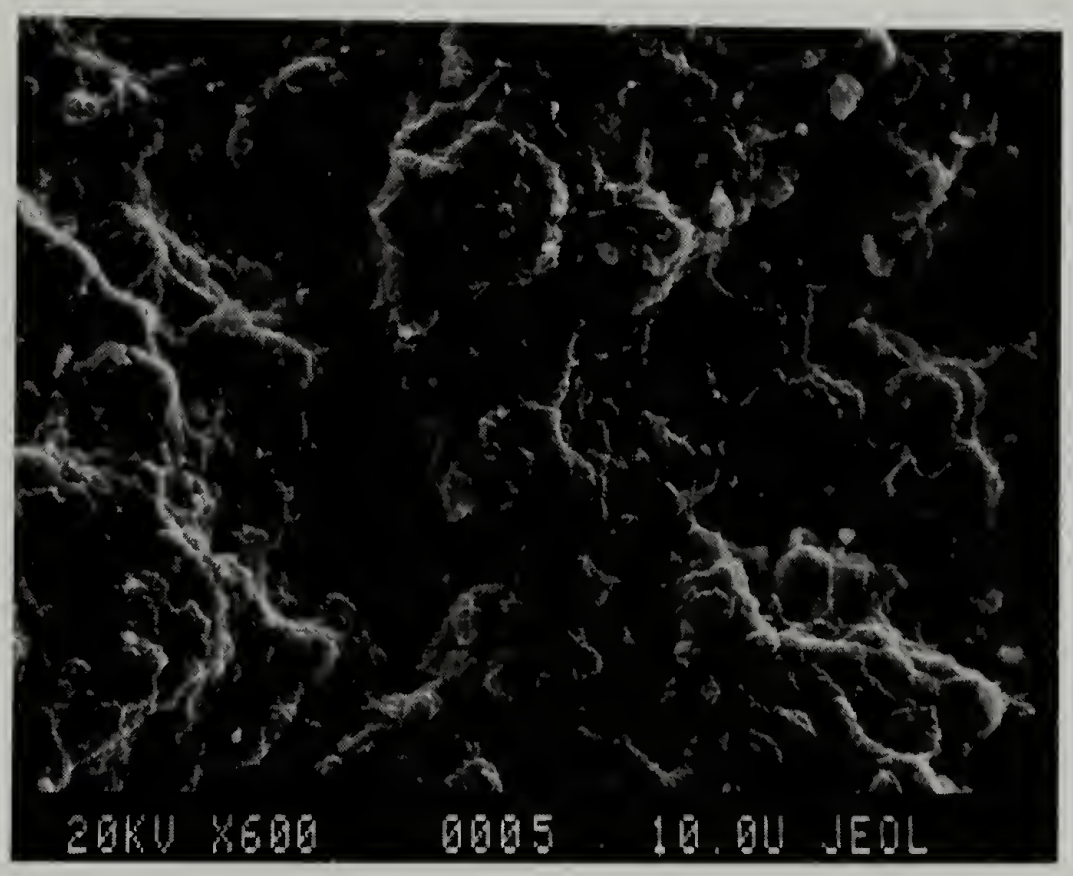

Figure 6.23. Fractured surface of tensile bar from 5% lignin incorporated 6-50 sample (heat treatment and improved catalyst package), higher magnification

In conclusion, good dispersion and improved specific interactions between lignin and polyol are essential to improve the adhesion between lignin and the polyurethane matrix and to minimize local defects. Lignin as a reinforcing component had little effect on the soft polyether chains, but functioned as the hard segment or multi-crosslinker to improve the interconnectivity between hard domains. In addition, the final phase separated morphology of polyurethane matrix was crucial for enhancing the mechanical properties of polyurethane materials.

The thermal stability of the polyurethane plaques was also studied using thermal gravimetric analysis(TGA) and the results are shown in Figure 6.24. It can be noted that the hardwood lignin started to decompose at around 150 °C and left 40 wt% of residues up to 600 °C.

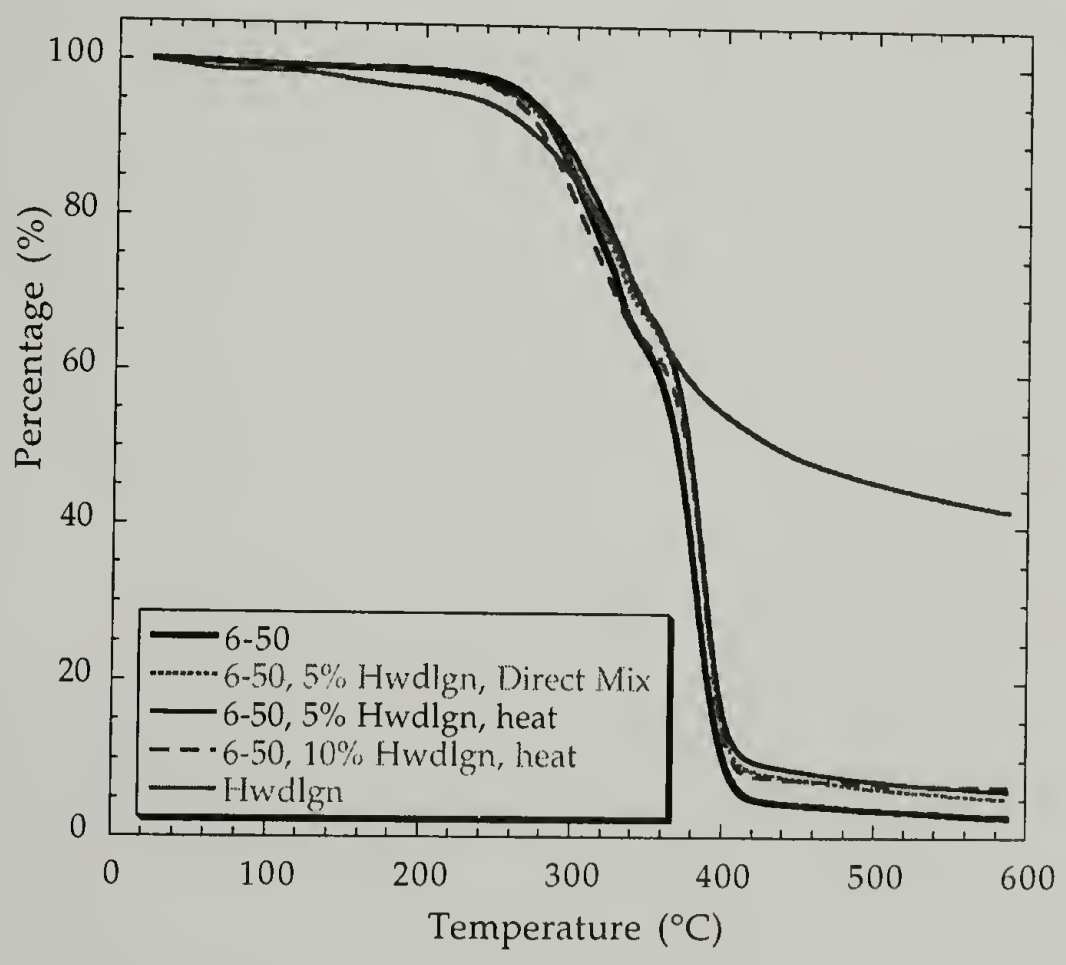

Figure 6.24. TGA analysis of lignin incorporated 6-50 polyurethane samples

The decomposition temperature of lignin incorporated polyurethane 6-50 samples showed no change, below 300 °C, but the amount of residues increases slightly with lignin content.

6.6. Conclusions

Lignin has been successfully incorporated into polyurethane to strengthen polyurethane materials. After improving the miscibility and dispersion of lignin in polyol and optimizing the processing conditions, including catalyst, both the modulus and strength can be enhanced for 5% hardwood lignin incorporated samples. The reinforcing mechanism is explored. Rather than strengthening the soft matrix, the lignin is most likely to function as the hard segment domain to achieve interconnectivity with the ordered urea domains. In addition, the phase separated morphology of the polyurethane matrix should be maintained to enhance the properties of the composite material. The success of incorporating lignin into polyurethane gives the potential of reduction in isocyanate consumption in polyurethane productions. Also it provides a new route to utilize this biomass effectively.

6.7. References

1) Feldman, D.; Banu, D.; Natansohn, A.; Wang, J. *J. Appl. Polym. Sci.* **1991**, *42*, 1537-1550.

2) Cousins, W. *J. For. Sci.* **1977**, *7*, 107.

3) Rouhi, A. M. *Lignin and Lignan Biosynthesis*, 2000; Vol. 78, pp 29-32.

4) Bolker, H. I.; Terashima, N. *Infrared Spectroscopy of Lignins. IV Isolation of Lignins by Solvolysis in Acetals*; American Chemical Society: Washington, D. C., **1966**.

5) Pearl, I. A. *The Chemistry of Lignin*; Marcel Dekker, Inc.: New York, 1967.

6) Robinson, P., Personal Communication.

7) Lindberg, J. J.; Kuusela, T. A.; Levon, K. *Specialty Polymers from Lignin*; American Chemical Society: Washington, D. C., **1989**.

8) Tan, T. T. M. *Polym. Int.* **1996**, 13-16.

9) Feldman, D.; Banu, D.; Luchian, C.; Wang, J. *J. Appl. Polym. Sci.* **1991**, *42*, 1307-1318.

10) Klason, C.; Kubat, J. *Plastics and Rubber Processing and Application* **1986**, *6*, 17-20.

11) Parkinson, D. *Reinforcement of Rubbers*; The Institution of the Rubber Industry:, **1957**.

12) Hess, W. M. *Microscopy in the Study of Elastomer Reinforcement by Pigment Fillers*; Kraus, G., Ed.; John Wiley & Sons, Inc.: New York, **1965**.

13) Hess, W. M. *Rubber Chemistry and Technology* **1991**, *64*, 386-449.

14) Raab, M.; Nezbedova, E. *Toughness of Ductile Polymers*; Hanser: Munich, 2000.

15) Nielsen, L. E. *Mechanical Properties of Polymers*; Reinhold Publishing Corporation: New York, **1962**.

16) Chow, T. S. *J. Polym. Sci. Polym. Phys. Ed.* **1982**, *20*, 2103-2109.

17) Wang, J.; St. John Manley, R.; Feldman, D. *Prog. Polym. Sci.* **1992**, *17*, 611-646.

18) Glasser, W. G.; Kelley, S. S. *J. Wood Chem. Technol.* **1988**, *8*, 341-359.

19) Glasser, W. G.; Barnett, C. A.; Rials, T. G.; Saraf, V. P. *J. Appl. Polym. Sci.* **1984**, *29*, 1815-1830.

20) Hirose, S.; Kobashigawa, K.; Izuta, Y.; Hatakeyama, H. *Polym. Int.* **1998**, *47*, 247-256.

21) Biermann, C. J.; Chung, J. B.; Narayan, R. *Macromolecules* **1987**, *20*, 954-957.

22) Herrington, R.; Hock, K. *Flexible Polyurethane Foams*; 2 ed.; The Dow Chemical Company: Midland, **1997**.

23) Ryan, A. J.; Stanford, J. L.; Still, R. H. *Plast. Rubber Proc. Appl.* **1990**, *13*, 99-110.

24) Koberstein, J.; Gancarz, I. *Journal of Polymer Scienc: Part B: Polymer Physics* **1986**, *24*, 2487-2498.

25) West, J. C.; Cooper, S. L. *J. Polym. Sci., Polym. Symp.* **1977**, *60*, 127-150.

26) Elwell, M. J.; Mortimer, S.; Ryan, A. J. *Macromolecules* **1994**, *27*, 5428-5439.

27) Elwell, M. J.; Ryan, A. J.; Grunbauer, H. J. M.; Van Lieshout, H. C. *Polymer* **1996**, *37*, 1353-1361.

28) Elwell, M. J.; Ryan, A. J.; Grunbauer, H. J. M.; Van Lieshout, H. C. *Macromolecules* **1996**, *29*, 2960-2968.

CHAPTER VII

CONCLUSIONS AND FUTURE WORK

7.1. Conclusions

The morphology and physical properties of polyurethanes have been studied in this work. Deuterium substitution has been used to study quantitatively the dispersion state of the interconnecting hard domain morphology. The surface, the disordered hard domain and the bulk hard domain have been specified for samples made at different temperatures. Based upon the new morphological picture, in addition to the direct bridges from the longer hard segments, the disordered hard domains can function to interconnect the ordered hard domains or between hard domain and soft matrix. The difference in the morphological features of samples made at different temperatures is attributed to the difference in the physical properties of the final materials. The degree of phase separation and the interconnecting region of the hard domain are determining factors for the mechanical properties of polyurethanes.

The deformation behavior of polyurethanes has been studied using infrared dichroic measurement. In addition to the amide I region, the amide II region has been shown to be important for the quantification on the deformation process. The hard domain is not "undeformable" but participates in stretching throughout the deformation process. Even at small strains, the interconnecting hard domain region takes the load from the soft polyether chains and distributes the stress evenly to eliminate stress concentration. Within the interfacial region, the soft chains are constrained by hard

segments, thus the effective hard domain volume fraction increases and interconnectivity between hard domains contributes to a higher modulus of the material. It is known that the bulk of the hard domain tends to rotate transverse to the stretching direction. The lower modulus of the interconnecting regions will experience plastic deformation. As a result, the hard segment chains in these regions slide away from the original position or pull out into the soft matrix and become dispersed hard segments. This points to an explanation of the large hysteresis and stress softening effect for polyurethanes found even at small strains. For high performance polyurethane materials, the interconnecting morphology and the compromise between bulk hard domain and interconnecting interfacial region determines the final performance of the material. Control of the right morphology is important to obtain higher modulus and more durable polyurethane materials.

The importance of interconnecting region of the hard domain to the overall properties of polyurethanes is further revealed from the stress relaxation experiment under humid environment. D_2O can be used as a probe in order to study simultaneously where the absorbed water is and the extent of interaction with the specific regions of the hard domain. The surface and interfacial regions of the interconnecting hard domains are accessible at room temperature. The excess accessibility of the hard domain in stretched thin film samples compared with that of the undeformed sample suggests that the hard domain undergoes large plastic deformation under stress. The small irreversible stress recovery on desorption suggests tremendous decrease in the interconnectivity. The diffusion coefficient of moisture in the polyurethane thin films was determined by swelling stress measurements. Deuterium substitution does not indicate any contribution from the soft matrix even though surely moisture diffuses through the soft matrix.

Emphasis on the hard domain contribution to the lower mechanical properties under water plasticization has been presented.

Lastly, the lignin has been successfully incorporated into polyurethane to improve the mechanical properties of the materials. The miscibility and dispersion of lignin in polyol and the optimization of the processing conditions, including catalyst use, are crucial issues to be solved for effective incorporation of lignin. It is found that both the modulus and strength increase for 5% incorporated lignin polyurethane samples. The reinforcing mechanism is also explored. Rather than strengthening the soft matrix, the lignin is most likely to function as the hard segment domain to achieve interconnectivity with the ordered urea domains. The phase separated morphology of the polyurethane matrix should be maintained to enhance the properties of this composite material.

7.2. Future Work

There is no doubt that the interconnecting morphology is the key for the reinforcement in polyurethane phase separated morphology. There are many different ways to enhance the interconnectivity as Figure 1.2 depicted. In this dissertation, the emphasis on the contribution of the hard segment domain has been presented. Further improvement can start from the weakest link, the soft segment domain. The introduction of the crystallizable polyester polyol as the new candidate for soft segment could possibly enhance the soft domain. [1-4] The "hardening" of the soft matrix can achieve better interconnectivity throughout the phase separated morphology. [5]

In addition to making polyblends such as incorporating lignin or polyhydroxybutyrate (PHB), copolymerization of crystallizable ester units or oligomers into the backbone of the polyol system could be effective. This not only strengthens the soft matrix intrinsically, but also provides a new route to form the physical network of the entire phase separated morphology. The crystallization kinetics and the crystallizing domain of those ester segments within the soft chains become an important subject to pursue for reinforcement. Since crystallization will compete against phase separation, various processing conditions need to be investigated. [6,7]

Infrared spectroscopy has been shown to be one of the most powerful techniques to study polyurethane materials. The band assignment of the complicated phase separated morphology of polyurethane can be further improved by simulation. [8-10] Using normal coordinate analysis of better model compounds, a more detailed band assignment that is associated with different regions of the hard domain can possibly be accomplished. [11] Therefore more complete analysis can be performed on the complicated polyurethane morphology.

The stress relaxation experiment certainly provides a unique way to investigate the hard domain reinforcement. If an establishment can be built that the difference in time scale of the relaxation spectra with different hard domain regions, the contributions of the interconnecting hard domain morphology can be explicit in more detail. The calculation of the relaxation spectra will be necessary for further studies. [12-15]

Miscibility is one of the fundamental issues in the production of polyurethanes. Beginning with water and polyol, the chemical composition and blockiness of ethylene

oxide in the backbone of polyol have shown strong effect on the dispersion of water molecules in the polyol/water mixture. [16-18] For filler or other components to be incorporated into the soft matrix, the miscibility issue not only affects the dispersion within the soft matrix before the reactive processing, but also determines the final interconnecting morphology of the multi-component system. The miscibility issue is also a matter of domain size of different components that coexist in the entire system. Using scattering and spectroscopy techniques, the domain organization and interactions between different domains can be characterized to understand the reinforcement from each component. [19-21]

The quantitative description of interconnectivity in affecting the physical properties of polyurethanes, such as modulus, hysteresis and wet compression set, is the ultimate goal of this research. However, not until those above issues have been solved will the reinforcement of the interconnecting hard domain morphology be understood completely.

7.3. References

1) Xiu, Y.; Wang, D.; Hu, C.; Ying, S.; Li, J. *Journal of Applied Polymer Science* **1993**, *48*, 867-869.

2) Petrovic, Z. S.; Ferguson, J. *Prog. Polym. Sci.* **1991**, *16*, 695.

3) Kanamoto, T.; Tanaka, K. *J. Polym. Sci., A-2* **1971**, *9*, 2043-2060.

4) Girolamo, M.; Keller, A.; Stejny, J. *Makromol. Chem.* **1975**, *176*, 1489-1502.

5) Lee, S. S.; Kim, S. C. *Polym. Eng. Sci.* **1993**, *33*, 598-606.

6) Skoglund, P.; Fransson, A. *Polymer* **1998**, *39*, 1899-1906.

7) Gilbert, M.; Hybart, F. J. *Polymer* **1972**, *13*, 327-332.

8) Bahl, S. K. *Structural an Vibrational Studies of Polyesters*; University of Connecticut: Storrs, 1976.

9) Boerio, F. J.; Bahl, S. k. *J. of Polymer Sci.: Polymer Physics Edition* **1976**, *14*, 1029-1046.

10) Cates, D. A.; Strauss, H. L.; Snyder, R. G. *J. of physics chemistry-US* **1994**, *98*, 4482-4488.

11) Kim, P. K.; Chang, C.; Hsu, S. L. *Polymer* **1986**, *27*, 34-46.

12) Monteiro, E. E. C.; Fonseca, J. L. C. *J. Appl. Polym. Sci.* **1997**, *65*, 2227-2236.

13) Smith, T. L.; Dickie, R. A. *J. Polymer Sci. Part C* **1969**, *26*, 163-187.

14) Rubinstein, M.; Obukhov, S. P. *Macromolecules* **1993**, *26*, 1740-1750.

15) Isono, Y.; Ferry, J. D. *Rubber Chem. Technol.* **1984**, *57*, 925-943.

16) Hespe, H.; Crone, J.; Mueller, E. H.; Schaefer, E. E. *J. Cell. Plastics* **1982**, *18*, 289-298.

17) Tabor, R. L.; Hinze, K. J.; Priester, R. D.; Turner, R. B. *The Compatibility of Water with Polyols*, **1992**; Vol. October 21-24, pp 514-528.

18) Gruenbauer, J. H. M.; Folmer, J. C. W.; van Lieshout, H. C.; Lidy, W. A.; Thoen, J. A. *Polym. Preprt.* **1991**, *32*, 517-518.

19) Strobl, G. *The Physics of Polymers*; 2nd ed.; Springer-Verlag: Berlin, **1997**.

20) Coleman, M. M.; Graf, J. F.; Painter, P. C. *Specific Interactions and the Miscibility of Polymer Blends*; Technomic Publishing Co.: Lancaster, **1991**.

21) Coleman, M. M.; Sobkowiak, M.; Pehlert, G. J.; Painter, P. C.; Iqbal, T. *Macromol. Chem. Phys.* **1997**, *198*, 117-136.

APPENDIX A

BASIC POLYURETHANE FOAM COMPONENTS

Flexible polyurethane foam recipes normally contain a host of ingredients, as listed in the following table, selected to aid in achieving the desired grade of foam. To understand these components and their functions can serve as a guide for new product design and improvement.

TABLE A.1. Formulation Basics for Flexible Polyurethane Foams [1]

Component	Parts by Weight
Polyol	100
Inorganic Fillers	0-150
Water	1.5-7.5
Silicone Surfactant	0.5-2.5
Amine Catalyst	0.1-1.0
Tin Catalyst	0.0-0.5
Chain-extender	0-10
Cross-linker	0-5
Additive	Variable
Auxiliary Blowing Agent	0-35
Isocyanate	25-85

Polyol is a source of hydroxyl or other isocyanate reactive groups, such as amine. Ninety percent of all flexible foams produced today are made from polyether type polyols. [1,2] Another commonly utilized polyol is polyester polyol.

Isocyanate provides the source of NCO groups to react with functional groups from the polyol, water, and cross-linkers in the formulation. [3,4] In flexible foams, the isocyanate most commonly used is toluene diisocyanate (TDI). The two isomers are illustrated in Chapter 2. Another common isocyanate is diphenylmethane diisocyanate (MDI) which is often used in high resiliency, semiflexible and micro-cellular foams, and adhesives. The chemical structure is shown in Figure A.1.

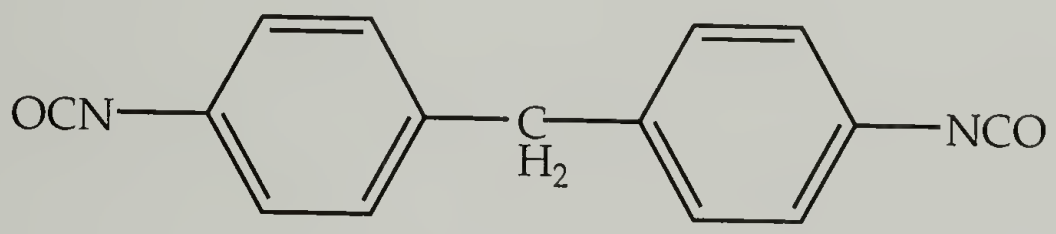

Figure A.1. Chemical structure of MDI

Chain extender uses only demineralized water in the foam formulation. Some short chain diol or diamines, e.g. 1,4-butane diol, are often found in the production of polyurethane or polyurea.

Isocyanate Index is the amount of isocyanate required to react with the polyol and any other reactive additives is calculated in terms of stoichiometric equivalents.

Equation A.1. $$\text{Isocyanate Index} = \frac{\text{Actual amount of isocyanate used}}{\text{Theoretical amount of isocyanate required}} \times 100$$

Variation of the index in the foam has a pronounced effect on the phase separated morphology and thus the physical properties, such as hardness of the final foam. The

increase in hardness has been shown to be directly related to increased covalent crosslinking, resulting from more complete consumption of isocyanate reactive sites caused by the presence of excess isocyanate groups. In general, foam becomes harder with increasing index as more isocyanate groups available for the hard segments. There is, however, a point beyond which hardness does not increase and other physical properties begin to suffer. In the production of flexible slabstock foams, the isocyanate index normally ranges from 105 to 115. The ability of excess isocyanate groups to react and build further load is dependent on the ambient humidity conditions during foam cure. [5,6]

Catalyst will be covered in Appendix B.

Surfactant is an indispensable component to make flexible foams. The non-ionic and silicone based surfactants serve to stabilize the cell-walls of the rising foam and prevent the coalescence of rapid growing cells until those cells have attained sufficient strength through polymerization to become self-supporting. [1] Surfactants also help to control the precise timing and the degree of cell-opening. Selection of a surfactant or surfactant combination for any given foam system is a task requiring literature review, supplier consultation and small-scale foam experimentation. [6-8]

Fillers, such as finely divided inert inorganic fillers are often purposely added to foam formulations to increase density, load bearing and sound attenuation, with the sacrifice of other physical properties. [9] Depending on the nature of the filler, the overall cost of the final foam may be reduced. [10]

Crosslinker are molecules that tie chains together to form branched chains or polymer networks, such as diethanolamine (DEOA). [11]

Additives can be incorporated into a foaming system to impart specific desired properties, including colorants, UV stabilizers, flame retardants, bacteriostats, plasticizers, cell-openers, anti-static agents, etc. [1]

Auxiliary blowing agents may be used in a foam formulation to aid in attaining densities and softness not obtainable with conventional water-isocyanate blowing chemistry. [12] Auxiliary blowing agents function as a heat sink for the exothermic reactions, vaporizing and providing additional gas useful in expanding the foam to a lower density. [13,14]

References:

1) Herrington, R.; Hock, K. *Flexible Polyurethane Foams*; 2 ed.; The Dow Chemical Company: Midland, **1997**.

2) Christianson, L. R.; Dheming, M.; Ochoa, E. L. *J. Cell Plast.* **1977**, *13*, 111-117.

3) Ozaki, S. *Chem. Rev.* **1972**, *72*, 457-496.

4) Ulrich, H. *Introduction to Industrial Polymers*; Hanser: Munich, **1982**.

5) Hogan, J. M.; Pearson, C. J.; Rogers, T. H.; White, J. R. *J. Cell Plast.* **1973**, *9*, 219-225.

6) Woods, G. *Flexible Polyurethane Foams: Chemistry and Technology*; Applied Science Publishers Ltd.: London, **1982**.

7) Hersch, P. *Plast. Tech.* **1967**, *13*, 49-53.

8) Rossmy, G. R.; Kollmeier, H. J.; Lidy, W.; Schator, H.; Wiemann, M. *J. Cell. Plast.* **1977**, *13*, 26-35.

9) Doyle, E. N. *The Development and Use of Polyurethane Products*; McGraw-Hill, Inc.: New York, **1971**.

10) Reilly, A. F. *Chem. Eng. Prog.* **1967**, *63*, 104-108.

11) Dounis, D. V.; Wilkes, G. L. *J. Appl. Polym. Sci.* **1997**, *65*, 525-537.

12) "Handbook for Reducing and Eliminating Chlorofluorocarbons in Flexible Polyurethane Foams," United States Environmental Protection Agency, **1991**.

13) Klesper, E. *Rubber Age* **1958**, 84-87.

14) Sayad, R. S.; Williams, K. W. *Methylene Chloride Urethane Grade as a Viable Auxiliary Blowing Agent in Flexible Slabstock Foam*; Technomic: Lancaster, PA, **1978**, pp 1-8.

APPENDIX B

CATALYSIS

Catalysts are employed whose functions are not only to bring about faster rates of reaction but also to establish a proper balance between the chain-propagating reaction (primarily the hydroxyl-isocyanate reaction, gelling reaction) and the foaming reaction (isocyanate-water reaction in the case of flexible foams, blowing reaction). [1-11] If gelling reaction occurs too fast, it will result in a closed cell and shrinkage. If a blowing reaction is too fast, it could results in collapse. Therefore a balance has to be established between polymer growth and gas formation in order to entrap the gas CO_2 efficiently and to develop sufficient strength in the cell walls at the end of the foaming reaction to maintain their structure without shrinkage or collapse. Another important function of catalysts is to bring about completion of the reactions, resulting in an adequate "cure" of the polymers. Completion of cure results in maximum strength properties, minimum compression set, and optimum chemical and weathering resistance. [12]

Based upon the above fundamental demands, a catalyst system should (1) allow a sufficient cream time. (The time between discharge of the foam ingredients from the mixing head and the beginning of the foam rise. At this point, the surface of the liquid will change color, usually turning lighter as a results of saturation of the liquid with evolving gas) (2) permit the attunement of cream time, rise time, rise profile and curing make possible changing the foam properties within a certain range. (3) have no disadvantages such as toxicity, odor or reducing the aging stability of the foam. [12]

The catalyst system used throughout this thesis research is a combination of tertiary amine and organotin compound catalyst package. The catalytic mechanism of organotin and amine catalysts has been proposed in the literature. XXX

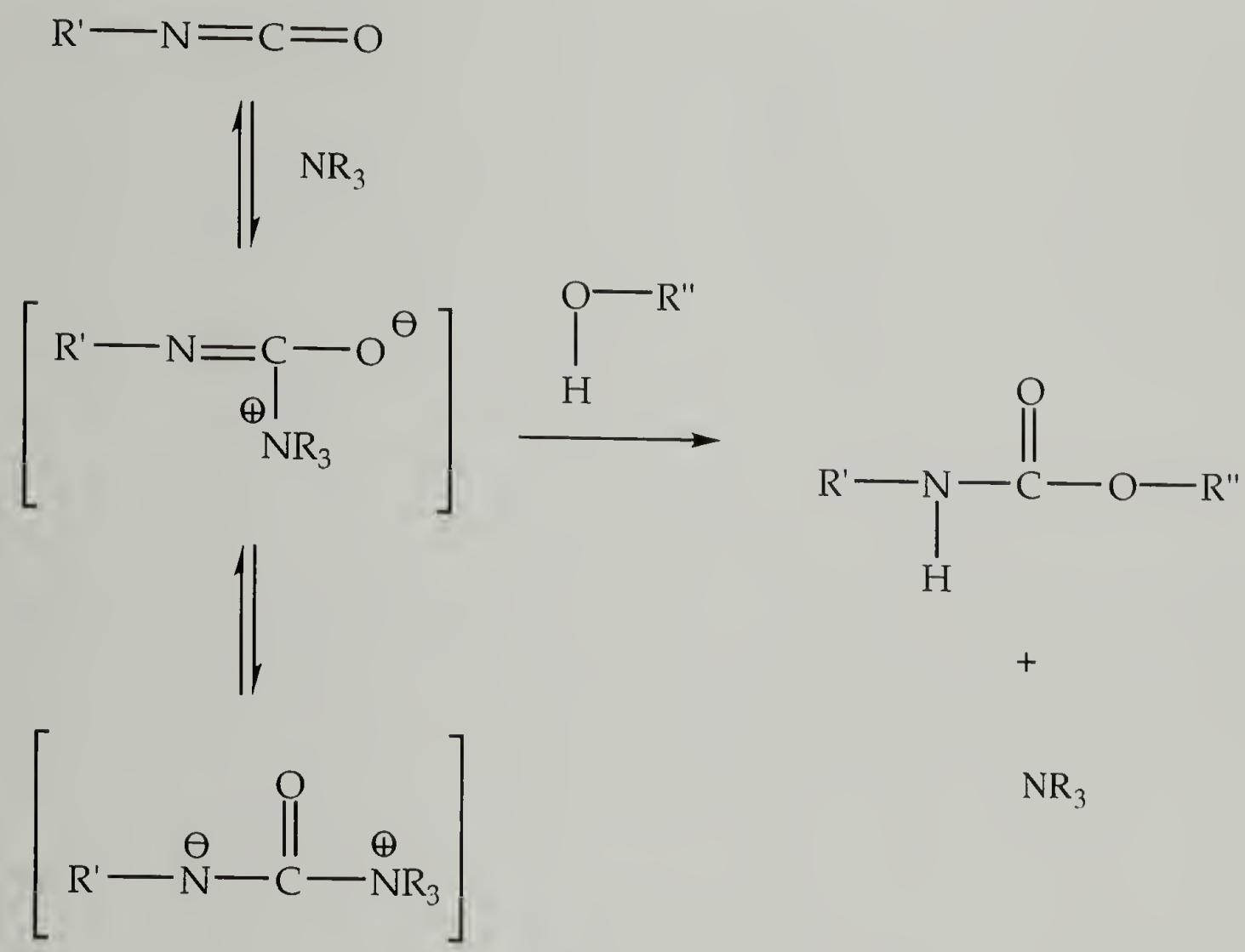

Figure B.1. Catalytic mechanism of amine catalyst

The catalytic activity of amines is due to the presence of a free electron pair on the nitrogen atom. Steric hindrance about the nitrogen atom and the electronic effects of substituent groups are the main factors influencing the relative catalytic activity of various amines. First proposed by Baker and Holdsworth in 1947, [13] the mechanism, as illustrated in Figure B.1, proposes reversible nucleophilic attack on the carbon atom by

the amine to form an activated complex. With aromatic isocyanates the carbonyl and aromatic groups both have moderate electron-withdrawing effects. With the formation of an amine-isocyanate complex, the nitrogen atom of the isocyanate group is activated and readily reacts with hydrogen atoms from any water or polyol sources in the vicinity.

A more recent mechanism (Figure B.2) is presented by Farkas and Strohm. [14] It involves the formation of an amine-active hydrogen complex. This latter mechanism supports the observed increase in catalytic activity of an amine with

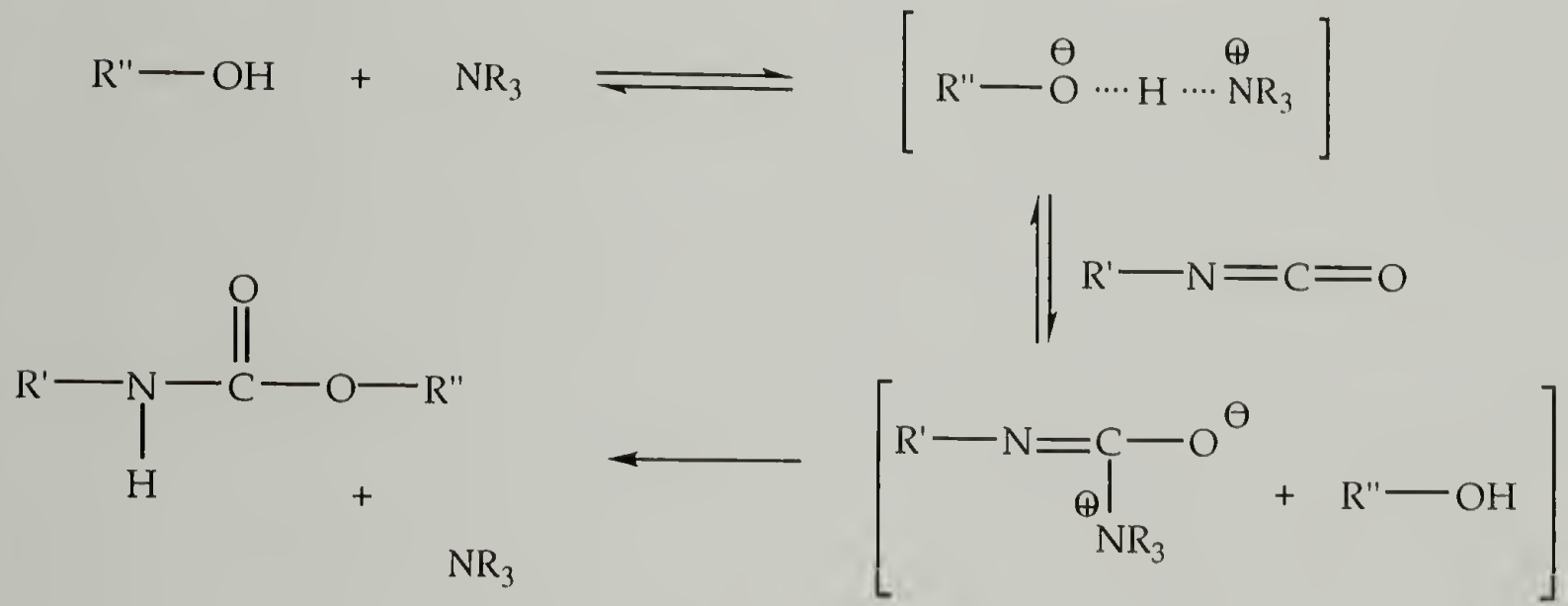

Figure B.2. Catalytic mechanism of amine catalyst

increasing basicity. Tertiary amine accelerates the isocyanate-water reaction more intensely than the isocyanate-polyol reaction because they form more stable hydrogen bonds with water. [2]

Of the many metal catalysts available, tin compounds are the most widely used. The compounds act as Lewis acids and are generally thought to function by interacting

with basic sites in the isocyanate and polyol compounds. [15-17] A few complementary mechanisms for activated complex formation can be envisaged. In the first, the polyol is activated by formation of a complex with the tin catalyst, as shown in Figure B.3. [2]

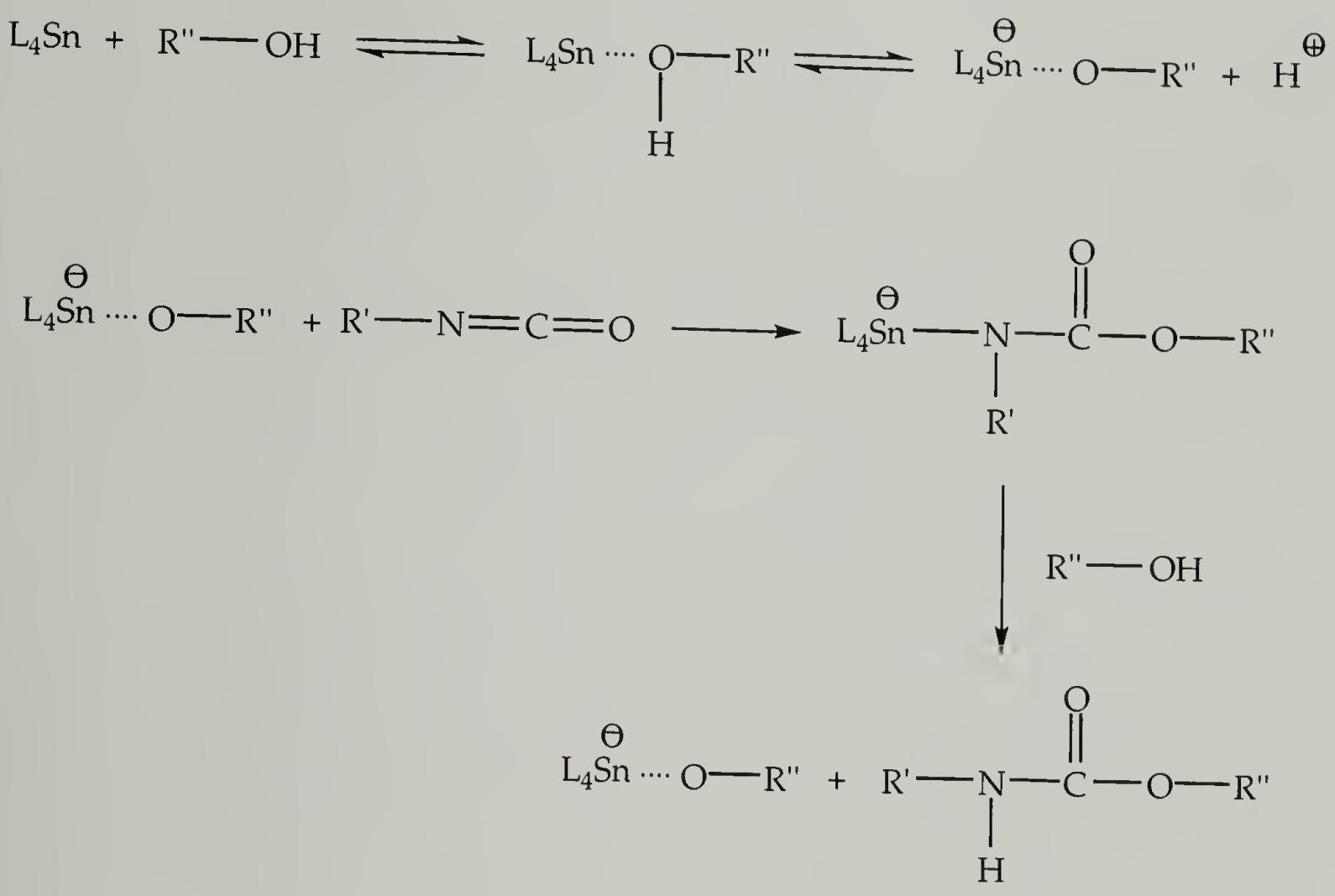

Figure B.3. Catalytic mechanism of organotin catalyst (Activation of polyol)

L symbolizes a ligand substituent to the tin molecule. From the tin alcohol adduct, the tin alkoxide can react with isocyanate to give a carbamate, which further reacts with additional polyol to propagate the polymer and regenerate the catalytic species.

The second mechanism (Figure B.4) involves activation of isocyanate molecules. Polyol attacks this complex at the isocyanate carbon atom to again propagate the polymer and regenerate the catalyst. [12]

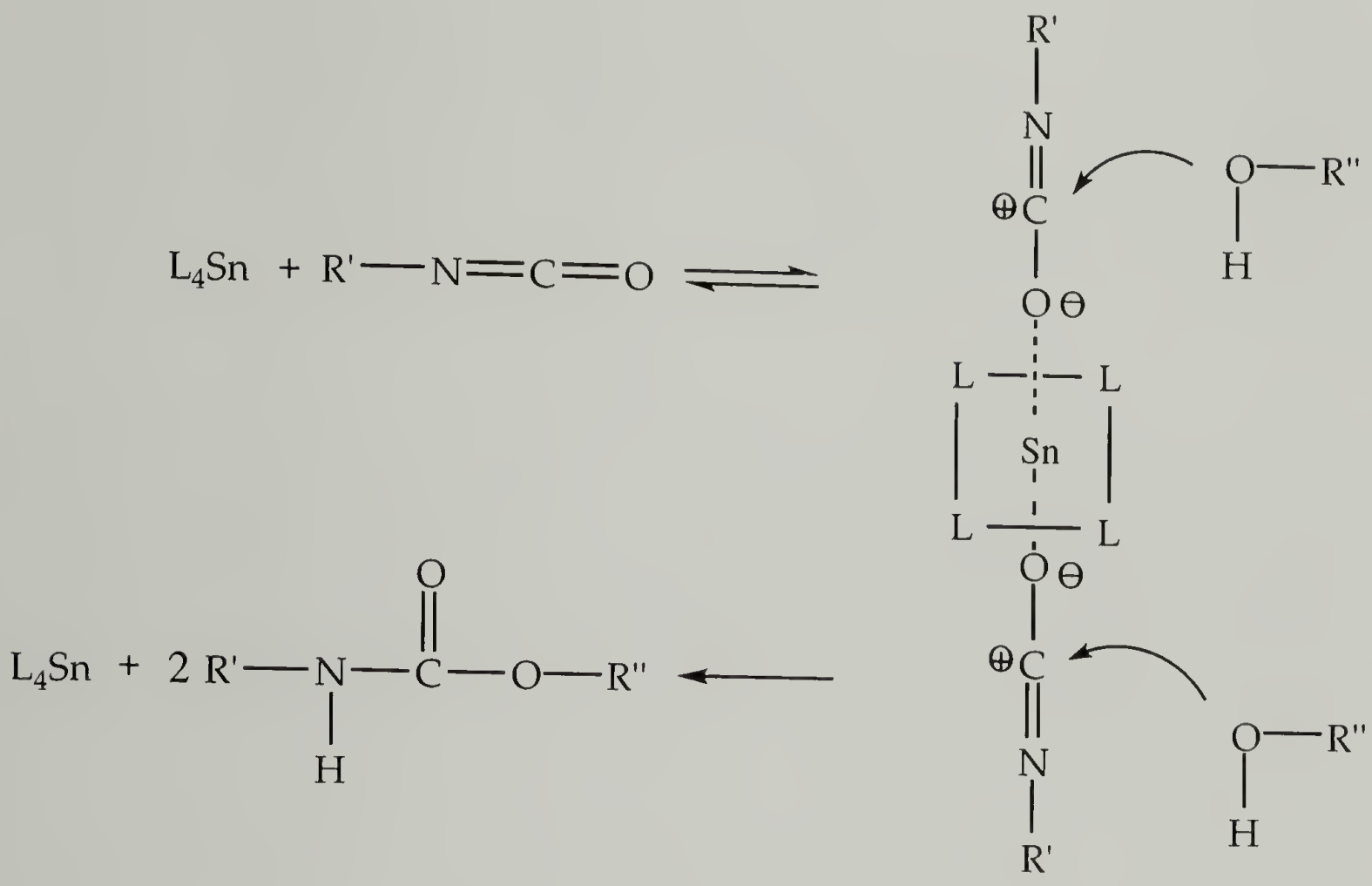

Figure B.4. Catalytic mechanism of organotin catalyst (Activation of isocyanate)

It is found experimentally that the combination of organometallic compounds and amine catalysts acts synergistically, which yields higher reaction rates. The last mechanism tends to give the interpretation. Tertiary amines are stronger Lewis bases

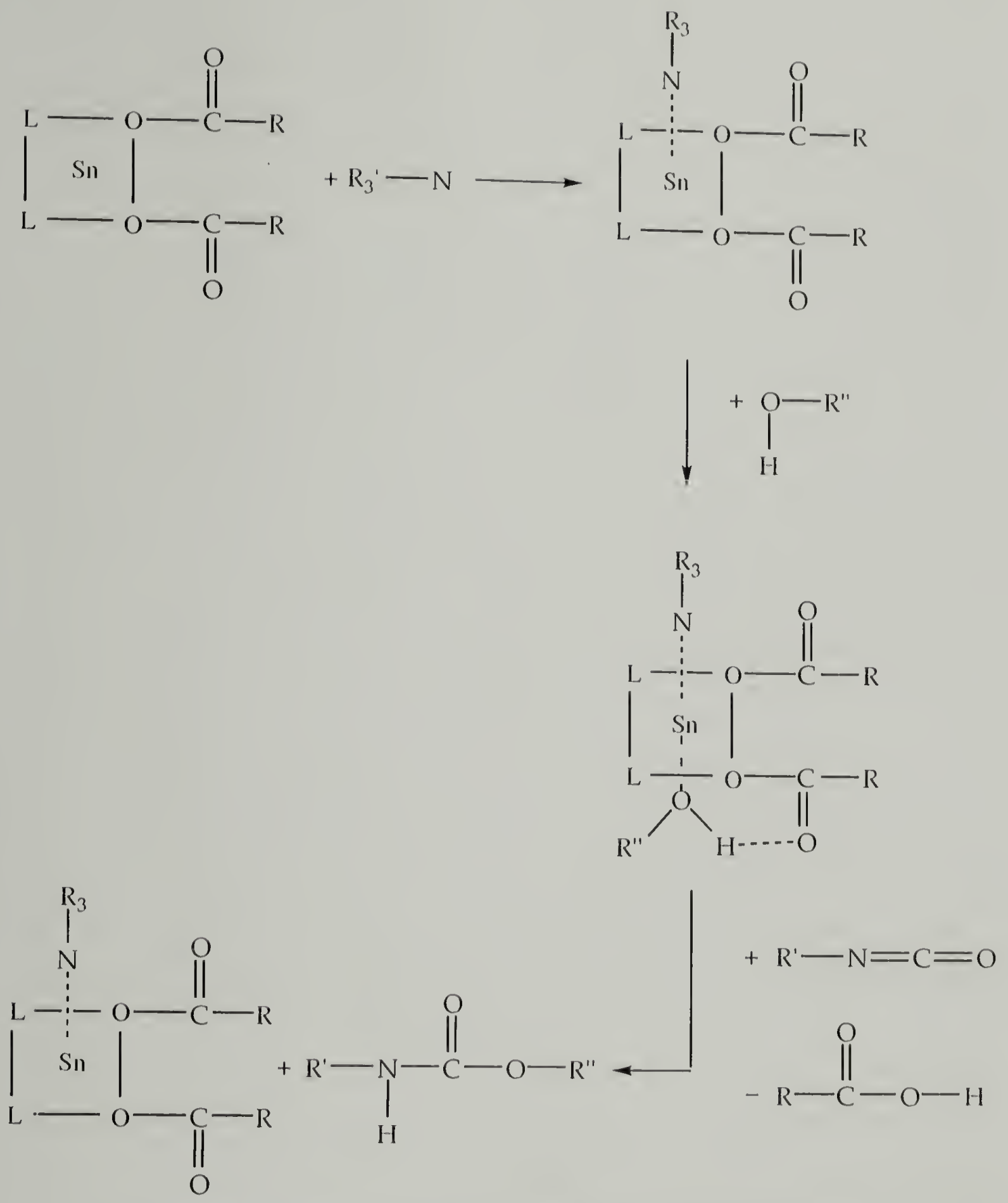

Figure B.5. Synergic mechanism of organotin and amine catalysts

than isocyanates and alcohols, and their complexation to metal compounds is expected. This tin-amine complex then accepts a polyol molecule to further activate the complex

and promote formation of a tin alkoxide. A leaving carboxylate group accepts the proton and opens a position for insertion of an isocyanate group. Further reaction of the complex with additional polyol propagates the polymer and regenerates the catalytic species.

In conclusion, the production of flexible polyurethane foams rests on a delicate balance in the timing of the two types of reactions. [18] The exothermic nature and the temperature profile of the process will have a substantial impact on the reactivity of various reactants and the sensitivity to catalyst variation, which will eventually affect the final phase separated morphology. [19,20] Besides, any possible additives, surfactants and fillers can alter the catalytic chemistry significantly.

References

1) Hostettler, F.; Cox, E. F. *Ind. Eng. Chem.* **1960**, *52*, 609-610.

2) Burkhart, G.; Kollmeier, H. J.; Schloens, H. H. *J. Cell. Plast.* **1984**, 37-41.

3) Wong, S.-W.; Frisch, K. C. *J. Polym. Sci. Part A: Polym. Chem. Ed.* **1986**, *24*, 2867-2875.

4) Malwitz, N.; Wong, S. W.; Frisch, K. C.; Manis, P. A. *J. Cell. Plast.* **1987**, *23*, 461-502.

5) Listemann, M. L.; Savoca, A. C.; Wressell, A. L. *J. Cell. Plast.* **1992**, *28*, 360-398.

6) Sojecki, R.; Trzcinski, S. *Eur. Polym. J.* **1998**, *34*, 1793-1799.

7) Sojecki, R. *Acta Polym.* **1992**, *43*, 96-98.

8) Sojecki, R. *Acta Polym.* **1991**, *42*, 411-414.

9) Sojecki, R. *Acta Polym.* **1991**, *41*, 518-520.

10) Sojecki, R. *Acta Polym.* **1989**, *40*, 487-492.

11) Sojecki, R. *Eur. Polym. J.* **1994**, *30*, 725-729.

12) Herrington, R.; Hock, K. *Flexible Polyurethane Foams*; 2 ed.; The Dow Chemical Company: Midland, **1997**.

13) Baker, J. W.; Holdsworth, J. B. *J. Chem. Soc.* **1947**, 713-726.

14) Farkas, A.; Strohm, P. F. *Ind. Eng. Chem. Fund.* **1965**, *4*, 32-38.

15) Doyle, E. N. *The Development and Use of Polyurethane Products*; McGraw-Hill, Inc.: New York, **1971**.

16) Hepburn, C. *Polyurethane Elastomers*; Applied Sciences Publishers: London, **1982**.

17) Woods, G. *Flexible Polyurethane Foams: Chemistry and Technology*; Applied Science Publishers Ltd.: London, **1982**.

18) Van Gheluwe, P.; Leroux, J. *J. Appl. Polym. Sci.* **1983**, *28*, 2053-2067.

19) Lowe, A. J.; Chandley, E. F.; Leigh, H. W.; Molinario, L. *J. Cell. Plastics* **1965**, *1*, 121-130.

20) Yontz, D. J.; Hsu, S. L.; Lidy, W. A.; Gier, D. R.; Mazor, M. H. *J. Polym. Sci., Polym. Phys.* **1998**, *36*, 3065-3077.

BIBLIOGRAPHY

Armistead, J. P.; Wilkes, G. L. *J. Appl. Polym. Sci.* **1988**, *35*, 601-629.

Arnold, K. R.; Meier, D. J. *J. Appl. Polym. Sci.* **1970**, *14*, 427-440.

Artavia, L. D.; Macosko, C. W. *J. Cell. Plast.* **1990**, *26*, 490-511.

Artavia, L. D.; Macosko, C. W.; Priester, R. D., Jr.; Shrock, A. K.; Turner, R. B. *An Integrated View of Reactive Urethane Foaming*: Nice, France, **1991**, pp 509-517.

Bailey, F. E. J.; Critchfield, F. E. *J. Cell. Plast.* **1981**, *17*, 333-339.

Bahl, S. K. *Structural an Vibrational Studies of Polyesters*; University of Connecticut: Storrs, 1976.

Balon, W. J. *Trifunction Isocyanate Trimers*; E.I. duPont de Nemours and Company: USA, **1957**.

Baker, J. W.; Holdsworth, J. B. *J. Chem. Soc.* **1947**, 713-726.

Bard, J. K.; Chung, C. I. *Modeling the Elastic Behavior of Poly(Styrene-b-Butadiene-b-Styrene) Block Copolymers*; Legge, N. R., Holden, G. and Schroeder, H. E., Ed.; Hanser: Munich, **1987**.

Bellamy, L. J. *The Infrared Spectra of Complex Molecules*; Chapman and Hall Ltd.: London, **1975**.

Bendit, E. G. *Biopolymers* **1966**, *4*, 539-559.

Bicerano, J.; Brewbaker, J. L. *J. Chem. Soc. Faraday Trans.* **1995**, *91*, 2507-2513.

Biermann, C. J.; Chung, J. B.; Narayan, R. *Macromolecules* **1987**, *20*, 954-957.

Boerio, F. J.; Bahl, S. k. *J. of Polymer Sci.: Polymer Physics Edition* **1976**, *14*, 1029-1046.

Bolker, H. I.; Terashima, N. *Infrared Spectroscopy of Lignins. IV Isolation of Lignins by Solvolysis in Acetals*; American Chemical Society: Washington, D. C., **1966**.

Bonart, R.; Morbitzer, L.; Hentze, G. *J. Macromol. Sci.-Phys.* **1969**, *B3*, 337-356.

Born, L.; Hespe, H. *Colloid Polym. Sci.* **1985**, *263*, 335-341.

Brodnyan, J. G. *Trans. Soc. Rheol.* **1959**, *3*, 61-68.

Brunette, C. M.; Hsu, S. L.; MacKnight, W. J. *Macromolecules* **1982**, *15*, 71-77.

Broos, R.; Herrington, R. M.; Casati, F. M. *Journal of Cellular Plastics* **2000**, *36*, 207-245.

Burkhart, G.; Kollmeier, H. J.; Schloens, H. H. *J. Cell. Plast.* **1984**, 37-41.

Callister, S.; Keller, A.; Hikmet, R. M. *Makromol. Chem. Macromol. Symp.* **1990**, *39*, 19-54.

Cates, D. A.; Strauss, H. L.; Snyder, R. G. *J. of physics chemistry-US* **1994**, *98*, 4482-4488.

Chen, C. C.; Krejchi, M. T.; Tirrell, D. A.; Hsu, S. L. *Macromolecules* **1995**, *28*, 1464-1469.

Chen, R.; Wu, Q. *J. Appl. Polym. Sci.* **1994**, *52*, 437-443.

Chow, T. S. *J. Polym. Sci. Polym. Phys. Ed.* **1982**, *20*, 2103-2109.

Christianson, L. R.; Dheming, M.; Ochoa, E. L. *J. Cell Plast.* **1977**, *13*, 111-117.

Clayden, N. J. N., C.; and Eeckhaut, G. *Macromolecules* **1998**, *31*, 7820-7828.

Coleman, M. M.; Lee, K. H.; Skrovanek, D. J.; Painter, P. C. *Macromolecules* **1986**, *19*, 2149-2157.

Coleman, M. M.; Skrovanek, D. J.; Hu, J.; Painter, P. C. *Macromolecules* **1988**, *21*, 59-65.

Coleman, M. M.; Graf, J. F.; Painter, P. C. *Specific Interactions and the Miscibility of Polymer Blends*; Technomic Publishing Co.: Lancaster, **1991**.

Coleman, M. M.; Sobkowiak, M.; Pehlert, G. J.; Painter, P. C.; Iqbal, T. *Macromol. Chem. Phys.* **1997**, *198*, 117-136.

Cooper, S. L.; Tobolsky, A. V. *J. Appl. Polym. Sci.* **1966**, *10*, 1837-1844.

Colthup, N. B.; Daly, L. H.; Wiberly, S. E. *Introduction to Infrared and Raman Spectroscopy*; 3rd ed.; Academic Press, Inc.: Boston, **1990**.

Cousins, W. *J. For. Sci.* **1977**, *7*, 107.

Crank, J. *The Mathematics of Diffusion*; Oxford University Press: Oxford, **1956**.

Creswick, M. W.; Lee, K. D.; Turner, R. B.; Huber, L. M. *J. Elast. Plast.* **1989**, *21*, 179-96.

Culbertson, B. M. *Multiphase Macromolecular Systems*; Plenum Publishing Corporation: New York, **1989**.

Dounis, J.; Moreland, J. C.; Wilkes, G. L.; Turner, R. B. *Polym. Prepr. (Am. Chem. Soc., Div. Polym. Chem.)* **1992**, *33*, 284-85.

Dounis, D. V.; Moreland, J. C.; Wilkes, G. L.; Dillard, D. A.; Turner, R. B. *J. Appl. Polym. Sci.* **1993**, *50*, 293-301.

Dounis, D. V.; Wilkes, G. L.; Turner, R. B. *Polym. Prepr. (Am. Chem. Soc., Div. Polym. Chem.)* **1994**, *35*, 781-82.

Dounis, D. V.; Wilkes, G. L. *Polymer* **1997**, *38*, 2819-2828.

Dounis, D. V.; Wilkes, G. L. *J. Appl. Polym. Sci.* **1997**, *65*, 525-537.

Doyle, E. N. *The Development and Use of Polyurethane Products*; McGraw-Hill, Inc.: New York, **1971**.

Eisenbach, C. D.; Stadler, E. *Macromol. Chem. Phys.* **1995**, *196*, 1981-1997.

Elwell, M. J.; Mortimer, S.; Ryan, A. J. *Macromolecules* **1994**, *27*, 5428-5439.

Elwell, M. J.; Ryan, A. J.; Grunbauer, H. J. M.; Van Lieshout, H. C. *Polymer* **1996**, *37*, 1353-1361.

Elwell, M. J.; Ryan, A. J.; Grunbauer, H. J. M.; Van Lieshout, H. C. *Macromolecules* **1996**, *29*, 2960-2968.

Estes, G. M.; Seymour, R. W.; Cooper, S. L. *Macromolecules* **1971**, *4*, 452-457.

Farkas, A.; Flynn, K. G. *J. Am. Chem. Soc.* **1960**, *82*, 642-645.

Farkas, A.; Strohm, P. F. *Ind. Eng. Chem. Fund.* **1965**, *4*, 32-38.

Feldman, D.; Banu, D.; Luchian, C.; Wang, J. *J. Appl. Polym. Sci.* **1991**, *42*, 1307-1318.

Feldman, D.; Banu, D.; Natansohn, A.; Wang, J. *J. Appl. Polym. Sci.* **1991**, *42*, 1537-1550.

Flory, P. J. *Principles of Polymer Chemistry*; Cornell University Press: Ithaca, NY, **1953**.

Fraser, R. D. B. *J. Chem. Phys.* **1953**, *21*, 1511.

Fukushima, K.; Zwolinski, J. B. *J. Chem. Phys.* **1969**, *50*, 737-749.

Garrett, J. T.; Runt, J.; Lin, J. S. *Macromolecules* **2000**, *33*, 6353-6359.

Gibson, L. J.; Ashby, M. F. *Proc. Roy. Soc. Lond. A* **1982**, *382*, 43-59.

Gilbert, M.; Hybart, F. J. *Polymer* **1972**, *13*, 327-332.

Girolamo, M.; Keller, A.; Stejny, J. *Makromol. Chem.* **1975**, *176*, 1489-1502.

Glasser, W. G.; Kelley, S. S. *J. Wood Chem. Technol.* **1988**, *8*, 341-359.

Glasser, W. G.; Barnett, C. A.; Rials, T. G.; Saraf, V. P. *J. Appl. Polym. Sci.* **1984**, *29*, 1815-1830.

Godovsky, Y., K.; Bessonov, N. P.; Mironova, N. N. *Colloid & Polymer Science* **1989**, *267*, 414-420.

Gorce, J.-N.; Hellgeth, J. W.; Ward, T. C. *Polym. Eng. Sci.* **1993**, *33*, 1170-1176.

Goring, D. A. I. *Lignin: Properties and Materials*; Glasser, W. G. and Sarkanen, S., Ed.; American Chemical Society: Toronto, Ontario, Canada, **1988**; Vol. 397, pp 1-10.

Grady, B. P.; O' Connell, E. M.; Yang, C. Z.; Cooper, S. L. *J. Polym. Sci., Part B: Polym. Phys.* **1994**, *32*, 2357-2366.

Gruenbauer, J. H. M.; Folmer, J. C. W.; van Lieshout, H. C.; Lidy, W. A.; Thoen, J. A. *Polym. Preprt.* **1991**, *32*, 517-518.

Grunbauer, H. J. M.; Folmer, J. C. W. *J. Appl. Polym. Sci.* **1994**, *54*, 935-949.

Guth, E. *J. Appl. Phys.* **1945**, *16*, 20-25.52) Brunette, C. M.; Hsu, S. L.; MacKnight, W. J. *Macromolecules* **1982**, *15*, 71-77.

Halpin, J. C. *Revised Primer on Composite Materials: Analysis*; Technomic Publishing Co., Inc.: Lancaster, **1984**.42) Harrell, L. L., Jr. *Macromolecules* **1969**, *2*, 607-612.

Hatakeyama, H.; Hirose, S.; Hatakeyama, T. *J. Macro. Sci.-Pure Appl. Chem.* **1995**, *A32*, 743-750.

Hepburn, C. *Polyurethane Elastomers*; Applied Sciences Publishers: London, **1982**.

Herrington, R. M.; Klarfeld, D. L. *Humid Aged Compression Set Phenomena in All Water Blown HR Molded Foams*; Technomic Publishing Co., Inc.: Lancaster, PA., **1983**, pp 177-182.

Herrington, R.; Hock, K. *Flexible Polyurethane Foams*; 2 ed.; The Dow Chemical Company: Midland, **1997**.

Hersch, P. *Plast. Tech.* **1967**, *13*, 49-53.

Hespe, H.; Crone, J.; Mueller, E. H.; Schaefer, E. E. *J. Cell. Plastics* **1982**, *18*, 289-298.

Hess, W. M. *Microscopy in the Study of Elastomer Reinforcement by Pigment Fillers*; Kraus, G., Ed.; John Wiley & Sons, Inc.: New York, **1965**.

Hess, W. M. *Rubber Chemistry and Technology* **1991**, *64*, 386-449.

Hirose, S.; Kobashigawa, K.; Izuta, Y.; Hatakeyama, H. *Polym. Int.* **1998**, *47*, 247-256.

Hoeker, J. *J. Appl. Polym. Sci.* **1980**, *25*, 2879-2889.

Hogan, J. M.; Pearson, C. J.; Rogers, T. H.; White, J. R. *J. Cell Plast.* **1973**, *9*, 219-225.

Hostettler, F.; Cox, E. F. *Ind. Eng. Chem.* **1960**, *52*, 609-610.

Huang, J. S.; Gibson, L. J. *J. Mater. Sci* **1991**, *26*, 637-646.

Hummel, D. O.; Ellinghorst, G.; Khatchatryan, A.; Stenzenberger, H. D. *Die Ange. Makrom. Chem.* **1979**, *82*, 129-148.

Ishihara, H.; Kimura, I.; Saito, S.; Ono, H. *J. Macromol. Sci. Phys.* **1974**, *B10*, 591-618.

Isono, Y.; Ferry, J. D. *Rubber Chem. Technol.* **1984**, *57*, 925-943.

Jou, C.; Sackinger, S. T.; Farris, R. J. *J. Coatings Technol.* **1995**, *67*, 71-77.

Kamykowski, G. W.; Ferry, J. D.; Fetters, L. J. *J. Polym. Sci: Polym. Phys. Ed.* **1982**, *20*, 2125-2134.

Kanamoto, T.; Tanaka, K. *J. Polym. Sci., A-2* **1971**, *9*, 2043-2060.

Kim, P. K.; Chang, C.; Hsu, S. L. *Polymer* **1986**, *27*, 34-46.

Klason, C.; Kubat, J. *Plastics and Rubber Processing and Application* **1986**, *6*, 17-20.

Klesper, E. *Rubber Age* **1958**, 84-87.

Koberstein, J. T.; Stein, R. S. *J. Polym. Sci., Part B: Polym. Phys.* **1983**, *21*, 2181-2200.

Koberstein, J. T.; Russell, T. P. *Macromolecules* **1986**, *19*, 714-720.

Koberstein, J.; Gancarz, I. *Journal of Polymer Scienc: Part B: Polymer Physics* **1986**, *24*, 2487-2498.

Kornfield, J. A.; Spiess, H. W.; Nefzger, H.; Eisenbach, C. D. *Macromolecules* **1991**, *24*, 4787-4795.9)

Korzyuk, E. L.; Zharkov, V. V.; Emelin, E. A. *J. Appl. Chem. USSR* **1981**, *54*, 1320-1324.

Kricheldorf, H. R.; Meier-Haack, J. *Makromol. Chem.* **1992**, *193*, 2631-2645.

Kurzer, F. *Chem. Rev.* **1956**, *56*, 95-197.68) Laws, N.; McLaughlin, R. *J. Mech. Phys. Solids* **1979**, *47*, 1-13.

Lee, S. S.; Kim, S. C. *Polym. Eng. Sci.* **1993**, *33*, 598-606.

Lee, H. S.; Wang, Y. K.; Hsu, S. L. *Macromolecules* **1987**, *20*, 2089.

Lee, H. S.; Wang, Y. K.; MacKnight, W. J.; Hsu, S. L. *Macromolecules* **1988**, *21*, 270-273.

Lee, H. S.; Hsu, S. L. *Macromolecules* **1989**, *22*, 1100-1105.

Lee, H. S.; Hsu, S. L. *Journal of Polymer Science: Part B: Polymer Physics* **1994**, *32*, 2085-2098

Levon, K.; Margolina, A.; Patashinsky, A. Z. *Macromolecules* **1993**, *26*, 4061-4063.

Li, Y.; Ren, Z.; Zhao, M.; Yang, H.; Chu, B. *Macromolecules* **1993**, *26*, 612-622.

Lin, S. B.; Hwang, K. S.; Tsay, S. Y.; Cooper, S. L. *Colloid Polym. Sci.* **1985**, *263*, 128-140.

Lindberg, J. J.; Kuusela, T. A.; Levon, K. *Specialty Polymers from Lignin*; American Chemical Society: Washington, D. C., **1989**.

Listemann, M. L.; Savoca, A. C.; Wressell, A. L. *J. Cell. Plast.* **1992**, *28*, 360-398.

Lowe, A. J.; Chandley, E. F.; Leigh, H. W.; Molinario, L. *J. Cell. Plastics* **1965**, *1*, 121-130.

Malwitz, N.; Wong, S. W.; Frisch, K. C.; Manis, P. A. *J. Cell. Plast.* **1987**, *23*, 461-502.

Martin, D. J.; Meijs, G. F.; Gunatillake, P. A.; Yozghatlian, S. P.; Renwick, G. M. *J. Appl. Polym. Sci.* **1999**, *71*, 937-952.

McClusky, J. V.; O'Neill, R. E.; Priester, R. D. J.; Ramsey, W. A. *J. Cell. Plast.* **1992**, *30*, 224-241.

McClusky, J. V.; Priester, R. D., Jr.; O'Neill, R. E.; Willkomm, W. R.; Heaney, M. D.; Capel, M. A. *J. Cell. Plast.* **1994**, *30*, 338-360.

Medalia, A. I. *Rubber Chemistry and Technology* **1973**, *46*, 877-896.

Merten, R.; Lauerer, D.; Dahm, M. *J. Cell. Plast.* **1968**, *4*, 262-275.

Mertes, J.; Stutz, H.; Schrepp, W.; Kreyenschmidt, M. *J. Cell. Plast.* **1998**, *34*, 526-543.

Meuse, C. W.; Yang, X.; Yang, D.; Hsu, S. L. *Macromolecules* **1992**, *25*, 925-932.

Meuse, C. W.; Tao, H.-J.; Hsu, S. L.; MacKnight, W. J. *Polym. Prepr. (Am. Chem. Soc., Div. Polym. Chem.)* **1993**, *34*, 266-267.

Miller, J. A.; Lin, S. B.; Hwang, K. K. S.; Wu, K. S.; Gibson, P. E.; Cooper, S. L. *Macromolecules* **1985**, *18*, 32-44.

Miyazawa, T.; Blout, E. R. *J. Am. Chem. Soc.* **1961**, *83*, 712-719.

Monteiro, E. E. C.; Fonseca, J. L. C. *J. Appl. Polym. Sci.* **1997**, *65*, 2227-2236.

Mooney, M. *J. Colloid Sci.* **1951**, *6*, 162-170.

Moreland, J. C.; Wilkes, G. L. *Journal of Applied Polymer Science* **1991**, *43*, 801-815.

Moreland, J. C.; Wilkes, G. L.; Turner, R. B. *Viscoelastic Behavior of Flexible Slabstock Polyurethane Foams as a Function of Temperature and Relative Humidity*: Nice, France, **1991**, pp 500-508.

Mullins, L.; Tobin, N. R. *Journal of Applied Polymer Science* **1965**, *9*, 2993-3009.

Nakayama, K.; Ino, T.; Matsubara, I. *J. Macromol. Sci.-Phys.* **1969**, *A3*, 1005.

Neff, R.; Macosko, C. W. *A Model for Modulus Development in Flexible Polyurethane Foam*: Chicago, IL, **1995**, pp 344-352.

Neff, R.; Adedeji, A.; Macosko, C. W.; Ryan, A. J. *J. Polym. Sci., Part B: Polym. Phys.* **1998**, *36*, 573-581.

Nielsen, L. E. *Mechanical Properties of Polymers*; Reinhold Publishing Corporation: New York, **1962**.

Oertel, G. *Polyurethane Handbook*; Hanser/Gardner Publications, Inc.: Cincinnati, **1993**.

Ozaki, S. *Chem. Rev.* **1972**, *72*, 457-496.

Paik Sung, C. S.; Schneider, N. S. *Macromolecules* **1975**, *8*, 68-73.

Paik Sung, C. S.; Smith, T. W.; Hu, C. B.; Sung, N.-H. *Macromolecules* **1979**, *12*, 538-540.

Paik Sung, C. S.; Smith, T. W.; Sung, N. H. *Macromolecules* **1980**, *13*, 117-121.

Parkinson, D. *Reinforcement of Rubbers*; The Institution of the Rubber Industry:, **1957**.

Pearl, I. A. *The Chemistry of Lignin*; Marcel Dekker, Inc.: New York, 1967.

Peterlin, A. *Plastic Deformation of Polymers*; Marcel Dekker, Inc.: New York, **1971**.

Petrovic, Z. S.; Javni, I. *Journal of Polymer Science: Part B: Polymer Physics* **1989**, *27*, 545-560.

Petrovic, Z. S.; Ferguson, J. *Prog. Polym. Sci.* **1991**, *16*, 695.

Pimentel, G. C.; Sederholm, C. H. *The Journal of Chemical Physics* **1956**, *24*, 639-641.

Pimentel, G. C.; L., M. A. *The Hydrogen Bond*; W. H. Freeman and Company: San Francisco, **1960**.

Priester, R. D.; McClusky, J. V.; O'Neill, R. E.; Harthcock, M. A.; Davis, B. L. *33rd Annual Polyurethane Technical/Marketing Conference* **1990**, *September 30-October 3*, 527-538.

Pukanszky, B. *Makromol. Chem. Macromol. Symp.* **1993**, *70/71*, 213-223.

Raab, M.; Nezbedova, E. *Toughness of Ductile Polymers*; Hanser: Munich, 2000.

Read, B. E.; Stein, R. S. *Macromolecules* **1968**, *1*, 116.

Reich, S. *Dynamics of Late Stage Phase Separation in Polymer Blends*; Rabin, Y. and Bruinsma, R., Ed.; Plenum Press: New York, **1994**, pp 73-98.

Reilly, A. F. *Chem. Eng. Prog.* **1967**, *63*, 104-108.

Robinson, P., Personal Communication.

Rosch, J.; Mulhaupt, R. *Polym. Bull.* **1994**, *32*, 361-365.

Rossmy, G. R.; Kollmeier, H. J.; Lidy, W.; Schator, H.; Wiemann, M. *J. Cell. Plast.* **1977**, *13*, 26-35.

Rouhi, A. M. *Lignin and Lignan Biosynthesis*, 2000; Vol. 78, pp 29-32.

Ryan, A. J.; Stanford, J. L.; Still, R. H. *Polym. Comm.* **1988**, *29*, 196-198.

Ryan, A. J.; Stanford, J. L.; Still, R. H. *Plast. Rubber Proc. Appl.* **1990**, *13*, 99-110.

Rubinstein, M.; Obukhov, S. P. *Macromolecules* **1993**, *26*, 1740-1750.

Sackinger, S. T. *The Determination of Swelling Stresses in Polyimide Film*; University of Massachusetts: Amherst, **1990**.

Samuels, R. J. *J. Polym. Sci., A* **1965**, *3*, 1741-1763.

Samuels, R. J. *J. Macromol. Sci. - Phys.* **1970**, *B4*, 701-759.

Sayad, R. S.; Williams, K. W. *Methylene Chloride Urethane Grade as a Viable Auxiliary Blowing Agent in Flexible Slabstock Foam*; Technomic: Lancaster, PA, **1978**, pp 1-8

Schneider, N. S.; Dusablon, L. V.; Snell, E. W.; Prosser, R. A. *J. Macromol. Sci.-Phys.* **1969**, *B3*, 623-644.

Schneider, N. S.; Paik Sung, C. S.; Matton, R. W.; Illinger, J. L. *Macromolecules* **1975**, *8*, 62-67.

Seymour, R. W.; Allegrezza, A. E.; Cooper, S. L. *Macromolecules* **1973**, *6*, 896-902.

Seymour, R. W.; Cooper, S. L. *J. Polym. Sci., Polym. Symp.* **1974**, *46*, 69-81.

Siesler, H. W.; Holland-Moritz, K. *Infrared and Raman Spectroscopy of Polymers*; Marcel Dekker, Inc.: New York, **1980**.

Siesler, H. W. *Polymer Bulletin* **1983**, *9*, 382-389.

Siesler, H. W. *Polymer Bulletin* **1983**, *9*, 557-562.

Siesler, H. W. *Rheo-Optical Fourier-Transform Infrared Spectroscopy: Vibrational Spectra and Mechanical Properties of Polymers*; Springer-Verlag: Berlin, **1984**; Vol. 65.

Siesler, H. W. *Berichte Der Bunsen-Gesellschaft-Physical Chemistry Chemical Physics* **1988**, *92*, 641-645.

Skoglund, P.; Fransson, A. *Polymer* **1998**, *39*, 1899-1906.

Smallwood, H. M. *J. Appl. Phys.* **1944**, *15*, 758-766.

Smith, T. L.; Dickie, R. A. *J. Polymer Sci. Part C* **1969**, *26*, 163-187.

Smith, T. L. *Polymer Engineering and Science* **1977**, *17*, 129-143.

Sojecki, R. *Acta Polym.* **1989**, *40*, 487-492.

Sojecki, R. *Acta Polym.* **1992**, *43*, 96-98.

Sojecki, R. *Acta Polym.* **1991**, *42*, 411-414.

Sojecki, R. *Acta Polym.* **1991**, *41*, 518-520.

Sojecki, R. *Eur. Polym. J.* **1994**, *30*, 725-729.

Sojecki, R.; Trzcinski, S. *Eur. Polym. J.* **1998**, *34*, 1793-1799.

Spirkova, M.; Kubin, M.; Dusek, K. *J. Macromol. Sci.-Chem.* **1987**, *A24*, 1151-1166.

Stephanou, A.; Pizzi, A. *Holzforschung* **1993**, *47*, 439-445.

Strobl, G. *The Physics of Polymers*; 2nd ed.; Springer-Verlag: Berlin, **1997**.

Suen, W.; Percy, J.; Hsu, S. L. *In Preparation* **2000**.

Sandridge, R. L.; Morecroft, A. S.; Hardy, E. E.; Saunders, J. H. *J. Chem. Eng. Data* **1960**, *5*, 495-498.

Tabor, R. L.; Hinze, K. J.; Priester, R. D.; Turner, R. B. *The Compatibility of Water with Polyols*, **1992**; Vol. October 21-24, pp 514-528.

Tan, T. T. M. *Polym. Int.* **1996**, 13-16.

Tao, H.-J.; Meuse, C. W.; Yang, X.; MacKnight, W. J.; Hsu, S. L. *Macromolecules* **1994**, *27*, 7146-7151.

Tao, H.-J.; Fan, C. F.; MacKnight, W. J.; Hsu, S. L. *Macromolecules* **1994**, *27*, 1720-1728.

Tao, H. J.; MacKnight, W. J.; Gagnon, K. D.; Lenz, R. W.; Hsu, S. L. *Macromolecules* **1995**, *28*, 2016-2022.

Thomas, O.; Priester, R. D., Jr.; Hinze, K. J.; Latham, D., D. *Journal of Polymer Science: Part B: Polymer Physics* **1994**, *32*, 2155-2169.

Tsuboi, M.; Nakanishi, M. *Adv. Biophys.* **1979**, *12*, 101-130.

Tsubomura, H. *J. Chem. Phys.* **1956**, *24*, 927-931.

Turner, R. B.; Wilkes, G. L. *Structure vs. Properties of Flexible Urethane Foams Used in the Home Furnishing Industry (Polymer-Morphology)*; Technomic Publishing Co., Inc.: Aachen, Federal Republic of Germany, **1987**, pp 935-939.

Uematsu, I.; Uematsu, Y. *Polypeptide Liquid Crystals*; Gordon, M., Ed.; Springer-Verlag: Berlin, **1984**.

Ulrich, H. *Introduction to Industrial Polymers*; Hanser: Munich, **1982**.

Van der Put, T. A. C. M. *Wood Fiber Sci.* **1989**, *21*, 219.

Van Gheluwe, P.; Leroux, J. *J. Appl. Polym. Sci.* **1983**, *28*, 2053-2067.

Varsanyi, G. *Vibrational Spectra of Benzene Derivatives*; New York: Academic Press, **1969**.

Vrtis, J. K. *Stress and Mass Transport in Polymer Coating and Films*; University of Massachusetts: Amherst, **1995**.

Wang, C. B.; Cooper, S. L. *Macromolecules* **1983**, *16*, 775-786.

Wang, F. C.; Feve, M.; Lam, T. M.; Pascault, J. *J. Polym. Sci., Part B: Polym. Phys.* **1994**, *32*, 1315-1320.

Wang, J.; St. John Manley, R.; Feldman, D. *Prog. Polym. Sci.* **1992**, *17*, 611-646.

West, J. C.; Cooper, S. L. *J. Polym. Sci., Polym. Symp.* **1977**, *60*, 127-150.

Wilkinson, A. N.; Naylor, S.; Elwell, M. J.; Draper, P.; Komanschek, B. U.; Stanford, J. L.; Ryan, A. J. *Polym. Commun.* **1996**, *37*, 2021-2024.

Wilkinson, S. L. *C & EN News* **2001**, *79*, 61-62.

Wong, S.-W.; Frisch, K. C. *J. Polym. Sci. Part A: Polym. Chem. Ed.* **1986**, *24*, 2867-2875.

Woods, G. *Flexible Polyurethane Foams: Chemistry and Technology*; Applied Science Publishers Ltd.: London, **1982**.

Wu, X.; Hsu, S. L. *PMSE Preprints* **2000**, *82*, 369.

Xiu, Y.; Wang, D.; Hu, C.; Ying, S.; Li, J. *Journal of Applied Polymer Science* **1993**, *48*, 867-869.

Yamamoto, T.; Shibayama, M.; Nomura, S. *Polymer Journal* **1991**, *23*, 311-320.

Yamamura, H.; Kuramoto, N. *J. Appl. Polym. Sci.* **1959**, *2*, 71-80.

Yang, C. Z.; Hwang, K. K. S.; Cooper, S. L. *Makromol. Chem.* **1983**, *184*, 651-668.

Yang, C. Z.; Li, C.; Cooper, S. L. *J. Polym. Sci., Polym. Phys. Ed.* **1991**, *29*, 75-86.

Yang, D. K.; Koros, W. J.; Hopfenberg, H. B.; Stannett, V. T. *J. Appl. Polym. Sci.* **1985**, *30*, 1035-1047.

Yang, X.; Hsu, S. L. *Macromolecules* **1993**, *26*, 1465.

Yontz, D. J.; Hsu, S. L.; Lidy, W. A.; Gier, D. R.; Mazor, M. H. *J. Polym. Sci., Polym. Phys.* **1998**, *36*, 3065-3077.

Yontz, D. J. *An Analysis of Molecular Parameters Governing Phase Seperation in a Reacting Polyurethane System*; University of Massachusetts: Amherst, MA, **1999**, pp 329.

Yontz, D. J.; Hsu, S. L. *Macromolecules* **2000**, *33*, 8415 - 8420.

Yoshida, H.; Morck, R.; Kringstad, K. P.; Hatakeyama, H. *J. Appl. Polym. Sci.* **1987**, *34*, 1187-1198.

Zbinden, R. *Infrared Spectroscopy of High Polymers*; Academic Press, Inc.: New York, **1964**.